TABLE OF CONTENTS

		Page	
SUMMARY		1	1/A7
1.0	INTRODUCTION	3	1/A9
2.0	CABOT BASELINE DATA	5	1/A11
	2.1 Materials	5	1/A11
	2.2 Texture	5	1/A11
	2.3 Tensile Properties	14	1/B7
	2.4 Stress Rupture Properties	17	1/B12
	2.5 Creep Properties	17	1/B12
	2.5.1 Creep life evaluation	17	1/B12
	2.5.2 Minimum creep rate evaluation	25	1/C9
	2.6 Static Oxidation Resistance	31	1/D5
	2.7 Dynamic Oxidation Resistance	31	1/D5
3.0	TEXTURE STUDY	39	1/E4
	3.1 Introduction	39	1/E4
	3.2 Initial Investigaton	40	1/E5
	3.2.1 Production of experimental sheet lots	40	1/E5
	3.2.2 Examination of crystallographic texture	40	1/E5
	3.2.3 Creep strength evaluation	61	1/G1
	3.3 Evaluation of Optimum Texture Sheets	65	1/G6
	3.3.1 Production of experimental sheet lots	65	1/G6
	3.3.2 Examination of grain size and crystallographic texture	65	1/G6

TABLE OF CONTENTS (Cont.)

		Page	
3.3.3	Bend ductility	65	1/G6
3.3.4	Tensile properties	65	1/G6
3.3.5	Stress rupture properties	67	1/G8
3.3.6	Creep life evaluation	67	1/G8
3.3.7	Minimum creep rate evaluation	79	2/B3
3.3.8	Examination of microstructure after creep testing	79	2/B3
3.3.9	Residual room temperature tensile properties after creep testing	88	2/C2
4.0	GRAIN SIZE STUDY	92	2/C8
4.1	Investigation of the Dependence of Creep Strength on Grain Size	92	2/C8
4.1.1	Production of experimental sheet lots	92	2/C8
4.1.2	Examination of crystallographic texture	92	2/C8
4.1.3	Creep strength evaluation	97	2/D3
4.1.4	Apparent activation energies for creep	101	2/D9
4.2	Evaluation of ASTM 5-6 Grain Size Sheets	103	2/D12
4.2.1	Production of experimental sheet lots	103	2/D12
4.2.2	Tensile properties	107	2/E2
4.2.3	Stress rupture properties	107	2/E2
4.2.4	Creep life evaluation	107	2/E2
4.2.5	Minimum creep rate evaluation	120	2/F11
4.3	Supplementary Grain Size Study: Investigation of the Dependence of Creep Strength on Sheet Thickness	120	2/F11
4.3.1	Production of experimental sheet	124	2/G3
4.3.2	Examination of crystallographic texture	124	2/G3

TABLE OF CONTENTS (Cont.)

	Page	
4.3.3 Tensile properties	124	2/G3
4.3.4 Stress rupture properties	128	2/G8
4.3.5 Creep life evaluation	128	2/G8
4.3.6 Minimum creep rates	140	3/B7
5.0 PRESTRAIN STUDY	144	3/B12
5.1 Materials and Experimental Procedure	144	3/B12
5.2 Creep Test Results	144	3/B12
5.3 Examination of Microstructures after Creep Testing	147	3/C3
6.0 DYNAMIC OXIDATION RESISTANCE OF EXPERIMENTAL SHEETS	154	3/C10
6.1 Materials and Experimental Procedure	154	3/C10
6.2 Dynamic Oxidation Test Results	154	3/C10
7.0 DISCUSSION AND CONCLUDING REMARKS	158	3/D2
APPENDIX A - Conversion of U.S. Customary Units to SI Units	160	3/D4
APPENDIX B - Creep Test Procedure	164	3/D8
APPENDIX C - Baseline Creep Test Data	168	3/D13
APPENDIX D - Texture Study Creep Test Data	173	3/E9
APPENDIX E - Grain Size Study Creep Test Data	179	3/F7
REFERENCES	186	3/G7

NAS 1.26:3013

OCT 4 1978

NASA Contractor Report 3013

COMPLETED

ORIGINAL

Thermomechanical Processing of HAYNES® Alloy No. 188 Sheet To Improve Creep Strength

D. L. Klarstrom

CONTRACT NAS1-13837
AUGUST 1978

NASA

194

NASA Contractor Report 3013

Thermomechanical Processing of HAYNES® Alloy No. 188 Sheet To Improve Creep Strength

D. L. Klarstrom
Cabot Corporation
Kokomo, Indiana

Prepared for
Langley Research Center
under Contract NAS1-13837

National Aeronautics
and Space Administration

Scientific and Technical
Information Office

1978

Blank

Page

SUMMARY

The purpose of this investigation was to improve the low strain (≤ 1 percent) creep strength of HAYNES alloy No. 188 sheet by means of thermo-mechanical processing (TMP). Research efforts were organized along two major approaches: One examined TMP designed to develop high degrees of preferred grain orientation in recrystallized thin gauge sheet; and the other concentrated on grain size control. Brief studies were also performed to examine the effects of thickness-to-grain diameter ratio and prestrain on low strain creep strength.

To assist in the performance of the program, the Stellite Division of the Cabot Corporation established baseline data for three production heats of HAYNES alloy No. 188 sheet nominally 0.38 mm (0.015-inch) thick. The data included tensile properties from room temperature to 1366K (2000°F), low strain creep strength in the temperature range of 922K (1200°F) to 1255K (1800°F), stress rupture properties at standard quality control test conditions, and static and dynamic oxidation resistance. In addition, the microstructural characteristics of the baseline sheets were documented.

Significant improvements in low strain creep strength were obtained in sheets with a strong recrystallized texture. The TMP considered to give optimum results consisted of 80 percent final cold work followed by an anneal at 1505K (2250°F) for 10 minutes. The major components of the texture resulting from this TMP schedule, with respect to the plane of the sheet and the rolling direction, were identified as (110) [$\bar{1}$10] and (112) [$\bar{1}$10].

Based on stress versus Larson-Miller parameter correlations obtained for 0.5 percent and 1.0 percent creep life data, the minus 3-sigma creep life minimums of the textured sheets were found to lie above the baseline average values over a range of test conditions corresponding to approximately 206.8 MPa/ 18×10^3 LMP-K (30 ksi/32.5×10^3 LMP-°R) to 17.2 MPa/23.5×10^3 LMP-K (2.5 ksi/ 42.3×10^3 LMP-°R).

Results of room temperature bend tests indicated no adverse effects of the preferred crystallographic texture on fabricability. The tensile and stress rupture properties of the textured sheets were found to be equivalent or superior to the baseline sheets except for ductility under certain test conditions. Specifically, elongation values obtained in tensile tests at temperatures of 1144K (1600°F) and above, in stress rupture tests at 1089K/ 165.4 MPa (1500°F/24 ksi), and in room temperature tensile tests conducted on samples which had been creep tested at 922K (1200°F) and at 1255K (1800°F) were less than those obtained for the baseline sheets. In all cases, however, the ductility values obtained were considered to be at acceptable levels.

In the investigation of TMP to optimize grain size, an initial study was carried out to determine the dependence of creep strength on grain size using a quality control test condition of 1200K/41.4 MPa (1700°F/6 ksi). Results of the study indicated no significant improvements over the baseline sheets. However, important findings were the deterioration in creep strength at a grain size of ASTM 7-8, and an increase in the amount of primary creep strain at a grain size of ASTM 2-4.

An attempt was made to gain a better understanding of the role of grain size on creep strength by determining activation energies for creep. Due to an apparent strain-aging effect, unreasonably high activation energy values were obtained. In the final phase of the investigation, sheets with a grain size of ASTM 5-6 were produced and evaluated. The results of the evaluation indicated that improvements in creep strength were obtained. These improvements were evidenced by increases in the creep life average values and increases in the minus 3-sigma minimums for both 0.5 percent and 1.0 percent creep strain levels. The 1-sigma values determined for the ASTM 5-6 grain size sheets were approximately two-thirds as large as those obtained for the baseline sheets. The evaluation of tensile and stress rupture properties of the ASTM 5-6 thin gauge sheets revealed trends similar to those observed in the textured sheets. Tensile and stress rupture strengths were equivalent or superior to those of the baseline sheets, but elongation values obtained in tensile tests at 1144K (1600°F) and above and in stress rupture tests at 1089K/165.4 MPa (1500°F/24 ksi) were less than the baseline values. The ductilities observed were judged to be at acceptable levels, however.

To investigate the effect of thickness-to-grain diameter ratio, a sheet 0.76 mm (0.030-inch) thick having a grain size of ASTM 5-6 was produced and evaluated. Comparisons were made to the ASTM 5-6 thin gauge sheets as well as the baseline sheets. In addition, creep data generated on the initial grain size study sheets were re-analyzed in terms of thickness-to-grain diameter ratio. The results indicated no meaningful correlation between creep strength and thickness-to-grain diameter ratio. Instead, the observed creep lives appeared to be related to grain size alone.

Following completion of the TMP studies, samples from the various experimental sheets and the baseline sheets were subjected to 100 hours of dynamic oxidation at a temperature of 1366K (2000°F). The test was conducted in a flame tunnel type rig which provided a combustion gas velocity of Mach 0.3. Results of the test indicated that the TMP used in the experimental studies had no effects on the dynamic oxidation resistance of HAYNES alloy No. 188 sheet.

In a final brief study, the effects of prestrain on creep strength at a quality control test condition of 1200K/41.4 MPa (1700°F/6 ksi) were examined using one of the baseline heats of production thin gauge sheet. Significant improvements were found with prestrains of 4-10 percent. Above 10 percent prestrain, recrystallization occurred and creep properties were degraded. The improvements obtained with prestrain were not as great as those obtained in the textured sheets.

1.0 INTRODUCTION

This investigation was undertaken to seek improvements in the low strain (≤ 1 percent) creep strength of HAYNES alloy No. 188 thin gauge sheet by means of thermomechanical processing. The potential application for such an optimized form of this material would be as heat shields for advanced re-entry and/or hypersonic vehicles.

In the design of metallic heat shields for reusable thermal protection systems, plastic deformation due to creep is considered to be a significant factor (ref. 1). Attention in design has been focused on low values of creep strain due to deflection limit criteria. Optimization of heat shields for maximum reuse with minimum weight further requires the use of thin gauge sheet materials. Thus, the successful candidate material must possess the required low strain creep strength in thin gauge form.

HAYNES alloy No. 188, a cobalt-base sheet alloy developed by the Stellite Division of the Cabot Corporation, has shown promise for heat shield applications. Like most alloys, lower strengths than normal result when the material is produced in thin gauge form using standard commercial practices. The creep properties of HAYNES alloy No. 188 thin gauge sheet were not characterized in the initial development work. However, the reduced high temperature load-bearing capability of thin gauge sheet was indicated by the lower stress rupture properties obtained in sheet 0.25 mm to 0.48 mm (0.010-0.019 inch) thick as compared to sheet 0.76 to 2.0 mm (0.030-0.080 inch) thick (ref. 2). It was the objective of this program, therefore, to seek improvement of the low strain creep strength of thin gauge HAYNES alloy No. 188 sheet by modification of thermomechanical processing procedures.

To assist in the performance of the program, the Stellite Division of the Cabot Corporation established baseline data for three production heats of HAYNES alloy No. 188 sheet nominally 0.38 mm (0.015 inch) thick. This included tensile properties from room temperature to 1366K (2000°F), low strain (1 percent) creep properties in the temperature range of 922K (1200°F) to 1255K (1800°F), standard quality control stress rupture properties, and 1366K (2000°F)/100 hour dynamic oxidation behavior. In addition, the crystallographic textures and the microstructural characteristics of the baseline sheets were examined.

The experimental program was performed on sheet produced in the laboratory from standard production hot rolled plate sheet feedstock. All mechanical property testing was done by a single inhouse testing group to eliminate lab-to-lab testing variations. Improvements in the low strain creep strength of HAYNES alloy No. 188 sheet nominally 0.38 mm (0.015 inch) thick were sought using two different approaches. One concentrated on thermomechanical processing to optimize grain size. The second approach examined thermomechanical processing which was designed to promote high degrees of perferred orientation in recrystallized thin gauge sheet.

In both studies, initial experimental sheets were screened to optimize creep strength using the standard 1200K/41.4 MPa (1700°F/6 ksi) quality

control test condition. Extensive mechanical property evaluations were then carried out within each study on sheet from three different heats produced in accordance with the selected thermomechanical processing scheme. The effects of the two processing procedures on the microstructure and surface stability of HAYNES alloy No. 188 were also evaluated. Auxiliary studies were also performed to examine the effects of sheet thickness-to-grain diameter ratio and prestrain on low strain creep strength.

Certain commercial materials are identified in this paper in order to specify adequately which materials were investigated in the research effort. In no case does such identification imply recommendation or endorsement of the product by the National Aeronautics and Space Administration.

2.0 CABOT BASELINE DATA

2.1 Materials

For the purpose of developing baseline data, three lots of HAYNES alloy No. 188 sheet nominally 0.38 mm (0.015 inch) thick were obtained from three different Stellite Division heats. All lots of material were received in the mill annealed (bright annealed at 1450K (2150°F) followed by rapid cooling) and roller leveled condition. The heat chemistries of these materials are listed in Table I. A summary of thickness data obtained on the selected thin gauge sheet lots is presented in Table II.

The as-received microstructure of each heat was also examined using both optical and electron metallographic techniques. Micrographs of representative structures are presented in Figures 1-3. These figures illustrate the typical mill annealed microstructure consisting of an f.c.c. matrix containing a dispersion of M_6C type carbides. Grain sizes were found to be in the range of ASTM 6-6 1/2 by the comparative method. No discernible difference in grain size was noted in sections taken parallel or transverse to the rolling direction.

2.2 Texture

The three baseline heats were examined for the presence of preferred crystallographic texture in the plane of the sheet using the diffractometer reflection method. Samples were first sheared into approximate 25.4 mm (1 inch) squares and spot welded at the corners to slightly oversized plates of HAYNES alloy No. 188 having a thickness of 4.57 mm (0.180 inch). This procedure facilitated handling during preparation and ensured a flat surface during X-ray exposure. The surface of each specimen was prepared by hand polishing on 220 grit through 600 grit silicon carbide papers then electropolishing for 15 seconds in a solution composed of 10 percent H_2SO_4-90 percent methanol. The prepared sample was then placed in a Phillips-Norelco pole figure device and exposed to CoK_α radiation. During exposure, the device tilted and rotated the sample about the X-ray beam such that the resultant motion described a spiral in the plane of the stereographic projection. The maximum angle of tilt was limited to 55 degrees due to absorption of the beam by the sample. The diffracted X-ray intensities were monitored by a solid state scintillation counter and recorded on a strip chart. Integrated intensities were also determined at 12 second intervals and recorded on paper tape. Upon completion of the X-ray scan, the integrated intensities were read into a computer for analysis. The computer program employed (ref. 3) corrected the data for background and absorption, converted the corrected data into relative intensities on a scale from 1 to 9, and printed out the results in a rectangular array which placed each value in its correct angular location on the stereographic projection. Computer operations were also employed to take advantage of symmetry across the planes normal to the rolling and transverse directions.

The (111) pole figures determined for the baseline heats are presented in Figures 4-6. Based on the fact that the relative intensities did not cover

TABLE I

HEAT ANALYSES FOR BASELINE THIN GAUGE SHEETS

	Composition - Weight Percent		
Element	Heat 2-1604	Heat 3-1622	Heat 4-1671
Cr	22.14	22.43	22.66
W	14.02	14.11	13.76
Fe	1.67	1.10	1.34
C	0.09	0.09	0.10
Si	0.32	0.43	0.41
Co	38.14	39.40	37.52
Ni	22.29	22.23	22.66
Mn	0.72	0.72	0.71
P	0.011	0.010	0.010
S	0.005	0.005	0.006
La	0.06	0.034	0.045
B	0.001	0.008	0.003

TABLE II

THICKNESS DATA FOR BASELINE THIN GAUGE SHEETS

Heat No.	Thickness Range mm	Thickness Range (inch)	Average Thickness mm	Average Thickness (inch)	Standard Deviation mm	Standard Deviation (inch)
2-1604	.3810-.4572	(.0150-.0180)	.3988	(.0157)	.0203	(.0008)
3-1622	.4445-.4699	(.0175-.0185)	.4547	(.0179)	.0051	(.0002)
4-1671	.3810-.4318	(.0150-.0170)	.3912	(.0154)	.0127	(.0005)

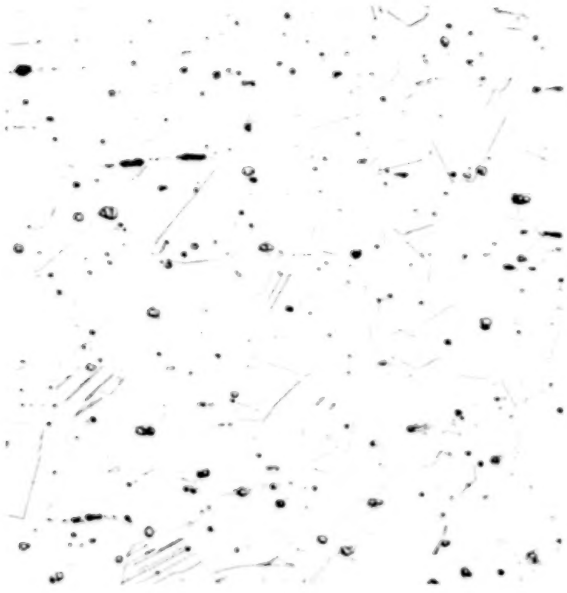

(a) Optical Micrograph. X300.

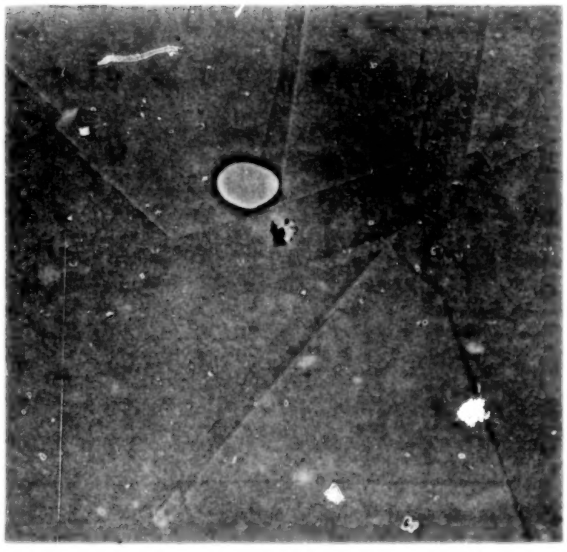

(b) Electron Micrograph of Replica. X3000.

Figure 1: Microstructure of Baseline Heat 2-1604, Grain Size ASTM 6.

(a) Optical Micrograph. X300.

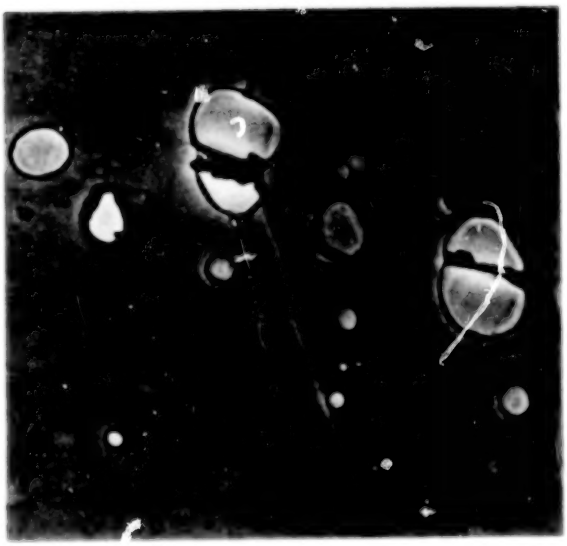

(b) Electron Micrograph of Replica. X3000.

Figure 2: Microstructure of Baseline Heat 3-1622, Grain Size ASTM 6.

(a) Optical Micrograph. X300.

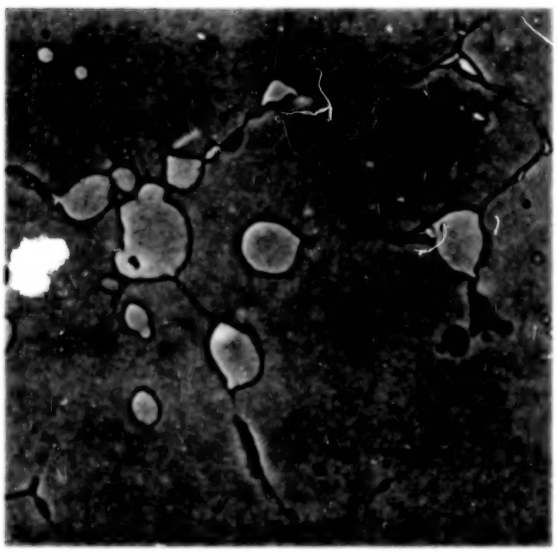

(b) Electron Micrograph of Replica. X3000.

Figure 3: Microstructure of Baseline Heat 4-1671, Grain Size ASTM 6-1/2.

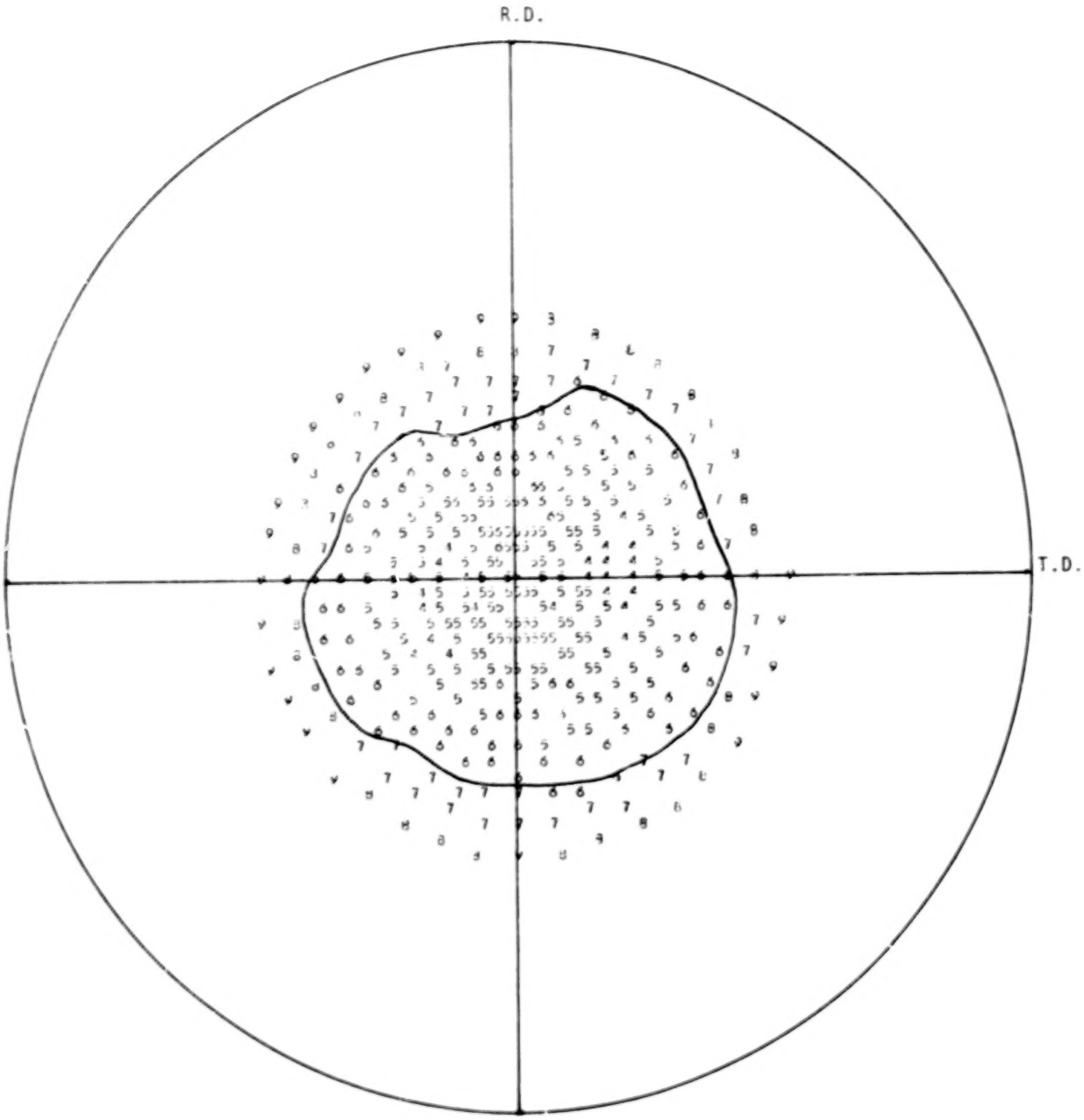

Figure 4: (111) pole figure for Heat 2-1604

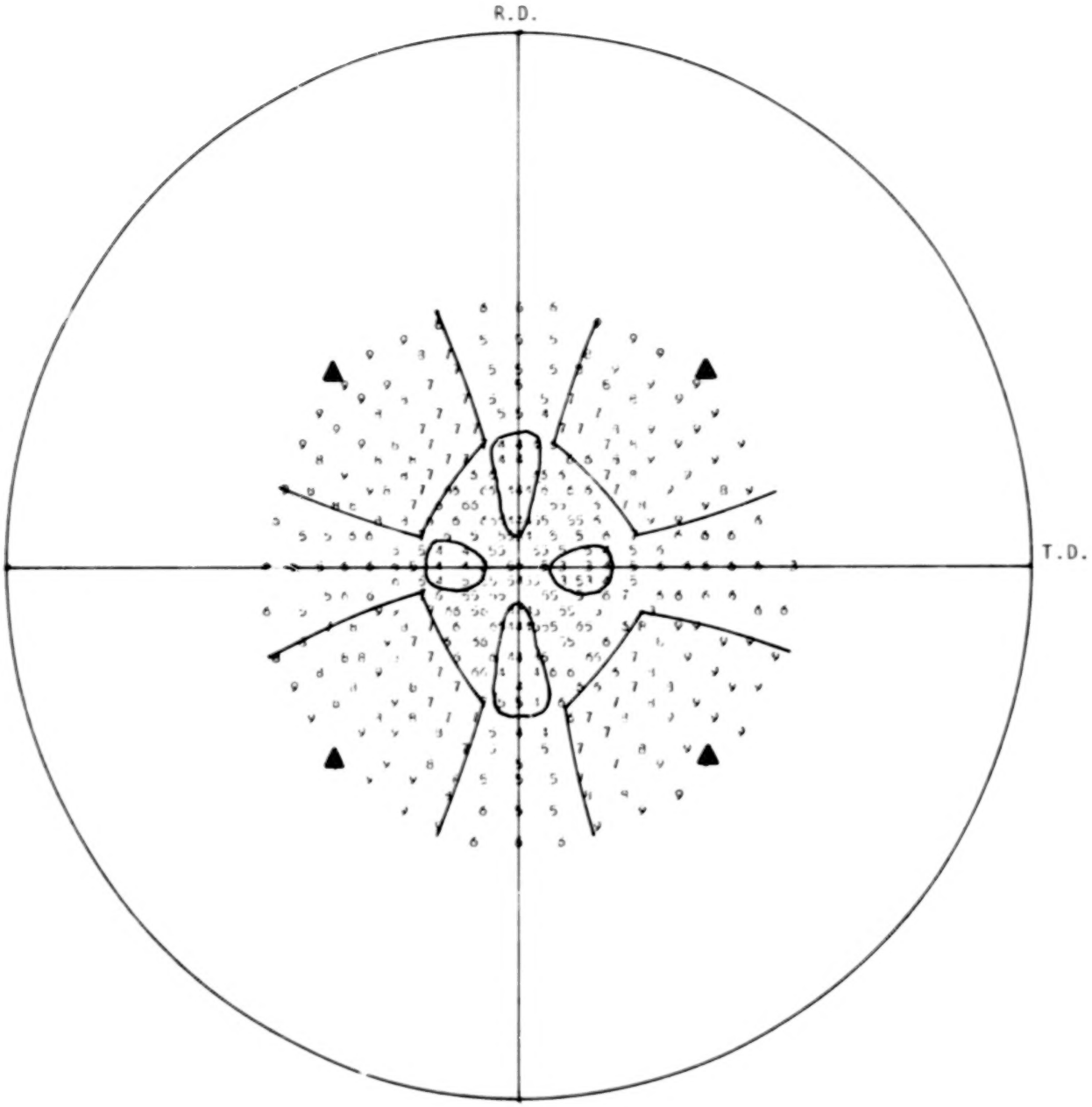

Figure 5: (111) pole figure for Heat 3-1622

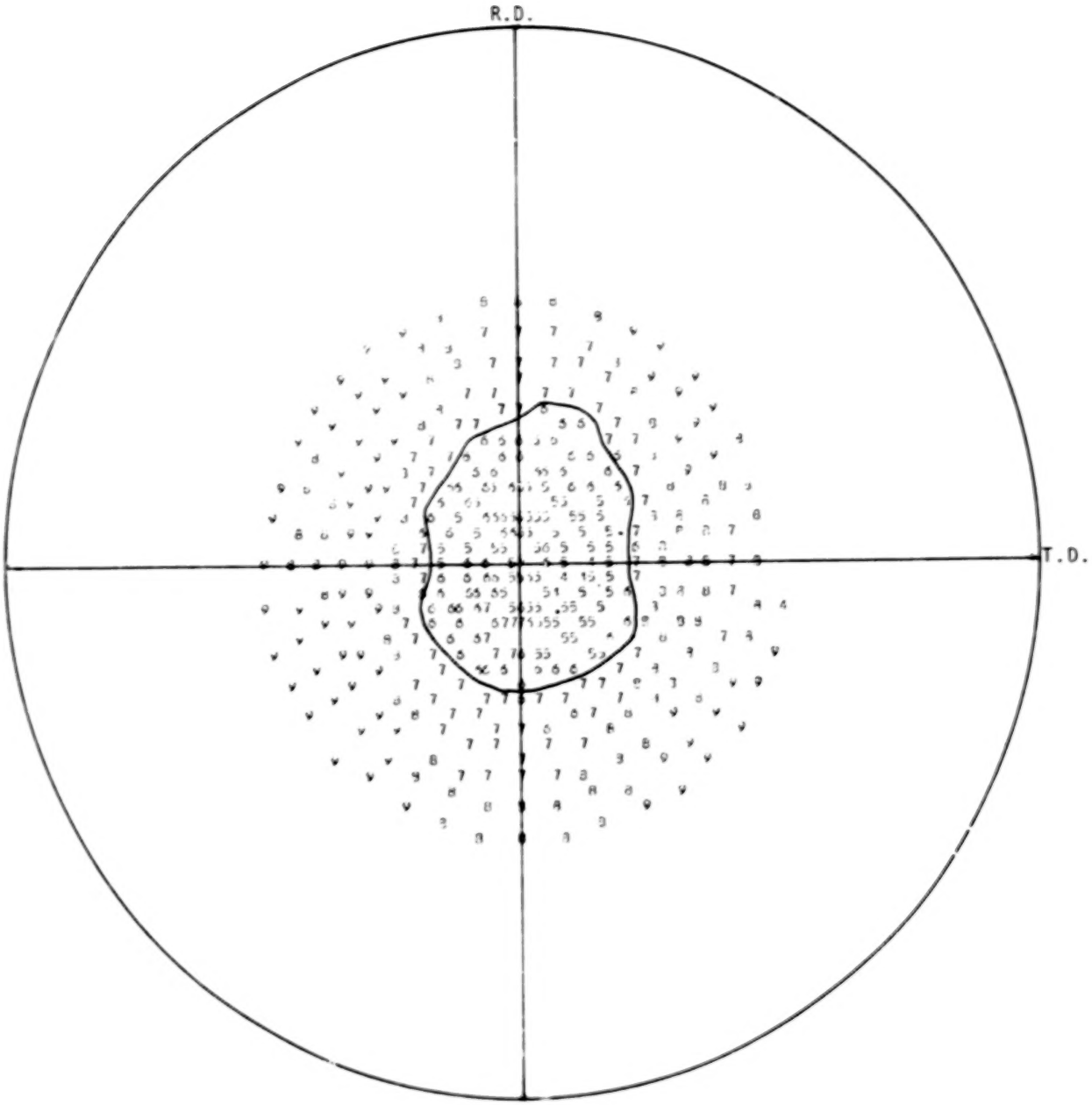

Figure 6: (111) pole figure for Heat 4-1671

the full range of 1-9, it can be stated that none of the observed textures were highly developed. That is, the intensity levels observed were not very much above the background levels. The strip chart recordings for each heat substantiated this conclusion. Scan recordings over angular regions of high relative intensity were jagged and not much above background levels which is indicative of a texture which is not highly developed.

Based on the form of the pole figures and the strip chart recordings, the ranking of the heats in the order of increasing texture development was 4-1671, 2-1604, and 3-1622. The pole figures for Heats 4-1671 and 2-1604 were not of a form that could be described in terms of simple crystal indices. However, Heat 3-1622 appeared to have a weakly defined cube texture. The locations of the four (111) poles have been indicated in Figure 5 with closed triangular symbols for a perfectly aligned cube texture. It can be seen that they lie in the regions of high relative intensities. However, the angular spread of these areas and the background levels which were still relatively strong indicate that the texture was not highly developed.

2.3 Tensile Properties

Duplicate longitudinal and transverse specimens from each heat were tensile tested in air at room temperature, 922K (1200°F), 1033K (1400°F), 1144K (1600°F), 1255K (1800°F) and 1366K (2000°F). The specimen configuration employed for these tests was the same as that illustrated in Appendix B. In addition, tabs were spot welded to the grip ends of each sample to prevent distortion from occurring around the pinning holes during testing. For elevated temperature tests, a radiant furnace equipped with quartz infrared lamps was used to maintain the temperature within ± 3K (± 5°F) of the desired test temperature. Two chromel-alumel thermocouples were wired to the center of the specimen gage length. One was used for control of the furnace while the other served as a means to independently monitor the sample temperature. Each specimen was allowed to soak at the test temperature for at least ten minutes before testing began. Crosshead speeds employed were 1.27 mm/min (0.05 in/min) through .2 percent yield strain then 12.7 mm/min (0.5 in/min) to failure. For the determination of 0.2 percent yield strengths in room temperature tests, strain was measured using a clip-on type extensometer with a 25.4 mm (1-inch) gage length. The maximum strain error of the extensometer was 0.00012 (Class B2). In elevated temperature tests, a rigid frame extensometer of the same type as that described in Appendix B was used. Strain was measured by a linear variable differential transformer which was an integral component of the extensometer. The maximum strain error of the LVDT measuring system was 0.0001 (Class B1). The results obtained from the tensile tests are listed in Table III. Within each heat, no major differences in properties were observed with respect to sample orientation. A summary of the overall average tensile properties at each test temperature is given in Table IV.

TABLE III

TENSILE PROPERTIES FOR BASELINE THIN GAUGE SHEETS

Test Temp.	Orient.	Heat 2-1604 0.2% YS MPa	Heat 2-1604 0.2% YS (ksi)	Heat 2-1604 UTS MPa	Heat 2-1604 UTS (ksi)	Heat 2-1604 El %	Heat 3-1622 0.2% YS MPa	Heat 3-1622 0.2% YS (ksi)	Heat 3-1622 UTS MPa	Heat 3-1622 UTS (ksi)	Heat 3-1622 El %	Heat 4-1671 0.2% YS MPa	Heat 4-1671 0.2% YS (ksi)	Heat 4-1671 UTS MPa	Heat 4-1671 UTS (ksi)	Heat 4-1671 El %
RT	L	505.0	(73.3)	988.7	(143.5)	66.3	548.4	(79.6)	1019.7	(148.0)	57.7	478.9	(69.5)	999.1	(145.0)	63.6
	L	510.6	(74.1)	1003.9	(145.7)	63.3	557.4	(80.9)	1017.0	(147.6)	58.0	480.2	(69.7)	999.7	(145.1)	62.7
	T	485.1	(70.4)	966.7	(140.3)	62.7	525.7	(76.3)	1017.7	(147.7)	59.5	485.1	(70.4)	1014.2	(147.2)	61.4
	T	489.2	(71.0)	995.6	(144.5)	66.1	536.0	(77.8)	1012.8	(147.0)	57.1	480.9	(69.8)	1010.8	(146.7)	61.5
922 K (1200°F)	L	292.8	(42.5)	675.2	(98.0)	65.4	347.3	(50.4)	773.8	(112.3)	64.0	298.3	(43.3)	737.9	(107.1)	63.3
	L	292.8	(42.5)	658.0	(95.5)	68.2	349.3	(50.7)	768.2	(111.5)	58.0	285.9	(41.5)	659.4	(95.7)	55.4
	T	294.9	(42.8)	663.5	(96.3)	59.9	333.5	(48.4)	763.4	(110.8)	62.0	294.9	(42.8)	731.0	(106.1)	60.8
	T	303.9	(44.1)	674.5	(97.9)	62.1	347.3	(50.4)	771.0	(111.9)	60.0	299.0	(43.4)	727.6	(105.6)	59.3
1033 K (1400°F)	L	259.8	(37.7)	557.4	(80.9)	40.4	316.9	(46.0)	627.0	(91.0)	56.8	292.1	(42.4)	585.7	(85.0)	50.8
	L	258.4	(37.5)	532.6	(77.3)	31.1	315.6	(45.8)	667.6	(96.9)	64.4	272.8	(39.6)	565.7	(82.1)	48.8
	T	255.6	(37.1)	547.1	(79.4)	35.1	305.9	(44.4)	623.6	(90.5)	63.6	280.4	(40.7)	598.7	(86.9)	49.5
	T	250.8	(36.4)	520.9	(75.6)	34.8	303.2	(44.0)	588.4	(85.4)	52.5	299.7	(43.5)	647.0	(93.9)	51.2
1144 K (1600°F)	L	244.6	(35.5)	425.8	(61.8)	49.1	272.8	(39.6)	390.7	(56.7)	56.5	273.5	(39.7)	439.6	(63.8)	44.5
	L	224.6	(32.6)	313.5	(45.5)	38.4	281.1	(40.8)	432.0	(62.7)	65.8	267.3	(38.8)	411.3	(59.7)	34.6
	T	237.0	(34.4)	382.4	(55.5)	48.0	268.7	(39.0)	367.2	(53.3)	53.3	257.0	(37.3)	407.9	(59.2)	43.5
	T	237.0	(34.4)	412.0	(59.8)	42.0	283.9	(41.2)	416.2	(60.4)	52.4	213.6	(31.0)	293.5	(42.6)	43.7
1255 K (1800°F)	L	162.6	(23.6)	243.9	(35.4)	44.4	156.4	(22.7)	247.4	(35.9)	49.3	166.1	(24.1)	241.2	(35.0)	35.9
	L	193.6	(28.1)	288.0	(41.8)	44.2	159.9	(23.2)	250.8	(36.4)	45.1	162.6	(23.6)	242.5	(35.2)	30.9
	T	159.9	(23.2)	244.6	(35.5)	33.6	175.7	(25.5)	259.1	(37.6)	58.0	173.6	(25.2)	247.4	(35.9)	33.2
	T	181.2	(26.3)	248.0	(36.0)	33.8	163.3	(23.7)	241.8	(35.1)	50.7	176.4	(25.6)	251.5	(36.5)	31.9
1366 K (2000°F)	L	62.7	(9.1)	127.5	(18.5)	24.4	72.4	(10.5)	139.2	(20.2)	33.0	87.5	(12.7)	118.5	(17.2)	23.3
	L	73.7	(10.7)	118.5	(17.2)	24.0	75.8	(11.0)	148.1	(21.5)	32.7	84.1	(12.2)	143.3	(20.8)	29.6
	T	58.6	(8.5)	126.8	(18.4)	20.2	85.4	(12.4)	135.0	(19.6)	29.5	77.2	(11.2)	121.3	(17.6)	23.9
	T	47.5	(6.9)	86.1	(12.5)	17.8	85.4	(12.4)	135.0	(19.6)	34.0	82.0	(11.9)	126.8	(18.4)	19.5

15

15

TABLE IV

AVERAGE BASELINE TENSILE PROPERTIES FOR THREE PRODUCTION HEATS OF "HAYNES" ALLOY NO. 188 THIN GAUGE SHEET*

Test Temp.	0.2% Y.S. MPa	0.2% Y.S. (ksi)	UTS MPa	UTS (ksi)	Elong. %
RT	507.1 (28.3)	73.6 (4.1)	1003.9 (15.2)	145.7 (2.2)	61.7 (3.1)
922 K (1200°F)	311.4 (24.8)	45.2 (3.6)	717.3 (47.5)	104.1 (6.9)	61.5 (3.4)
1033 K (1400°F	284.6 (24.1)	41.3 (3.5)	588.4 (46.2)	85.4 (6.7)	48.3 (10.9)
1144 K (1600°F)	254.9 (23.4)	37.0 (3.4)	391.4 (46.2)	56.8 (6.7)	47.7 (8.5)
1255 K (1800°F)	169.5 (11.0)	24.6 (1.6)	250.8 (13.1)	36.4 (1.9)	40.8 (9.0)
1366 K (2000°F)	74.4 (12.4)	10.8 (1.8)	127.5 (15.9)	18.5 (2.3)	26.0 (5.6)

* Average of twelve tests. Standard deviations are given in parenthesis.

2.4 Stress Rupture Properties

Duplicate longitudinal and transverse specimens from each heat were stress rupture tested at 1089K/165.5 MPa (1500°F/24 ksi) and 1311K/31 MPa (1900°F/4.5 ksi) which are standard quality control conditions. The specimen configuration was the same as that illustrated in Appendix B. The results are summarized in Table V. Normal heat to heat variations are apparent. The only significant variation with respect to test direction occurred in the 1089K/165.5 MPa stress rupture lives for Heat 3-1622. The values obtained for the transverse direction were slightly higher than those for the longitudinal direction. Average property values based on the log transformation are also given in the table.

2.5 Creep Properties

2.5.1 Creep life evaluation. - All creep testing was performed using the procedure described in Appendix B. Each of the baseline heats was initially tested in the transverse direction in duplicate under the standard quality control condition of 1200K/41.4 MPa (1700°F/6,000 psi). In order to develop an adequate description of baseline creep strength, further tests were conducted on each heat at temperatures of 922K (1200°F), 1033K (1400°F), 1144K (1600°F) and 1255K (1800°F) and at a minimum of five stress levels at each temperature. Among the five tests at each temperature, three tests were conducted with longitudinally oriented specimens and two with transverse oriented specimens with respect to the rolling direction.

Originally, it was planned to select stresses to give 1 percent creep lives in the range of roughly 25-500 hours. The initial stress levels were selected on the basis of previous studies performed by Stellite Division on HAYNES alloy No. 188 sheet >0.76 mm (0.030 inch) thick. From these results, additional stresses were selected so as to obtain a broad description of the low strain creep behavior over the temperature range of interest. In accomplishing this, some stresses were selected which gave 1 percent creep lives outside of the originally planned 25-500 hour range. A complete listing of the creep test results is given in Appendix C.

In order to characterize the creep strength of the baseline thin gauge sheets over the range of test conditions, the 0.5 percent and 1.0 percent creep strain data were subjected to a least squares optimization of the Larson-Miller parameter equation in the following form (ref. 4):

$$\log t = C_1 + \frac{C_2}{T} + \frac{C_3}{T} \log s + \frac{C_4}{T} (\log s)^2$$

where T = absolute temperature (K or °R)

t = time to given creep strain, hours

s = stress (MPa or ksi)

TABLE V

SUMMARY OF BASELINE STRESS RUPTURE DATA FOR "HAYNES" ALLOY NO. 188 THIN GAUGE SHEET

Heat No.	Sample Orientation	1089 K/165.5 MPa (1500°F/24,000 psi) Life, Hours	1089 K/165.5 MPa (1500°F/24,000 psi) Elong. %	1311 K/31 MPa (1900°F/4,500 psi) Life, Hours	1311 K/31 MPa (1900°F/4,500 psi) Elong. %
2-1604	L	41.0	38.2	26.8	39.5
	L	32.6	29.0	21.8	16.8
	T	36.9	32.7	25.3	24.4
	T	27.9	21.1	23.3	27.6
3-1622	L	77.9	52.1	19.8	25.5
	L	77.2	44.9	21.7	37.2
	T	97.8	46.8	18.9	19.6
	T	94.1	48.7	20.0	24.0
4-1671	L	25.3	42.0	12.0	33.5
	L	38.2	44.0	12.7	38.8
	T	26.4	44.3	15.1	29.2
	T	37.7	Void*	11.0	35.9
Log Average Values**		45.2	39.2	18.3	28.4
Standard Deviation, Log Units***		(.219)	(.116)	(.130)	(.120)

---

* Multiple Fracture

** mean $(\bar{X})$ = antilog $\left(\frac{\Sigma \log X_i}{n}\right)$

*** standard deviation = $\left(\frac{\Sigma (\log X_i - \log \bar{X})^2}{n - 1}\right)^{1/2}$

where, X_i = observed data value

n = number of data points

C_1 = optimized Larson-Miller constant

C_2, C_3, C_4 = optimized constants

Results of the analyses are summarized in Table VI. Plots of the actual data and the lines given by the parameter equation are presented in Figures 7-8. The fit of the data to the parameter equation was reasonably good with correlation coefficients of .884 and .903 for the 0.5 percent and 1.0 percent creep strain data, respectively. To obtain a better appreciation of the fit provided by the parameter equation to the data at individual test temperatures, two approaches were taken. In one case, root mean square (RMS) errors were computed at each temperature using the logarithmic creep life values predicted by the Larson-Miller parameter analysis and those of the actual data. In the second case, root mean square (RMS) errors at the individual test temperatures were obtained by fitting the creep data to an equation in the form of

$$\log t = B_1 + B_2 \log s + B_3(\log s)^2$$

where t and s have the meanings previously given, and B_1, B_2, and B_3 are optimized constants. The root mean square (RMS) error was selected as the means of comparing the data correlations since it includes both random error and functional bias. Results of these analyses are presented in Tables VII and VIII.

From the information contained in Table VII, it is clear that the optimized Larson-Miller parameter analysis fits the data at each temperature differently. One might suspect this from inspection of the plots shown in Figures 7 and 8. Of particular note are the lower RMS values obtained for the 922K (1200°F) test temperature in comparison to those obtained in the overall analysis listed in Table VI. For the other temperatures, the RMS values of Table VII were higher than the overall RMS values, but the differences were not found to be very great. In summary, the Larson-Miller parameter analysis provided a variable fit for the data at individual temperatures. Its overall estimate of error exaggerated the fit of the data at the 922K (1200°F) test temperature, but was fairly representative of the fits obtained for data at the other temperatures.

The comparison of the optimized Larson-Miller parameter analysis isolated at individual temperatures to separate analyses of individual test temperature data is provided by Tables VII and VIII. Although a better fit was always obtained through separate analysis of the data at individual temperatures, the differences between RMS values were, for the most part, not very great. Exceptions to this occurred for the 0.5 percent creep strain data at 922K (1200°F) and the 1.0 percent creep strain data at 1144K (1600°F) in which cases the RMS values of the Larson-Miller parameter analysis were approximately 25 percent higher.

In addition to the description of the baseline creep properties through the optimized larson-Miller parameter equation, there was a need to present the data in a form which would facilitate comparison to the creep properties of experimental sheets produced in subsequent portions of the program. Since each data set would probably have a different Larson-Miller constant, compari-

TABLE VI

OPTIMIZED LARSON-MILLER PARAMETER ANALYSIS OF
BASELINE THIN GAUGE SHEETS

Regression equation: $Y = \log t = C_1 + \frac{C_2}{T} + \frac{C_3}{T} \log S + \frac{C_4}{T} (\log S)^2$

A. where T = absolute temperature, Kelvin
t = time to given creep strain, hours
S = stress, MPa

Creep Strain	Equation Parameters				Fit of test data: Std. error of Estimate, log units	Correlation Coefficient	Number of Tests	RMS*
	C_1	C_2	C_3	C_4				
0.5%	15.3550	26315.4	-3619.76	-281.34	.371	.884	74	.361
1.0%	16.1772	27446.9	-2966.27	-549.79	.356	.903	74	.347

B. where T = absolute temperature, degrees Rankine
t = time to given creep strain, hours
S = stress, ksi

0.5%	15.3550	41548.3	-7364.84	-506.41	.371	.884	74	.361
1.0%	16.1772	44231.4	-6998.92	-989.62	.356	.903	74	.347

* Root Mean Square (RMS) $= \left(\frac{\Sigma (\log t_i - \log t_{i_p})^2}{n} \right)^{1/2}$, where $\log t_i$ = observed log time to given creep strain

$\log t_{i_p}$ = predicted log time to given creep strain

n = number of observations in data set

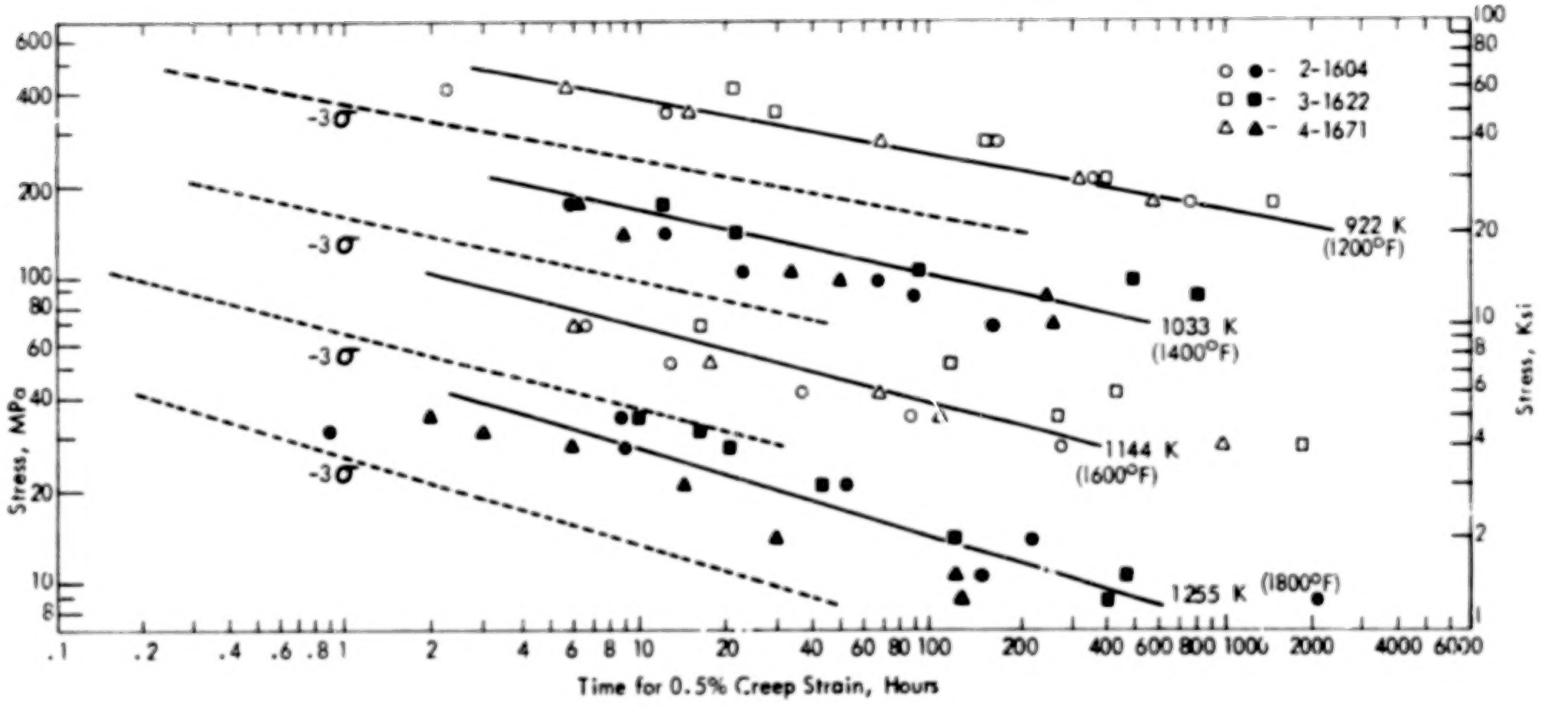

Figure 7: Stress vs. 0.5% Creep Life for HAYNES alloy No. 188 Baseline Sheets (Actual Data and Parametric Evaluation)

21

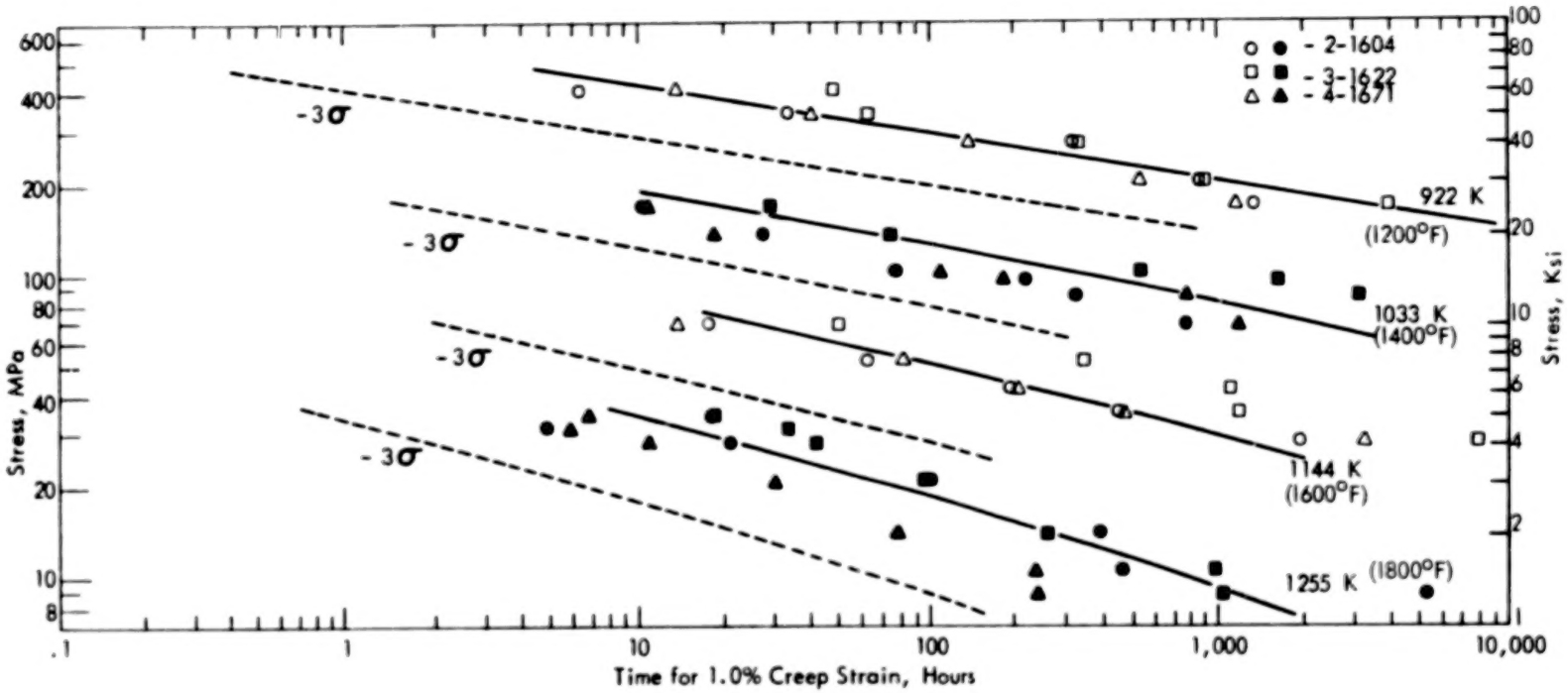

Figure 8: Stress vs. 1.0% Creep Life for HAYNES alloy No. 188 Baseline Sheets (Actual Data and Parametric Evaluation).

TABLE VII

COMPARISON OF PREDICTIONS OF LARSON-MILLER PARAMETER ANALYSIS TO ACTUAL DATA AT INDIVIDUAL TEST TEMPERAUTRES

Temp	RMS* Values for Given Creep Strain Data 0.5%	1.0%
922 K (1200°F)	.293	.257
1033 K (1400°F)	.370	.380
1144 K (1600°F)	.377	.369
1255 K (1800°F)	.383	.358

* Root Mean Square (RMS) = $\left(\frac{\Sigma (\log t_i - \log t_{i_p})^2}{n}\right)^{1/2}$

where $\log t_i$ = observed log time to given creep strain

$\log t_{i_p}$ = predicted log time to given creep strain

n = number of observations in data set

TABLE VIII

FIT OF BASELINE THIN GAUGE SHEET CREEP DATA AT INDIVIDUAL TEST TEMPERATURES*

Temp	RMS Values for Given Creep Strain Data 0.5%	1.0%
922 K (1200°F)	.234	.229
1033 K (1400°F)	.339	.355
1144 K (1600°F)	.353	.288
1255 K (1800°F)	.381	.338

* Equation Form: $\log t = B_1 + B_2 \log S + B_3 (\log S)^2$

sons of creep properties using combined plots of log-stress versus Larson-Miller parameter would require a nomographic tool. Therefore, in an effort to develop a unified presentation of the data for the purpose of direct comparison, the baseline creep data was force-fit using a value of 17 for the Larson-Miller constant. The choice of C_1 = 17 was based on the average of the values obtained from the analyses of 0.5 percent creep strain results for the baseline and for experimental sheets described in later sections of this report. Results of previous work at Stellite Division on HAYNES alloy No. 188 sheet 0.76-2.29 mm (0.030-0.090 inch) thick also indicated that the optimized Larson-Miller constant was close to a value of 17.

Results of the force-fit analyses for the baseline data are presented in Table IX. Graphical presentations of the analyses are also given in Figures 9 and 10. The data correlations of the force-fit approach were equivalent to those of the optimized Larson-Miller parameter analysis judging from the RMS values obtained, and the figures provide a basis for clear comparisons to subsequent data sets.

2.5.2 Minimum Creep Rate Evaluation. - Minimum creep rate data determined at each test temperature were subjected to multiple regression analyses to obtain fits to the two well known phenomenological equations:

$$\log \dot{\epsilon}_{min} = \log A + n \log s \quad (1)$$

$$\text{and } \log \dot{\epsilon}_{min} = \log A' + \beta s \quad (2)$$

where $\dot{\epsilon}_{min}$ = minimum creep rate, percent/hour

s = stress (MPa or ksi)

n = stress exponent

A, A', β = constants

Results of these analyses are summarized in Tables X and XI. Essentially equivalent fits of the data were obtained with either equation form. According to Garofalo (ref. 5), minimum creep rates should conform to a single stress function given by

$$\log \dot{\epsilon}_{min} = \log A'' + n \log (\sinh \alpha s) \quad (3)$$

where A'' and α are constants at a constant temperature. For values of $\alpha s < .8$, equation (3) reduced to the form given by equation (1) and $A'' \alpha^n = A$. For values of $\alpha s > 1.2$, equation (3) reduced to the form given by equation (2) from which it can be determined that $A''/2^n = A'$ and $n\alpha = \beta$. In order to evaluate α, results at both low and high stresses are required. In the present case, it appears that neither inequality for αs has been entirely fulfilled, and within the range of stresses employed at each temperature, the overlap is sufficient to provide a reasonable fit by either function.

TABLE IX

FORCE-FIT OF BASELINE CREEP DATA TO THE LARSON-MILLER PARAMETER EQUATION WITH A LARSON-MILLER CONSTANT OF 17

Regression Equation: $P = T (\log t + 17) = C_2 + C_3 \log S + C_4 (\log S)^2$

A. Where T = absolute temperature, Kelvin
t = time to given creep strain, hours
S = stress, MPa

	Equation Parameters			Fit of Test Data			
Strain	C_2	C_3	C_4	Std. Error of Estimate, LM Parameter Units	Correlation Coefficient	Number of Tests	RMS
0.5%	28429.1	-3489.62	-435.01	424.72	.984	74	.367
1.0%	28321.0	-2690.88	-683.38	400.82	.986	74	.349

B. Where T = absolute temperature, degrees Rankine
t = time to given creep strain, hours
s = stress, ksi

0.5%	45354.8	-7594.46	-783.01	764.50	.984	74	.367
1.0%	46051.4	-6906.48	-1230.08	721.47	.986	74	.349

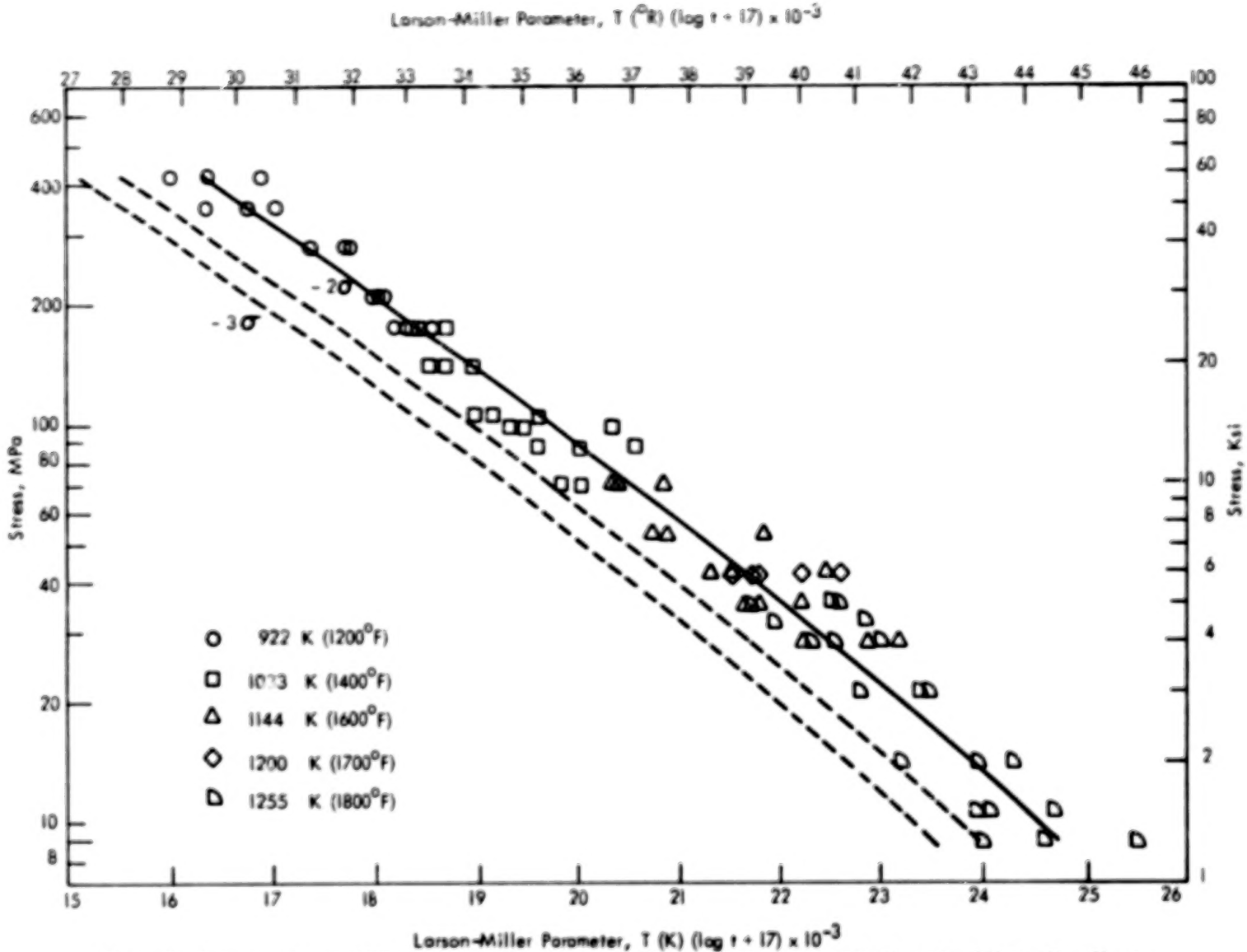

Figure 9: Stress vs. Larson-Miller Parameter (C_1 = 17) for 0.5% Creep Life of HAYNES alloy No. 188 Baseline Sheets

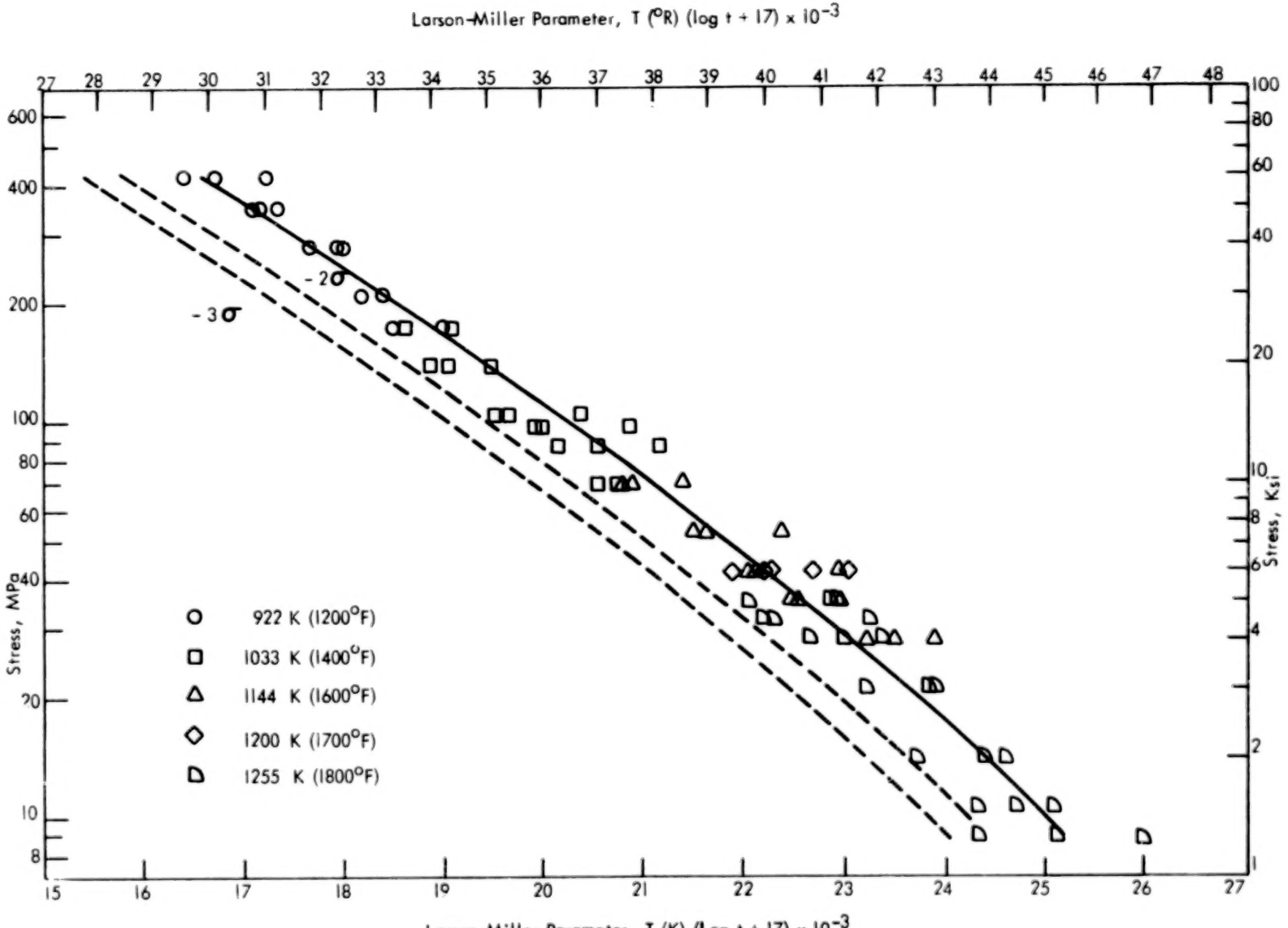

Figure 10: Stress vs. Larson-Miller Parameter (C_l = 17) for 1.0% Creep Life of HAYNES alloy No. 188 Baseline Sheets.

TABLE X

ANALYSIS OF BASELINE MINIMUM CREEP RATES AS A POWER FUNCTION OF STRESS*

Temp.	log A		n	Std. Error of Estimate, Log Units,	Correlation Coefficient
	Stress as MPa	Stress as ksi			
922 K (1200°F)	-15.734	(-11.127)	5.49	.262	.953
1033 K (1400°F)	-13.748	(-9.130)	5.51	.472	.893
1144 K (1600°F)	-12.659	(-7.564)	6.08	.265	.975
1255 K (1800°F)	-6.608	(-3.569)	3.62	.358	.921

---

* $\log \dot{\epsilon}_{min} = \log A + n \log S$

$\dot{\epsilon}_{min}$ = minimum creep rate, %/hr

S = stress (MPa or ksi)

A,n = constants estimated by method of least squares

TABLE XI

ANALYSIS OF BASELINE MINIMUM CREEP RATES AS AN EXPONENTIAL FUNCTION OF STRESS*

Temp	log A′	β		Std. Error of Estimate, Log Units,	Correlation Coefficient
		Stress as MPa	Stress as ksi		
922 K (1200°F)	-4.846	.0087	(.0600)	.253	.956
1033 K (1400°F)	-4.956	.0210	(.144)	.430	.912
1144 K (1600°F)	-5.388	.0571	(.394)	.267	.974
1255 K (1800°F)	-3.766	.0837	(.577)	.364	.918

$\log \dot{\epsilon}_{min} = \log A' + \beta S$

$\dot{\epsilon}_{min}$ = minimum creep rate, %/hr

S = stress (MPa or ksi)

A′, β = constants estimated by method of least squares

Since the stress exponent, n, is fundamentally important to the description of creep rate phenomena, it was considered more useful to portray the minimum creep rates as a power function of stress. Plots of the data in this form are presented in Figure 11. As the figure and the data in Table X indicate, the slopes of the lines are approximately constant in the 922K (1200°F) - 1144K (1600°F) temperature range with n = 5.5-6. At the 1255K (1800°F) test temperature, and from Table X, a value of approximately 3.6 is indicated for the stress exponent. The data of Table X indicate that a large reduction in A, the so-called structure factor, also occurred between the 1144K (1600°F) and 1255K (1800°F) test temperatures.

These differences, which imply a change in the creep kinetics, are most likely attributable to changes in the precipitation characteristics known to occur in HAYNES alloy No. 188 at those temperatures (ref. 2 and 6). That is, at 1255K (1800°F) the microstructure contains large M_6C carbides distributed randomly and relatively coarse secondary M_6C carbides precipitated at grain boundaries. At 1144K (1600°F), in addition to the large random primary M_6C carbides, fine secondary M_6C and $M_{23}C_6$ carbides are found distributed along twin and grain boundaries.

2.6 Static Oxidation Resistance

Triplicate samples of each baseline sheet lot were subjected to 300 hours of static oxidation testing at a temperature of 1422K (2100°F). The samples measured 19.05 mm x 19.05 mm (3/4 inch x 3/4 inch), and they had a 4.76 mm (3/16 inch) diameter hole located at mid-width and 6.35 (1/4 inch) from the top edge for suspension on the test rack. Testing was carried out in the constant temperature zone of a tube furnace. An air flow of 0.2 m^3/hour (7 ft^3/hour) was maintained through the furnace to ensure a constant supply of oxygen to the samples. Every 25 hours the samples were cooled to a temperature of 422K (300°F) or less and rotated to an adjacent peg such that the surface facing the rack faced away. After testing, the oxidized samples were chemically descaled and weighed. The metal loss per side was then computed from the recorded weight change. One of the samples from each heat was also sectioned 3.18 mm (1/8 inch) from the bottom edge and prepared for metallographic examination.

The parameters measured by this procedure are schematically illustrated in Figure 12. The test results obtained for the three baseline heats are summarized in Table XII. Heat-to-heat differences are apparent from the metal loss data. However, in consideration of the test duration, these differences are not very large. The oxidation penetration data, which are more reliable for evaluating oxidation resistance, indicate that the differences between the three heats are minor.

2.7 Dynamic Oxidation Resistance

Triplicate samples of each baseline heat were subjected to dynamic oxidation testing for 100 hours at a temperature of 1366K (2000°F). The test was

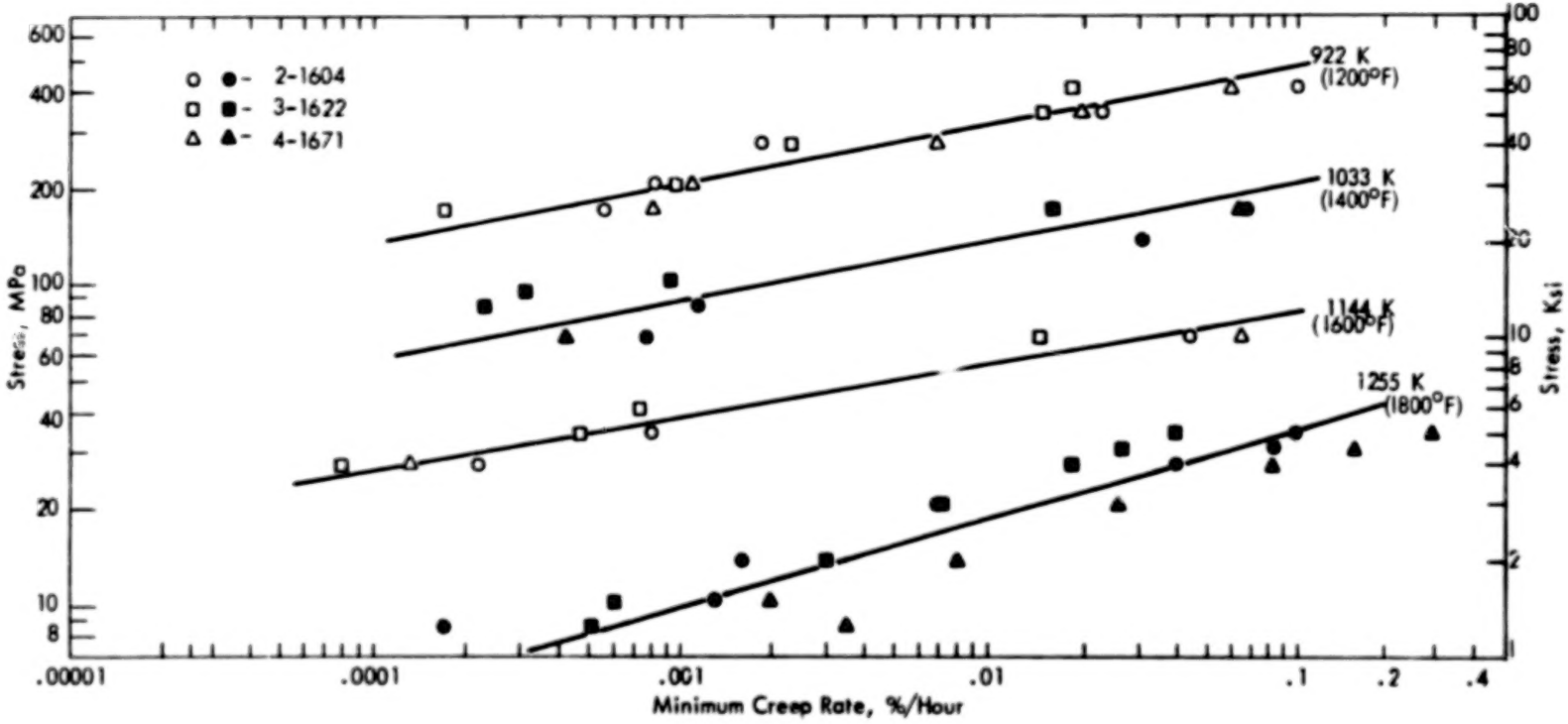

Figure 11: Stress vs. Minimum Creep Rate for HAYNES alloy No. 188 Baseline Sheets.

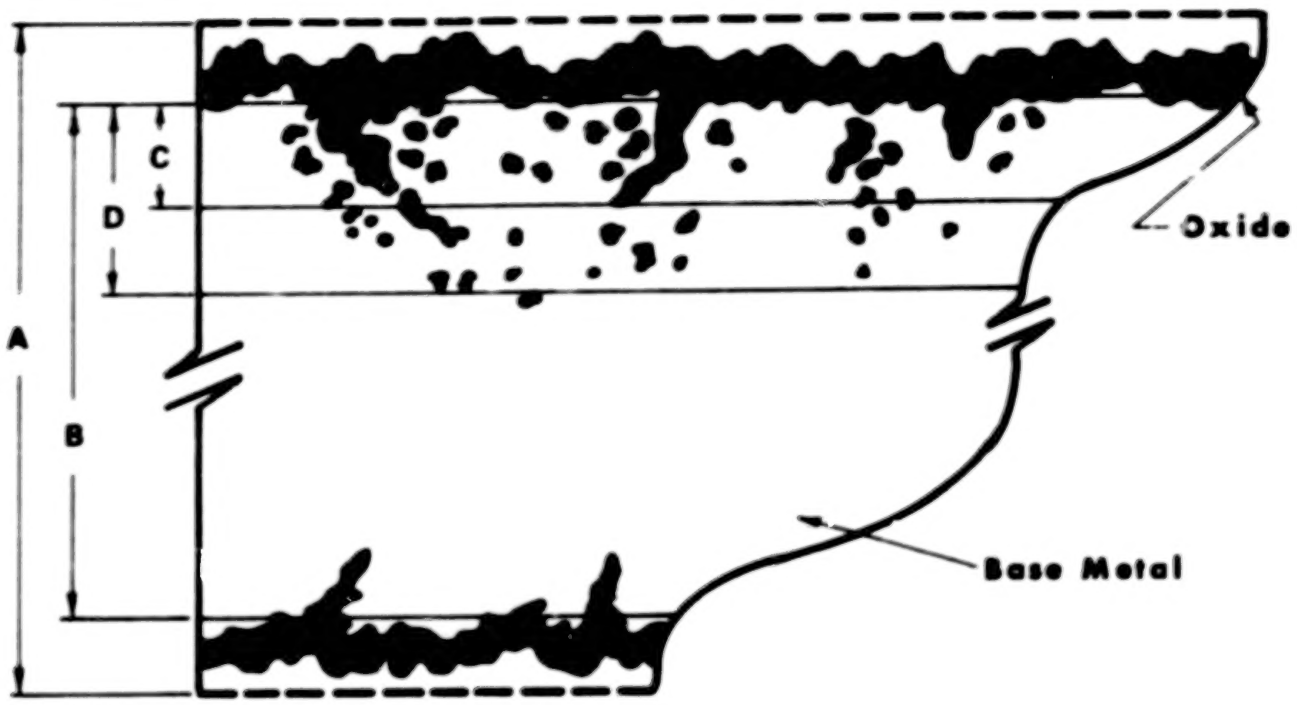

1. Metal Loss, $\left[(A-B)/2\right]$

2. Continuous Penetration, $\left[C\right]$

3. Maximum Penetration, $\left[D\right]$

4. Total Metal Affected, $\left[((A-B)/2) + D\right]$

Figure 12: Schematic of Metallographic Measurement Technique

TABLE XII

1422 K (2100°F)/300 HOUR STATIC OXIDATION DATA FOR
"HAYNES" ALLOY NO. 188 BASELINE THIN GAUGE SHEETS

Heat No.	Metal Loss mm/side	Metal Loss (mils/side)	Continuous Penetration mm/side	Continuous Penetration (mils/side)	Maximum Penetration um/side	Maximum Penetration (mils/side	Total Affected Metal mm/side	Total Affected Metal (mils/side)
2-1604	.01939	(.7634)	.0102	(.4)	.0406	(1.6)	.0610	(2.4)
	.01971	(.7761)						
	.02026	(.7975)						
3-1622	.01465	(.5768)	.0076	(.3)	.0457	(1.8)	.0610	(2.4)
	.01466	(.5873)						
	.01546	(.6085)						
4-1671	.01118	(.4402)	.0102	(.4)	.0533	(2.1)	.0635	(2.5)
	.01223	(.4814)						
	.01087	(.4279)						
Average	.01541	(.6066)	.0094	(.37)	.0465	(1.83)	.0617	(2.43)
Std. Dev.	.0037	(.1442)	.0015	(.06)	.0064	(.25)	.0015	(.06)

conducted in a flame tunnel type rig schematically illustrated in Figure 13 which provided a gas velocity of Mach 0.3. The combustible mixture was composed of air and No. 2 fuel oil (0.3-0.5 sulfur) in a weight ratio of approximately 54:1. The test specimens were sheared from the respective sheets. The sheared edges of the samples were then ground to provide maximum lateral dimensions of 1 cm x 7.6 cm (0.375 inch x 3.0 inches). Each specimen was subsequently surface ground to a 120 grit finish to achieve a uniform starting surface condition. Sample dimensions were measured to ±.01 cm and the surface area was calculated in cm^2. After measurement, the samples were ultrasonically degreased in thicklorethane, dried, weighed on a microbalance to ± .0005 gm, and then placed in test. During testing, the specimens were subjected to cycles consisting of 30 minutes in the test chamber followed by withdrawal and a two minute air quench to a temperature <533K (500°F). Periodically, the specimens were removed from test and weighed to document weight changes. At the conclusion of the test, the specimens were sectioned, nickel plated and prepared metallographically to determine oxidation penetration characteristics.

A summary of the 1366K (2000°F) dynamic oxidation test results is given in Table XIII. Average weight change data and the range for each test period are also presented in Figure 14. The weight change results reflect heat-to-heat differences. However, the range of values, even after 100 hours, is considered small. The oxidation penetration data, which provide a more reliable and unambiguous basis for evaluating dynamic oxidation resistance, indicate only minor differences between the three baseline heats.

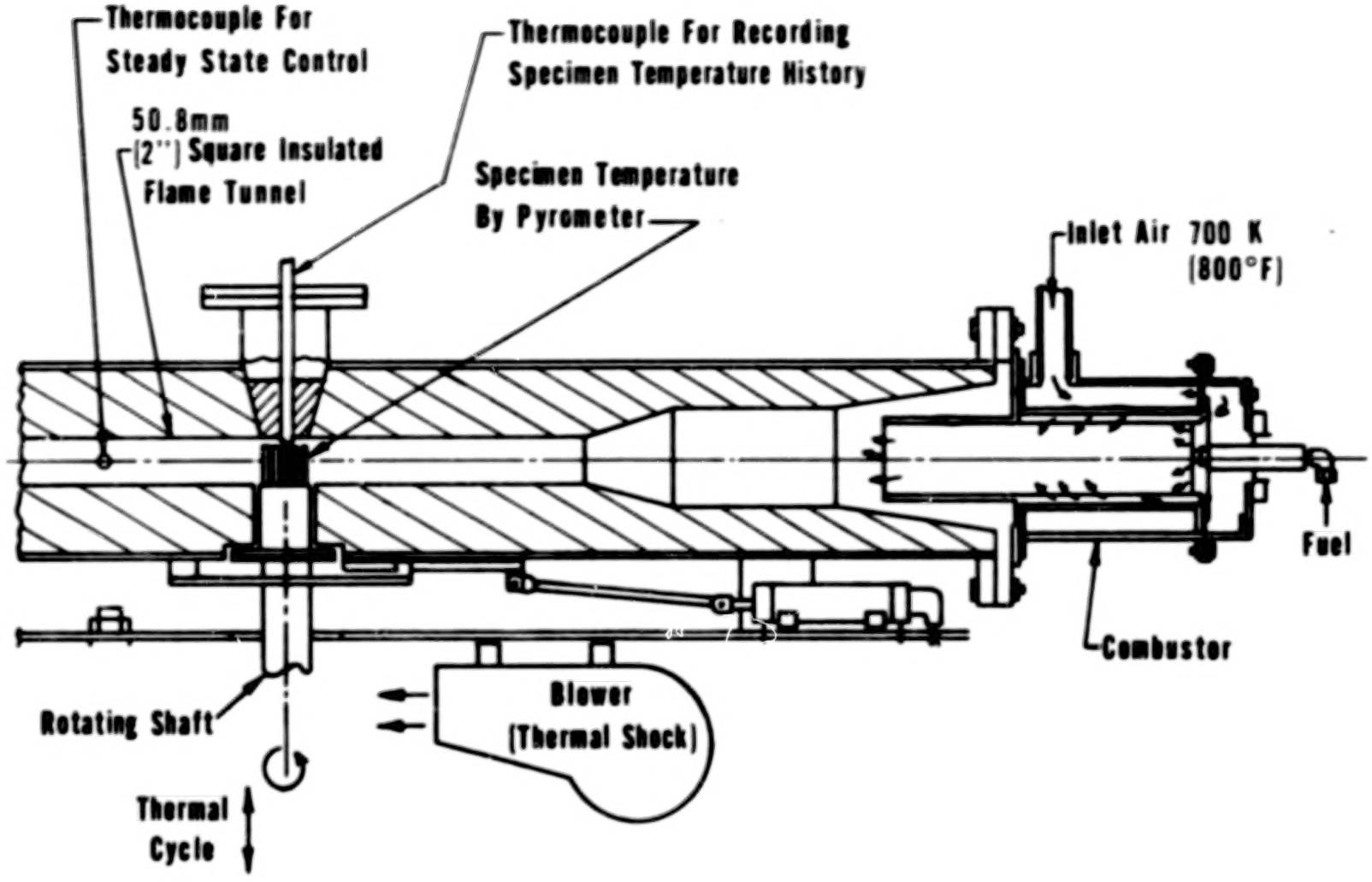

Figure 13: Flame Tunnel Cross Section

TABLE XIII

1366 K (2000°F)/100 HOUR DYNAMIC OXIDATION DATA FOR
"HAYNES" ALLOY NO. 188 BASELINE THIN GAUGE SHEETS

Heat No.	Weight Change, mg/cm^2				Continuous Oxidation Penetration		Maximum Penetration	
	20 hr.	40 hr.	60 hr.	100 hr.	mm/side	(mils/side)	mm/side	(mils/side)
2-1604	.148	-.058	-.388	-1.18	.0231	(.91)	.0356	(1.40)
	.148	-.058	-.395	-1.23	.0196	(.77)	.0381	(1.50)
	.189	-.008	-.345	-1.17	.0183	(.72)	.0384	(1.51)
3-1622	.033	-.388	-.884	-1.82	.0180	(.71)	.0404	(1.59)
	.025	-.394	-.895	-1.81	.0178	(.70)	.0391	(1.54)
	.025	-.388	-.876	-1.79	.0185	(.73)	.0406	(1.60)
4-1671	.247	-.107	-.657	-3.19	.0185	(.73)	.0389	(1.53)
	.218	-.143	-.680	-3.04	.0170	(.67)	.0422	(1.66)
	.252	-.118	-.673	-3.15	.0196	(.77)	.0409	(1.61)
Average	.143	-.185	-.644	-2.04	.0191	(.75)	.0394	(1.55)
Std. Dev.	.094	.159	.222	.857	.0018	(.07)	.0020	(.08)

37

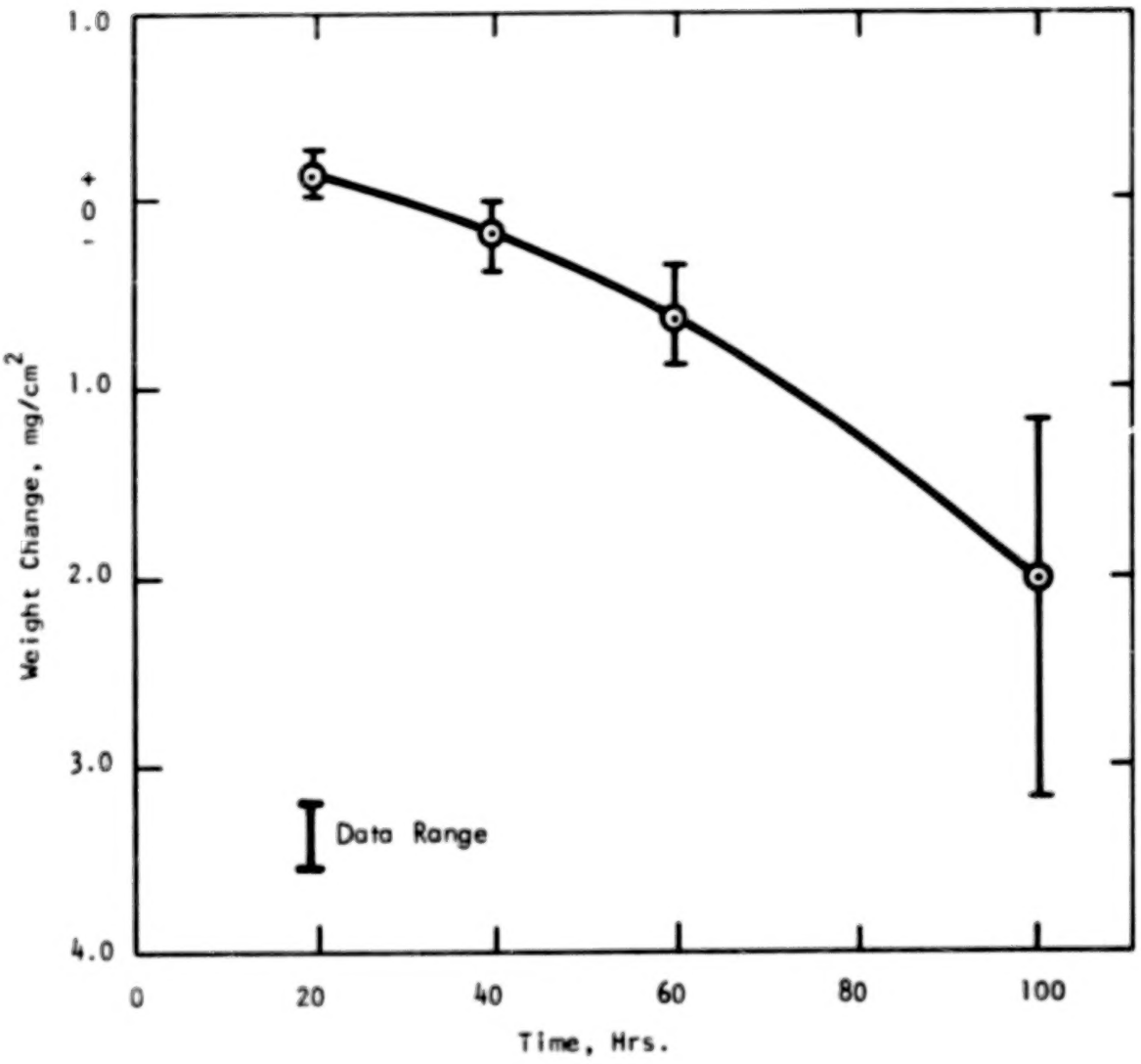

Figure 14: 1366 K (2000°F), Mach 0.3 Dynamic Oxidation Weight Change Characteristics for HAYNES alloy No. 188 Baseline Thin Gauge Sheets

3.0 TEXTURE STUDY

3.1 Introduction

The development of a HAYNES alloy No. 188 thin gauge sheet with a preferred crystallographic texture after recrystallization offered a potential means of improving creep strength. Barrett, et al (ref. 7), investigated the effect of the cube texture on creep in copper and found significant benefits. The cube textured copper sheet was produced by cold rolling 97 percent and annealing which yielded an average recrystallized grain diameter of 0.03 mm (ASTM 7). The steady-state creep rates of the textured copper sheet were found to be about half those for random polycrystals, and independent of sample orientation in the plane of the sheet. No evidence of grain boundary displacement or grain growth was observed in the textured copper sheet. The samples with randomly oriented grains, on the other hand, were found to have a grain boundary sliding strain component which was independent of the amount of strain and which decreased as the average grain diameter increased. Evidence of grain size instability was also observed in some of the random polycrystals. The beneficial effects of the cube texture were interpreted in terms of the low angle grain boundaries (~5° average misorientation angle) serving as poor vacancy sources for dislocation climb.

No previous work had been done to intentionally develop a preferred crystallographic texture in HAYNES alloy No. 188 sheet. Accordingly, the plan of investigation was designed to obtain the following information:

1. The amount of cold work required to develop a well defined texture.

2. The roles of cold reduction and annealing temperature in determining the type and extent of the texturing.

3. The effects of texture processing on microstructure.

4. Determination of any improvements in the low strain ($\leq$ 1 percent) creep strength at a common quality control test condition.

5. The range of creep conditions over which improvements would exist for the optimum texture.

6. The effect of texture on other mechanical properties.

7. The effects of texture and texture processing on fabricability and oxidation resistance.

The experimental work plan was facilitated by limiting initial investigations (items 1 through 4) to a single heat of material. Upon defining an optimum textured sheet, three heats of material were employed to perform the evaluations required by items 5 through 7. The starting materials used in

this and in subsequent experimental portions of the program were 4.57 mm (.180 inch) thick, hot-rolled plates which serve as the feedstock for the production cold strip mill. The heat analyses for these materials are listed in Table XIV. A typical starting material microstructure is shown in Figure 15.

3.2 Initial Investigation

3.2.1 Production of expeirmental sheet lots. - Sheets nominally .38 mm (.015 inch) thick for the initial investigation were produced from Heat 3-1655 using strips measuring 4.57 mm x 25.4 mm x 152.4 mm (.180 inch x 1 inch x 6 inches). The resulting strips measured approximately .38 mm x 28.57 mm x 127 cm (.015 inch x 1.125 inch x 50 inches). The cold-rolling schedules, which are illustrated in Table XV, were planned such that final cold reductions of 70 percent, 80 percent and 90 percent would be obtained. Three strips were processed to eacn level of final cold work and then final annealed for 10 minutes at a temperature of 1394K (2050°F), 1450K (2150°F), or 1505K (2250°F) and rapid air cooled. The strips so produced thus represented nine different final cold work and annealing temperature combinations. After final annealing, each strip was salt bath descaled and flattened by stretcher leveling. The samples were coded using the numbers 7, 8, and 9 to represent final cold-work levels of 70 percent, 80 percent, and 90 percent, respectively, and the letters A, B, and C to represent the final annealing temperature in the order of increasing temperature. For example, the code designation 7A would represent 70 percent final cold work and a final annealing temperature of 1394K (2050°F).

A sample from each experimental strip was examined metallographically. Micrographs illustrating typical structures are presented in Figures 16-18. No discernible grain size differences were noted with respect to sections oriented parallel or perpendicular to the rolling direction. As might be expected, the final grain size at each level of cold work changed dramatically from very fine to coarse as the annealing temperature was increased. At constant annealing tempeature, differences in the final grain sizes with respect to the level of final cold work were not very great. The carbide sizes and distributions were also observed to coarsen with increasing annealing temperature, and it was evident that those samples which had been annealed at 1505K (2250°F) retained more carbon in solution.

3.2.2 Examination of crystallographic texture. - Samples from the experimental strips were examined for crystallographic texture using the procedure previously described in Section 2.2. The strip chart recordings of diffracted X-ray intensities indicated that all samples had well defined textures. The results of the computer analyses of integrated diffracted beam intensities also indicated that the full range of relative intensities (1 to 9) was obtained for each sample. The resulting pole figures, shown in Figures 19-27, are presented using only the three highest intensity levels so that this principal texture feature can be easily appreciated.

TABLE XIV

HEAT ANALYSES FOR "HAYNES" ALLOY NO. 188, 4.57mm (.180-INCH) THICK, HOT ROLLED PLATES USED AS STARTING MATERIALS IN EXPERIMENTAL SHEET STUDIES

	Composition - Weight Percent		
Element	Heat 3-1655	Heat 4-1696	Heat 4-1697
Cr	22.52	22.58	22.57
W	14.06	14.29	14.10
Fe	1.78	1.50	1.38
C	0.10	0.11	0.10
Si	0.33	0.34	0.35
Co	37.95	36.86	37.00
Ni	22.54	22.74	22.28
Mn	0.65	0.71	0.64
P	0.012	0.011	0.011
S	0.005	0.007	0.006
La	0.040	0.099	0.104
B	0.006	0.004	0.004

Figure 15: Microstructure of Heat 3-1655, 4.57 mm (.180-inch) Thick Starting Stock, Grain Size ASTM 6-1/2 to 7. X300.

TABLE XV

COLD ROLLING SCHEDULES FOR TEXTURE STUDY
SHEETS: INITIAL INVESTIGATION

70% Final Reduction

4.57mm (.180") — Cold Roll — 1.27mm (.050") — Cold Roll — .38mm (.015")

Anneal at
1450 K (2150°F)
10 min.

80% Final Reduction

4.57mm (.180") — Cold Roll — 1.91mm (.075") — Cold Roll — .38mm (.015")

Anneal at
1450 K (2150°F)
10 min.

90% Final Reduction

4.57mm (.180") — Cold Roll — .38mm (.015")

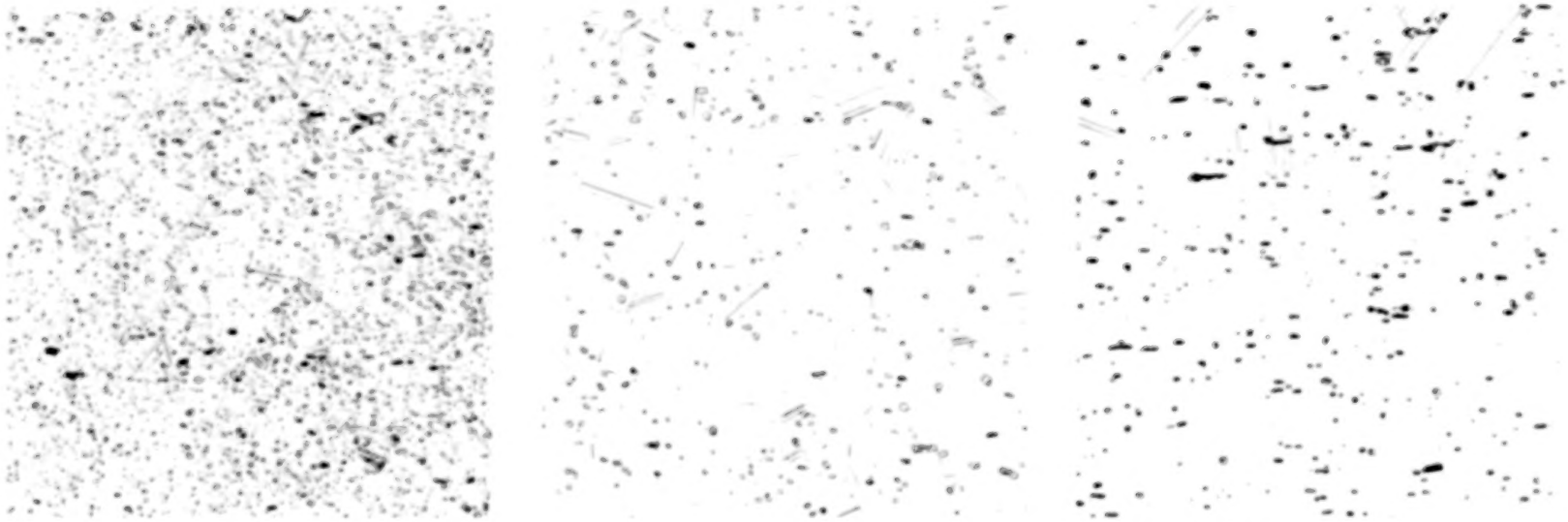

(a) 7A - 1394K (2050°F)/10 min. Grain Size ASTM 8-10 & Finer. X300.

(b) 7B - 1450K (2150°F)/10 min. Grain Size ASTM 6-1/2-7. X300.

(c) 7C - 1505K (2250°F)/10 min. Grain Size ASTM 4-1/2. X300.

Figure 16: Microstructures of Texture Study Sheet Lots of Heat 3-1655 Given 70% Cold Reduction Prior to Final Annealing at the Indicated Temperatures

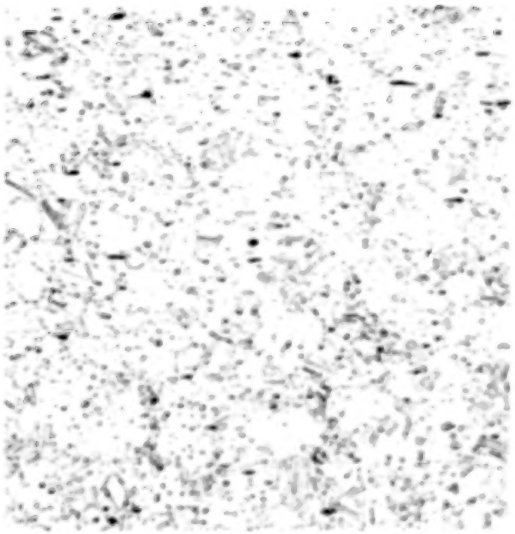

(a) 8A - 1394K (2050°F)/10 min. Grain Size ASTM 9-10 & Finer. X300.

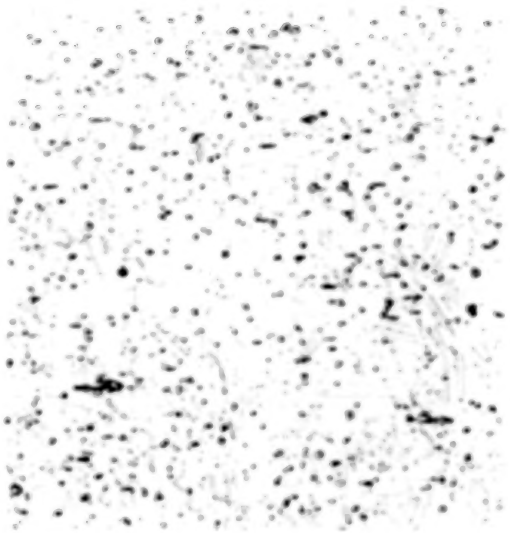

(b) 8B - 1450K (2150°F)/10 min. Grain Size ASTM 7-1/2. X300.

(c) 8C - 1505K (2250°F/10 min. Grain Size ASTM 5-5-1/2. X300.

Figure 17: Microstructures of Texture Study Sheet Lots of Heat 3-1655 Given 80% Cold Reduction Prior to Final Annealing at the Indicated Temperatures

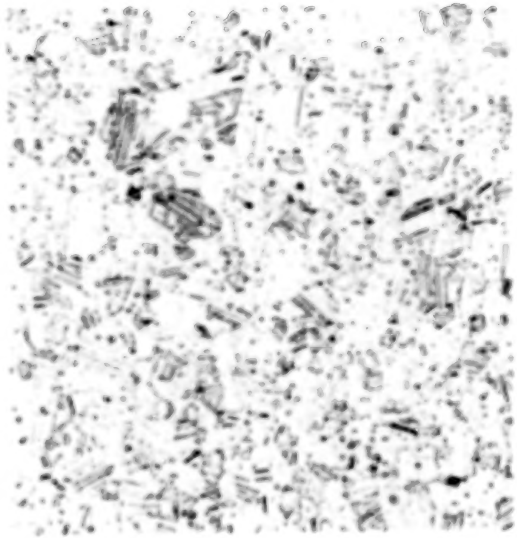

9A - 1394K (2050°F)/10 min.
Grain Size ASTM 8-1/2-10 & Finer.
X300.

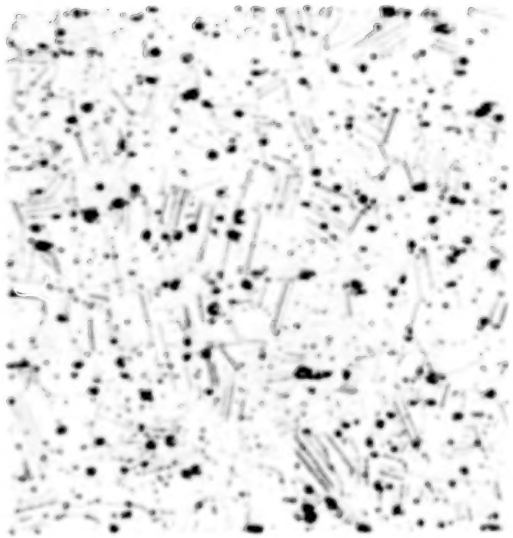

(b) 9B - 1450K (2150°F)/10 min.
Grain Size ASTM 7-1/2.
X300.

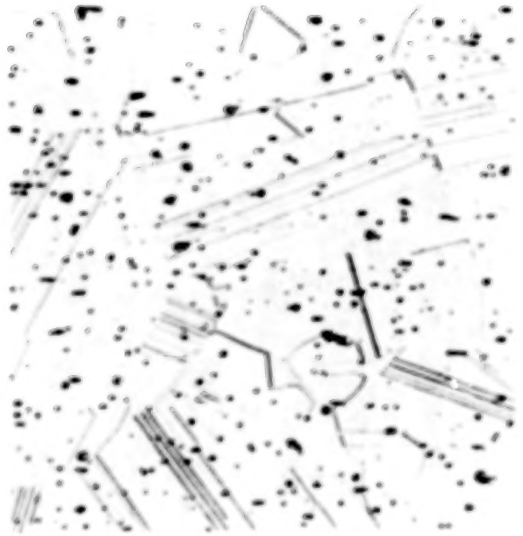

(c) 9C - 1405K (2250°F)/10 min.
Grain Size ASTM 3-1/2-5-1/2.
X300.

Figure 18: Microstructures of Texture Study Sheet Lots of Heat 3-1655 Given 90% Cold Reduction Prior to Final Annealing at the Indicated Temepratures

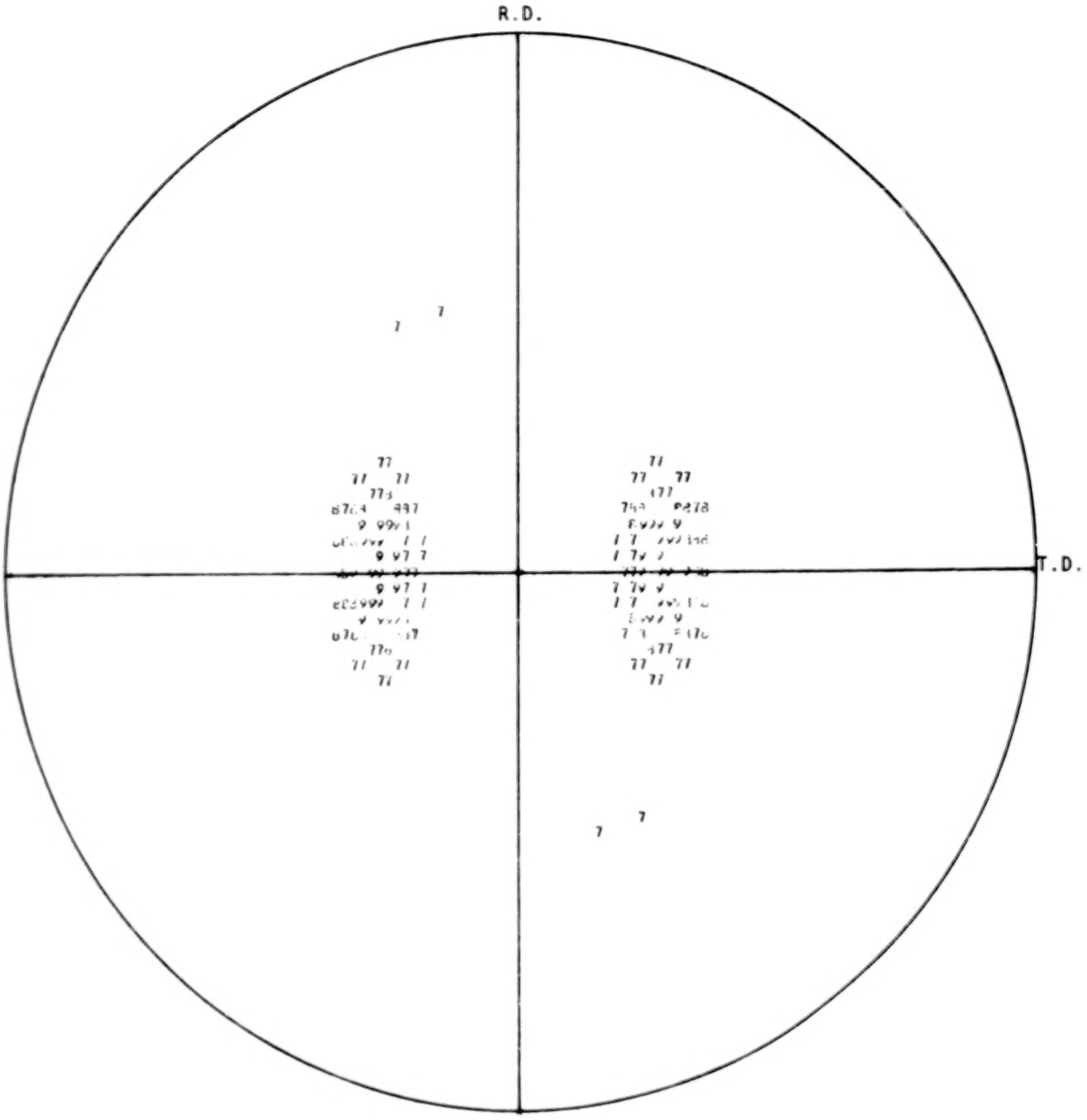

Figure 19: (111) pole figure for 7A - cold reduced 70% and annealed at 1394 K (2050°F) for 10 minutes

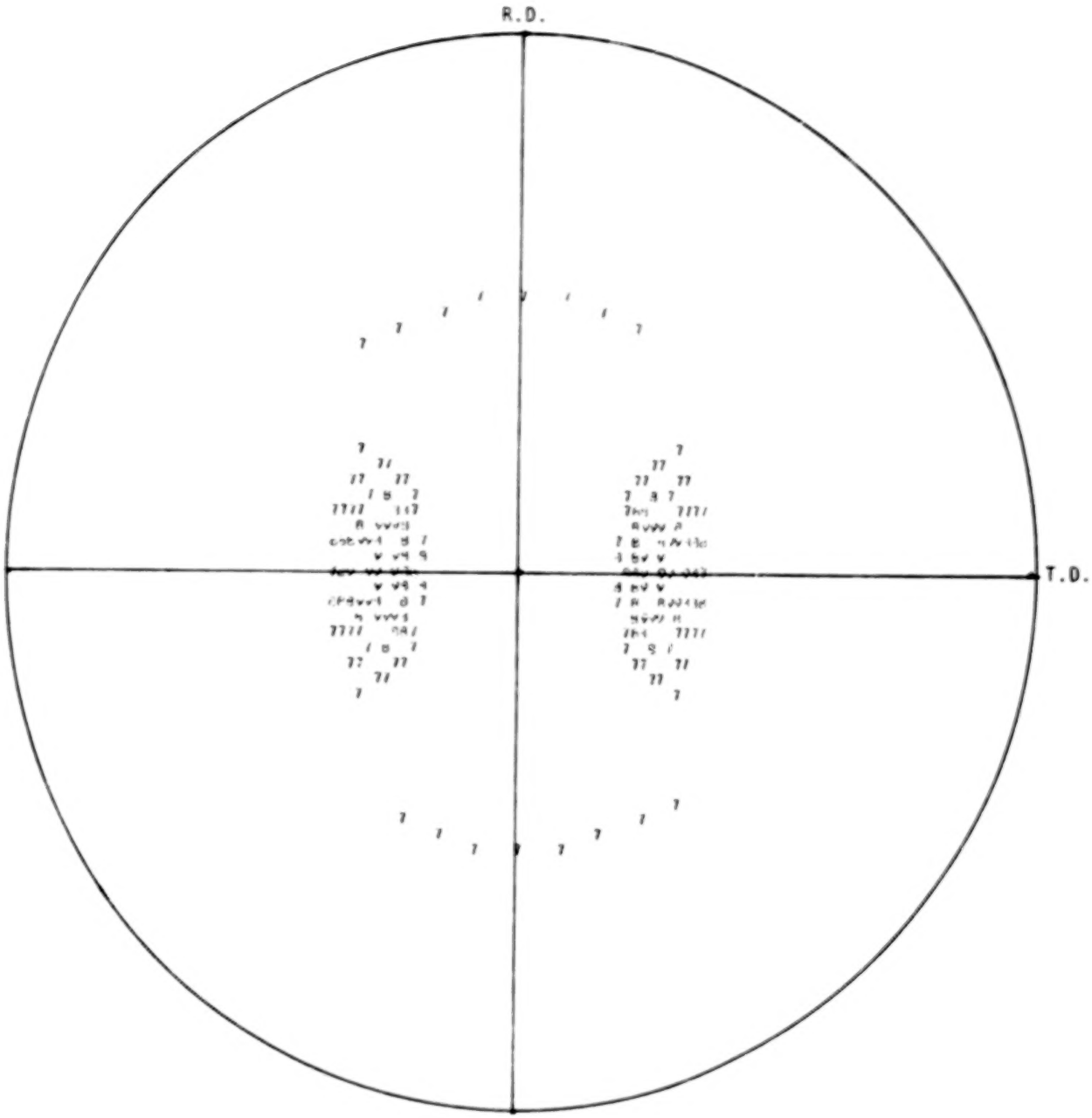

Figure 20: (111) pole figure for 7B - cold reduced 70% and annealed at 1450 K (2150°F) for 10 minutes

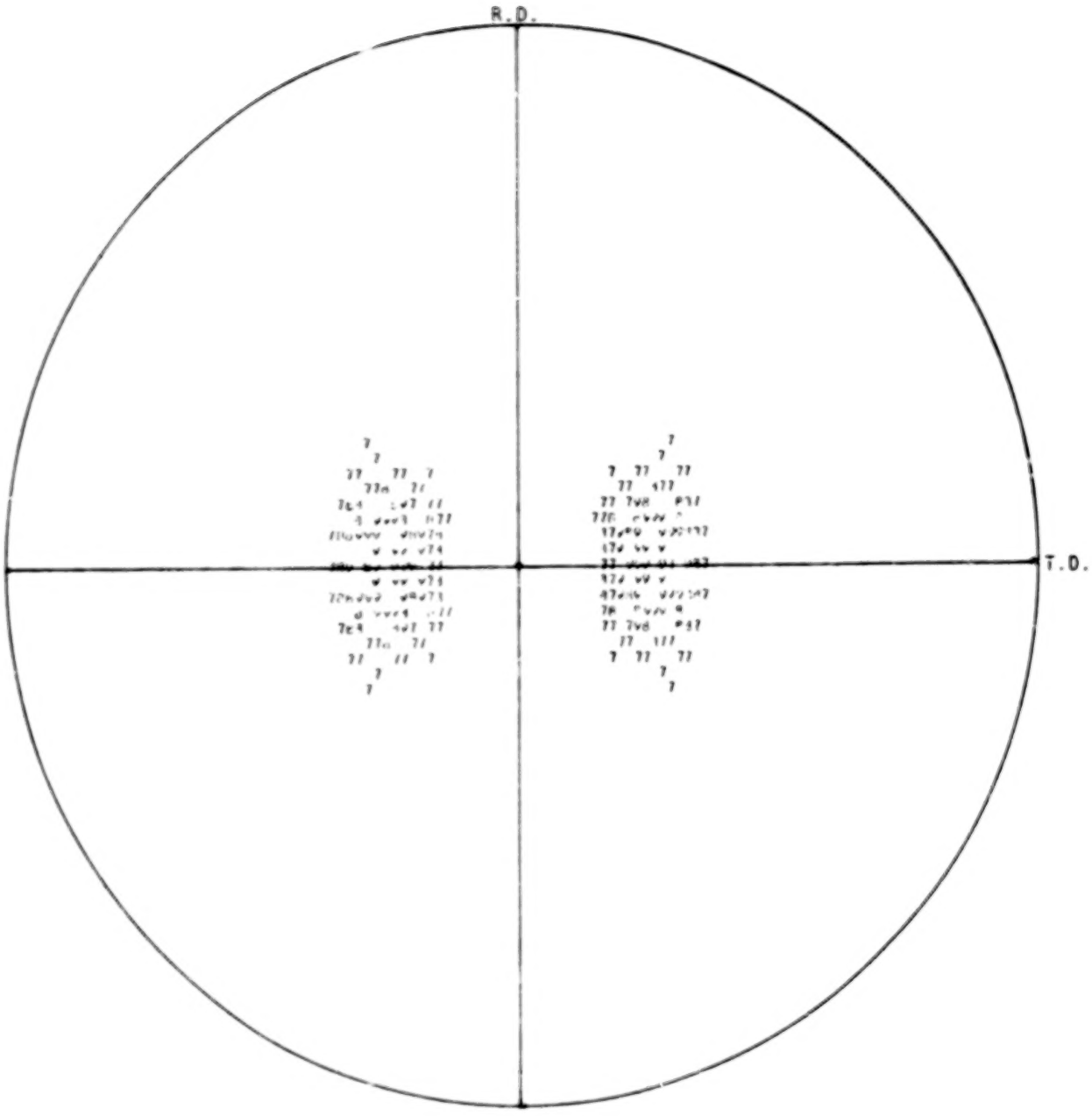

Figure 21: (111) pole figure for 7C - cold reduced 70% and annealed at 1505 K (2250°F) for 10 minutes

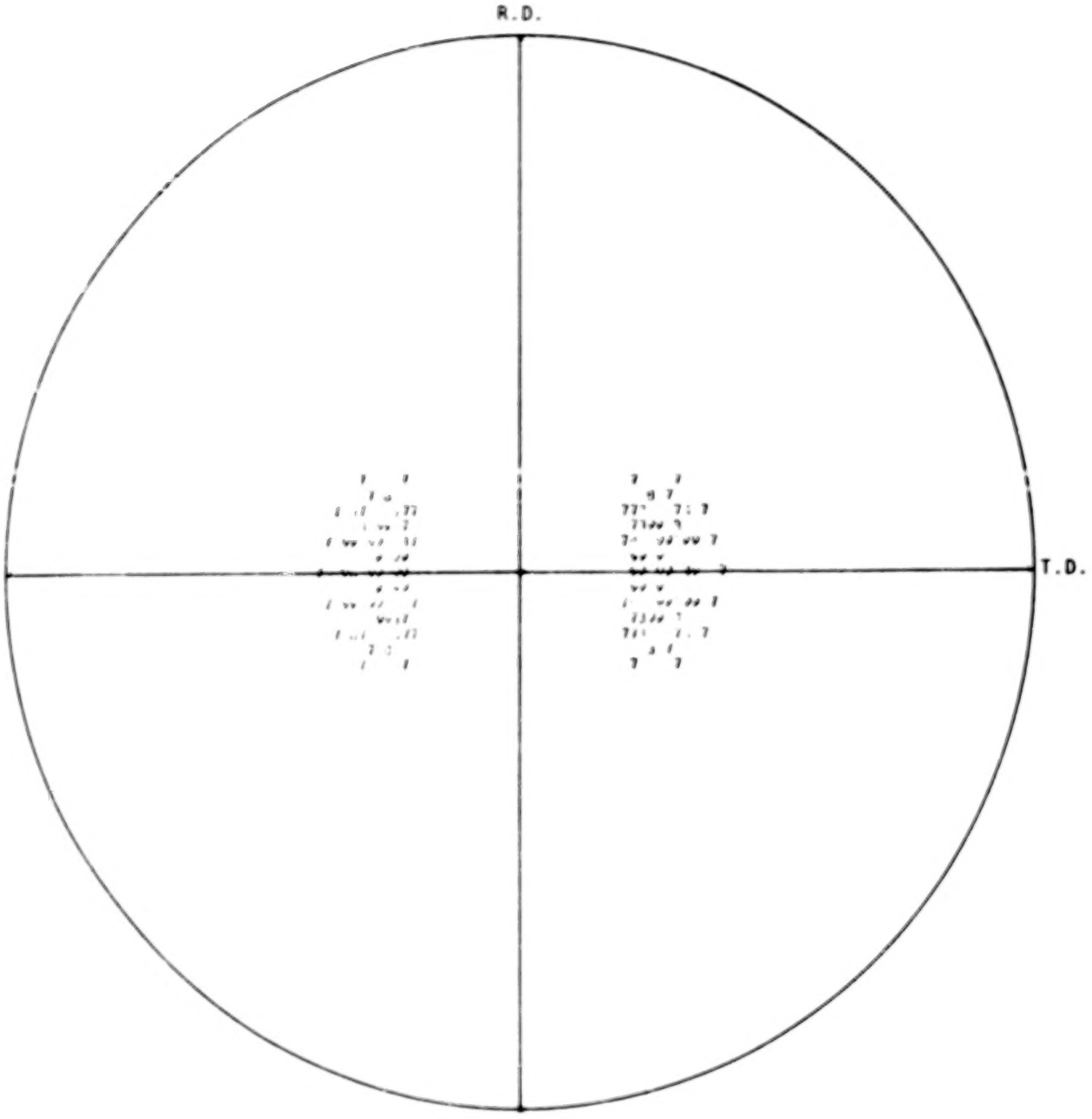

Figure 22: (111) pole figure for 8A - cold reduced 80% and annealed at 1394 K (2050°F) for 10 minutes

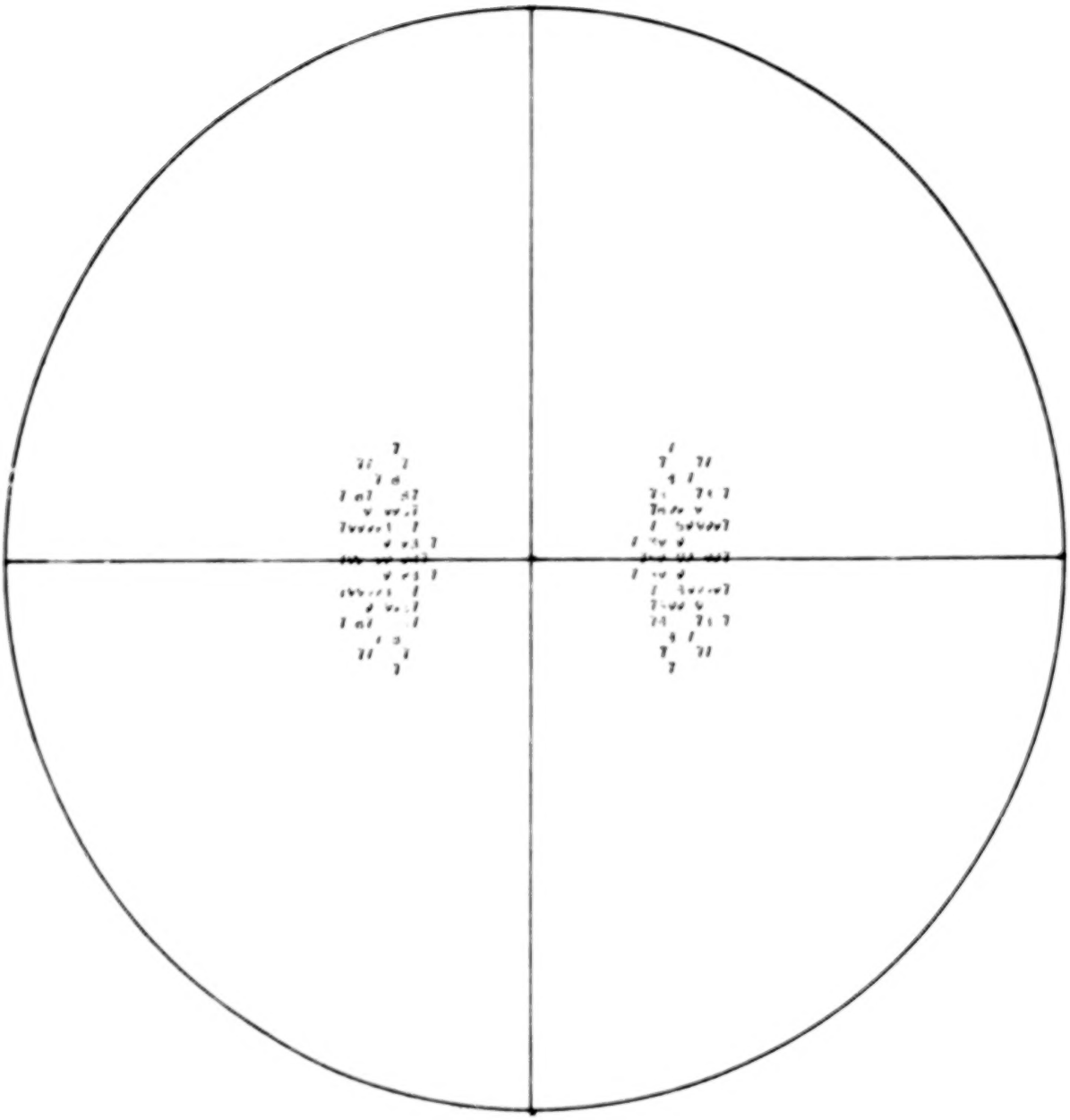

Figure 23: (111) pole figure for 8B - cold reduced 80% and annealed at 1450 K (2150°F) for 10 minutes

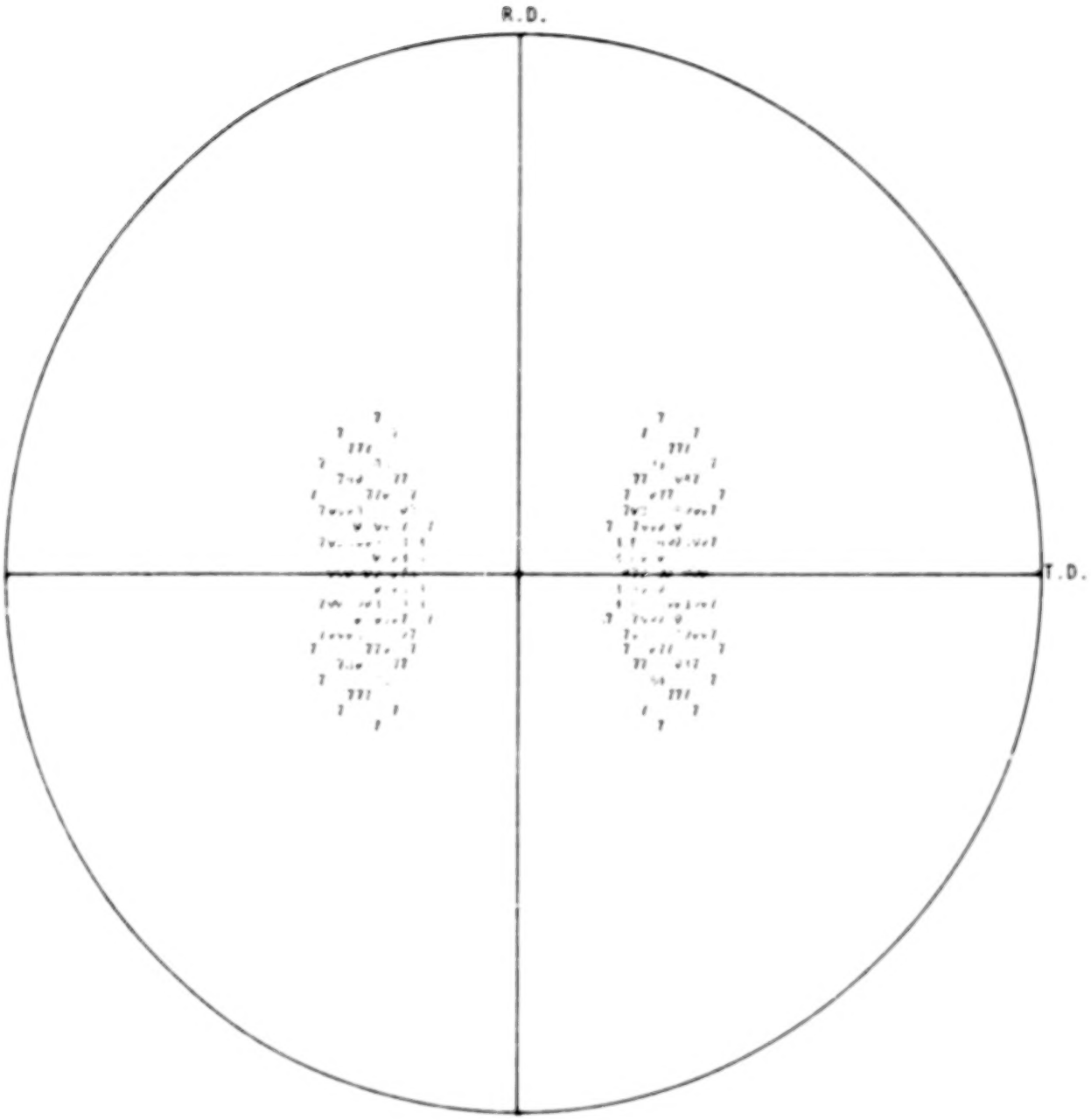

Figure 24: (111) pole figure for 8C - cold reduced 80% and annealed at 1505 K (2250°F) for 10 minutes

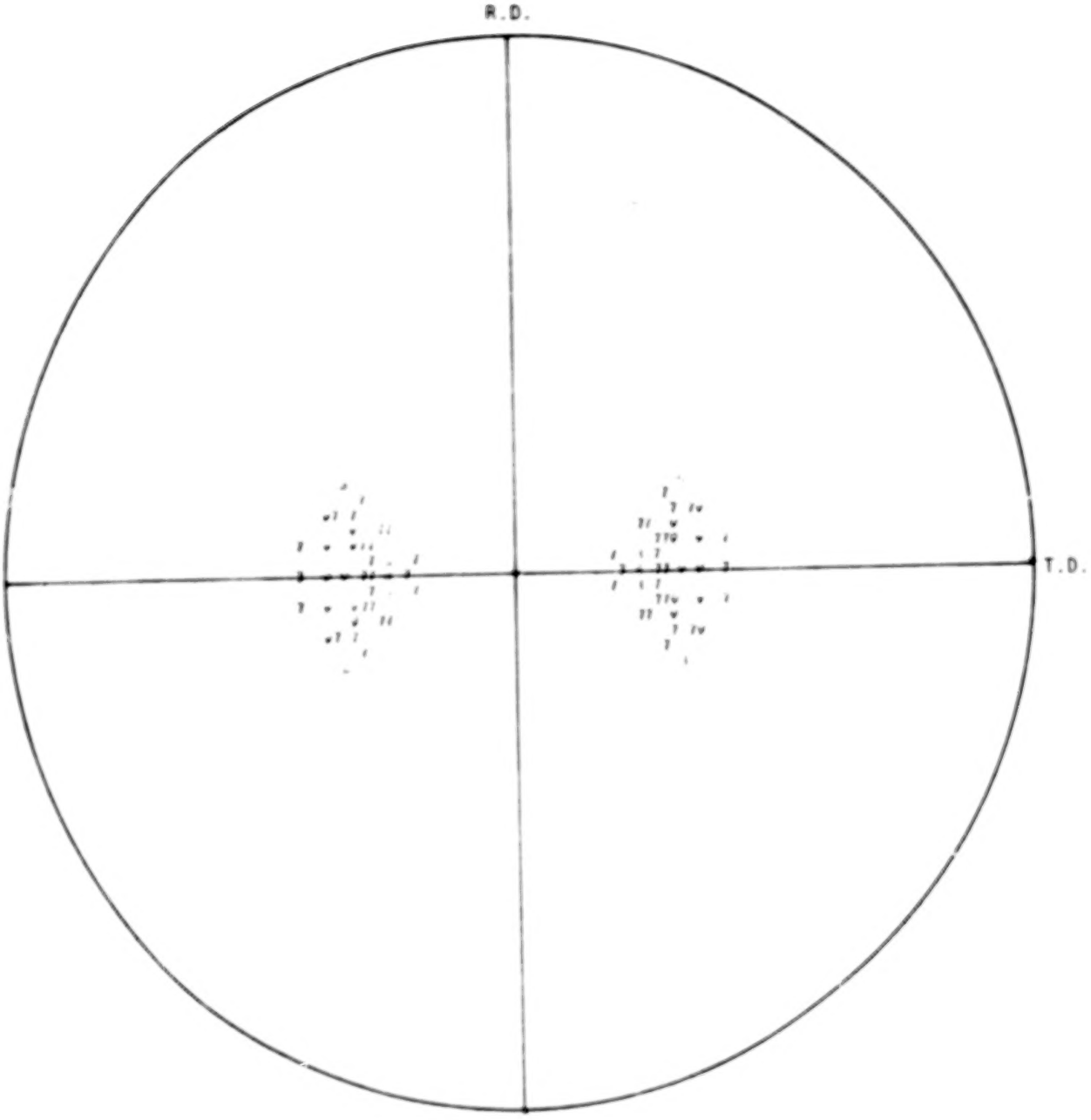

Figure 25: (111) pole figure for 9A - cold reduced 90% and annealed at 1394 K (2050°F) for 10 minutes

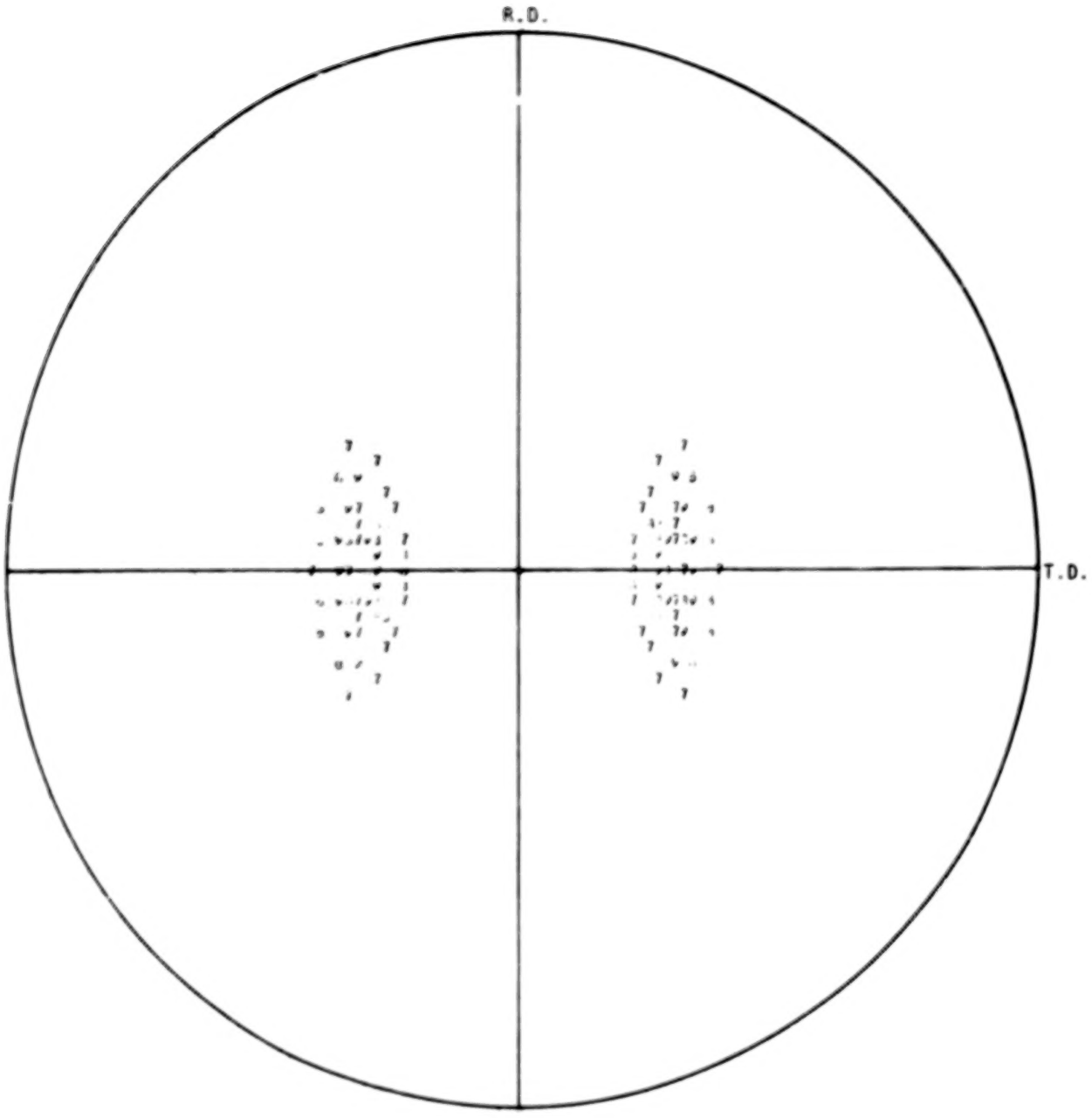

Figure 26: (111) pole figure for 9B - cold reduced 90% and annealed at 1450 K (2150°F) for 10 minutes

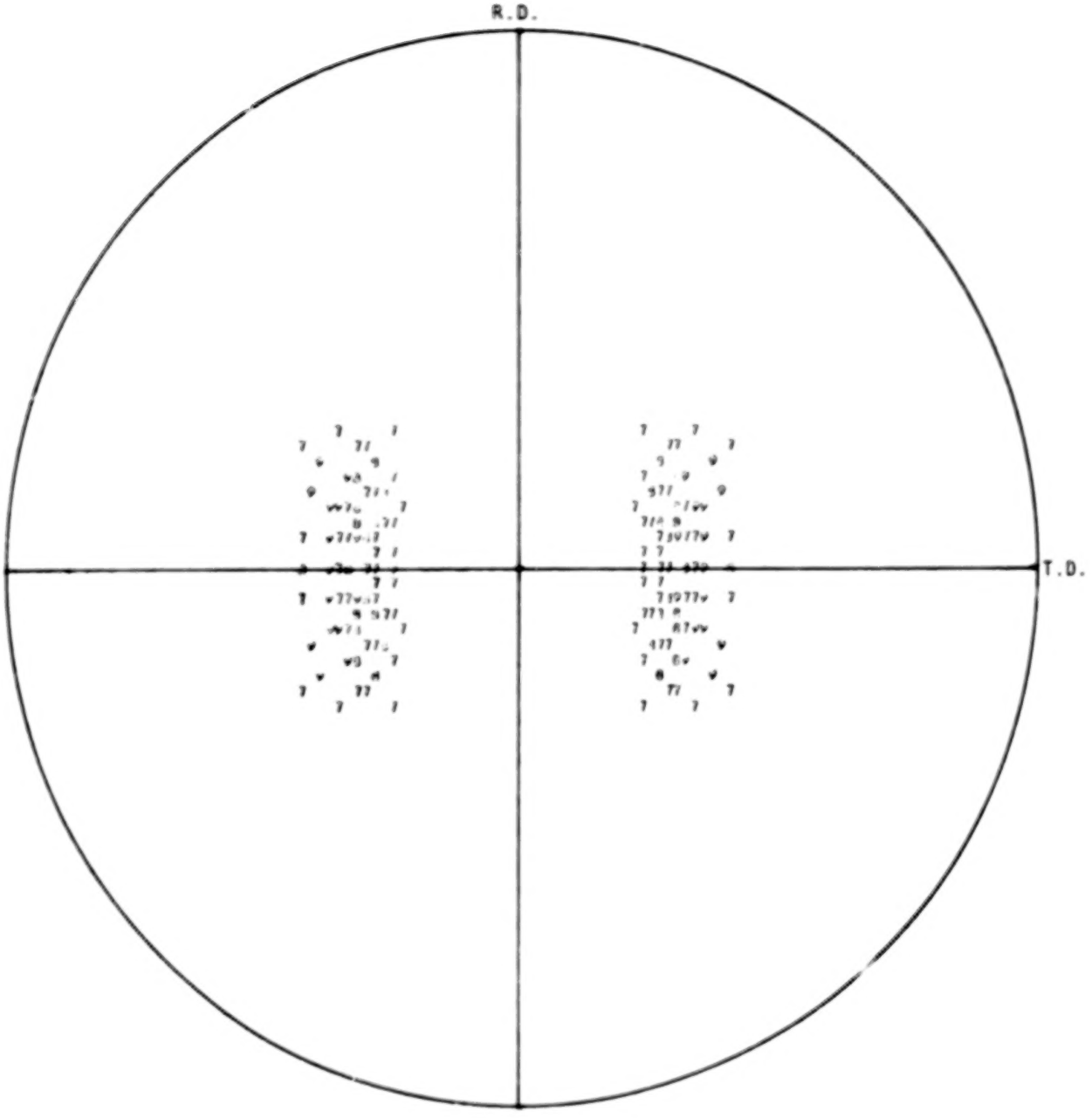

Figure 27: (111) pole figure for 9C - cold reduced 90% and annealed at 1505 K (2250°F) for 10 minutes

Comparison of the pole figures indicated that all of the experimental sheets possessed the same type of texture. The centers of the (111) high intensity regions all lay on the equator of the stereographic projection with respect to the axis defined by the rolling direction. Only the angular spreading of these areas was observed to vary with the different thermomechanical processing conditions. From the positioning of the (111) high intensity reflections, it was clear that the texture obtained was not the cube texture, and since each pole figure covered only the central 55 degrees of the stereographic projection, insufficient data was available to define the texture type in a specific manner. To remedy this situation, sample 8B was arbitrarily selected in view of the similarities between the (111) pole figures, and its corresponding (200) and (220) pole figures were determined. These pole figures are presented in Figures 28 and 29, respectively. By Comparing the three pole figures of sample 8B to the (001), (110), (111), and (112) standard projections, it became clear that more than one textural component was present. A satisfactory fit was obtained by assuming the presence of two components. These were (1) (110) parallel to the sheet plane with $[\bar{1}10]$ parallel to the rolling direction and [001] parallel to the transverse direction, and (2) (112) parallel to the sheet plane with [110] parallel to the rolling direction and $[11\bar{1}]$ parallel to the transverse direction. A composite stereographic projection containing these components is illustrated in Figure 30. According to the condition of symmetry (ref. 8), each pole indicated should have a "mirror image" across the planes normal to the rolling and transverse directions. When these allowances are made, the agreement between the ideal and the experimental pole figures is quite good.

In an attempt to quantify the degree of texturing observed, the angular spreading of the high intensity regions about the rolling and transverse directions was measured on the (111) pole figures. Due to symmetry, only one-half of each pole figure needed to be considered. In this treatment, the angular spreading which occurred about each of the major axes should be considered as phenomenological and independent of one another. However, the composite projection model predicts that the (111) poles belonging to the (112) and (110) components should be scattered about positions on the equator of 15.8° and 35.3° from the center of the projection, respectively. This would give rise to a natural spread of 15.8" around the rolling direction if both components were present in appreciable amounts. Therefore, by considering the actual angular locations of the high intensity regions with respect to the rolling direction, a qualitative assessment could be made regarding the presence of each component.

A summary of the angular data obtained from the (111) pole figures is presented in Table XVI. Generally, the angular spreading about the transverse direction increased with annealing temperature at each level of cold work. The changes which occurred at the 70 percent level were not as great as those for the 80 percent and 90 percent cold-work levels, however. At constant annealing temperature, the changes in the amount of angular spreading about the transverse direction with cold work were not consistent. It appeared, however, that increasing cold work suppressed the (112) component and increased the spreading of the (110) component about the rolling direction.

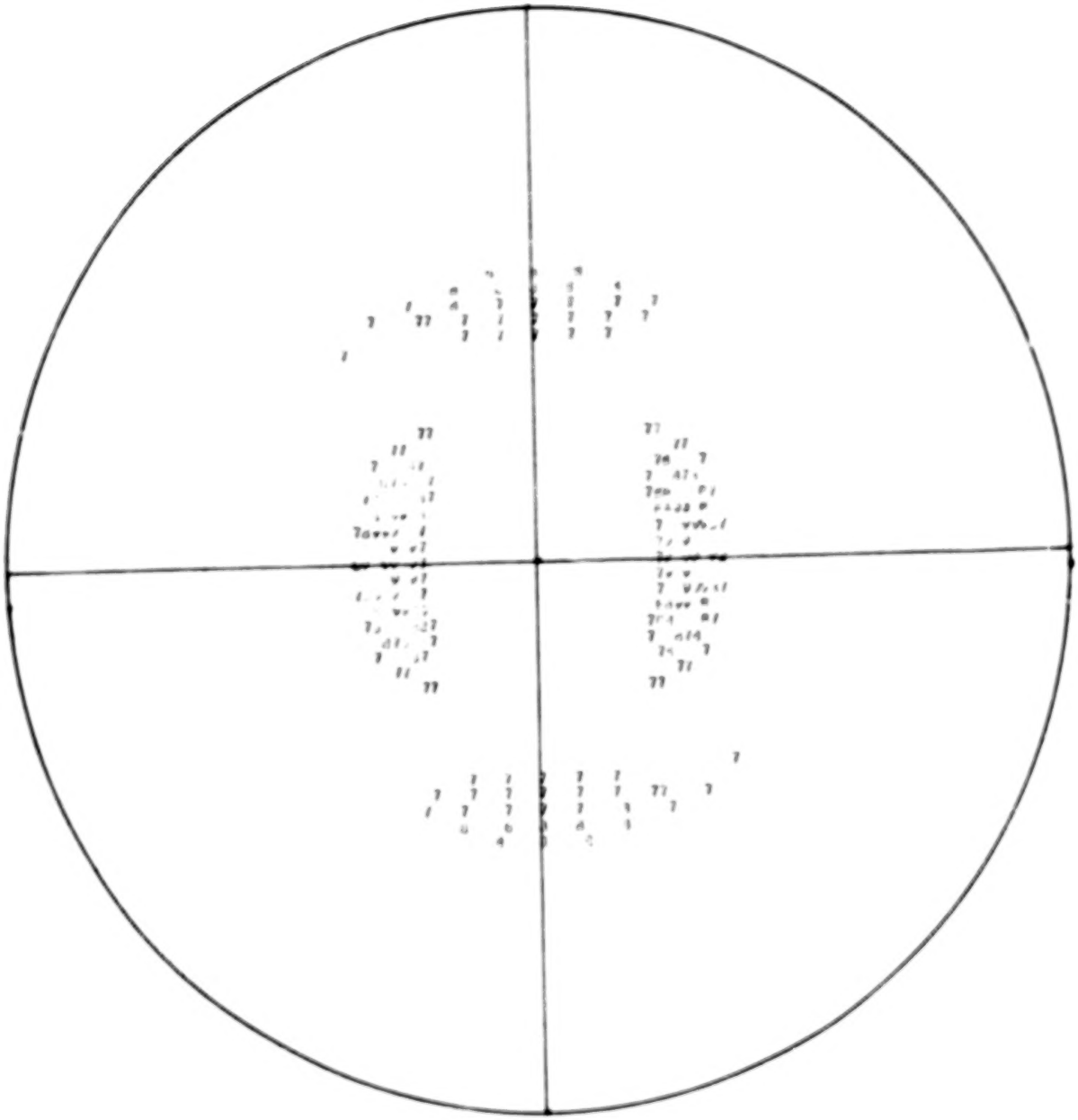

Figure 28: (200) pole figure for 8B - cold reduced 80% and annealed at 1450 K (2150°F) for 10 minutes

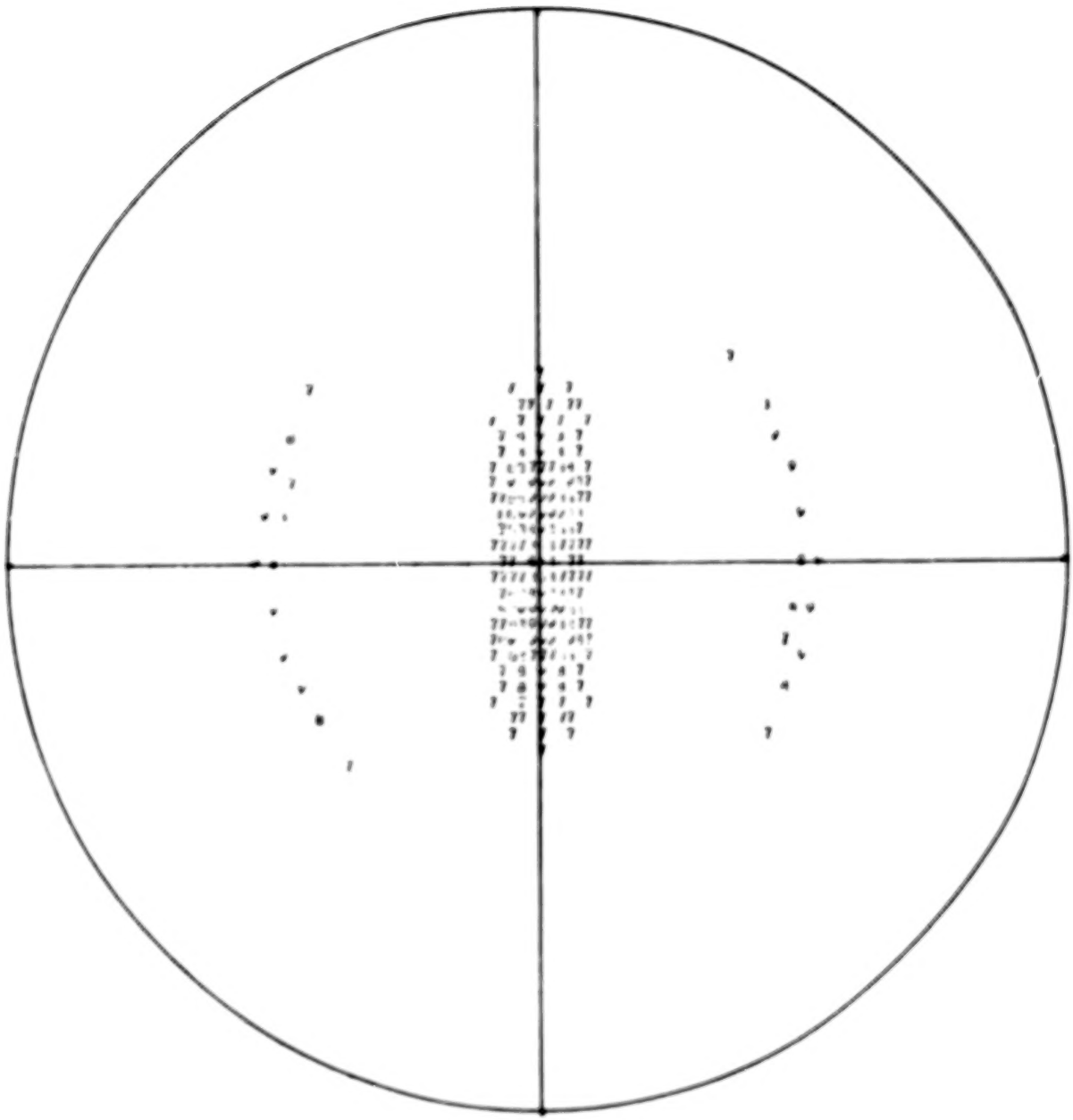

Figure 29: (220) pole figure for 8B - cold reduced 80% and annealed at 1450 K (2150°F) for 10 minutes

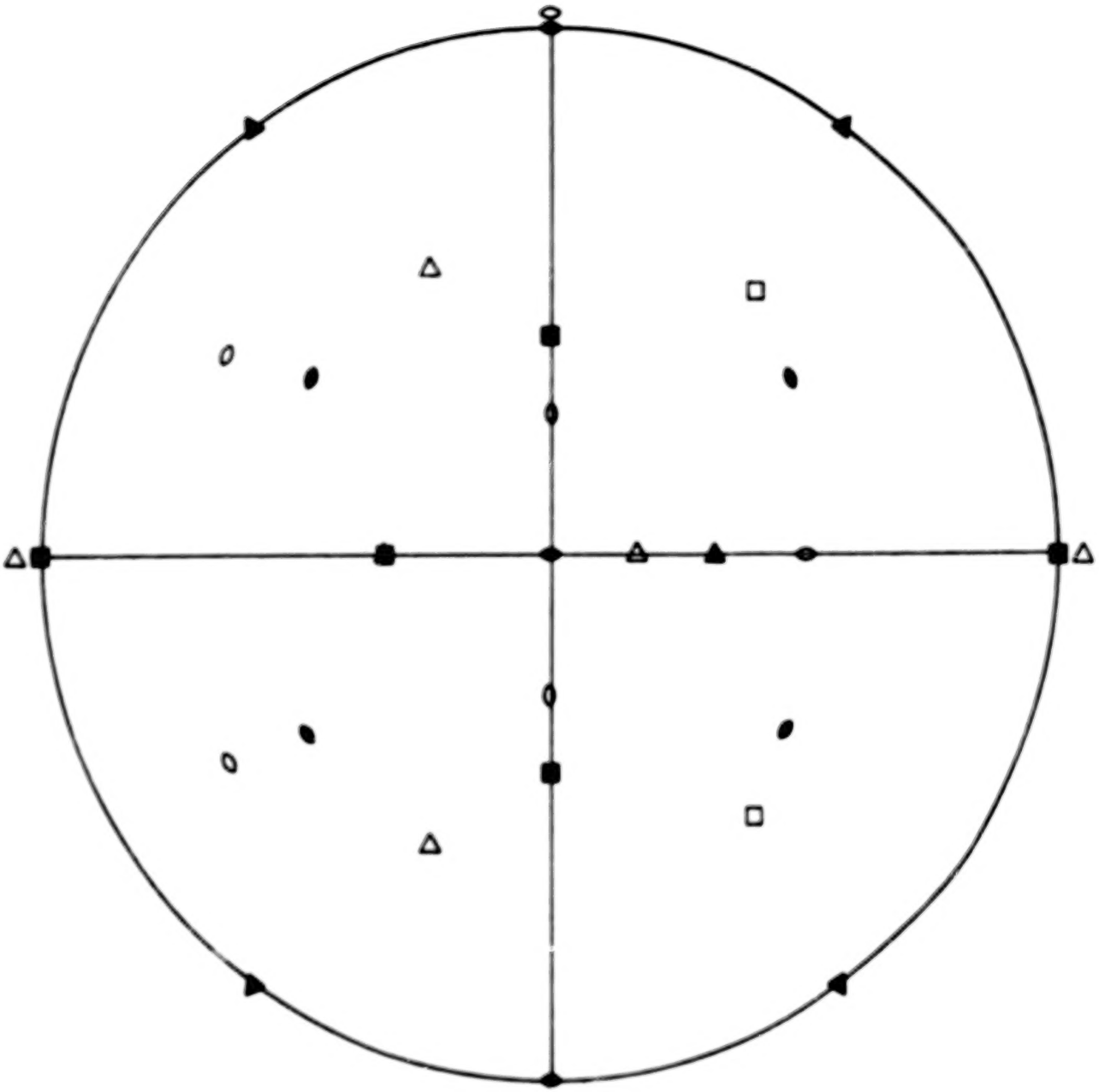

Figure 30: Composite projection containing (110) [$\bar{1}$10], closed symbols, and (112) [$\bar{1}$10], open symbols

TABLE XVI

ANGULAR DATA OF HIGH INTENSITY REGIONS FOR (111) POLE FIGURES DETERMINED FOR TEXTURE STUDY THIN GAUGE SHEET LOTS

Spec. No.*	Around Rolling Direction		Around Transverse Direction	
	Angular Locations	Angular Spread	Angular Locations	Angular Spread
7A	21-40°	19°	±25°	50°
7B	20-40°	20°	±28°	56°
7C	15-40°	25°	±28°	56°
8A	18-48°	30°	±21°	42°
8B	21-40°	19°	±24°	48°
8C	19-42°	23°	±34°	68°
9A	21-45°	24°	±21°	42°
9B	25-43°	18°	±29°	58°
9C	24-45°	21°	±32°	64°

* 7, 8 and 9 indicate 70, 80, and 90% cold reductions, respectively; A, B and C indicate final annealing temperatures of 1394 K (2050°F), 1450 K (2150°F), and 1505 K (2250°F), respectively.

3.2.3 Creep strength evaluation. - Initially, duplicate specimens from each experimental sheet were creep tested to a strain of $\geq$ 1 percent at a test condition of 1200K/41.4 MPa (1700°F/6 ksi) in accordance with the procedure described in Appendix B. A complete listing of the creep test data is contained in Appendix D. For the purpose of the present discussion, the log time averages of the test results for creep strain levels of 0.5 percent and 1.0 percent were determined. The antilogs of the average values were then computed to facilitate comparisons in terms of time units. The results are summarized in Table XVII.

Within each sheet lot, the creep strength based on the amount of time to a given strain level was found to increase with increasing annealing temperature. Recalling the microstructures presented in Section 3.2.1, this behavior appeared to be directly correlated with grain size. That is, the average grain diameter increased (or average ASTM No. decreased) with increasing annealing temperature. Among the experimental sheets, the best creep strengths were obtained for samples 7C, 8C and 9C. Due to the small number of test results, significant differences between these materials could not be fully appreciated. Further testing was therefore carried out until a total of five replicate tests had been completed for each of the three sheet lots. The additional test data are listed in Appendix D. The log average creep results obtained are presented in Table XVIII along with those for the baseline sheets for the purpose of comparison.

In order to detect statistically significant differences between the three texture study sheet lots, the creep data, transformed into log units, were compared using the t-test (ref. 9). Comparisons were also made to the baseline results in order to assess any improvement in creep strength at 1200K/41.4 MPa (1700°F/16 ksi). In each case, the null hypothesis was that the means of the samples tested were equal, and the alternative hypothesis was that the means were not equal. The results of these statistical tests are summarized in Table XIX. All three textured sheet lots were found to have creep lives significantly higher than those of the baseline at both the 0.5 percent and 1.0 percent creep strain levels. Among the textured sheet lots, 8C was found to be significantly superior to 7C ($\geq$ 99 percent confidence level) at both creep strain levels. The tests between sheets 7C and 9C indicated the superiority of 9C for the 0.5 percent creep strain level, but the results for the 1.0 percent creep strain level indicated a confidence level of ~89.4 percent which is normally not considered to be statistically significant. Results of the t-tests between sheets 8C and 9C showed no statistically significant differences. These results established that a sheet processed with 80 percent cold work prior to a final anneal at 1505K (2250°F)/10 minutes was superior to a sheet given 70 percent cold work prior to the same final annealing treatment, and that such a sheet offered a significant improvement in creep strength over the baseline at 1200K/41.4 MPa (1700°F/6 ksi). The fact that no statistical differences could be detected between experimental sheets 8C and 9C made it clear that 90 percent cold work prior to the final anneal offered no advantages over the 80 percent cold work level. Therefore, the combination of 80 percent final cold work followed by a final anneal at 1505K (2205°F)/10 minutes was judged to represent the optimum TMP sequence for producing a textured HAYNES alloy No. 188 thin gauge sheet.

TABLE XVII

SUMMARY OF LOG AVERAGE DATA FOR INITIAL 1200 K/41.4 MPa (1700°F/6 ksi) CREEP TESTS OF THE EXPERIMENTAL TEXTURE STUDY SHEETS

Specimen No.*	0.5% Creep Strain			1.0% Creep Strain		
	Avg Log Time**	Antilog, Hrs	Std. Dev.***	Avg Log Time**	Antilog Hrs	Std. Dev.***
7A	-.126	0.7	.041	.75	1.5	.041
7B	1.237	17.3	.129	1.577	37.7	.131
7C	1.605	40.2	.069	1.931	85.3	.047
8A	-.189	0.6	.146	.110	1.3	.097
8B	1.006	10.1	.027	1.315	20.6	.019
8C	1.923	83.8	.044	2.210	162.3	.074
9A	-.141	0.7	.114	.222	1.7	.130
9B	.872	7.5	.430	1.203	16.0	.432
9C	1.716	52.0	.280	1.991	97.9	.266

* 7, 8, and 9 indicate 70, 80, and 90% final cold reductions, respectively; A, B, and C indicate final annealing temperatures of 1394 K (2050°F), 1450 K (2150°F), and 1505 K (2250°F), respectively.

** $\log \bar{t} = \frac{\Sigma \log t_i}{n}$ t_i = observed time to given creep strain

n = no. of observations

*** log units

TABLE XVIII

SUMMARY OF LOG AVERAGE DATA FOR
1200 K/41.4 MPa (1700°F/6 ksi) CREEP TESTS
OF BASELINE AND TEXTURE STUDY SHEET LOTS

Sheet Lot	No. of Tests, N	0.5% Creep Strain			1.0% Creep Strain		
		Avg Log Time*	Antilog, Hrs	Std. Dev.**	Avg Log Time*	Antilog, Hrs	Std. Dev.**
Baseline	6	1.280	19.1	.339	1.631	42.8	.346
7C***	5	1.660	45.7	.098	1.974	94.2	.062
8C***	5	1.866	73.5	.100	2.169	147.6	.071
9C***	5	1.899	79.3	.218	2.200	158.6	.235

* $\log \bar{t} = \frac{\Sigma \log t_i}{n}$ where t_i = observed time to given creep strain

n = no. of observations

** log units

*** 7C, 8C, 9C = 70%, 80%, and 90% cold work prior to 1505 K (2250°F)/10 min. final anneal

63

TABLE XIX

SUMMARY OF STATISTICAL COMPARISON FOR BASELINE AND TEXTURE STUDY SHEET LOTS

Test	D.F.	t	2-Tailed Probabilities
		Time to 0.5% Creep Strain	
7C vs. 8C	8	-3.2958	.01093
7C vs. 9C	8	-2.23778	.05562
8C vs. 9C	8	-.30703	.76666
7C vs. baseline	6.37	2.61478	.03986
8C vs. baseline	6.43	4.02753	.00690
9C vs. baseline	9	3.50522	.00667
		Time to 1.0% Creep Strain	
7C vs. 8C	8	-4.63314	.00168
7C vs. 9C	4.84	-2.08166	.10582
8C vs. 9C	5.08	-.28290	.78859
7C vs. baseline	5.54	2.37891	.06325
8C vs. baseline	5.69	3.70777	.01389
9C vs. baseline	9	3.11043	.01251

Hypotheses: Null (Ho) $\bar{X}_1 = \bar{X}_2$

Alternative (H_1) $\bar{X}_1 \neq \bar{X}_2$

where $\bar{X}_1$ and $\bar{X}_2$ are the sample means

3.3 Evaluation of Optimum Texture Sheets

3.3.1 Production of experimental sheet lots. - To obtain material for an extensive property evaluation, sheets nominally .38 mm (.015 inch) thick were produced from Heats 3-1655, 4-1696, and 4-1697. The processing schedule was the same as that employed in the production of experimental sheet sample 8C (see Table XV). The actual production of the sheets was accomplished by cold rolling two pieces of each heat measuring 4.57 mm x 11.4 cm wide x 15.24 cm long (.180 inch x 4.5 inches x 6 inches) parallel to the original sheet plate rolling direction. The sheets were purposely made wider than the original strip to enable testing to be carried out in the transverse direction. After the first cold rolling session to a thickness of 1.91 mm (.075 inch), each piece was cut in half to facilitate cold rolling on the 4-Hi laboratory mill. The resulting pieces measured approximately .38 mm x 12.7 cm wide x 63.5 cm long (.015 inch x 5 inches x 25 inches). Following the final annealing treatment, each piece was salt bath descaled and flattened by stretcher leveling.

3.3.2 Examination of grain size and crystallographic texture. - Each cold-rolled sheet selected for mechanical property evaluation was examined for grain size, and (111) crystallographic texturing using the pole figure method previously described. The results of these analyses are presented in Table XX. In all cases, the grain sizes obtained were slightly coarser than that of the original strip produced from Heat 3-1655 (ASTM 4-5 1/2 as compared to ASTM 5-5 1/2).

There were also variations in the textures of the sheets. Those produced from Heat 3-1655 had slightly less angular spreading of the (111) high intensity regions about the rolling direction as compared to the original 8C strip. The angular spreading about the transverse direction for the sheets of Heat 3-1655 was also observed to be significantly less than in the original strip (48-50° versus 68°). Sheets from Heat 4-1696 had slightly higher spreading around the rolling direction and much higher spreading around the transverse direction. For Heat 4-1697, more variation in texture was observed among the individual pieces than was observed between pieces of the other two heats. The amounts of angular spreading of the (111) high intensity regions around both the rolling and transverse directions were found to vary above and below the values obtained on the original strip.

3.3.3 Bend ductility. - As a check on room temperature fabricability, duplicate longitudinal and transverse samples from each heat of textured sheet were subjected to guided bend tests around a diameter equal to 1.5 times the nominal sheet thickness. The samples measured 25.4 mm long x 19 mm wide x .38 mm thick (1 inch x .75 inch x .015 inch). Prior to testing, the sheared edges of the samples were rounded by belt grinding to prevent edge cracking. In all cases, a 180° bend was obtained without any signs of sample cracking.

3.3.4 Tensile properties. - Duplicate longitudinal and transverse tensile tests were performed on samples from each heat of the Type 8C textured sheets

TABLE XX

GRAIN SIZE AND (111) POLE FIGURE DATA FOR TYPE 8C* TEXTURE STUDY SHEETS PRODUCED FOR EXTENSIVE EVALUATION

Piece No.	ASTM G.S.	Around R.D.		Around T.D.	
		Angular Locations	Angular Spread	Angular Locations	Angular Spread
		Heat 3-1655			
2	4-5 Pred 5	21-40°	19°	±25°	50°
3	4-1/2-5-1/2 Pred** 5	20-40°	20°	±25°	50°
4	4-1/2-5-1/2 Pred 5	21-40°	19°	±24°	48°
		Heat 4-1696			
1	4	20-48"	28°	±50°	100°
2	4-4-1/2	19-43°	24°	±49°	98°
4	4-4-1/2	19-45°	26°	±49°	98°
		Heat 4-1697			
2	4-4-1/2 Pred 4-1/2	20-40°	20°	±28°	56°
3	4-4-1/2 Pred 4-1/2	18-42°	24°	±50°	100°
4	4-1/2	16-40°	24°	±38°	76°
		Original Strip, Heat 3-1655			
8C	5-5-1/2	19-42°	23°	±34°	68°

* 80% cold work + final anneal at 1505 K (2250°F)/10 min.

** Pred = Predominantly

over the temperature range of room temperature to 1366K (2000°F). The procedures employed were the same as those described in Section 2.3. A complete listing of the test results is given in Table XXI. These data indicate that there were no significant differences in the tensile properties with respect to test direction. Average tensile property values for the three heats are presented in Table XXII. The yield and ultimate strengths were similar to those obtained for the baseline (Table IV) over the full range of test temperatures. The average elongations were equivalent to those of the baseline through 1033K (1400°F), but significantly lower at temperatures of 1144K (1600°F) and above. Presumably, the lower ductilities of the textured sheets at the three highest temperatures can be attributed to their coarser grain size (ref. 10).

3.3.5 Stress rupture properties. - Duplicate longitudinal and transverse samples from each heat were stress rupture tested at 1089K/165.4 MPa (1500°F/24 ksi) and at 1311K/31 MPa (1900°F/4.5 ksi). The specimen configuration employed was the same as that illustrated in Appendix B. A summary of the results of these tests is given in Table XXIII. At the 1089K/165.4 MPa (1500°F/24 ksi) test condition, the rupture lives of the textured sheets were similar to those of the baseline sheets (Table V), but the elongations were significantly lower. No significant differences were noted in the properties obtained with respect to test direction. At the 1311K/31 MPa (1900°F/4.5 ksi) test condition, the rupture lives of the textured sheets were significantly higher than the baseline values, and independent of test direction. The elongations, on the other hand, were dependent on test direction. The values obtained in the transverse direction were lower than those for the longitudinal direction and significantly different (~99 percent confidence level). The longitudinal elongation values were equivalent to those of the baseline.

3.3.6 Creep life evaluation. - As an initial check on the quality of the textured sheets as compared to the original 8C strip, duplicate longitudinal and transverse samples from each heat were creep tested at 1200K/41.4 MPa (1700°F/6 ksi). All creep tests were conducted in accordance with the procedure given in Appendix B. Complete test data are contained in Appendix D. A summary of the log average data for creep strain levels of 0.5 percent and 1.0 percent is presented in Table XXIV along with the corresponding results for the original 8C strip and the baseline heats for comparison. Among the textured sheets of the three different heats, creep lives were found to vary above and below those for the original strip. However, the combined averages were essentially equivalent to those of the original strip. In all cases, the creep lives of the textured sheets were significantly superior to those obtained for the baseline heats.

In order to obtain a more detailed characterization of the creep strength of the textured sheets, further creep testing was conducted on each heat at temperatures of 922K (1200°F), 1144K (1600°F) and 1255K (1800°F), and at three stress levels at each temperature. All tests were performed using longitudinally oriented samples. As with the baseline, it was planned to select stresses which would give 1 percent creep lives in the range of roughly 25-500 hours. The initial stress levels selected were based on the baseline creep

TABLE XXI

TENSILE PROPERTIES OF TEXTURE STUDY SHEET - TYPE 8C*

Test Temp.	Orient.	Heat 3-1655 0.2% YS MPa	Heat 3-1655 0.2% YS (ksi)	Heat 3-1655 UTS MPa	Heat 3-1655 UTS (ksi)	Heat 3-1655 El %	Heat 4-1696 0.2% YS MPa	Heat 4-1696 0.2% YS (ksi)	Heat 4-1696 UTS MPa	Heat 4-1696 UTS (ksi)	Heat 4-1696 El %	Heat 4-1697 0.2% YS MPa	Heat 4-1697 0.2% YS (ksi)	Heat 4-1697 UTS MPa	Heat 4-1697 UTS (ksi)	Heat 4-1697 El %
R.T.	L	553.3	(80.3)	1020.4	(148.1)	57.8	475.4	(69.0)	989.4	(143.6)	59.7	474.0	(68.8)	994.2	(144.3)	62.0
	L	565.7	(82.1)	1012.8	(147.0)	54.0	487.1	(70.7)	956.3	(138.8)	64.4	483.0	(70.1)	946.0	(137.3)	65.2
	T	570.5	(82.8)	1008.7	(146.4)	64.1	460.3	(66.8)	962.5	(139.7)	68.6	494.7	(71.8)	967.4	(140.4)	68.5
	T	544.3	(79.0)	983.2	(142.7)	62.9	449.9	(65.3)	984.6	(142.9)	65.4	450.6	(65.4)	985.3	(143.0)	61.7
922 K (1200°F)	L	321.1	(46.6)	691.1	(100.3)	48.8	300.4	(43.6)	715.9	(103.9)	57.6	268.7	(39.0)	653.9	(94.9)	63.8
	L	307.3	(44.6)	713.8	(103.6)	51.6	270.8	(39.3)	669.7	(97.2)	67.5	269.4	(39.1)	696.6	(101.1)	69.3
	T	338.3	(49.1)	678.0	(98.4)	49.5	283.2	(41.1)	674.5	(97.9)	67.6	281.1	(40.8)	665.6	(96.6)	69.5
	T	328.0	(47.6)	702.1	(101.9)	59.1	281.1	(40.8)	684.2	(99.3)	70.2	309.4	(44.9)	664.9	(96.5)	61.2
1033 K (1400°F)	L	331.4	(48.1)	643.5	(93.4)	40.3	311.4	(45.2)	606.3	(88.0)	46.2	274.2	(39.8)	582.9	(84.6)	44.5
	L	336.2	(48.8)	638.0	(92.6)	38.7	305.2	(44.3)	569.1	(82.6)	42.0	307.2	(44.6)	618.0	(85.8)	47.5
	T	330.0	(47.9)	589.8	(85.6)	33.3	301.8	(43.8)	560.2	(81.3)	44.4	281.8	(40.9)	591.2	(85.8)	47.5
	T	315.6	(45.8)	602.2	(87.4)	43.1	303.8	(44.1)	613.2	(89.0)	51.1	280.4	(40.7)	533.3	(77.4)	40.0
1144 K (1600°F)	L	304.5	(44.2)	429.9	(62.4)	31.1	270.1	(39.2)	372.1	(54.0)	23.5	234.9	(34.1)	361.7	(52.5)	23.6
	L	299.7	(43.5)	425.8	(61.8)	32.4	259.1	(37.6)	372.1	(54.0)	25.5	267.3	(38.8)	392.0	(56.9)	26.6
	T	295.6	(42.9)	443.0	(64.3)	33.1	283.2	(41.1)	390.0	(56.6)	24.7	276.3	(40.1)	407.9	(59.2)	34.0
	T	296.5	(43.0)	400.3	(58.1)	31.6	263.2	(38.2)	396.2	(57.5)	37.6	283.9	(41.2)	380.3	(55.2)	29.2
1255 K (1800°F)	L	113.7	(16.5)	176.4	(25.6)	37.1	149.5	(21.7)	224.6	(32.6)	23.8	164.7	(23.9)	245.3	(35.6)	25.6
	L	159.2	(23.1)	241.2	(35.0)	26.0	146.8	(21.3)	214.3	(31.1)	26.9	145.4	(21.1)	226.0	(32.8)	23.0
	T	143.3	(20.8)	208.1	(30.2)	27.8	155.0	(22.5)	229.4	(33.3)	30.1	164.0	(23.8)	233.6	(33.9)	26.5
	T	159.2	(23.1)	229.4	(33.3)	24.8	155.0	(22.5)	227.4	(33.0)	26.8	150.9	(21.9)	210.8	(30.6)	20.8
1366 K (2000°F)	L	81.3	(11.8)	122.6	(17.8)	19.9	77.2	(11.2)	121.3	(17.6)	17.1	84.1	(12.2)	131.6	(19.1)	16.1
	L	78.5	(11.4)	124.0	(18.0)	17.6	75.1	(10.9)	122.6	(17.8)	18.6	86.8	(12.6)	130.2	(18.9)	14.3
	T	93.0	(13.5)	146.1	(21.2)	16.5	89.6	(13.0)	137.8	(20.0)	19.8	84.1	(12.2)	120.6	(17.5)	13.3
	T	77.2	(11.2)	117.1	(17.0)	14.5	75.1	(10.9)	120.6	(17.5)	15.6	91.6	(13.3)	134.4	(19.5)	11.9

* 80% cold work + 1505 K (2250°F)/10 min. final anneal

L = longitudinal

T = transverse

TABLE XXII

AVERAGE TENSILE PROPERTIES FOR TEXTURE STUDY SHEET - TYPE 8C*

Test Temp.	0.2% YS MPa	0.2% YS (ksi)	UTS MPa	UTS (ksi)	Elong. %
R.T.	500.9 (44.8)	72.7 (6.5)	984.6 (22.7)	142.9 (3.3)	62.9 (4.2)
922 K (1200°F)	296.3 (24.1)	43.0 (3.5)	684.2 (20.0)	99.3 (2.9)	61.3 (8.0)
1033 K (1400°F)	306.6 (20.0)	44.5 (2.9)	596.0 (31.7)	86.5 (4.6)	43.2 (4.8)
1144 K (1600°F)	277.7 (20.0)	40.3 (2.9)	397.6 (25.5)	57.7 (3.7)	29.2 (4.8)
1255 K (1800°F)	150.9 (13.8)	21.9 (2.0)	222.5 (17.9)	32.3 (2.6)	26.4 (4.2)
1366 K (2000°F)	82.7 (6.2)	12.0 (0.9)	127.5 (9.0)	18.5 (1.3)	16.3 (2.5)

* Standard deviations are given in parentheses.

TABLE XXIII

STRESS RUPTURE DATA FOR TEXTURE STUDY TYPE BC* SHEETS

Sample Orientation	1089 K/165.4 MPa (1500°F/24 ksi) Life Hours	Elongation %	1311 K/31 MPa (1900°F/4.5 ksi) Life Hours	Elongation %
		Heat 3-1655		
L	57.1	14.3	129.6	34.8
L	39.5	15.9	67.2	30.8
T	51.9	14.3	62.5	23.0
T	43.1	15.4	56.7	21.4
Log Avg.**	47.4	15.0	74.1	27.0
Std. Dev. (Log Units)	(.073)	(.023)	(.159)	(.101)
		Heat 4-1696		
L	26.7	20.0	64.8	23.6
L	36.2	20.7	30.8	40.4
T	43.5	20.3	59.1	23.5
T	29.2	17.3	39.9	21.8
Log Avg.**	33.3	21.6	46.6	26.4
Std. Dev. (Log Units)	(.095)	(.101)	(.151)	(.124)
		Heat 4-1697		
L	43.1	19.8	46.3	31.1
L	36.8	19.9	71.1	28.5
T	49.2	18.6	71.8	13.3
T	38.5	19.8	67.2	17.0
Log Avg.**	41.6	19.5	63.1	21.2
Std. Dev. (Log Units)	(.056)	(.014)	(.091)	(.177)
		Heats 3-1655, 4-1696 and 4-1697 Combined		
Log Avg.	40.3	18.5	60.2	24.7
Std. Dev. (Log Units)	(.096)	(.089)	(.151)	(.134)

* 80% cold work + 1505 K (2250°F)/10 min. final anneal

** $\bar{t}$ = antilog $\left(\frac{\Sigma \log t_i}{n}\right)$

L = longitudinal

T = transverse

TABLE XXIV

SUMMARY OF LOG AVERAGE DATA FOR 1200 K/41.4 MPa (1700°F/6 ksi) CREEP TESTS OF TYPE 8C TEXTURE SHEET LOTS WITH COMPARISON TO THE ORIGINAL 8C STRIP AND THE BASELINE

Sheet Lot	No. of Tests, N	0.5% Creep Strain			1.0% Creep Strain		
		Avg Log Time*	Antilog, Hrs	Std. Dev.**	Avg Log Time*	Antilog, Hrs	Std. Dev.**
Heat 3-1655	4	1.876	75.1	.093	2.270	186.2	.073
Heat 4-1696	4	1.663	46.0	.237	2.043	110.3	.222
Heat 4-1697	4	1.914	82.0	.223	2.258	181.2	.295
Combined Heats	12	1.817	65.7	.211	2.190	155.0	.225
Original 8C Strip	5	1.866	73.5	.100	2.169	147.6	.071
Baseline Heats	6	1.280	19.1	.339	1.631	42.8	.346

* $\log \bar{t} = \frac{\Sigma \log t_i}{n}$ where t_i = observed time to given creep strain

n = no. of observations

** log units

71

TABLE OF CONTENTS

		Page	
SUMMARY		1	1/A7
1.0	INTRODUCTION	3	1/A9
2.0	CABOT BASELINE DATA	5	1/A11
	2.1 Materials	5	1/A11
	2.2 Texture	5	1/A11
	2.3 Tensile Properties	14	1/B7
	2.4 Stress Rupture Properties	17	1/B12
	2.5 Creep Properties	17	1/B12
	2.5.1 Creep life evaluation	17	1/B12
	2.5.2 Minimum creep rate evaluation	25	1/C9
	2.6 Static Oxidation Resistance	31	1/D5
	2.7 Dynamic Oxidation Resistance	31	1/D5
3.0	TEXTURE STUDY	39	1/E4
	3.1 Introduction	39	1/E4
	3.2 Initial Investigaton	40	1/E5
	3.2.1 Production of experimental sheet lots	40	1/E5
	3.2.2 Examination of crystallographic texture	40	1/E5
	3.2.3 Creep strength evaluation	61	1/G1
	3.3 Evaluation of Optimum Texture Sheets	65	1/G6
	3.3.1 Production of experimental sheet lots	65	1/G6
	3.3.2 Examination of grain size and crystallographic texture	65	1/G6

TABLE OF CONTENTS (Cont.)

		Page	
3.3.3	Bend ductility	65	1/G6
3.3.4	Tensile properties	65	1/G6
3.3.5	Stress rupture properties	67	1/G8
3.3.6	Creep life evaluation	67	1/G8
3.3.7	Minimum creep rate evaluation	79	2/B3
3.3.8	Examination of microstructure after creep testing	79	2/B3
3.3.9	Residual room temperature tensile properties after creep testing	88	2/C2
4.0	GRAIN SIZE STUDY	92	2/C8
4.1	Investigation of the Dependence of Creep Strength on Grain Size	92	2/C8
4.1.1	Production of experimental sheet lots	92	2/C8
4.1.2	Examination of crystallographic texture	92	2/C8
4.1.3	Creep strength evaluation	97	2/D3
4.1.4	Apparent activation energies for creep	101	2/D9
4.2	Evaluation of ASTM 5-6 Grain Size Sheets	103	2/D12
4.2.1	Production of experimental sheet lots	103	2/D12
4.2.2	Tensile properties	107	2/E2
4.2.3	Stress rupture properties	107	2/E2
4.2.4	Creep life evaluation	107	2/E2
4.2.5	Minimum creep rate evaluation	120	2/F11
4.3	Supplementary Grain Size Study: Investigation of the Dependence of Creep Strength on Sheet Thickness	120	2/F11
4.3.1	Production of experimental sheet	124	2/G3
4.3.2	Examination of crystallographic texture	124	2/G3

TABLE OF CONTENTS (Cont.)

	Page	
4.3.3 Tensile properties	124	2/G3
4.3.4 Stress rupture properties	128	2/G8
4.3.5 Creep life evaluation	128	2/G8
4.3.6 Minimum creep rates	140	3/B7
5.0 PRESTRAIN STUDY	144	3/B12
5.1 Materials and Experimental Procedure	144	3/B12
5.2 Creep Test Results	144	3/B12
5.3 Examination of Microstructures after Creep Testing	147	3/C3
6.0 DYNAMIC OXIDATION RESISTANCE OF EXPERIMENTAL SHEETS	154	3/C10
6.1 Materials and Experimental Procedure	154	3/C10
6.2 Dynamic Oxidation Test Results	154	3/C10
7.0 DISCUSSION AND CONCLUDING REMARKS	158	3/D2
APPENDIX A - Conversion of U.S. Customary Units to SI Units	160	3/D4
APPENDIX B - Creep Test Procedure	164	3/D8
APPENDIX C - Baseline Creep Test Data	168	3/D13
APPENDIX D - Texture Study Creep Test Data	173	3/E9
APPENDIX E - Grain Size Study Creep Test Data	179	3/F7
REFERENCES	186	3/G7

test results. Additional stresses were then selected to obtain the required description of creep strength over the temperature range of interest. A complete listing of the creep test data is contained in Appendix D.

Characterization of the creep properties of the textured sheet was accomplished by subjecting the 0.5 percent and 1.0 percent creep strain data to a least squares optimization of the Larson-Miller parameter equation described in Section 2.5.1. Results of this analysis are presented in Table XXV. Plots showing the actual data and the lines given by the parameter equation are illustrated in Figures 31 and 32. The fit of the data to the Larson-Miller equation was very good with correlation coefficients of ~.94 at both creep strain levels. In comparison to the baseline (Table VI), much less scatter was observed. The standard error of the estimate and RMS values obtained were approximately half of those reported for the baseline sheets.

A comparison of Figures 31 and 32 to their baseline counterparts (Figures 7 and 8) indicated that the textured sheets provided definite improvements in creep strength at each of the temperatures investigated. To afford a more direct means of comparison, the 0.5 percent and 1.0 percent creep strain data were force-fit to the parameter equation using a value of 17 for the Larson-Miller constant as was done previously for the baseline data. The results of the force-fit analyses are presented in Table XXVI. The RMS value for the 0.5% creep strain data was equivalent to that obtained in the optimized Larson-Miller analysis, while that obtained for the 1.0% creep strain data was slightly higher. These variations in agreement reflect the difference between the values obtained for the Larson-Miller constant in the optimized analyses and the value of 17 assumed in the forced-fit approach.

Comparison plots of the baseline and texture study creep properties based on the force-fit of the Larson-Miller parameter equation are presented in Figures 33 and 34. The minus 2-sigma and minus 3-sigma limits based on the standard errors of the estimates are also illustrated for the texture study sheets so that the significance of the differences in creep properties can be appreciated. That is, only 2.27 percent of the test results at a given creep test condition are expected to be less than the value given by the minus 2-sigma limit, and only 0.13 percent are expected to be less than the value given by the minus 3-sigma limit. Using these criteria, Figures 33 and 34 indicate that the textured sheet offer a significant improvement in creep strength over the baseline over most of the range of test conditions. Specifically, the minus 3-sigma limits of the textured sheets are above the baseline average from approximately 206.8 MPa/18 x 10^3 LMP-K (30 ksi/32.5 x 10^3 LMP-°R) to 17.2 MPa/23.5 x 10^3 LMP-K (2.5 ksi/42.3 x 10^3 LMP-°R) for 0.5% creep strain, and from 172.4 MPa/18.9 x 10^3 LMP-K (25 ksi/34 x 10^3 LMP-°R) for 1.0% creep strain. The minus 2-sigma limits of the textured sheets are superior to the baseline average from approximately 290 MPa/17.2 x 10^3 LMP-K (42 ksi/31 x 10^3 LMP-°R) to 12.4 MPa/24.1 x 10^3 LMP-K (1.8 ksi/43.4 x 10^3 LMP-°R) for 0.5% creep strain, and from 297 MPa/17.5 x 10^3 LMP-K (43 ksi/31.5 x 10^3 LMP-°R) to 8.6 MPa/25.2 x 10^3 LMP-K (1.25 ksi/45.4 x 10^3 LMP-°R) for 1.0% creep strain.

TABLE XXV

OPTIMIZED LARSON-MILLER PARAMETER ANALYSIS OF TYPE 8C TEXTURE STUDY SHEETS

Regression Equation: $Y = \log t = C_1 + \frac{C_2}{T} + \frac{C_3}{T} \log S + \frac{C_4}{T} (\log S)^2$

A. Where T = Absolute temperature, Kelvin

t = Time to fiven creep strain, hours

S = Stress, MPa

Creep Strain	Equation Parameters				Fit of Test Data			
	C_1	C_2	C_3	C_4	Std. Error of Estimate	Correlation Coefficient	Number of Tests	RMS
0.5%	17.2025	25789.5	933.04	-1690.86	.185	.941	39	.176
1.0%	19.6910	30433.8	256.59	-1726.15	.198	.946	39	.187

B. Where T = Absolute temperature, degrees Rankine

t = Time to fiven creep strain, hours

S = Stress, ksi

0.5%	17.2025	45689.2	-3424.68	-3043.55	.185	.941	39	.176
1.0%	19.6910	52983.5	-4748.79	-3107.06	.198	.946	39	.187

73

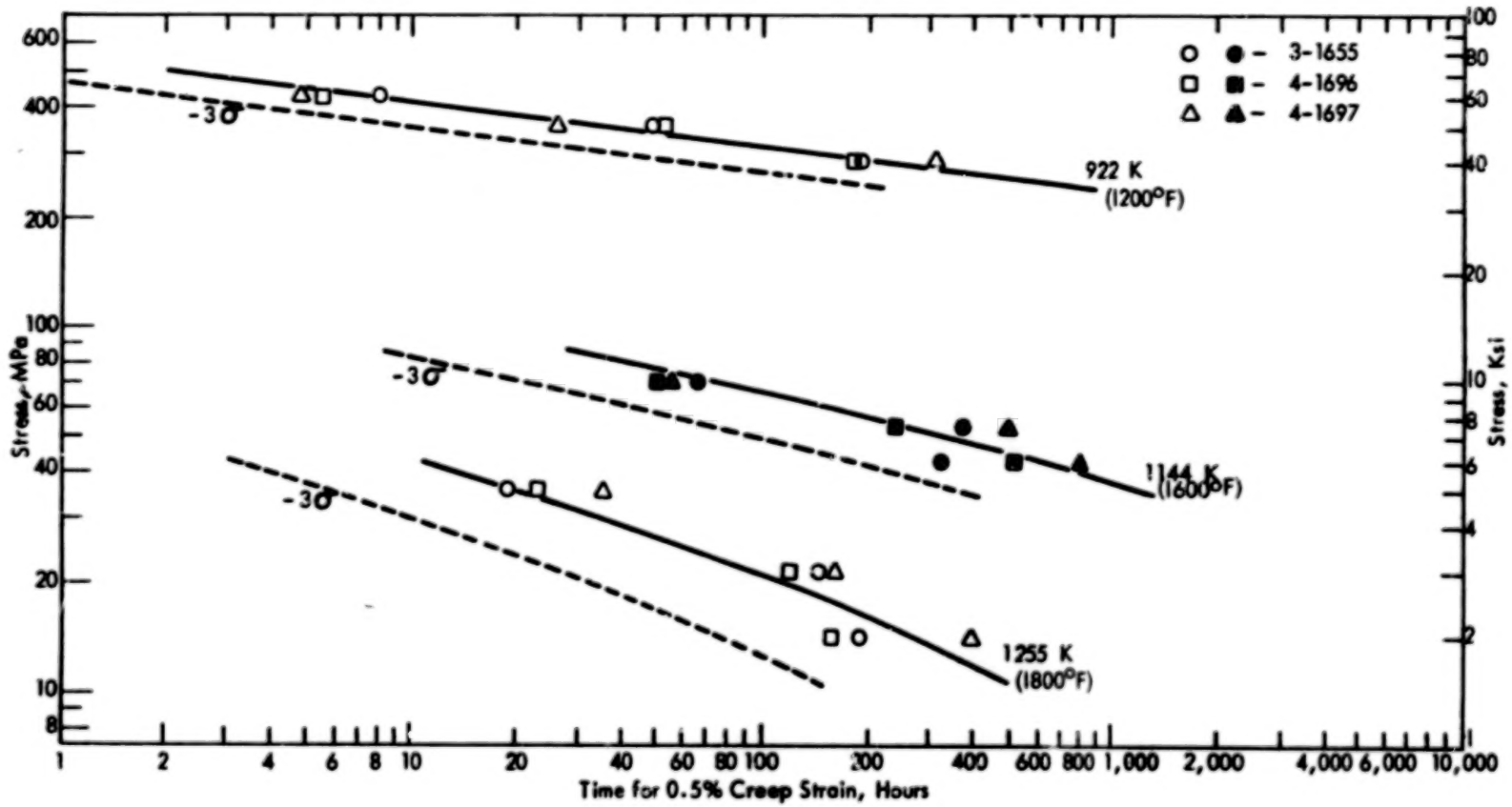

Figure 31: Stress vs. 0.5% Creep Life for Texture Study Sheets (Actual Data and Parametric Evaluation).

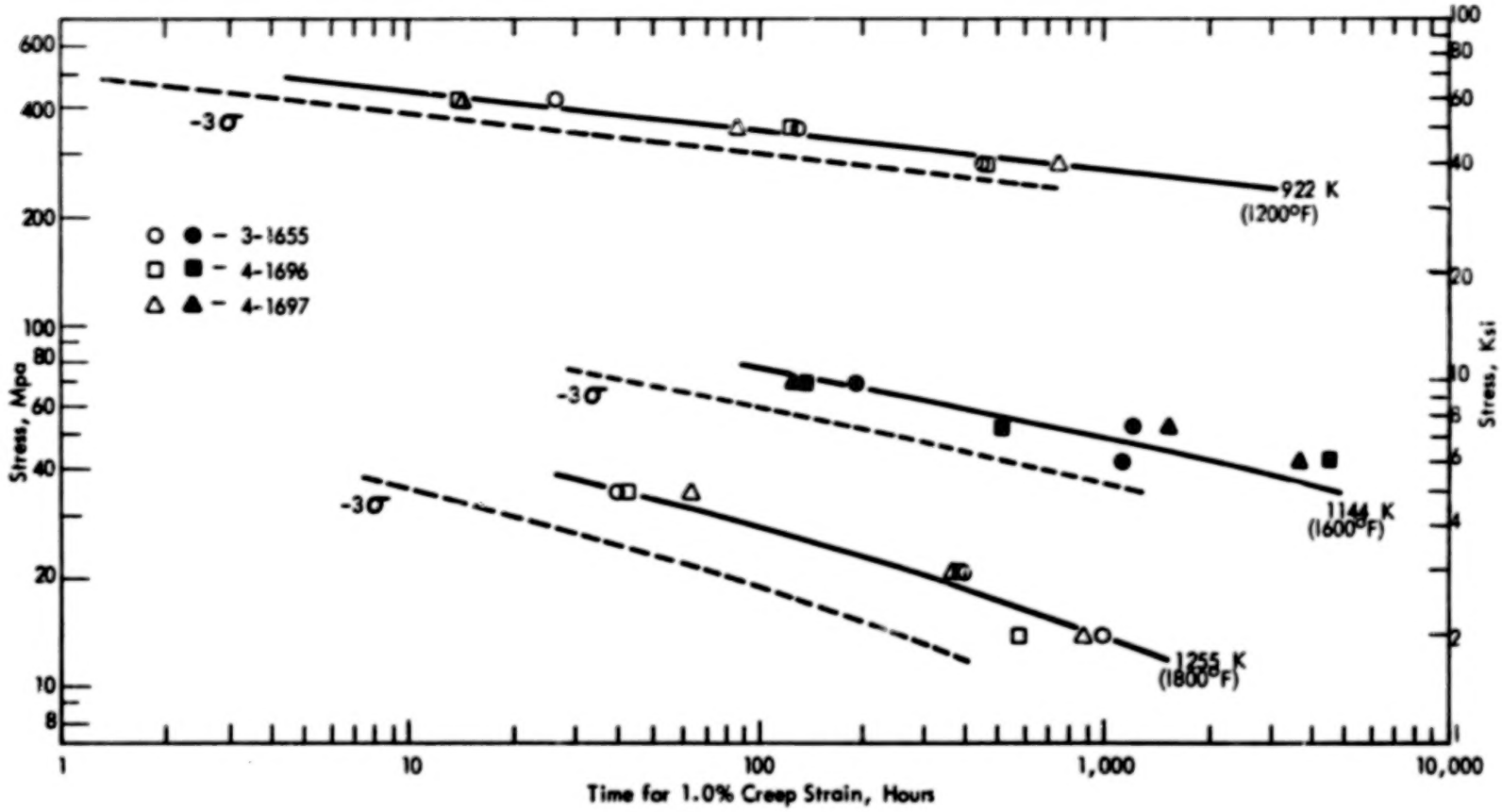

Figure 32: Stress vs. 1.0% Creep Life for Texture Study Sheets. (Actual Data and Parametric Evaluation)

75

TABLE XXVI

FORCE-FIT OF TEXTURE STUDY CREEP DATA TO THE LARSON-MILLER PARAMETER EQUATION WITH A LARSON-MILLER CONSTANT OF 17

Regression Equation: $P = T (\log t + 17) = C_2 + C_3 \log S + C_4 (\log S)^2$

A. Where T = Absolute temperature, Kelvin

t = Time to given creep strain, hours

S = Stress, MPa

Creep Strain	Equation Parameters			Fit of Test Data			
	C_2	C_3	C_4	Std. Error of Estimate, LM Parameter Units	Correlation Coefficient	Number of Tests	RMS
0.5%	25565.8	879.14	-1664.23	212.96	.997	39	.176
1.0%	26813.0	184.60	-1521.45	237.72	.996	39	.197

B. Where T = Absolute temperature, degrees Rankine

t = Time to given creep strain, hours

S = Stress, ksi

0.5%	45239.0	-3441.29	-2995.61	383.34	.997	39	.176
1.0%	46614.5	-4260.47	-2739.61	427.90	.996	39	.197

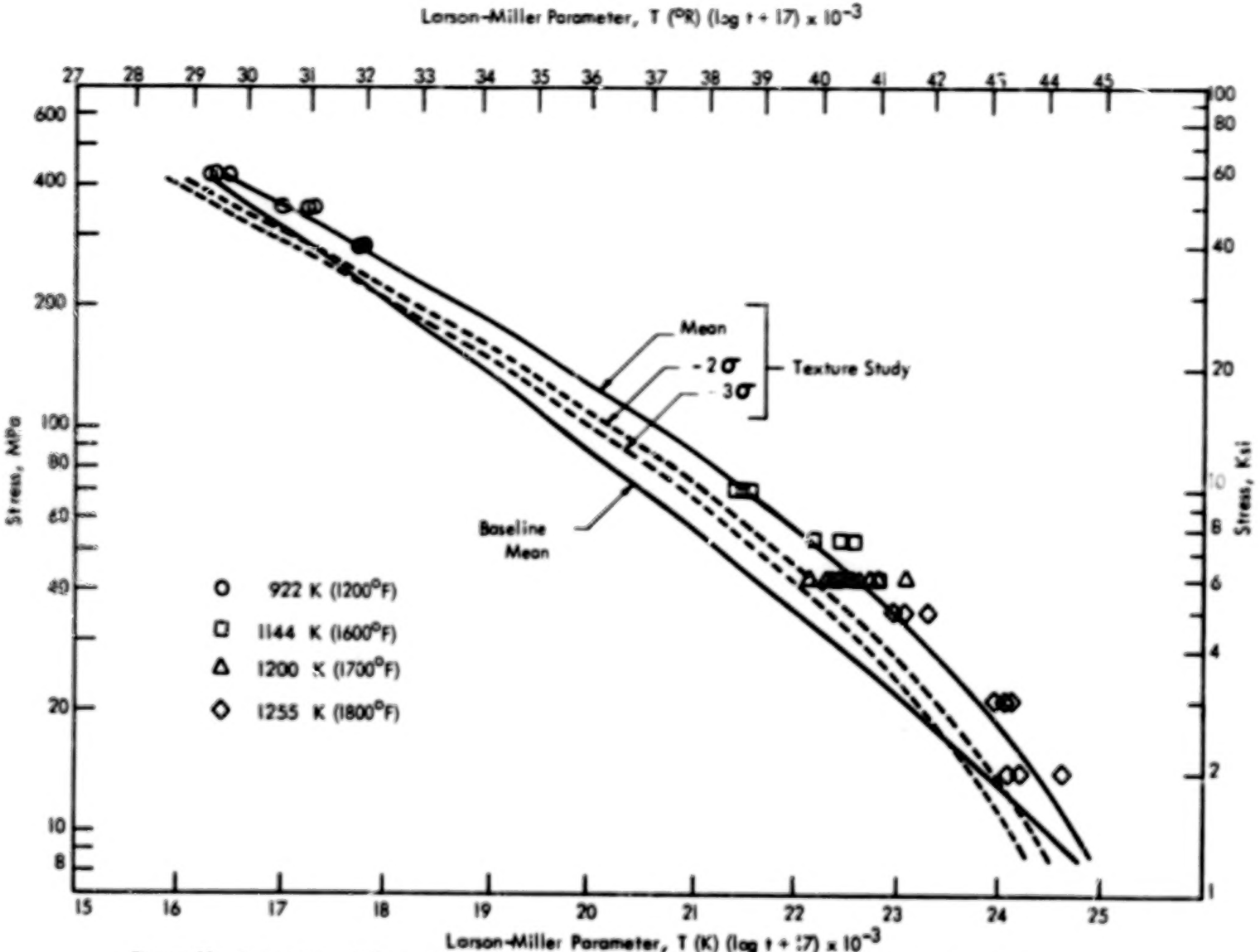

Figure 33: Comparison of Stress vs. Larson-Miller Parameter (C_1 = 17) for 0.5% Creep Lives of Baseline and Texture Study Sheets.

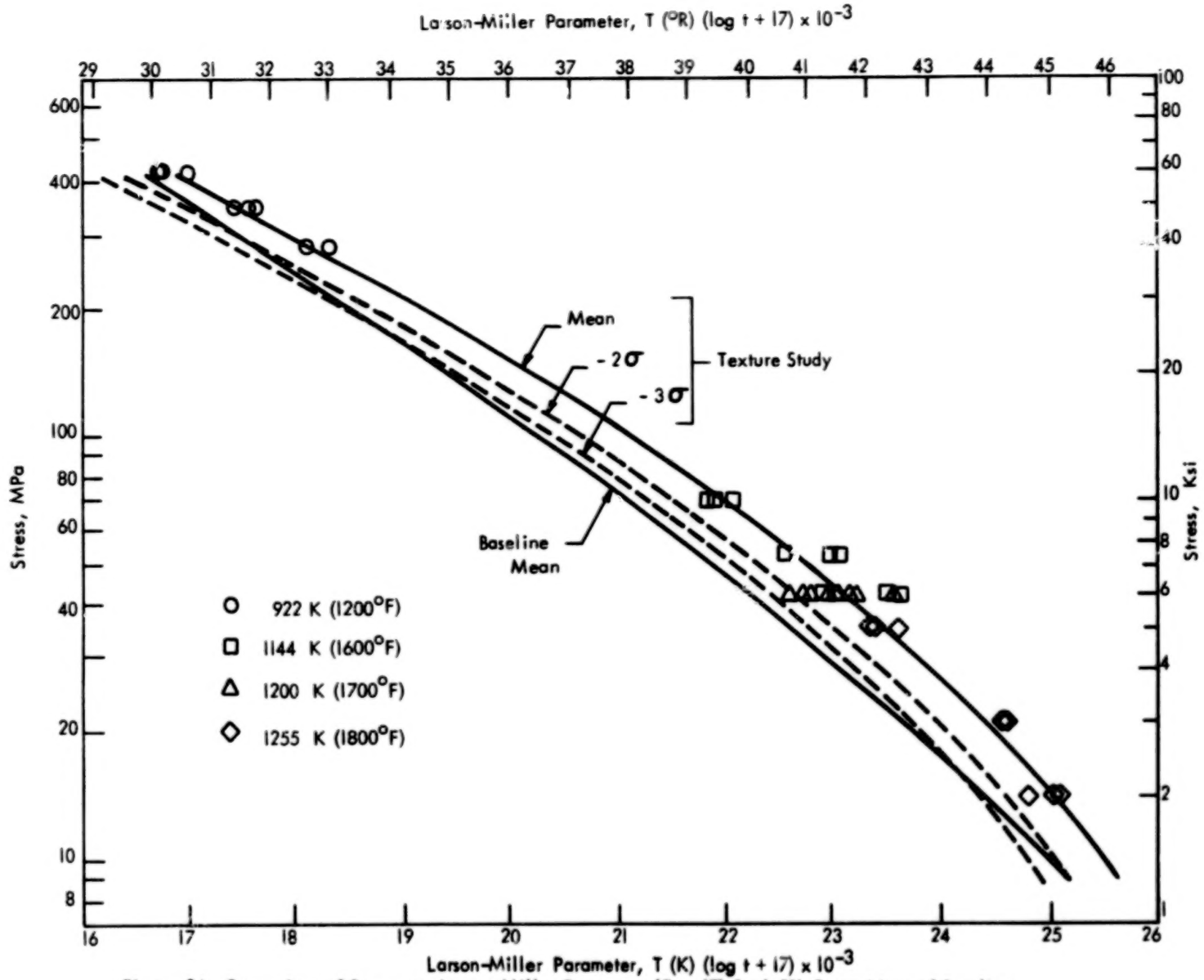

Figure 34: Comparison of Stress vs. Larson-Miller Parameter (C_1 = 17) for 1.0% Creep Lives of Baseline and Texture Study Sheets.

3.3.7 Minimum creep rate evaluation. - The minimum creep rate data obtained for the texture study sheets were subjected to multiple regression analyses assuming both power and exponential stress functional relationships as described in Section 2.5.2 Results of these analyses are presented in Tables XXVII and XXVIII. As was found in the analyses of the baseline data, essentially equivalent fits were obtained with either equation form. The explanation of this behavior is likely the same as that described for the baseline. Namely, the inequalities for αS based on the hyperbolic sine law were not fulfilled, and the overlap in αS allowed either function to provide a reasonable fit to the data.

As in the case of the baseline data, it was considered more useful to describe the minimum creep rates of the textured sheets in terms of the power function of stress. Plots of the data in this form are shown in Figure 35. The minimum creep rates of the textured sheets were generally lower than those observed in the baseline sheets (Figure 11) at equivalent stress levels. These differences were most pronounced at the 1144K (1600°F) and 1255K (1800°F) test temperatures where the minimum creep rates of the textured sheets were more than five times lower than those of the baseline sheets. Examination of the power function parameters contained in Tables X and XXVII also revealed some striking differences. At the 922K (1200°F) and 1144K (1600°F) test temperatures, the "structure factor" parameters of the textured sheets were several order of magnitude smaller than those of the baseline. At the same time, however, the stress exponents of the textured sheets were higher, indicating a greater sensitivity to the level of stress which resulted in a reduction of the overall effects on the minimum creep rates. At the 1255K (1800°F) test temperature, the stress exponents of the textured and the baseline sheets were approximately equal, but the "structure factor" parameter of the textured sheets was still approximately one-half an order of magnitude less than that of the baseline.

3.3.8 Examination of microstructures after creep testing. - The differences noted between the textured and the baseline sheets with respect to their low strain creep lives and minimum creep rates strongly suggested the possibility of significant microstructural differences. To test this hypothesis, a brief investigation was conducted on the samples which had been creep tested at 1200K/41.4 MPa (1700°F/6 ksi). The crept samples were examined using the techniques of both optical metallography and transmission electron microscopy so that bulk as well as microstructural features could be appreciated.

Optical photomicrographs of typical structures observed in the three baseline heats and in the textured sheets produced from Heat 3-1655 are presented in Figures 36 and 37, respectively. In all cases, the metallographic sections were prepared and photographed such that the specimen tensile axis lies in the field of view parallel to the horizontal axis of the photograph. This was done to detect any structural changes that might be associated with the direction of stress.

TABLE XXVII

ANALYSIS OF TEXTURE STUDY MINIMUM CREEP RATES
AS A POWER FUNCTION OF STRESS*

Temp.	log A		n	Std. Error of Estimate, Log Units	Correlation Coefficient
	Stress as MPa	Stress as KSI			
922 K (1200°F)	-22.206	(-13.572)	7.92	.142	.977
1144 K	-14.979	(-9.181)	6.91	.313	.915
1255 K (1800°F)	-7.098	(-4.225)	3.43	.154	.972

* $\log \dot{\epsilon}_{min} = \log A = n \log S$

$\dot{\epsilon}_{min}$ = minimum creep rate, %/hr

S = stress (MPa or ksi)

A, n = constants estimated by method of least squares

TABLE XXVIII

ANALYSIS OF TEXTURE STUDY MINIMUM CREEP RATES
AS AN EXPONENTIAL FUNCTION OF STRESS*

Temp.	log A'	β		Std. Error of Estimates, Log Units	Correlation Coefficient
		Stress as MPa	Stress as KSI		
922 K (1200°F)	-5.661	.0102	(.0703)	.125	.982
1144 K (1600°F)	-6.040	.0551	(.3796)	.317	.913
1255 K (1800°F)	-4.052	.0659	(.4541)	.107	.986

---

* $\log \dot{\epsilon}_{min} = \log A' + \beta S$

$\dot{\epsilon}_{min}$ = minimum creep rate, %/hr

S = stress (MPa or KSI)

A', β = constants estimated by method of least squares

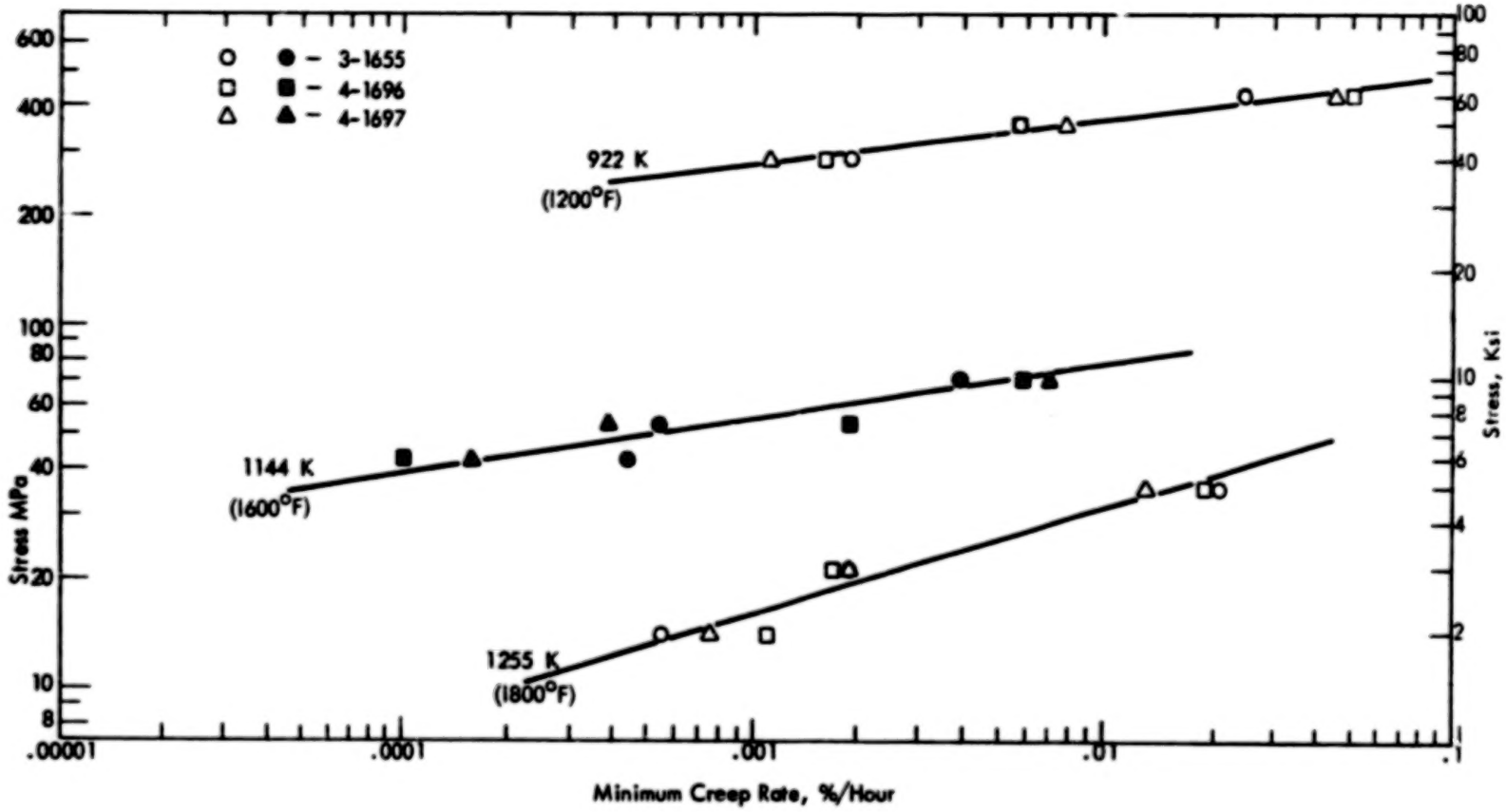

Figure 35: Stress vs. Minimum Creep Rate for Texture Study Sheets.

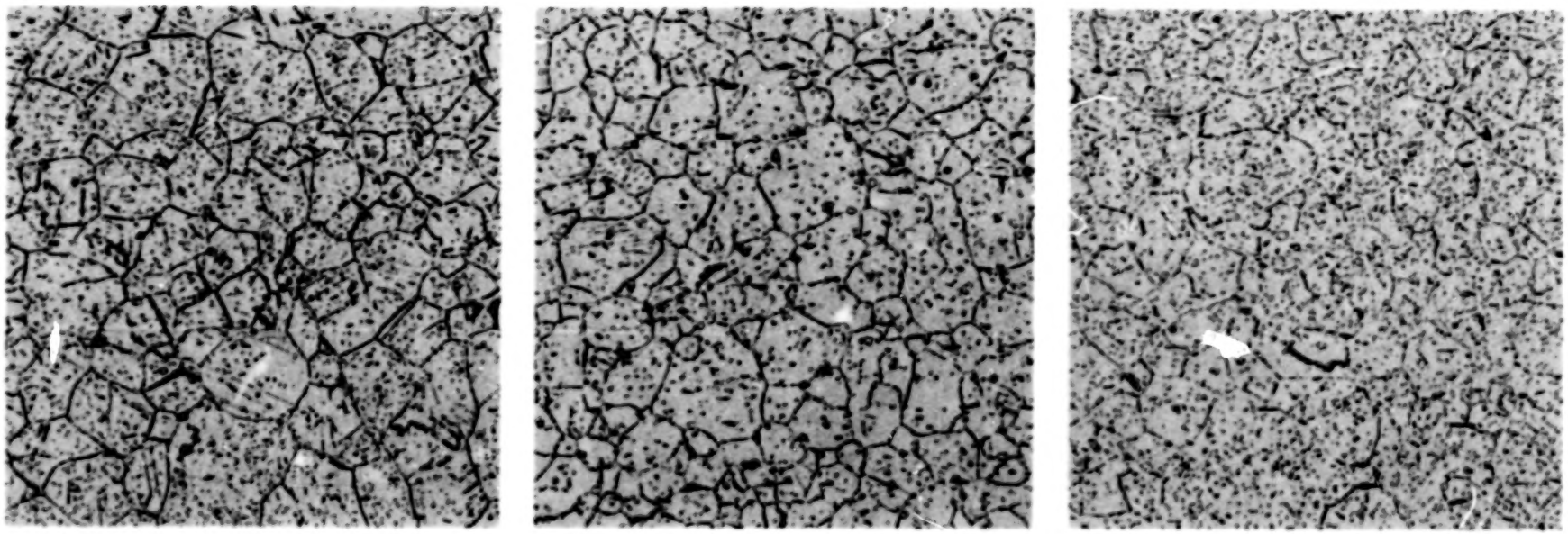

(a) (b) (c)

Figure 36: Optical Photomicrographs of Baseline Sheets after Creep Testing at 1200K/41.4 MPa (1700°F/6 ksi): (a) Heat 2-1604, (b) Heat 3-1622, (c) Heat 4-1671. Test specimens were oriented transverse to the rolling direction. X300.

(a) (b) (c)

Figure 37: Optical photomicrographs of Textured Sheet Produced from Heat 3-1655 after Creep Testing at 1200K/41.4 MPa (1700°F/6 ksi): (a) Original 8C Strip, Tensile Axis Parallel to Rolling Direction, (b) Type 8C Sheet, Tensile Axis Parallel to Rolling Direction, (c) Type 8C Sheet, Tensile Axis Transverse to Rolling Direction. X300.

The extent of secondary carbide precipitation in the various samples after creep testing was quite pronounced as judged from the as-annealed microstructures (Figures 1-3 for the baseline sheets and Figure 17(c) for the original 8C textured strip). However, this type of precipitation behavior can be considered normal for HAYNES alloy No. 188 based on its aging response at 1200K (1700°F) (ref. 2 and 6) albeit somewhat accelerated due to the condition of continual plastic deformation. The crept microstructures of the baseline sheets were typified by fine precipitates distributed both randomly and in grain boundaries. Twin boundaries contained few precipitates. In contrast, the microstructures of the textured sheets contained relatively coarse carbides distributed randomly and in grain boundaries, and precipitation on twin boundaries was much more in evidence. Neither the baseline sheets nor the textured sheets showed any signs of grain size instability, or any microstructural feature which could be associated with the direction of the tensile stress.

Information on the substructures produced during creep deformation was obtained through examination of the crept samples by transmission electron microscopy. Representative electron micrographs of the baseline and textured sheets are illustrated in Figures 38 and 39, respectively. Comparison of the photographs reveals some major substructural differences. Typical dislocation structures in the baseline sheets consisted of tangles produced by the intersection and reaction of the glide dislocations, and pile-ups at relatively large carbide particles and grain boundaries. For the textured sheets, on the other hand, there was a marked tendency toward the formation of dislocation subboundaries. These occurred in the form of loosely constructed subgrain walls as shown in Figure 39(a), or as well defined planar networks resulting from the interaction of the primary glide dislocations as shown in Figure 39(b). In addition to this, fine carbide precipitates were observed within the dislocation boundaries and on tangled dislocations as shown in Figures 39(b), (c), and (d).

These observations provide the basis for explaining the improved creep resistance of the textured sheets:

1. The preferred grain orientations promote the formation of dislocation subboundaries which represents an effective stalemating process for the glide dislocations.

2. The carbon taken into solution during the high temperature final annealing treatment provides an additional source of impediment to dislocation flow through the precipitation of fine carbides on partially immobilized dislocations.

Using this model, the observed temperature and stress effects can be qualitatively understood. At the lowest test temperature, 922K (1200°F), carbide precipitation kinetics are slow. At high stress levels such as 413.7 MPa (60 ksi), creep resistance is principally a function of dislocation dynamics the driving force of which is too high for effective stalemating by dislocation boundaries. As the stress level is reduced, subboundary stalemating becomes more effective, and the reduced deformation rate allows sufficient time for carbide precipitation to become effective. This might ex-

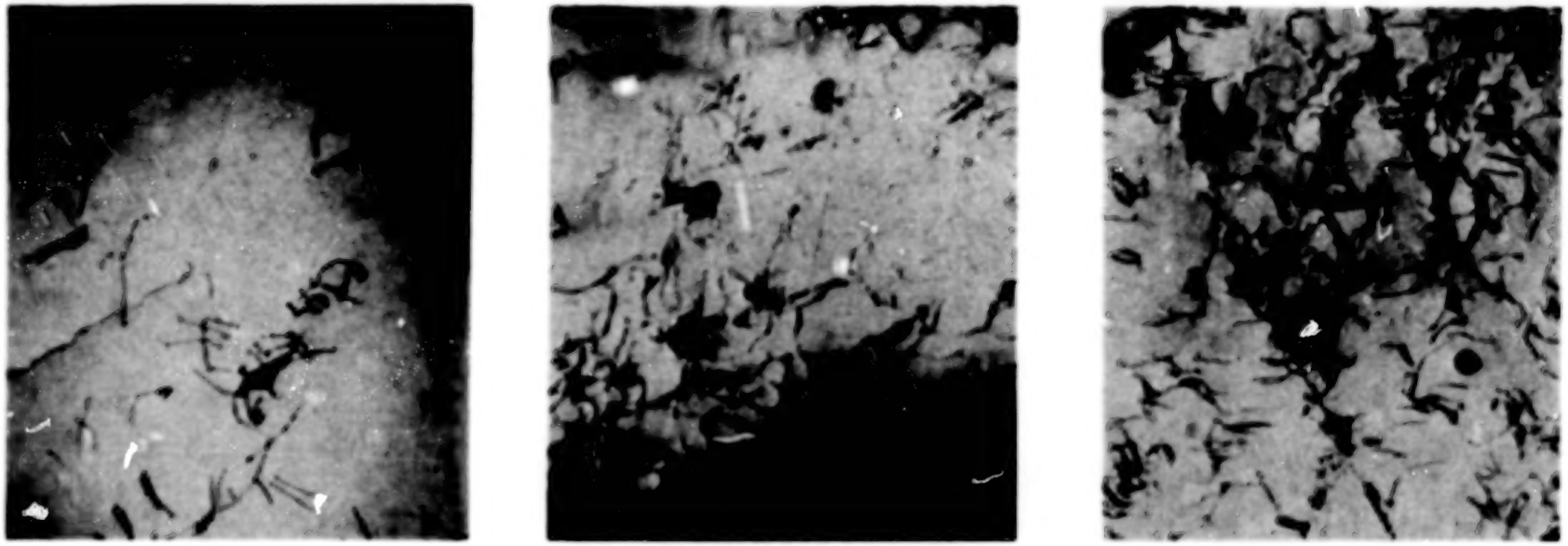

(a) Heat 2-1604 (b) Heat 3-1622 (c) Heat 4-1671

Figure 38: Substructures Observed in "HAYNES" ALLOY No. 188 Baseline Thin Gauge Sheets after Creep Testing at 1200K/41.4 MPa (1700°F/6 ksi). X23,900.

(a) Heat 3-1655
Original 8C Strip. X9,500

(b) Heat 3-1655
Type 8C. X15,100.

(c) Heat 4-1696
Type 8C. X23,900.

(d) Heat 4-1697
Type 8C. X23,900.

Figure 39: Substructures Observed in Textured Thin Gauge Sheets after Creep Testing at 1200K/41.4 MPa (1700°F/6 ksi)

plain why the stress dependence of the minimum creep rate at 922K (1200°F) is so great. At the intermediate test temperature, 1144K (1600°F), carbide precipitation kinetics are much more rapid, and the stress level, within the range investigated, was not so important. At the highest test temperature, 1255K (1800°F), carbide precipitation kinetics are very rapid. However, the nature of the carbides is different in terms of type (principally M_6C) and tendency toward coarse sizes. At high stress levels, there should be an abundance of dislocation sites available for carbide nucleation so that an effective distribution of relatively fine carbides should be obtained. At low stress levels, fewer dislocation nucleation sites would be available. This would make grain boundary precipitation more favorable, and the carbides precipitated on dislocations would be expected to be relatively coarse and sparsely distributed. The creep resistance would, therefore, again depend principally on dislocation subboundary formation.

3.3.9 Residual room temperature tensile properties after creep testing. - Due to the significant improvement in creep strength obtained in the textured sheets, it was considered important to examine the residual room temperature tensile properties of the crept specimens in order to assess any creep damage effects. For the purpose of comparison, creep specimens from the baseline sheets were also examined. Samples were selected so as to include both short- and long-term tests in order to appreciate any effects due to aging. The data obtained for the baseline and textured sheets are listed in Tables XXIX and XXX, respectively. Comparisons to the room temperature tensile properties of these materials in the as-annealed condition can be made by referring to Tables III and XXI, respectively.

Observations on the residual tensile properties can be summarized according to creep test temperature in the following manner:

922K (1200°F) Creep Test Samples

A large increase in yield strength and a slight increase in ultimate tensile strength were obtained in both the baseline and the texture study sheets. No significant differences were noted for the texture study sheets with respect to test duration. For the baseline sheets, on the other hand, yield strength levels obtained in long-term tests were less than those for short-term tests. Although the materials of both studies exhibited a significant decrease in ductility, the residual levels of elongation were still reasonably high. Aside from one test, residual baseline ductilities were on the average slightly higher than those of the textured sheets.

1144K (1600°F) Creep Test Samples

For HAYNES alloy No. 188, it is known that maximum property degradation occurs on aging at 1144K (1600°F) (ref. 2) and the property most affected is ductility. The much lower elongation values obtained from the samples, therefore, were not surprising. To emphasize the effect of time at temperature, samples representing short, intermediate, and long-term tests were evaluated. The trend of decreasing residual ductility with increasing exposure time

TABLE XXIX

RESIDUAL ROOM TEMPERATURE TENSILE PROPERTIES OF BASELINE SHEETS

Heat No.	Creep Condition	Total Time, hr.	0.2%, YS MPa	0.2%, YS (ksi)	UTS MPa	UTS (ksi)	Elong. %
2-1604	922 K/206.8MPa (1200°F/30 ksi)	950.8	587.0	(85.2)	966.7	(140.3)	44.3
"	922 K/344.7MPa (1200°F/50 ksi)	65.5	700.0	(101.6)	832.3	(120.8)	11.2
3-1622	922 K/206.8MPa (1200°F/30 ksi)	949.5	856.6	(95.3)	1075.5	(156.1)	37.8
"	922 K/344.7MPa (1200°F/50 ksi)	90.0	698.7	(101.4)	1083.8	(157.3)	43.0
4-1671	922 K/206.8MPa (1200°F/30 ksi)	558.0	627.7	(91.1)	1026.6	(149.0)	33.5
"	922 K/344.7MPa (1200°F/50 ksi)	92.1	735.2	(106.7)	1043.2	(151.4)	31.8
2-1604	1144 K/27.6MPa (1600°F/4 ksi)	2031.9	440.3	(63.9)	777.9	(112.9)	7.1
"	1144 K/51.7MPa (1600°F/7.5 ksi)	90.0	467.1	(67.8)	875.7	(127.1)	15.8
"	1144 K/68.9MPa (1600°F/10 ksi)	21.4	476.1	(69.1)	913.6	(132.6)	33.7
3-1622	1144 K/27.6MPa (1600°F/4 ksi)	7864.5	396.2	(57.5)	703.5	(102.1)	6.4
"	1144 K/51.7MPa (1600°F/7.5 ksi)	357.3	462.3	(67.1)	800.6	(116.2)	7.2
"	1144 K/68.9MPa (1600°F/10 ksi)	63.8	474.0	(68.8)	989.4	(143.6)	33.8
4-1671	1144 K/27.6MPa (1600°F/4 ksi)	3545.0	417.5	(60.6)	767.6	(111.4)	8.4
"	1144 K/51.7MPa (1600°F/7.5 ksi)	114.3	475.4	(69.0)	967.4	(140.4)	23.2
"	1144 K/68.9MPa (1600°F/10 ksi)	17.8	483.7	(70.2)	961.8	(139.6)	28.3
2-1604	1255 K/13.8MPa (1800°F/2 ksi)	425.9	407.2	(59.1)	868.1	(126.0)	40.1
"	1255 K/27.6MPa (1800°F/4 ksi)	62.8	439.6	(63.8)	921.2	(133.7)	37.5
3-1622	1255 K/13.8MPa (1800°F/2 ksi)	280.3	425.8	(61.8)	919.1	(133.4)	43.9
"	1255 K/27.6MPa (1800°F/4 ksi)	47.0	432.0	(62.7)	955.6	(138.7)	47.8
4-1671	1255 K/13.8MPa (1800°F/2 ksi)	164.7	415.5	(60.3)	872.3	(126.6)	23.5
"	1255 K/27.6MPa (1800°F/4 ksi)	16.4	435.5	(63.2)	968.1	(140.5)	47.4

89

TABLE XXX

RESIDUAL ROOM TEMPERATURE TENSILE PROPERTIES OF TEXTURE STUDY - TYPE 8C SHEETS

Heat No.	Creep Condition	Total Time, hrs.	0.2%, YS		UTS		Elong. %
			Mpa	(ksi)	MPa	(ksi)	
3-1655	922 K/275.8MPa (1200°F/40 ksi)	478.2	708.3	(102.8)	1088.6	(158.0)	29.3
"	922 K/344.7MPa (1200°F/50 ksi)	142.4	693.8	(100.7)	1022.5	(148.4)	23.2
4-1696	922 K/275.8MPa (1200°F/40 ksi)	501.1	730.3	(106.0)	1107.2	(160.6)	29.4
"	922 K/344.7MPa (1200°F/50 ksi)	160.0	714.5	(103.7)	1087.9	(157.9)	32.3
4-1697	922 K/275.8MPa (1200°F/40 ksi)	834.0	724.1	(105.1)	1045.9	(151.8)	23.4
"	922 K/344.7MPa (1200°F/50 ksi)	136.0	734.5	(106.6)	1065.2	(154.6)	30.9
3-1655	1144 K/41.4MPa (1600°F/6 ksi)	1247.3	467.8	(67.9)	844.7	(122.6)	8.6
"	1144 K/51.7MPa (1600°F/7.5 ksi)	1292.3	455.4	(66.1)	692.5	(100.5)	4.2
"	1144 K/68.9MPa (1600°F/10 ksi)	238.6	502.3	(72.9)	884.7	(128.4)	13.6
4-1696	1144 K/41.4MPa (1600°F/6 ksi)	4842.4	398.9	(57.9)	634.6	(92.1)	2.9
"	1144 K/51.7MPa (1600°F/7.5 ksi)	545.2	442.3	(64.2)	776.5	(112.7)	7.0
"	1144 K/68.9MPa (1600°F/10 ksi)	191.8	467.8	(67.9)	789.6	(114.6)	9.9
4-1697	1144 K/41.4MPa (1600°F/6 ksi)	3886.3	410.0	(59.5)	737.9	(107.1)	5.6
"	1144 K/51.7MPa (1600°F/7.5 ksi)	1647.6	447.2	(64.9)	729.7	(.05.9)	4.4
"	1144 K/68.9MPa (1600°F/10 ksi)	159.5	480.2	(69.7)	848.9	(123.2)	14.5
3-1655	1255 K/13.8MPa (1800°F/2 ksi)	1127.5	364.5	(52.9)	736.5	(106.9)	14.8
"	1255 K/34.5MPa (1800°F/5 ksi)	63.4	425.1	(61.7)	897.8	(130.3)	27.1
4-1696	1255 K/13.8MPa (1800°F/2 ksi)	642.2	387.9	(56.3)	842.7	(122.3)	26.6
"	1255 K/34.5MPa (1800°F/5 ksi)	64.6	384.5	(55.8)	797.9	(115.8)	18.8
4-1697	1255 K/13.8MPa (1800°F/2 ksi)	909.6	374.1	(54.3)	781.3	(113.4)	21.4
"	1255 K/34.5MPa (1800°F/5 ksi)	90.6	426.5	(61.9)	908.8	(131.9)	31.5

is clearly evident from the values listed in the tables. The minimum levels reported for the baseline and texture study sheets for long-term tests are essentially equivalent. Due to the large differences in short-term test durations between the baseline and textured sheets, a direct comparison of the residual ductilities cannot be made. It is conceivable, however, that the textured sheet with its higher solution temperature, would exhibit a more rapid initial decrease in ductility with exposure time than would the baseline sheets.

Strength values were also found to decrease with exposure. Yield strengths were not as greatly affected as ultimate strength values. The minimums found for long-term tests were roughly equivalent for the baseline and textured sheets.

1255K (1800°F) Creep Test Samples

Samples creep tested at 1255K (1800°F) exhibited residual ductility levels which were comparable to those obtained for the 922K (1200°F) test samples. The elongation values for the baseline sheets were significantly higher than those for the textured sheets. However, the residual ductility levels of the textured sheets were still reasonably high.

The yield strength values of the baseline and textured sheets were slightly lower than those obtained for the 1144K (1600°F) creep test samples. Values reported for the baseline sheets were slightly higher than those for the textured sheets. The residual ultimate tensile strengths were comparable to those of the 1144K (1600°F) samples. Based on values obtained for short-term tests, the rate of decline was greater in the textured sheets.

In summary, the room temperature tensile properties of both the baseline and the textured sheets were generally adversely affected by high-temperature creep. The property most affected in a detrimental way was ductility. The baseline sheets tended to be superior to the textured sheets in terms of the amount of ductility retained after creep test exposure. However, the residual ductilities obtained for the textured sheets in this investigation were at levels which would not discourage consideration of using such materials for high-temperature applications.

4.0 GRAIN SIZE STUDY

4.1 Investigation of the Dependence of Creep Strength on Grain Size

The purpose of this investigation was to determine whether a significant improvement in the low strain ($\leq$ 1 percent) creep strength of HAYNES alloy No. 188 thin gauge sheet could be achieved through the optimization of grain size. To accomplish this, sheets nominally .38 mm (.015 inch) thick having uniform grain sizes corresponding to ASTM 7-8, ASTM 5-6, and ASTM 2-4 were evaluated. These sheets were produced in the laboratory from three heats of standard production hot-rolled sheet plate nominally 4.57 mm (.180 inch) thick. In order to determine the TMP schedules which would provide the required grain sizes, an initial laboratory processing study was carried out. The variables employed in this study were limited to amounts of cold work, annealing temperature and time at temperature. The range of each variable was also restricted to be within current production capabilities. In addition, emphasis was placed on determining processing schedules which would minimize microstructural variations other than grain size. The final TMP schedules resulting from this study are presented in Table XXXI.

4.1.1 Production of experimental sheet lots. - Using the processing schedules listed in Table XXXI, strips nominally .38 mm (.015 inch) thick were produced with grain sizes of ASTM 7-8, ASTM 5-6, and ASTM 2-4 using 4.57 mm (.180 inch) thick hot-rolled plate from each of Heats 3-1655, 4-1696, and 4-1697 as starting material. The chemical analyses of these heats were previously given in Table XIV. The starting pieces measured 4.57 mm x 25.4 mm wide x 152.4 mm long (.180 inch x 1 inch x 6 inches). All cold rolling was carried out parallel to the original hot-rolling direction. The resulting strips measured approximately .38 mm x 28.6 mm wide x 127 cm long (.015 inch x 1.125 inches x 50 inches). After the final annealing treatment, each strip was salt bath descaled and flattened by stretcher leveling. Optical photomicrographs illustrating typical structures observed in the initial sheet lots are presented in Figures 40-42.

4.1.2 Examination of crystallographic texture. - Samples from the experimental strips were examined for crystallographic texture in the plane of the sheet using the diffractometer reflection method previously described in Section 2.2. In each case, the (111) pole figure was determined and evaluated.

Judging from the strip chart recordings of the diffracted X-ray intensities, the strips comprising the ASTM 2-4 sheet lot were very weakly textured. That is, the diffracted beam intensity scans were jagged and not much above the background levels. Furthermore, the scans did not possess distinct intensity maxima or minima which are indicative of crystallographic texturing.

TABLE XXXI

THERMOMECHANICAL PROCESSING SCHEDULES FOR GRAIN SIZE STUDY SHEETS

ASTM 2-4

4.57mm (.180") — Cold Roll — 2.29mm* (.090") — Cold Roll — .89mm* (.035") — Cold Roll — .38mm* (.015") — Stretcher Level 3% — .38mm (.015")

*Intermediate and final anneals at 1463 K (2175°F)/10 min.

ASTM 5-6

4.57mm (.180") — Cold Roll — 2.29mm (.090") — Cold Roll — .89mm (.035") — Cold Roll — .38mm (.015")

Anneal at 1463 K(2175°F)/10 min — Anneal at 1478 K(2200°F)/10 min — Anneal at 1463 K(2175°F)/10 min

ASTM 7-8

4.57mm (.180") — Cold Roll — 2.54mm* (.100") — Cold Roll — 1.52mm* (.060") — Cold Roll — .38mm (.015")

*Intermediate and final anneals at 1450 K (2150°F)/10 min.

93

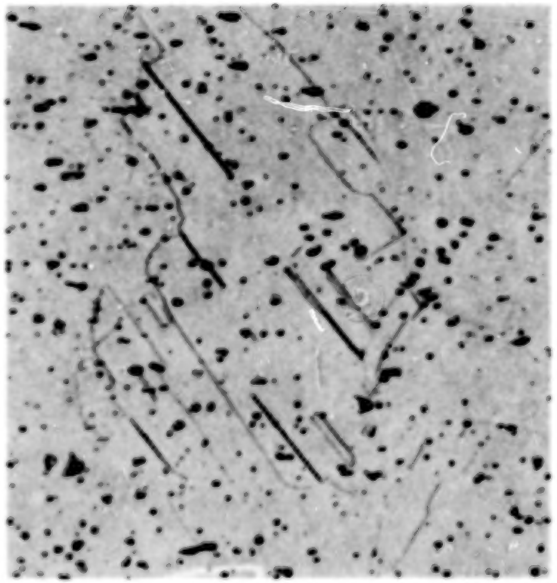

(a) Heat 3-1655
Grain Size ASTM 2-1/2-3-1/2.
X300.

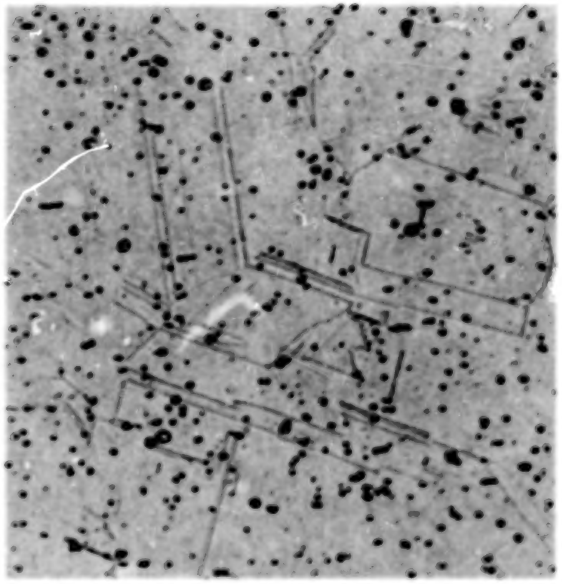

(b) Heat 4-1696
Grain Size ASTM 3.
X300.

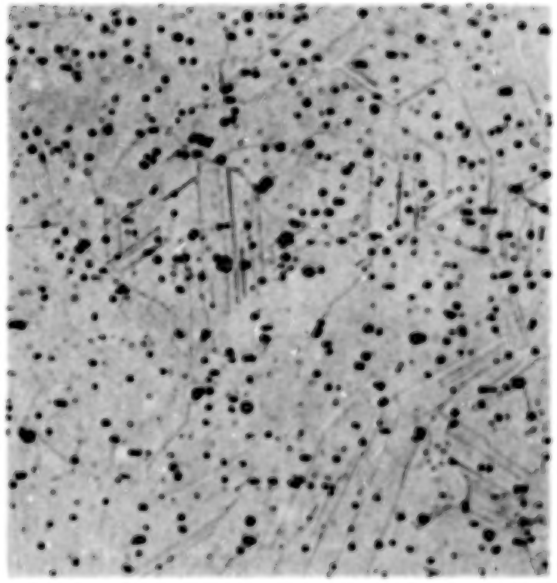

(c) Heat 4-1697
Grain Size ASTM 4-4-1/2.
X300.

Figure 40: Typical Microstructures of Grain Size Sheet - Lot ASTM 2-4

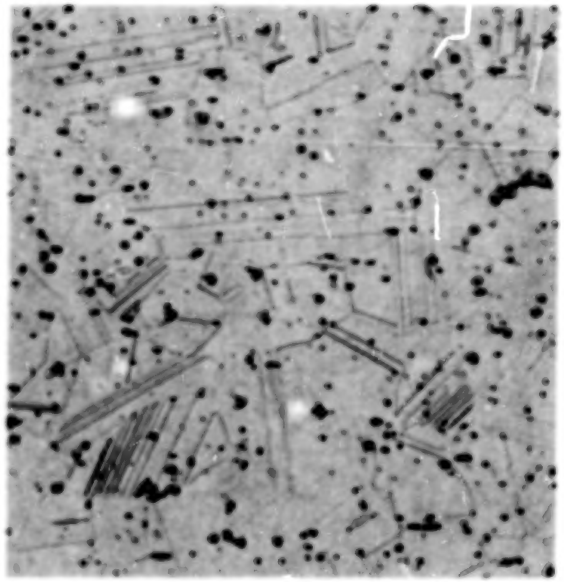

(a) Heat 3-1655
Grain Size 4-1/2-6.
Pred. 5-1/2.
X300.

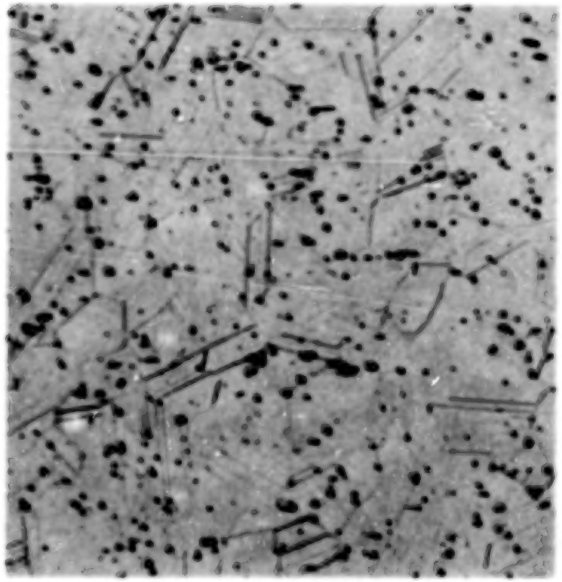

(b) Heat 4-1696
Grain Size ASTM 5-5-1/2.
X300.

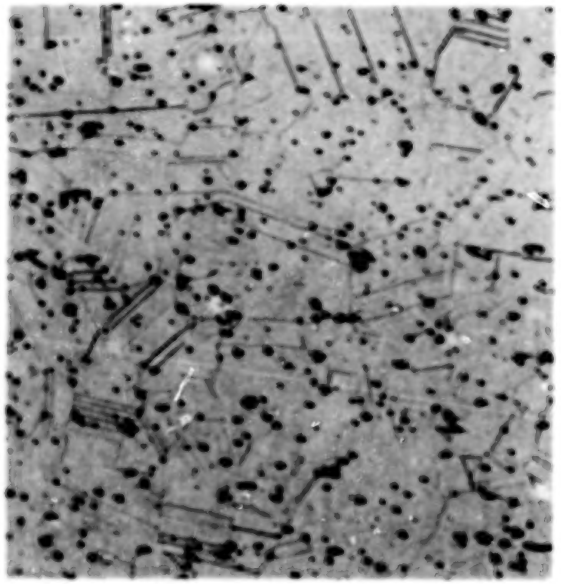

(c) Heat 4-1697
Grain Size ASTM 5-6-1/2.
Pred. 6
X300.

Figure 41: Typical Microstructures of Grain Size Sheet - Lot ASTM 5-6

95

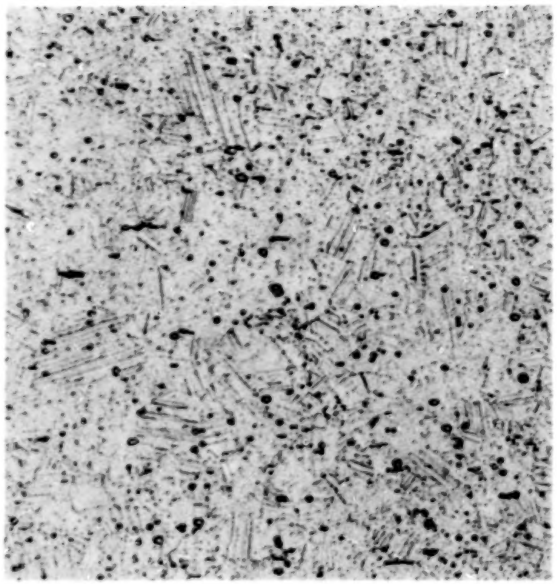

(a) Heat 3-1655
Grain Size ASTM 7-7-1/2.
Pred. 7-1/2.
X300.

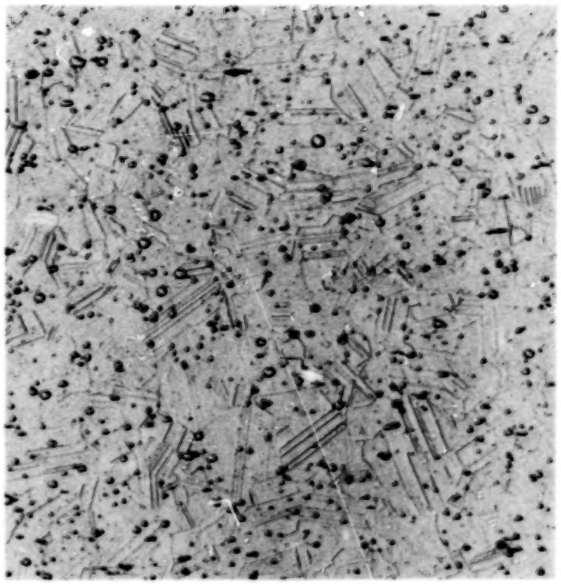

(b) Heat 4-1696
Grain Size ASTM 7.
X300.

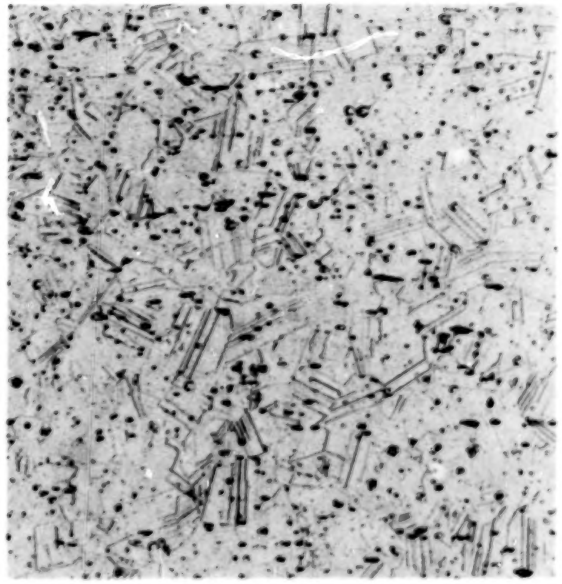

(c) Heat 4-1697
Grain Size ASTM 7.
X300.

Figure 42: Typical Microstructures of Grain Size Sheet - Lot ASTM 7-8

Definite texturing was found in the ASTM 5-6 and ASTM 7-8 sheet lots. The form was the same as that observed in the texture study sheets. Angular data obtained for the high intensity regions are summarized in Table XXXII. Due to its more diffuse nature, no angular spreading measurements were made for Heat 3-1655, ASTM 5-6 grain size. The degree of texturing observed in these sheets could be correlated to the amount of cold reduction prior to the final annealing treatment as was found for the texture study sheets. That is, the degree of texturing increased as the amount of final cold work increased.

4.1.3 Creep strength evaluation. - To evaluate the dependence of creep strength on grain size, duplicate samples from each experimental strip were creep tested to a strain of $\geq$ 1 percent at a test condition of 1200K/41.4 MPa in accordance with the procedure described in Appendix B. A complete listing of the creep test data is contained in Appendix E. The log averages of the test results for creep strain levels of 0.5 percent and 1.0 percent are summarized in Table XXXIII along with those obtained for the baseline sheets for the purpose of comparison.

Using these data, statistical comparisons were made between the baseline and grain size study lots by means of the t-test (ref. 9). In each case, the null hypothesis was that the means of the samples tested were equal, and the alternative hypothesis was that the means were not equal. The results of these statistical comparisons are listed in Table XXXIV.

The results of the statistical comparisons substantiated the following conclusions:

1. The ASTM 2-4 and ASTM 5-6 grain size lots were significantly superior in creep strength to the ASTM 7-8 lot.

2. The ASTM 2-4 and ASTM 5-6 lots were not significantly different.

3. The ASTM 2-4 and ASTM 5-6 lots were not significantly different from the baseline sheets.

4. The ASTM 7-8 lot was significantly inferior to the baseline sheets.

Although these results indicated that no significant improvement over the baseline 1200K/41.4 MPa (1700°F/6 ksi) creep strength was achieved by varying the grain size, it was clearly established that the creep strength of HAYNES alloy No. 188 deteriorates markedly with a grain size of ASTM 7 or finer. The reason for this behavior was not determined. However, a possible explanation might be an increase in the contribution of grain boundary sliding to the overall creep strain as the average grain diameter decreased. The opposite response was expected with increasing average grain diameter. The fact that the ASTM 2-4 and ASTM 5-6 lots were not significantly different with respect to the times to 0.5 percent and 1.0 percent creep strain was, therefore, somewhat surprising. Review of the creep data in Appendix E indicates that this might be explained by the larger amount of primary creep which occurred in the ASTM 2-4 grain size sheets. Determination of the causes of this difference

TABLE XXXII

ANGULAR DATA OF HIGH INTENSITY REGIONS FOR (111) POLE FIGURES
DETERMINED FOR GRAIN SIZE STUDY SHEET LOTS

	Final Cold Reduction, %	Final Annealing Condition	Around Rolling Direction		Around Transverse Direction	
			Angular Locations	Angular Spread	Angular Locations	Angular Spread
G.S. Study ASTM 5-6						
Heat 4-1696	57	1463K(2175°F)/10 min	21-45°	24°	±42°	84°
Heat 4-1697	57	1463K(2175°F)/10 min	19-45°	26°	±40°	80°
G.S. Study ASTM 7-8						
Heat 3-1655	75	1450K(2150°F)/10 min	21-40°	19°	±25°	50°
Heat 4-1696	75	1450K(2150°F)/10 min	21-40°	19°	±22°	44°
Heat 4-1697	75	1450K(2150°F)/10 min	22-43°	21°	±24°	48°

TABLE XXXIII

SUMMARY OF LOG AVERAGE DATA FOR 1200 K/41.4 MPa
(1700°F/6 ksi) CREEP TESTS OF BASELINE AND GRAIN SIZE
STUDY SHEET LOTS

Sheet Lot	Number of Tests, N	0.5% Creep Strain			1.0% Creep Strain		
		Avg. Log Time*	Antilog, Hrs	Std. Dev.**	Avg. Log Time*	Antilog, Hrs	Std. Dev.**
Baseline	6	1.280	19.1	.339	1.631	42.8	.346
ASTM 2-4	6	1.359	22.8	.174	1.821	62.2	.109
ASTM 5-6	6	1.279	19.0	.278	1.646	44.3	.260
ASTM 7-8	6	.907	8.1	.370	1.203	16.0	.356

* $\log \bar{t} = \frac{\Sigma \log t_i}{n}$ where t_i = observed time to given creep strain

n = no. of observations

** log units

99

TABLE XXXIV

SUMMARY OF STATISTICAL COMPARISONS FOR THE BASELINE AND GRAIN SIZE STUDY SHEET LOTS

Test	D.F.	t	2-Tailed Probabilities
Time to 0.5% Creep Strain			
2-4 vs. 5-6	10	.59824	0.56298
2-4 vs. 7-8	10	2.71053	0.02191
5-6 vs. 7-8	10	1.96336	0.07800
2-4 vs. baseline	10	0.50314	0.62576
5-6 vs. baseline	10	-0.01121	0.99127
7-8 vs. baseline	10	-1.82189	0.09847
Time to 1.0% Creep Strain			
2-4 vs. 5-6	7.37	1.52262	0.17167
2-4 vs. 7-8	6.28	4.06028	0.00665
5-6 vs. 7-8	10	2.46022	0.03366
2-4 vs. baseline	6.35	1.28543	0.24603
5-6 vs. baseline	10	0.09061	0.92959
7-8 vs. baseline	10	-2.10133	0.06194

Hypothesis: Null (Ho) $\bar{X}_1 = \bar{X}_2$

Alternative $\bar{X}_1 \neq \bar{X}_2$

where $\bar{X}$ and $\bar{X}_2$ are the sample means

was beyond the scope of this brief study. However, it might be postulated that the steady-state dislocation substructure is achieved more rapidly in the smaller grain size sheet lots. Such a trend is apparent from the data for the range of grain sizes investigated. Similar behavior with grain size has also been reported in the literature (ref. 7 and 11).

In spite of the fact that none of the grain sizes investigated provided an improvement in creep strength at the 1200K/41.4 MPa (1700°F/6 ksi) test condition, it was desired to select an optimum sheet lot for creep strength evaluation over a wide range of temperature and stress conditions. The foregoing statistical tests indicated a choice between grain sizes of ASTM 2-4 and ASTM 5-6 which were judged not to be significantly different. Consideration of primary creep characteristics and the TMP schedules of these materials, therefore, lead to the selection of ASTM 5-6 as the optimum grain size.

4.1.4 Apparent activation energies for creep. - In an attempt to gain a better understanding of the observed variation in creep properties with grain size, the apparent activation energies for creep were determined for each of the grain size study sheet lots. To accomplish this, minimum creep rates were determined for additional creep tests at a stress of 41.4 MPa (6 ksi) at temperatures of 1172K (1650°F), 1227K (1750°F) and 1255K (1800°F). Complete results of these tests are given in Appendix E. The apparent activation energies for creep were determined assuming the following relationship to exist:

$$\dot{\epsilon}_{min} = C\,(S)\; e^{\frac{-\Delta H_c}{RT}}$$

where $\dot{\epsilon}_{min}$ = minimum creep rate, percent/hour

$C\,(S)$ = constant for a constant stress level, percent/hour

ΔH_c = apparent activation energy for creep, J/mole (cal/mole)

R = gas constant = 8.31434 J/mole · K
(1.9872 cal/mole · K)

T = absolute temperature, K

This relationship predicts a straight line for a plot of the natural logarithm of the minimum creep rate versus the reciprocal of the absolute temperature, the slope of which is equal to the negative of the apparent activation energy for creep divided by the gas constant. Determination of the slopes required for the activation energy computations was made by obtaining least squares fits of the appropriately transformed data. Analyses were performed for the data of individual heats and for the data of all heats combined for each grain size range. A summary of the results obtained is presented in Table XXXV. Within each grain size range, agreement with the assumed relationship was quite good. However, heat-to-heat variations were apparent with respect to the activation energy values obtained. Among the three grain size groups, significantly

TABLE XXXV

APPARENT ACTIVATION ENERGIES FOR CREEP IN GRAIN SIZE STUDY SHEETS

Heat No.	Slope (-ΔHc/R)	Apparent Activation Energy for Creep, ΔHc J/mole	(Cal/mole)	Correlation Coefficient	Minimum Creep Rate Std. Dev. Log e
		ASTM 2-4			
3-1655	-67,147.8	558.294	(133,436)	.9882	.31084
4-1696	-68,444.7	569,078	(136,013)	.9931	.24045
4-1697	-77,961.9	648,210	(154,926)	.9920	.29576
Combined Heats	-71,184.8	591,860	(141,458)	.9852	.28662
		ASTM 5-6			
3-1655	-58,429.7	485,808	(116,111)	.9505	.57054
4-1696	-47,066.4	391,330	(93,530)	.9923	.17516
4-1697	-59.954.0	498,486	(119.141)	.9859	.30394
Combined Heats	-55,150.0	458,541	(109,594)	.8935	.64109
		ASTM 7-8			
3-1656	-63,286.9	526,197	(125,764)	.9573	.57028
4-1696	-50,653.6	421,157	(100,659)	.9734	.35584
4-1697	-58,268.4	484,470	(115,791)	.9694	.44075
Combined Heats	-57,403.0	477,273	(114,071)	.9035	.26962

higher apparent activation energies were found for the ASTM 2-4 sheets. Those obtained for the ASTM 5-6 and ASTM 7-8 sheets were essentially equivalent.

Semi-log plots based on the combined heat analyses are illustrated in Figures 43-45. Comparison of the figures indicates a trend of decreasing minimum creep rate with increasing average gain diameter (decreasing ASTM No.) at each temperature investigated. As far as low strain ($\leq$ 1 percent) creep life is concerned, however, review of the creep data in Appendix E indicates that the extent of primary creep increases as the average grain diameter increases. These offsetting responses to grain size help explain the similarity in low strain creep lives of the ASTM 2-4 and ASTM 5-6 sheets previously noted in the initial quality control creep tests.

The apparent activation energies for creep determined for each grain size range are much higher than the activation energy for self-diffusion that would be expected for HAYNES alloy No. 188. Based on results for β-cobalt and cobalt-nickel alloys (ref. 12), the activation energy for self-diffusion in HAYNES alloy No. 188 should be approximately 271,960 J/mole (65,000 cal/mole). These findings are not without precedent, however. Similar results have been reported for Nimonic 80A, Nimonic 90 and dispersion strengthened alloys such as S.A.P., TD-Ni, etc. (ref. 5, p. 97). More specifically, an investigation performed on HAYNES alloy No. 25 (L-605) which is closely related to HAYNES alloy No. 188 in terms of composition, yielded an apparent activation energy for creep of 502 KJ/mole (120 Kcal/mole) in the 1255K (1800°F) - 1478K (2200°F) temperature range (ref. 13). One obvious explanation of the high activation energies obtained is that more than one rate controlling mechanism is operative. If the activation energies for these mechanisms are of the same order of magnitude, the computed activation energies will not be true activation energies. That is, the value obtained will be fictitious since it does not correspond to a single process. In the present case, a possible physical explanation might be the phenomenon of strain-aging with the precipitation of carbides thus significantly affecting the minimum creep rate. The strain-aging behavior obtained should also depend on TMP. This might explain why the ASTM 2-4 sheets have higher apparent activation energies than the ASTM 5-6 and ASTM 7-8 sheets as opposed to attributing this difference to grain size. Previous studies have not shown a dependence of activation energy on grain size (ref. 5, p. 99).

4.2 Evaluation of ASTM 5-6 Grain Size Sheets

4.2.1 Production of experimental sheet lots. - In order to perform an extensive evaluation of the ASTM 5-6 grain size material, larger sized sheets nominally 0.38 mm (0.015 inch) thick were produced from Heats 3-1655, 4-1696 and 4-1697 using the previously defined processing schedule contained in Table XXXI. This was accomplished by cold rolling two pieces of each heat measuring 4.57 mm thick by 11.4 cm wide by 15.24 cm long (0.180 inch x 4.5 inches x 6 inches) parallel to the original hot-rolling direction. After the second cold-rolling session, each piece was cut in half to facilitate rolling to final gauge on the 4-Hi laboratory mill. The resulting pieces measured approximately

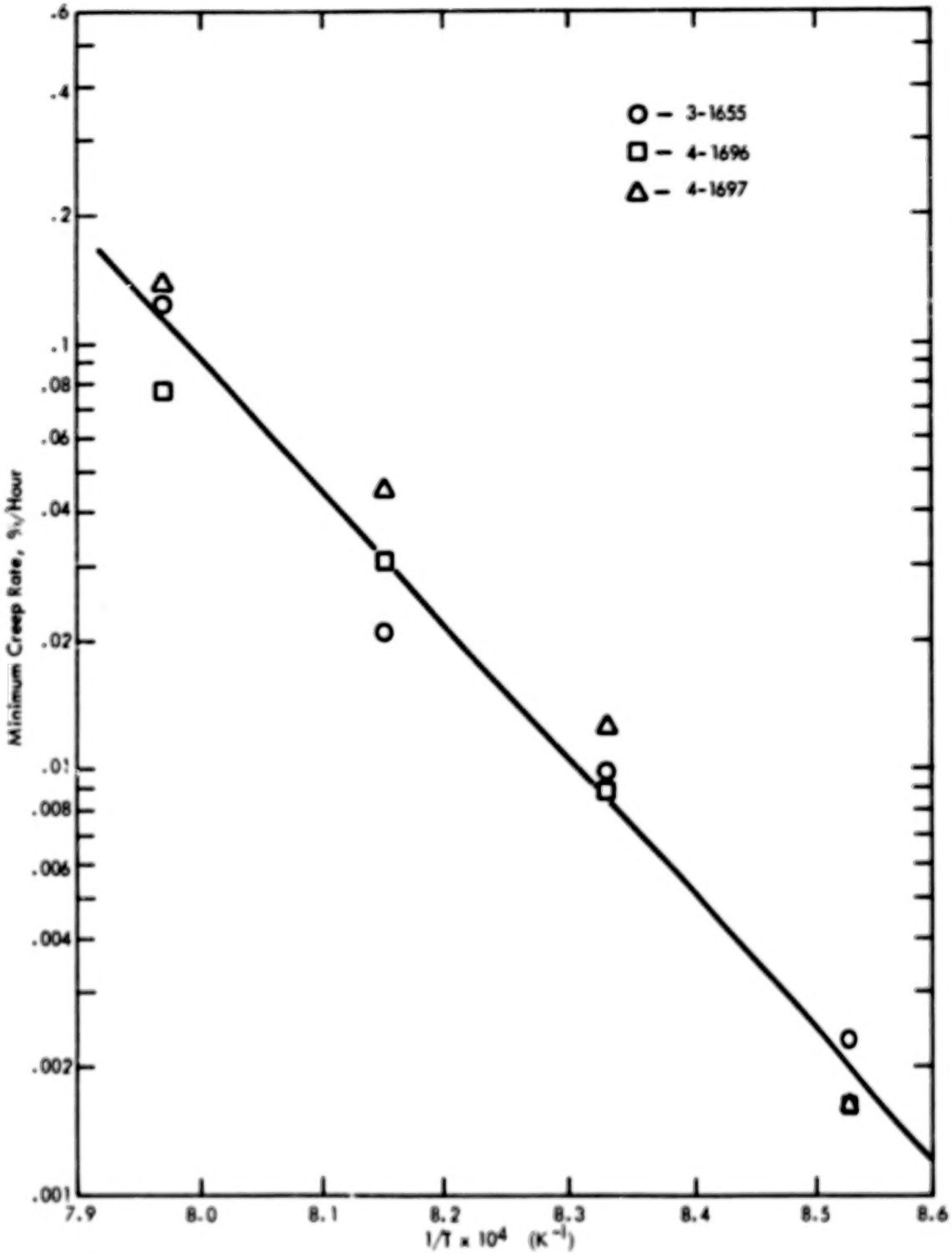

Figure 43: Minimum Creep Rate vs. Reciprocal of the Absolute Temperature for the ASTM 2-4 Grain Size Study Sheets.

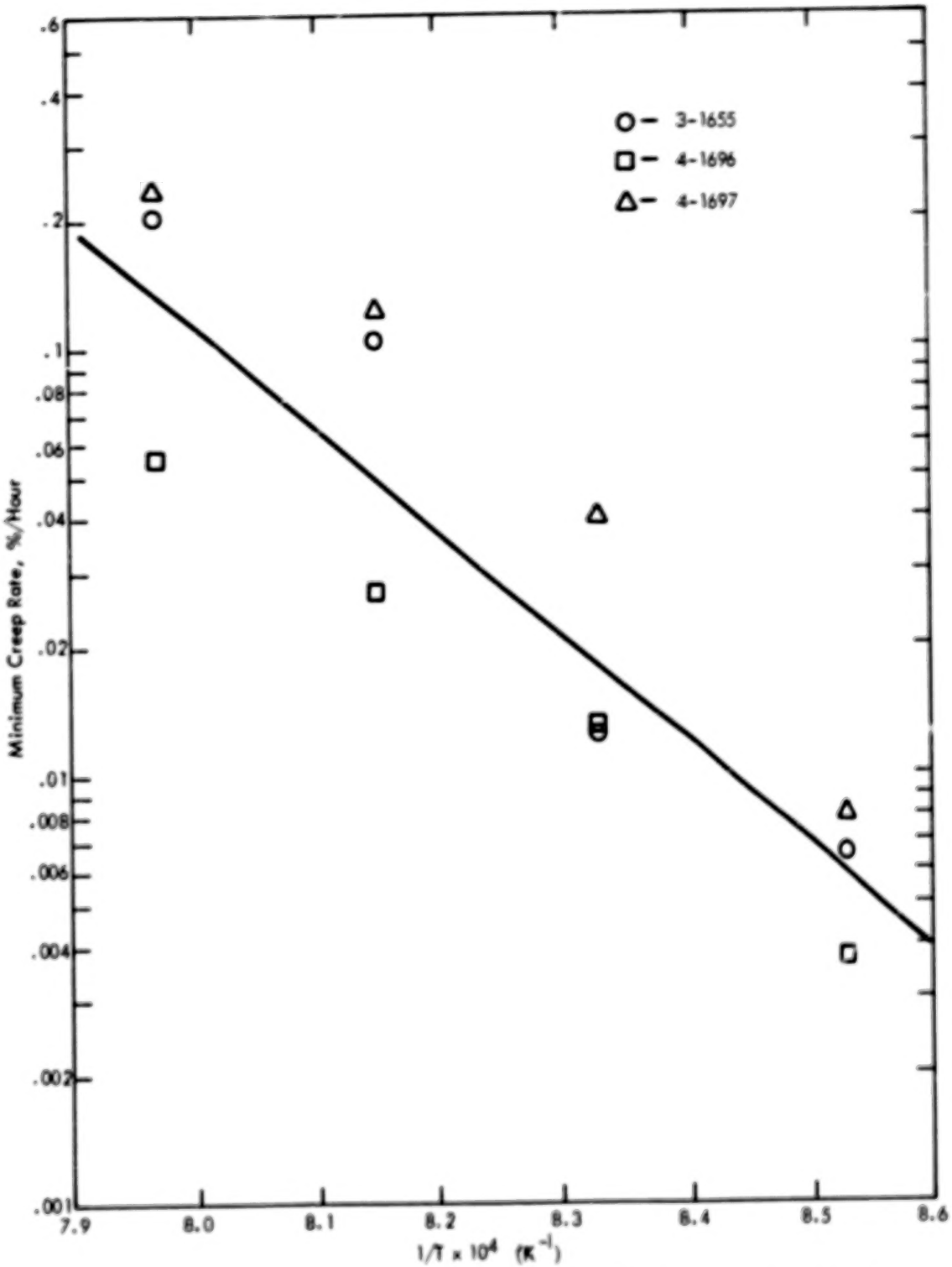

Figure 44: Minimum Creep Rate vs. Reciprocal of the Absolute Temperature for the ASTM 5-6 Grain Size Study Sheets.

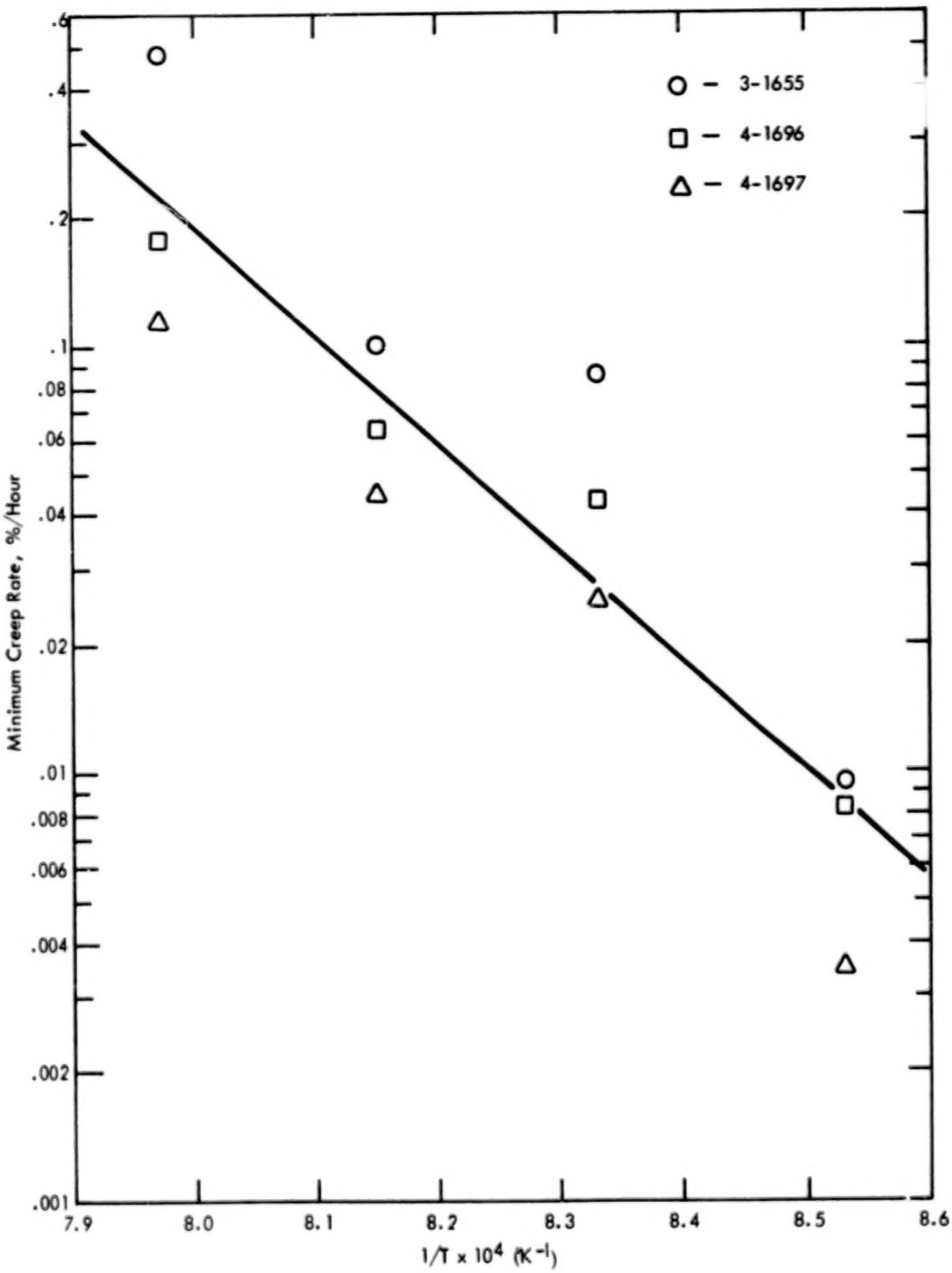

Figure 45: Minimum Creep Rate vs. Reciprocal of the Absolute Temperature for the ASTM 7-8 Grain Size Study Sheets.

0.38 mm by 12.7 cm by 63.5 cm long (0.015 inch x 5 inches x 25 inches). Following the final annealing treatment, each piece was salt bath descaled and flattened by stretcher leveling. Metallographic analysis of samples from the sheets indicated that the desired ASTM 5-6 grain size was obtained in all the pieces produced.

4.2.2 Tensile properties. - Duplicate longitudinal specimens from each heat were tensile tested in air over the temperature range of room temperature to 1366K (2000°F). The procedures employed were the same as those described in Section 2.3. A summary of the results obtained is presented in Table XXXVI. Average tensile properties for the three heats are listed in Table XXXVII.

The values obtained for 0.2 percent offset yield and ultimate strengths were similar to those reported for the baseline sheets (Table IV). With regard to the elongations, the same trend was apparent as noted previously for the textured sheets. That is, the elongations obtained were equivalent to those of the baseline sheets through 1033K (1400°F), but significantly lower at 1144K (1600°F) and above. Presumably, this effect was due to the coarser grain size of the grain size study sheets.

4.2.3 Stress rupture properties. - Duplicate longitudinal specimens from each heat were stress rupture tested at 1089K/165.4 MPa (1500°F/24 ksi) and 1311K/31 MPa (1900°F/4.5 ksi). The specimen configuration was the same as that illustrated in Appendix B. A summary of the data obtained is presented in Table XXXVIII.

The results of the 1089K/165.4 MPa (1500°F/24 ksi) tests indicate that the grain size study sheets had essentially the same rupture strength as the baseline sheets (Table V), but lower ductility. The decrease in ductility was most likely due to the coarser grain size of the grain size study sheets. Such a trend is supported by the values obtained for the textured sheets (Table XXIII).

At the 1311K/31 MPa (1900°F/4.5 ksi) test condition, the grain size study sheets had greater strength than the baseline sheets with essentially equivalent elongation. These data substantiate the well known trend that high temperature rupture strength increases as the average grain diameter increases (ASTM grain size decreases). Apparently, at lower temperatures (1089K ~.7 Tm), this advantage disappears.

4.2.4 Creep life evaluation. - To obtain a detailed characterization of the low strain ($\leq$ 1 percent) creep properties of the grain size study sheets, creep tests were conducted on samples from each heat at temperatures of 922K (1200°F), 1144K (1600°F) and 1255K (1800°F), and at three stresses at each temperature. All tests were performed using longitudinally oriented specimens. The testing procedure was the same as that described in Appendix B. As with the baseline, it was planned to select stresses which would give 1 percent creep lives in the range of roughly 25-500 hours. The initial stress levels selected were based on creep test results obtained for the baseline sheets.

TABLE XXXVI

LONGITUDINAL TENSILE PROPERTIES OF GRAIN SIZE STUDY SHEET: ASTM 5-6

	Heat 3-1655					Heat 4-1696					Heat 4-1697				
	0.2% YS		UTS		El	0.2% YS		UTS		El	0.2% YS		UTS		El
Test Temp.	MPa	(ksi)	MPa	(ksi)	%	MPa	(ksi)	MPa	(ksi)	%	MPa	(ksi)	MPa	(ksi)	%
R.T.	503.7	(73.1)	992.2	(144.0)	60.9	558.1	(81.0)	1023.2	(148.5)	55.9	503.7	(73.1)	994.9	(144.4)	60.9
	463.7	(67.3)	956.3	(138.8)	64.9	533.3	(77.4)	992.9	(144.1)	56.9	497.5	(72.2)	968.7	(140.6)	61.4
922 K	308.0	(44.7)	704.8	(102.3)	62.6	356.9	(51.8)	745.5	(108.2)	61.8	319.0	(46.3)	695.9	(101.0)	63.5
(1200°F)	301.1	(43.7)	691.1	(100.3)	62.4	338.3	(49.1)	717.3	(104.1)	61.6	299.7	(43.5)	691.1	(100.3)	61.3
1033 K	292.8	(42.5)	555.3	(80.6)	43.9	311.4	(45.2)	549.8	(79.8)	37.3	339.0	(49.2)	611.8	(88.8)	45.2
(1400°F)	292.8	(42.5)	540.2	(78.4)	43.8	313.5	(45.5)	626.3	(90.9)	42.8	275.6	(40.0)	593.9	(86.2)	45.9
1144 K	279.7	(40.6)	411.3	(59.7)	26.6	311.4	(45.2)	436.8	(63.4)	32.3	292.1	(42.4)	409.3	(59.4)	29.1
(1600°F)	272.2	(39.5)	408.6	(59.3)	36.4	292.1	(42.4)	415.5	(60.3)	45.5	274.2	(39.8)	383.6	(55.7)	30.9
1255 K	124.0	(18.0)	188.1	(27.3)	20.4	164.0	(23.8)	250.1	(36.3)	29.4	155.0	(22.5)	232.2	(33.7)	24.7
(1800°F)	148.1	(21.5)	224.6	(32.6)	23.6	141.3	(20.5)	234.9	(34.1)	26.9	139.2	(20.2)	215.7	(31.3)	24.3
1366 K	66.1	(9.6)	99.2	(14.4)	12.6	64.1	(9.3)	95.8	(13.9)	16.0	64.8	(9.4)	109.6	(15.9)	15.1
(2000°F)	73.0	(10.6)	121.3	(17.6)	15.0	78.6	(11.4)	124.0	(18.0)	16.6	75.1	(10.9)	114.4	(16.6)	13.4

TABLE XXXVII

AVERAGE LONGITUDINAL TENSILE PROPERTIES FOR GRAIN SIZE STUDY SHEET: ASTM 5-6*

Test Temp.	0.2% YS MPa	0.2% YS (ksi)	UTS MPa	UTS (ksi)	Elong. %
R. T.	509.9 (32.4)	74.0 (4.7)	988.0 (23.4)	143.4 (3.4)	60.2 (3.3)
922 K (1200°F)	320.4 (22.7)	64.5 (3.3)	707.6 (21.4)	102.7 (3.1)	62.2 (0.8)
1033 K (1400°F)	304.5 (22.0)	44.2 (3.2)	579.4 (35.8)	84.1 (5.2)	43.2 (3.1)
1144 K (1600°F)	287.3 (14.5)	41.7 (2.1)	410.6 (17.2)	59.6 (2.5)	33.5 (6.7)
1255 K (1800°F)	145.4 (13.8)	21.1 (2.0)	224.6 (21.4)	32.6 (3.1)	24.9 (3.1)
1366 K (2000°F)	70.3 (6.2)	10.2 (0.9)	110.9 (11.7)	16.1 (1.7)	14.8 (1.5)

* Standard deviations are given in parentheses

TABLE XXXVIII

LONGITUDINAL STRESS RUPTURE DATA FOR GRAIN SIZE
STUDY SHEET - ASTM 5-6

	1089 K/165.4 MPa (1500°F/24 ksi)		1311 K/31 MPa (1900°F/4.5 ksi)	
Heat No.	Life Hours	Elongation %	Life Hours	Elongation %
3-1655	47.7	24.9	44.0	32.1
	43.3	27.8	35.5	33.2
4-1696	31.2	25.1	47.9	39.7
	35.0	29.6	27.9	20.3
4-1697	29.4	22.7	43.6	34.1
	40.3	23.8	38.8	44.4
Log Avg.	37.3	25.5	39.0	33.0
Std. Dev. (Log Units)	(.083)	(.043)	(.085)	(.117)

* $\bar{t} = \text{antilog}\left(\frac{\Sigma \log t_i}{n}\right)$

Additional stresses were then selected so as to obtain the required description of creep strength over the temperature range of interest. A complete listing of the creep test data is contained in Appendix E. It should be noted that two of the tests performed at 1255K/113.8 MPa (1800°F/2 ksi) ran much longer than anticipated and were terminated before 1.0 percent creep strain had been reached. Only the 0.5 percent creep strain lives obtained for these tests were used in the subsequent creep life evaluation.

The creep life characterization of the grain size study sheets was accomplished by subjecting the 0.5 percent and 1.0 percent creep strain data to a least squares optimization of the Larson-Miller parameter equation described in Section 2.5.1. Results of this analysis are presented in Table XXXIX. Plots showing the actual data and the lines given by the parameter equation are illustrated in Figures 46 and 47. The fit of the data to the Larson-Miller parameter equation was relatively good with correlation coefficients of 0.93 and 0.95 for the 0.5 percent and 1.0 percent creep strain levels, respectively. In comparison to the baseline (Table VI), less scatter was observed. The standard error of the estimate and RMS values obtained for the grain size study sheets were approximately two-thirds the values determined for the baseline sheets.

To provide a basis for direct comparisons to other materials, the 0.5 percent and 1.0 percent creep strain data were also force-fit to the parameter equation using a value of 17 for the Larson-Miller constant. Results of these analyses are listed in Table XL. The agreement obtained to this form of the parameter equation was quite good with RMS values slightly higher than those obtained in the optimized parameter analysis. As already noted previously, the agreement in the RMS values of the two analysis methods reflects the differences between the optimized Larson-Miller constants and the value of 17 selected in the forced-fit approach.

Comparison plots of the baseline and grain size study creep properties based on the forced-fit to a Larson-Miller constant of 17 are presented in Figures 48 and 49. These figures indicate that improvements over the baseline low strain creep strength were obtained in the ASTM 5-6 grain size study sheets, but the improvements were not as great as those found for the textured sheets. The average creep strength of the grain size study sheets was greater than that of the baseline sheets for both the 0.5 percent and 1.0 percent creep strain levels. In addition, with reference to Figures 9 and 10, the minus 3-sigma limits of the grain size study sheets were found to lie above the minus 2-sigma limits of the baseline sheets for both strain levels.

Comparisons of the 0.5 percent and 1.0 percent creep strengths of the grain size and texture study sheets are presented in Figures 50 and 51. For 0.5 percent creep, the minus 2-sigma limits of the texture study sheets are above the average of the grain size study sheets from approximately 186 MPa/18.6 x 10^3 LMP-K (27 ksi/33.5 x 10^3 LMP-°R) to 38 MPa/22.4 x 10^3 LMP-K (5.5 ksi/40.3 x 10^3 LMP-°R). Beyond the latter point, differences in the creep strengths of both materials become less significant. Figure 51 indicates that the mean of the grain size study is within or at the minus 2-sigma limit over the full range of

TABLE XXXIX

OPTIMIZED LARSON-MILLER PARAMETER ANALYSIS FOR GRAIN SIZE STUDY SHEETS: ASTM 5-6

Regression Equation: $Y = \log t = C_1 + \frac{C_2}{T} + \frac{C_3}{T} \log S + \frac{C_4}{T} (\log S)^2$

A. Where T = Absolute temperature, Kelvin

t = Time to given creep strain, hours

S = Stress, MPa

Creep Strain	Equation Parameters				Fit of Test Data			
	C_1	C_2	C_3	C_4	Std. Error of Estimate	Correlation Coefficient	Number of Tests	RMS
0.5%	18.6476	31052.4	-3019.60	-767.26	.252	.933	27	.233
1.0%	19.7198	31813.2	-1782.29	-1158.46	.205	.955	25	.188

B. Where T = Absolute temperature, degrees Rankine

t = Time to given creep strain, hours

S = Stress, ksi

0.5%	18.6476	50365.8	-7751.37	-1381.06	.252	.933	27	.233
1.0%	19.7198	53107.5	-6705.13	-2085.23	.205	.955	25	.188

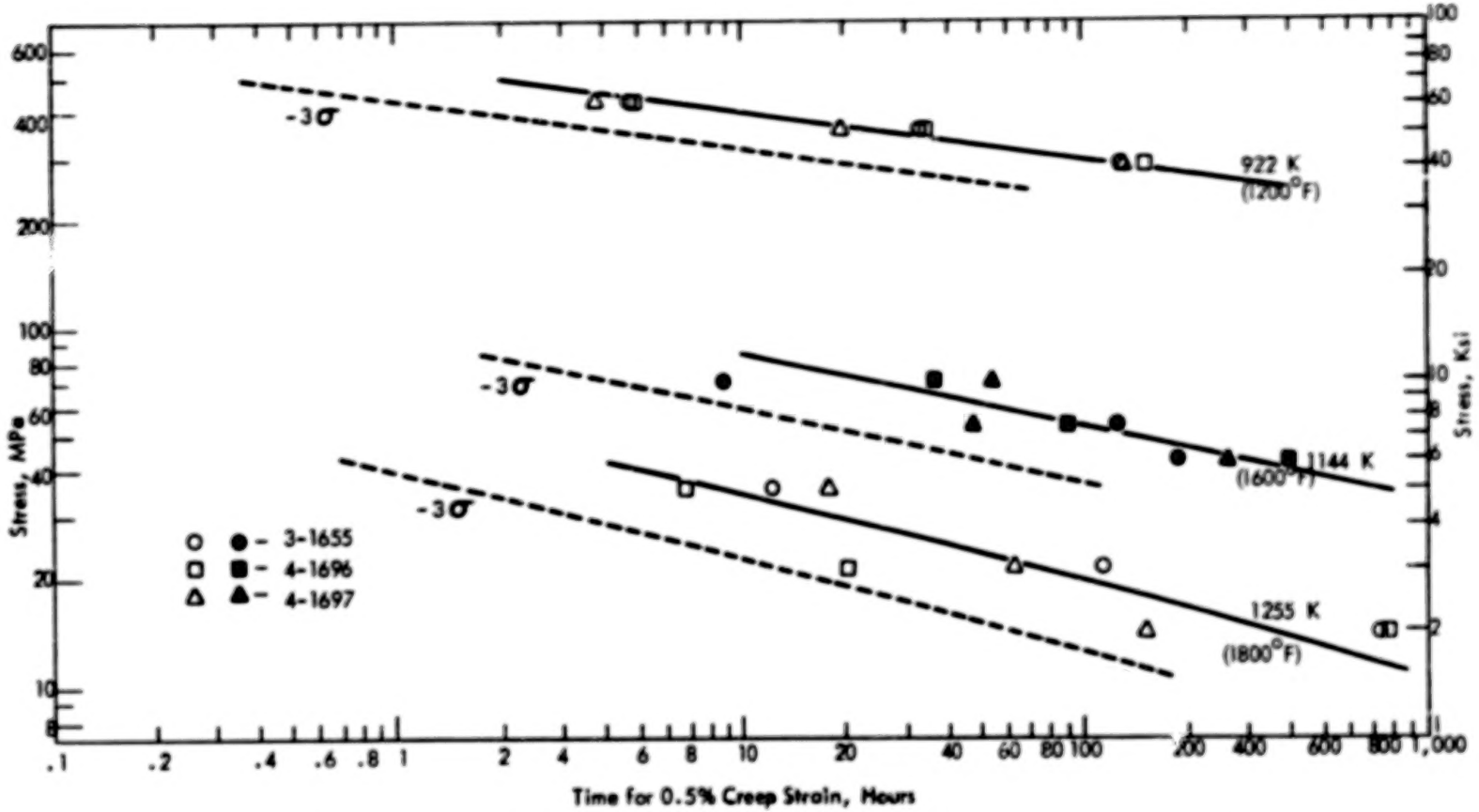

Figure 46: Stress vs. 0.5% Creep Life for Grain Size Study Sheets: ASTM 5-6 (Actual Data and Parametric Evaluation).

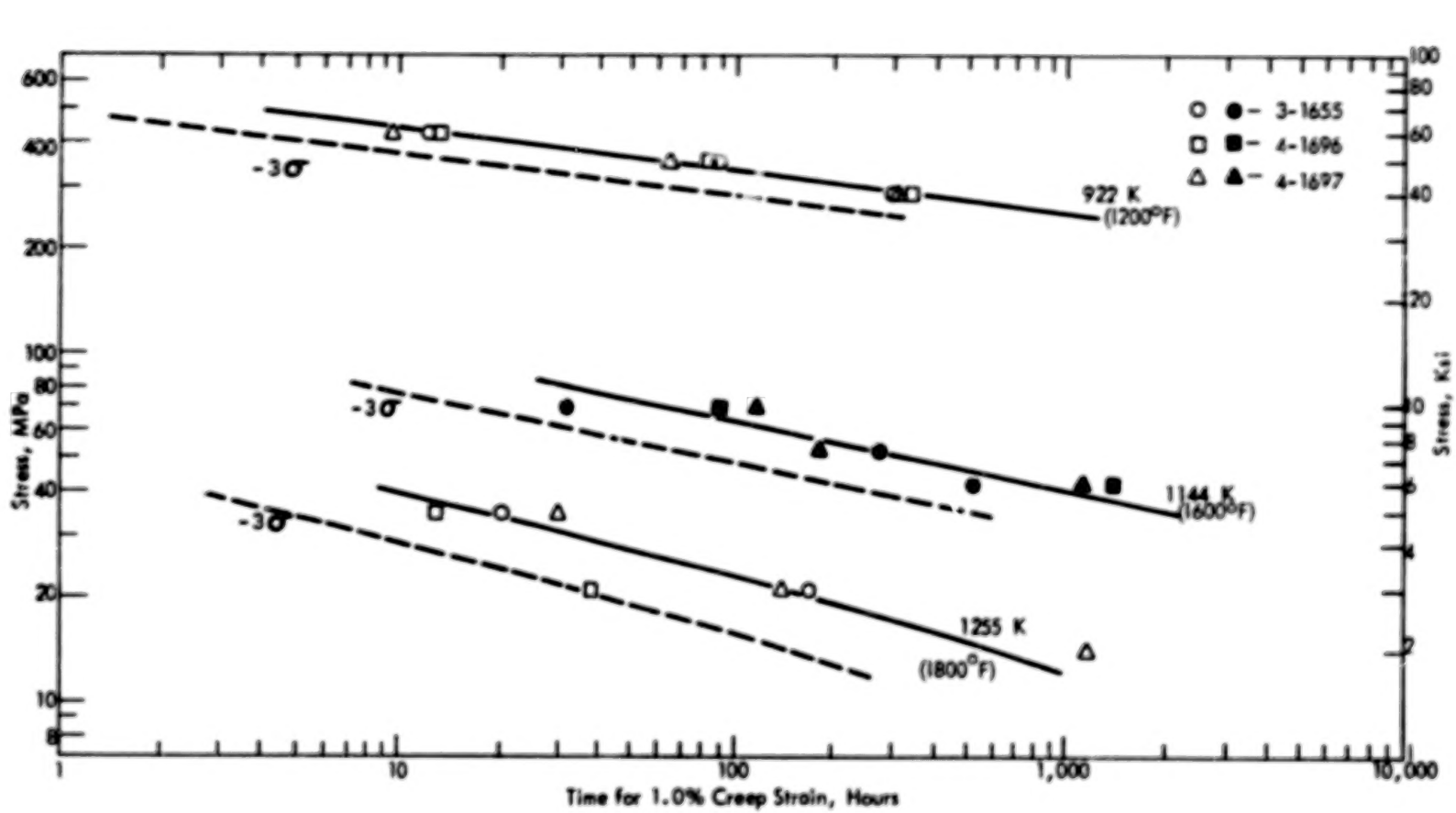

Figure 47: Stress vs. 1.0% Creep Life for Grain Size Study Sheets: ASTM 5-6 (Actual Data and Parametric Evaluation)

TABLE XL

FORCE-FIT ANALYSIS OF ASTM 5-6 GRAIN SIZE STUDY SHEETS TO THE LARSON-MILLER PARAMETER EQUATION WITH A LARSON-MILLER CONSTANT OF 17

Regression Equation: $P = T (\log t + 17) = C_2 + C_3 \log S + C_4 (\log S)^2$

A. Where T = Absolute temperature, Kelvin

t = Time to given creep strain, hours

S = Stress, MPa

Creep Strain	Equation Parameters			Fit of Test Data			
	C_2	C_3	C_4	Std. Error of Estimate, LM Parameter Units	Correlation Coefficient	Number of Tests	RMS
0.5%	28877.7	-3092.40	-636.96	296.66	.995	27	.236
1.0%	27791.0	-1458.07	-1051.43	252.32	.996	25	.200

B. Where T = Absolute temperature, degrees Rankine

t = Time to given creep strain, hours

S = Stress, ksi

0.5%	46506.2	-7489.10	-1146.53	533.99	.995	27	.236
1.0%	46492.4	-5798.43	-1892.57	454.17	.996	25	.200

115

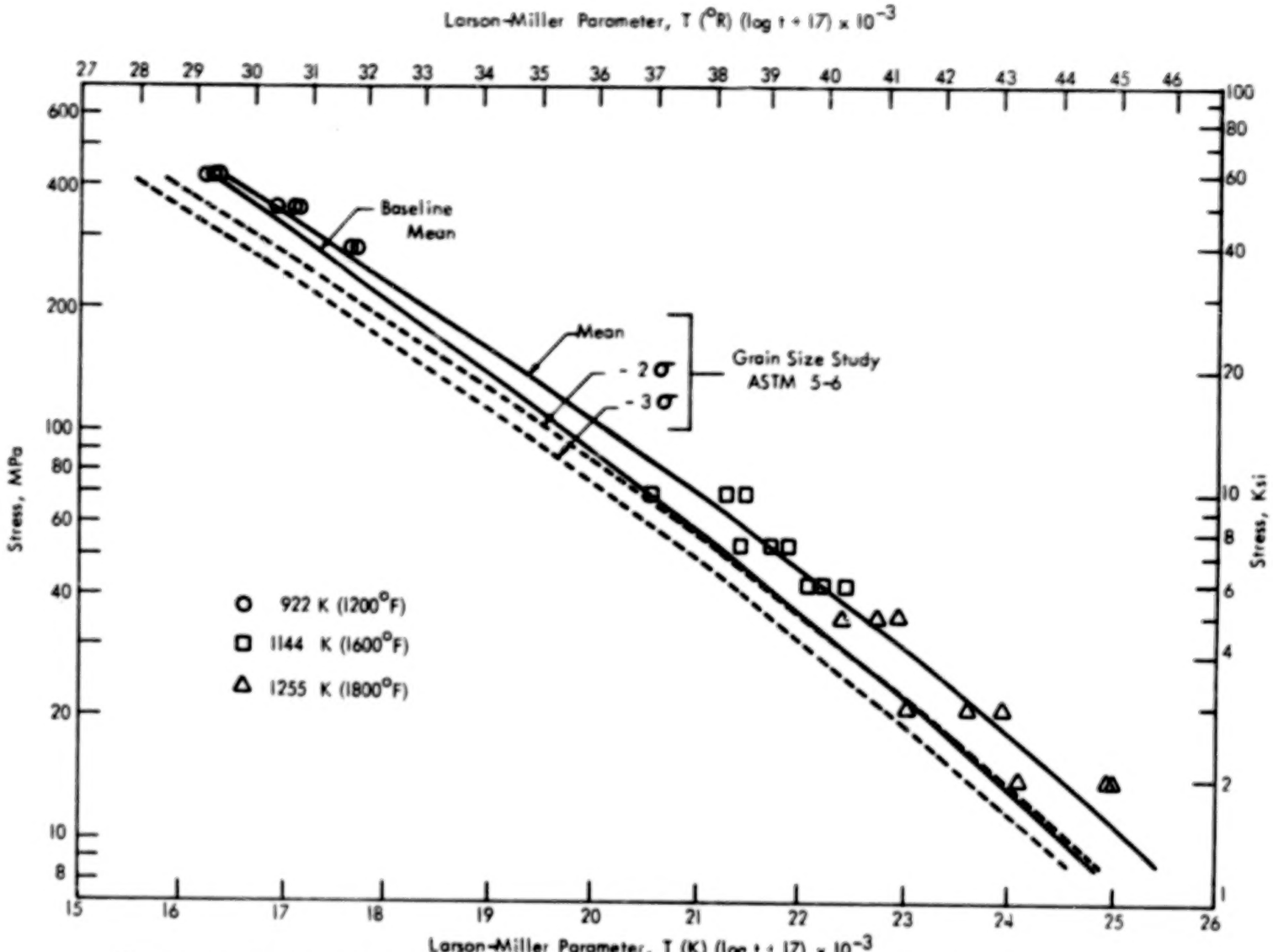

Figure 48: Comparison of Stress vs. Larson-Miller Parameter ($C_1 = 17$) for 0.5% Creep Lives of Baseline and ASTM 5-6 Grain Size Study Sheets.

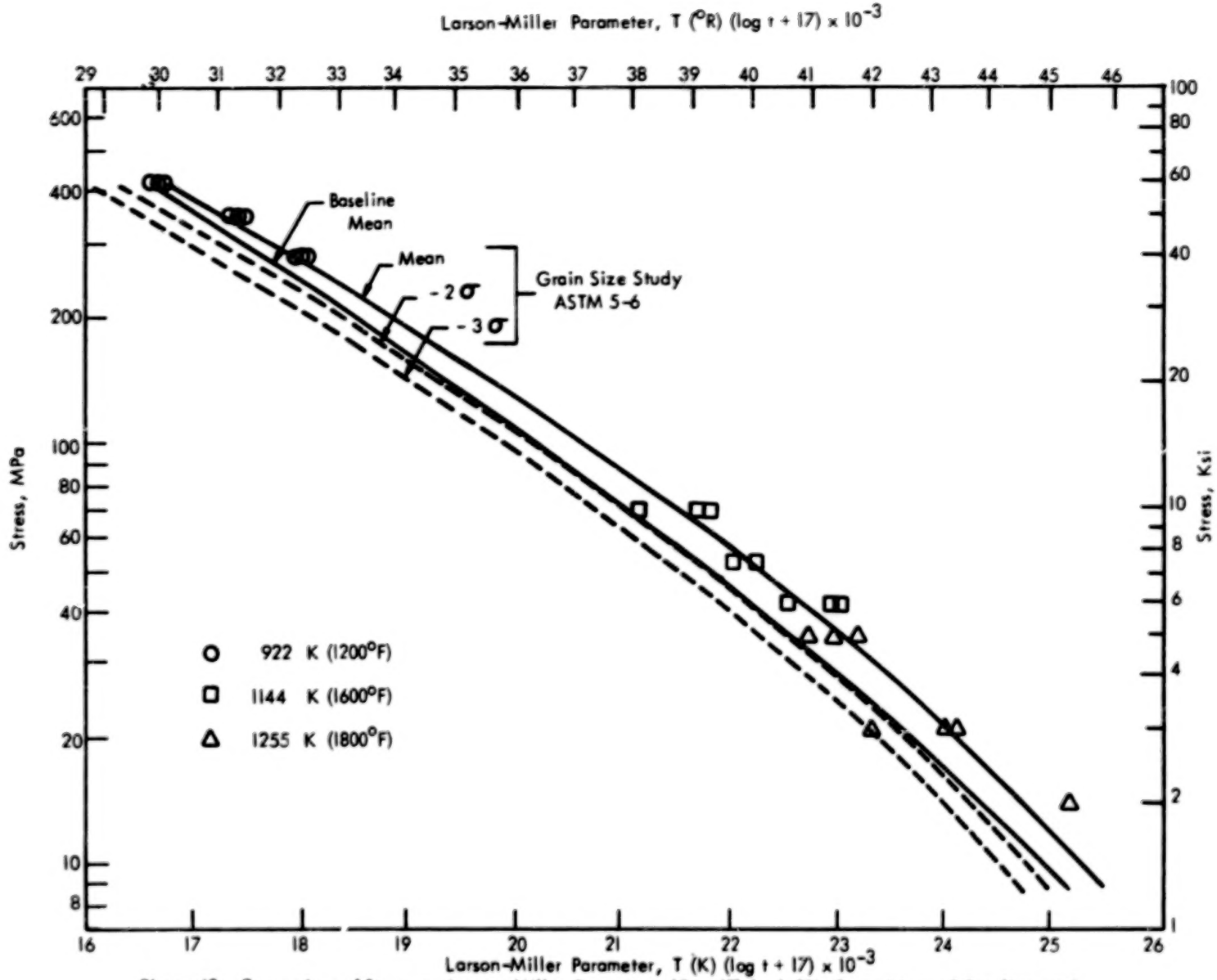

Figure 49: Comparison of Stress vs. Larson-Miller Parameter ($C_1 = 17$) for 1.0% Creep Lives of Baseline and ASTM 5-6 Grain Study Sheets.

117

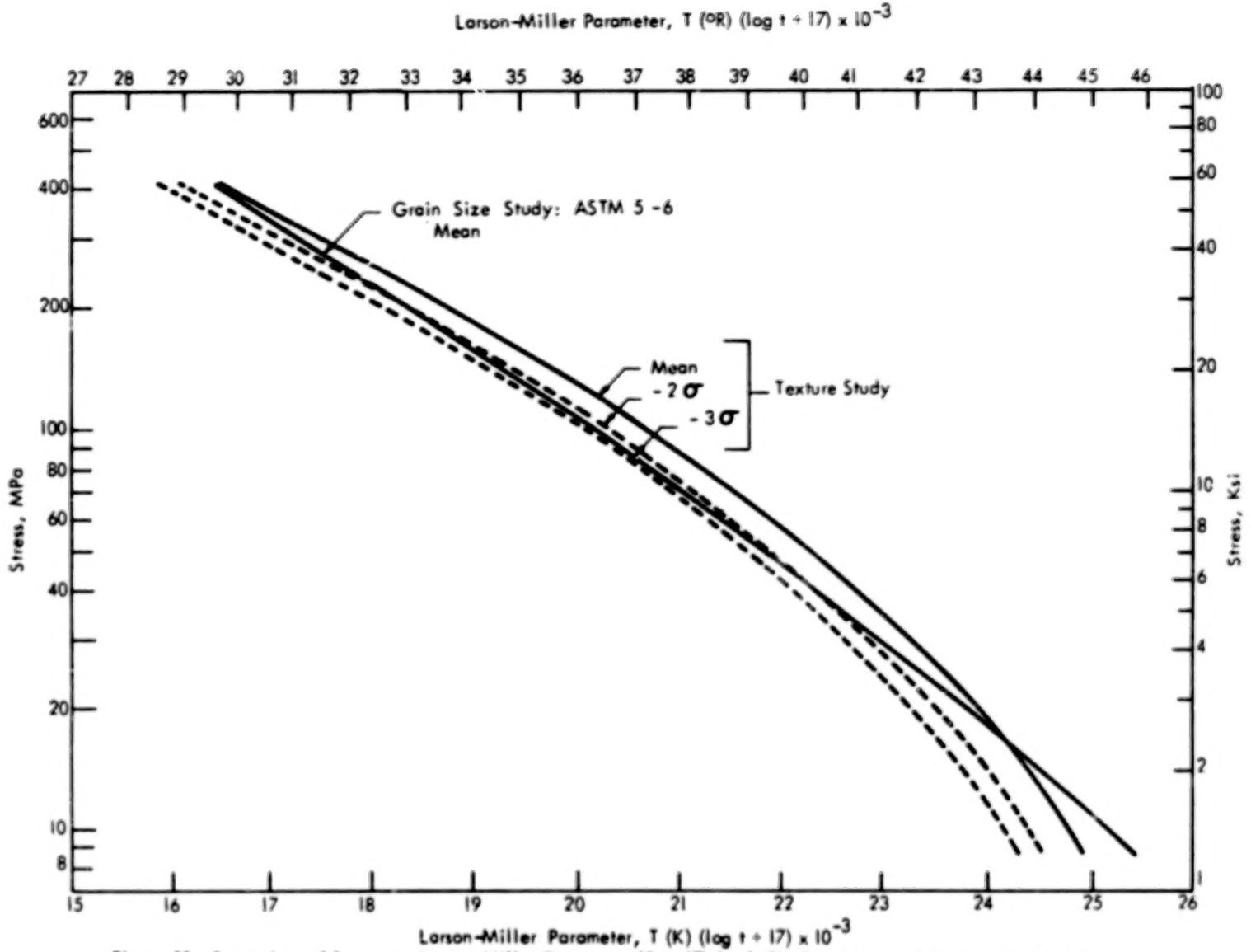

Figure 50: Comparison of Stress vs. Larson-Miller Parameter (C_1 = 17) for 0.5% Creep Lives of Texture Study and ASTM 5 -6 Grain Size Study Sheets.

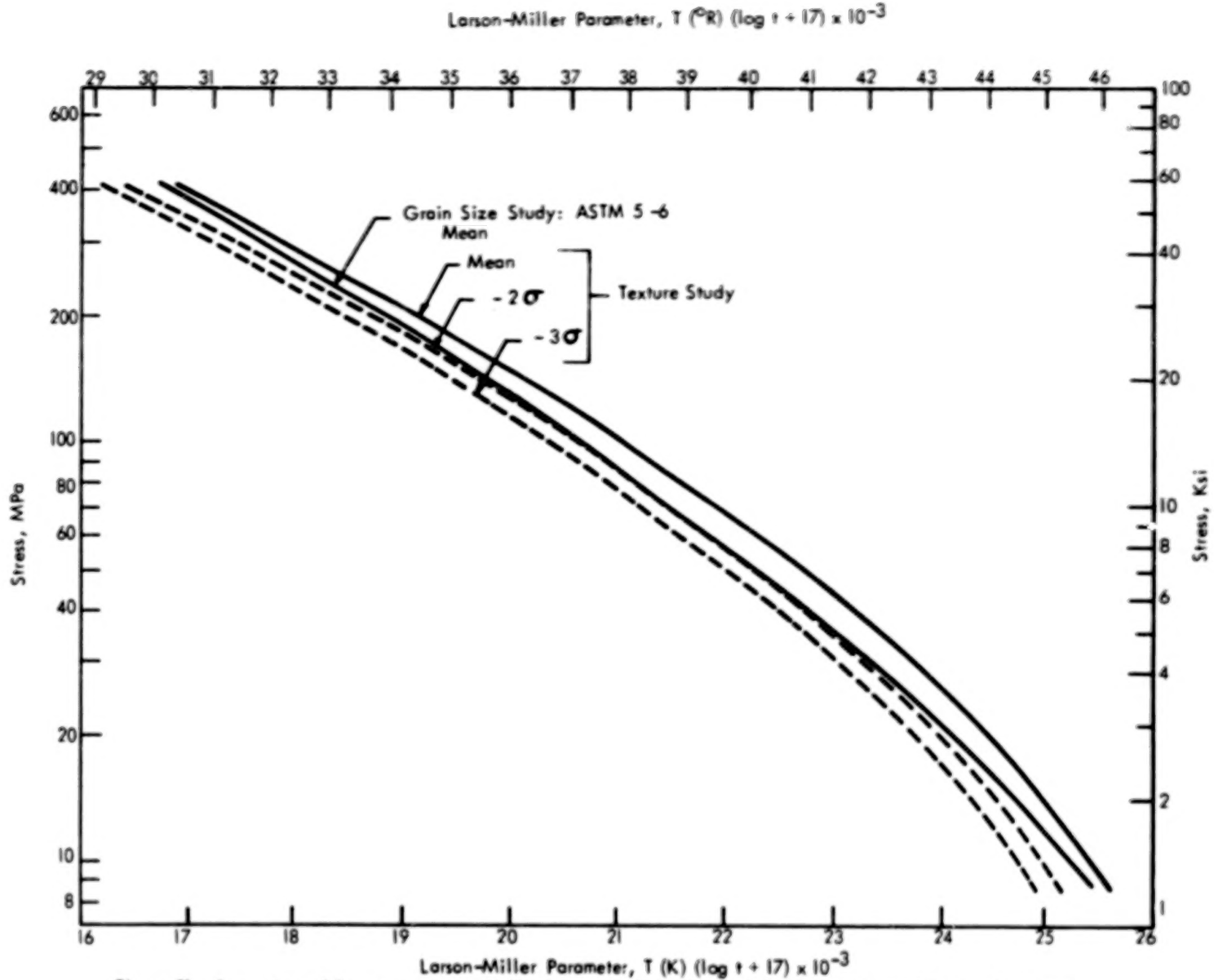

Figure 51: Comparison of Stress vs. Larson-Miller Parameter (C_1 = 17) for 1.0% Creep Lives of Texture Study and ASTM 5-6 Grain Size Study Sheets.

119

test conditions for 1.0% creep. Aside from these observations, reference to previous Figures 48 and 49 reveals that the minus 3-sigma limits of the textured sheet lie above the minus 2-sigma limits of the grain size study sheets from 413.7 MPa/15.8 x 10^3 LMP-K (60 ksi/28.4 x 10^3 LMP-°R) to approximately 17.2 MPa/23.5 x 10^3 LMP-K (2.5 ksi/42.3 x 10^3 LMP-°R) for 0.5 percent creep and essentially over the entire range for 1.0 percent creep.

4.2.5 Minimum creep rate evaluation. - The minimum creep rates determined for the ASTM 5-6 grain size study sheets were examined by multiple regression analysis assuming both a power and an exponential dependence on stress as described in Section 2.5.2. Results of these mathematical treatments are given in Tables XLI and XLII. The fit of the data to either functional relationship was essentially equivalent. This behavior was also observed for the baseline and textured sheets, and an explanation based on the hyperbolis sine law is described in Section 2.5.2.

Plots of the data conforming to the power function of stress are illustrated in Figure 52. Comparison of this figure to that obtained for the baseline (Figure 11), indicates that the minimum creep rates for the grain size study sheets and the baseline sheets were approximately the same at the 922K (1200°F) and 1144K (1600°F) test temperatures. However, at 1255K (1800°F), the minimum creep rates of the grain size study sheets were lower and divergent from those of the baseline. In terms of the power function parameters of Tables X and XLI, the grain size study sheets exhibited greater stress sensitivity at 922K (1200°F) which was offset by a much lower "structure factor." At 1144K (1600°F), the response of the two materials was approximately the same. At 1255K (1800°F), the grain size study sheets again exhibited greater stress sensitivity but a lower "structure factor." In this case, the two effects were not offsetting due to the lower stresses employed at that temperature.

In comparison to the textured sheets (Figure 35), the minimum creep rates of the grain size study sheets were about the same at 922K (1200°F) and slightly higher at 1144K (1600°F). At 1255K (1800°F), the grain size study sheets exhibited higher creep rates at stresses greater than about 20.7 MPa (3 ksi), but lower creep rates at stresses below that value. Reference to the power function parameter of Tables XXVII and XLI reveals the offsetting effects between the stress sensitivities and "structural factors" of these two materials at 922K (1200°F) so that approximately equivalent minimum creep rates result. At 1144K (1600°F), due to the lower stress values, these effects are not quite offsetting, and the textured sheets have slightly lower creep rates. At 1255K (1800°F), the stress sensitivity and "structure factor" effects reverse for the two materials which accounts for the observed changes with respect to the level of stress.

4.3 Supplementary Grain Size Study: Investigation of the Dependence of Creep Strength on Sheet Thickness

The purpose of this supplementary investigation was to determine if the creep strength of HAYNES alloy No. 188 is affected by grain size alone or by

TABLE XLI

ANALYSIS OF MINIMUM CREEP RATES OF ASTM 5-6
GRAIN SIZE STUDY SHEETS AS A POWER FUNCTION OF STRESS*

Temp.	log A		n	Std. Error of Estimate, Log Units	Correlation Coefficient
	Stress as MPa	Stress as KSI			
922 K (1200°F)	-20.168	(-14.135)	7.20	.106	.984
1144 K (1600°F)	-12.053	(-7.446)	5.49	.222	.931
1255 K (1800°F)	-10.517	(-5.450)	6.04	.480	.919

* $\log \dot{\epsilon}_{min} = \log A + n \log S$

$\dot{\epsilon}_{min}$ = minimum creep rate, %/hr

S = stress (MPa or KSI)

A, n = constants estimated by method of least squares

TABLE XLII

ANALYSIS OF MINIMUM CREEP RATES OF ASTM 5-6 GRAIN SIZE STUDY SHEETS AS AN EXPONENTIAL FUNCTION OF STRESS*

Temp.	log A'	β		Std. Error of Estimate, Log Units	Correlation Coefficient
		Stress as MPa	Stress as KSI		
922 K (1200°F)	-5.151	.0093	(.0640)	.075	.992
1144 K (1600°F)	-4.941	.0436	(.3004)	.231	.925
1255 K (1800°F)	-4.998	.1098	(.7570)	.574	.881

* $\log \dot{\epsilon}_{min} = \log A' + \beta S$

$\dot{\epsilon}_{min}$ = minimum creep rate, %/hr

S = stress (MPa or KSI)

A', β = constants estimated by method of least squares

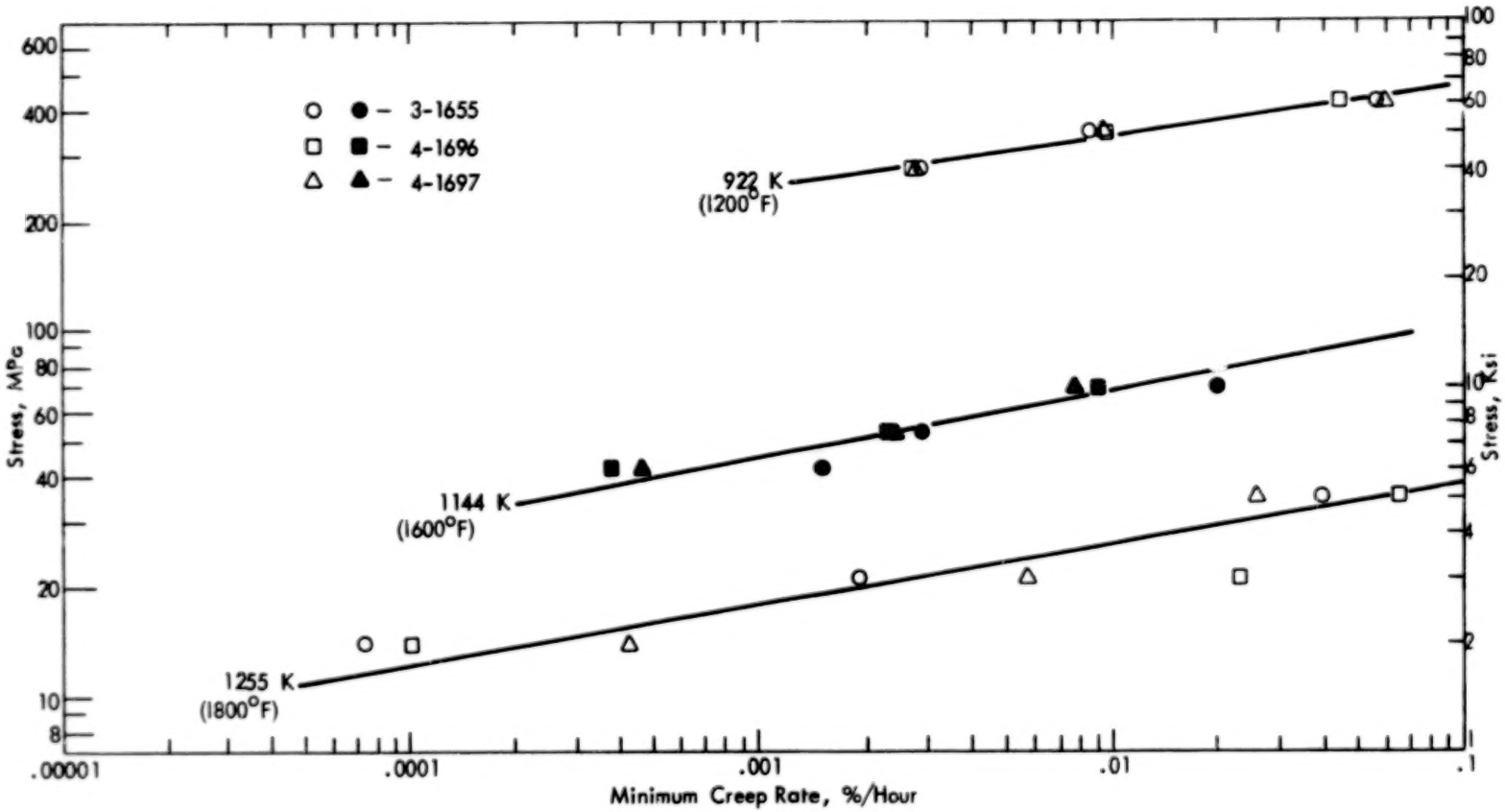

Figure 52: Stress vs. Minimum Creep Rate for ASTM 5-6 Grain Size Study Sheets.

123

thickness-to-grain diameter ratio. Richards (ref. 15), convincingly showed that the thickness-to-grain diameter ratio was more fundamental to the creep strength of several nickel-base sheet alloys than was grain size alone. There was ample reason, therefore, to suspect that thickness-to-grain diameter ratio might be similarly fundamental to the creep strength of thin-gauge HAYNES alloy No. 188. To assess this possibility, a sheet 0.76 mm (.030 inch) thick with a grain size of ASTM 5-6 was produced and evaluated. This selection provided a thickness-to-grain diameter ratio of approximately 14:1 for comparison to the experimental strips having a grain size of ASTM 7-8. Further compariosns were also afforded to the thin gauge sheets having the same grain size. In addition to this, creep properties developed on the initial grain size study strips were re-examined in search of any thickness-to-grain diameter effects.

4.3.1 Production of experimental sheet. - Sheet for the supplementary grain size study was produced from Heat 4-1697 using the thermomechanical processing schedule given in Table XLIII. In terms of the percentage of cold reduction and the annealing treatments, the rolling schedule was equivalent to the latter portion of the processing schedule used to produce the ASTM 5-6 grain size thin gauge sheets.

Production of the sheet was accomplished by rolling a piece of production hot rolled plate from Heat 4-1697 measuring 4.57 mm thick by 12.7 cm wide by 30.48 cm long (0.180 inch x 5 inches x 12 inches) parallel to the original hot rolling direction. The resulting sheet measured approximately 0.76 mm thick by 13.97 cm wide by 165.10 cm long (0.030 inch x 5.5 inches x 65 inches). After the final annealing treatment, the sheet was salt bath desclaed and flattened by stretcher leveling. To ensure that the desired grain size was obtained, metallographic samples were prepared from material taken from the center and both edges of the sheet at locations near the middle of the length and at both ends of the sheet. Results of the metallographic analyses confirmed that a grain size of ASTM 5-6 was achieved. The typical microstructure obtained in the sheet is illustrated in Figure 53.

4.3.2 Examination of crystallographic texture. - A sample of the supplementary grain size study sheet was examined for the presence of crystallographic texture in the sheet plane using the same experimental procedure described in Section 2.2 The type of texturing was the same as that observed in the texture study sheets and some of the grain size study sheets. Angular data measured for the high intensity regions are given in Table XLIV. In comparison to the ASTM 5-6 thin gauge strips (Table XXXII), the angular spreading around the rolling direction was equivalent, but less spreading was found around the transverse direction.

4.3.3 Tensile properties. - Duplicate longitudinal specimens were tensile tested in air at room temperature, 922K (1200°F), 1033K (1400°F), 1144K (1600°F), 1255K (1800°F), and 1366K (2000°F). The procedures employed were the same as those described in Section 2.3. A summary of the results is given in Table XLV. The values obtained were essentially equivalent to those reported

TABLE XLIII

THERMOMECHANICAL PROCESSING SCHEDULE FOR
SUPPLEMENTARY GRAIN SIZE STUDY SHEET LOT

4.57mm (0.180")	Cold Roll	1.78mm (0.070")	Cold Roll	.76mm (0.030")
		Anneal at 1478 K(2200°F)/10 min		Anneal at 1464 K(2175°F)/10 min

TABLE XLIV

ANGULAR DATA FOR HIGH INTENSITY REGIONS
OF (111) POLE FIGURE DETERMINED FOR SUPPLEMENTARY
GRAIN SIZE STUDY SHEET

Around Rolling Direction		Around Transverse Direction	
Angular Locations	Angular Spread	Angular Locations	Angular Spread
19-45°	26°	±34°	68°

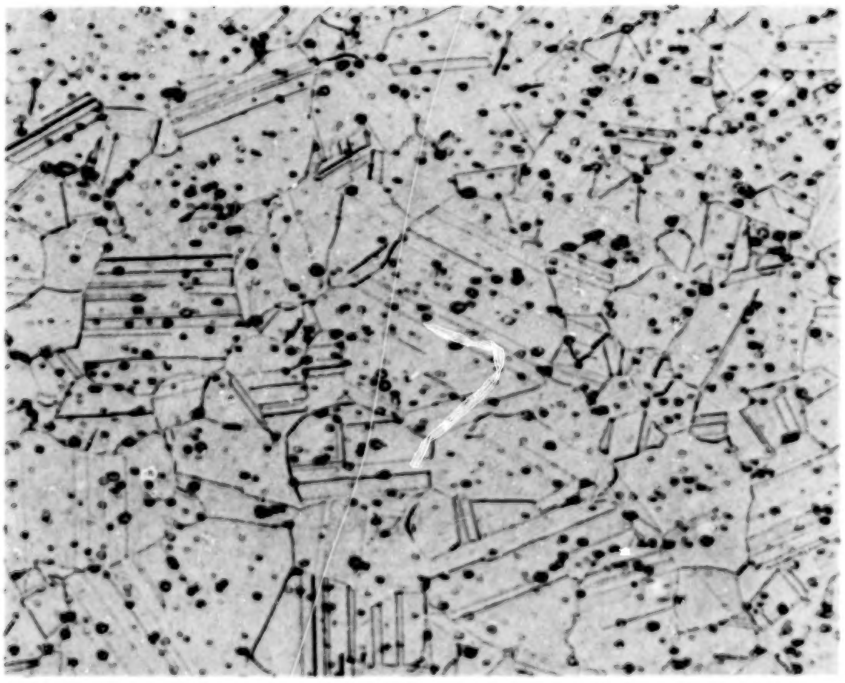

Figure 53: Microstructure of .76 mm (0.030 inch) Thick Supplementary Grain Size Study Sheet Produced from Heat 4-1697. Grain Size ASTM 5-6, Predominantly 5-1/2. X300.

TABLE XLV

LONGITUDINAL TENSILE TEST DATA FOR SUPPLEMENTARY GRAIN SIZE STUDY SHEET LOT - HEAT 4-1697
[0.76 mm (0.030-inch) thick, ASTM 5-6]

Test Temperature	0.2% YS		UTS		Elong.
	MPa	(ksi)	MPa	(ksi)	%
R.T.	521.9	(75.7)	1034.9	(150.1)	59.3
	488.8	(70.9)	980.4	(142.2)	64.4
922 K (1200°F)	316.5	(45.9)	797.0	(115.6)	63.1
	293.7	(42.6)	736.4	(106.8)	70.5
1033 K (1400°F)	302.0	(43.8)	582.6	(84.5)	47.1
	291.6	(42.3)	638.5	(92.6)	53.2
1144 K (1600°F)	272.3	(39.5)	399.9	(58.0)	41.8
	263.4	(38.2)	430.2	(62.4)	53.0
1255 K (1800°F)	151.0	(21.9)	226.8	(32.9)	31.3
	167.5	(24.3)	261.3	(37.9)	40.4
1366 K (2000°F)	79.3	(11.5)	124.8	(18.1)	22.8
	86.2	(12.5)	135.1	(19.6)	25.7

127

for the baseline sheets (Tables III and IV). In comparison to the tensile properties of the ASTM 5-6 grain size thin gauge sheets (Tables XXXVI and XXXVII), the yield and tensile strengths were essentially the same, but the elongations obtained in the supplementary grain size study sheet were higher at test temperatures of 1144K (1600°F) and above.

These observations indicate that yield and ultimate strength properties were not affected by sheet thickness of thickness-to-grain diameter ratios within the range investigated. Approximate values for the thickness-to-grain diameter ratios for the baseline, grain size study and supplementary grain size study sheets were 8.5:1, 7.1:1 and 14.3:1, respectively. From these values, it does not seem likely that the ductility differences between these materials is simply related to thickness-to-grain diameter ratio. If the baseline sheets are excluded from the comparison due to their different TMP and lack of crystallographic texture, a thickness-to-grain diameter effect might seem plausible. However, one could also attribute the differences in elongation to differences in cross-sectional area which would change the amount of necking strain at fracture (ref. 16). Furthermore, it does not seem reasonable that a thickness-to-grain diameter effect would be evident only at temperatures of 1144K (1600°F) and above. This suggests that some other causes might be responsible.

4.3.4 Stress rupture properties. - Duplicate longitudinal and transverse samples from the supplementary grain size study sheet were stress rupture tested at 1089K/165.4 MPa (1500°F/24 ksi) and 1300K/31 MPa (1900°F/4.5 ksi). The results of these tests are listed in Table XLVI. The stress rupture properties were similar to those reported for the baseline thin gauge sheets (Table V) except that elongations for the 1311K/31 MPa (1900°F/4.5 ksi) tests were generally lower. Comparison to the results for the ASTM 5-6 thin gauge sheets (Table XXXVIII) indicates that equivalent life and slightly higher elongation values were obtained in the supplementary grain size study sheet for the 1089K/165.4 MPa (1500°F/24 ksi) test condition, but lower life and elongation values were obtained at the 1311K/31 MPa (1900°F/4.5 ksi) test condition. These data do not reveal any correlation between stress rupture properties and thickness-to-grain diameter ratio that might be expected based on the work of Richards (ref. 15).

4.3.5 Creep life evaluation. - To characterize the low strain ($\leq$ 1 percent) creep properties of the supplementary grain size study sheet, creep tests were conducted on longitudinally oriented samples at temperatures of 922K (1200°F), 1144K (1600°F) and 1255K (1800°F) and at three stresses at each temperature. The testing procedure was the same as that described in Appendix B. As with the other materials evaluated, it was planned to select stresses which would give 1.0 percent creep strain lives in the range of roughly 25-500 hours. Initial stress levels were selected on the basis of results obtained for the baseline sheets. Additional stresses were then selected so as to obtain the required description of creep strength over the temperature range of interest. Duplicate longitudinal and transverse samples were also tested at 1200K/41.4 MPa (1700°F/6 ksi) so that comparisons could be made at the standard

TABLE XLVI

STRESS RUPTURE DATA FOR SUPPLEMENTARY GRAIN SIZE STUDY SHEET LOT - HEAT 4-1697
[0.76 mm (0.030-inch) thick, ASTM 5-6]

Sample Orientation	1089 K/165.4 MPa (1500°F/24 ksi) Life, Hours	1089 K/165.4 MPa (1500°F/24 ksi) Elongation %	1311 K/31 MPa (1900°F/4.5 ksi) Life, Hours	1311 K/31 MPa (1900°F/4.5 ksi) Elongation %
L	38.9	40.6	31.4	15.2
L	39.8	28.3	9.9	40.4
T	36.0	32.3	26.3	13.2
T	40.6	28.6	25.6	15.5
*Log Avg.	38.8	32.1	21.4	18.8
Std. Dev. (Log Units)	(.023)	(.073)	(.226)	(.223)

L = Longitudinal

T = Transverse

* $\bar{t} = \text{antilog}\left(\frac{\Sigma \log t_i}{n}\right)$

129

quality control test condition. A complete listing of the creep test data is contained in Appendix E.

The creep life characterization of the supplementary grain size study sheet was obtained by subjecting the 0.5 percent and 1.0 percent creep strain data to a least squares optimization of the Larson-Miller parameter. The results of this analysis are presented in Table XLVII. Plots of the actual data and the lines given by the parameter equation are illustrated in Figures 54 and 55. The fit of the data to the parameter equation was quite good with correlation coefficients > .95 for both creep strain levels.

The 0.5 percent and 1.0 percent creep data were also force-fit to the parameter equation using a value of 17 for the Larson-Miller constant to provide a basis for direct comparison to the creep properties of the baseline and ASTM 5-6 grain size study sheets. Results of these analyses are presented in Table XLVIII. Agreement to the parameter equation in this form was good, but the RMS values obtained were higher than those of the optimized analyses due to the differences between the optimized Larson-Miller constants and the value of 17 used in the forced-fit approach.

Plots comparing the 0.5 percent and 1.0 percent creep strengths of the baseline, grain size study and supplementary grain size study sheets based on the forced-fit analyses are presented in Figures 56 and 57. These figures indicate equivalent creep strengths at both creep strain levels for the thin gauge grain size study sheets and the supplementary grain size study sheet at conditions corresponding to tests performed at 922K (1200°F) and 1144K (1600°F). However, at conditions corresponding to the 1255K (1800°F) creep tests, the creep strength of the supplementary grain size study was inferior to and below the minus 3-sigma limits (see Figures 48 and 49) of the thin gauge grain size study sheets. Reference to Figures 9 and 10 indicates that although the average creep strength of the supplementary grain size study sheet was below that of the baseline at 1255K (1800°F), it was within the baseline scatter band. These comparisons clearly indicate that no improvement in low strain creep strength was obtained through an increase in the thickness-to-grain diameter ratio.

As a further test of the thickness-to-grain diameter ratio hypothesis, the creep data obtained at 1200K/41.4 MPa (1700°F/6 ksi) for the initial grain size study thin gauge strips were re-analyzed in terms of thickness-to-grain diameter ratio. Plots of the times to 0.5 percent and 1.0 percent creep strain versus thickness-to-grain diameter ratios obtained for these sheets are presented in Figures 58 and 59. Results of statistical comparisons reported in Section 4.1.3 indicated no significant differences in the creep properties of the ASTM 2-4 and the ASTM 5-6 grain size sheets. Therefore, the low strain creep lives of these materials showed no dependence on thickness-to-grain size ratio. For the ASTM 7-8 grain size sheets, creep lives were found to decrease with increasing thickness-to-grain diameter ratio rather than the opposite as might be expected. With reference to the data contained in Table XLIX, it can be seen that this trend is not supported by the results obtained for the ASTM 5-6 supplementary grain size study sheets. Instead, the results for the supplementary grain size study sheet were essentially equivalent to

TABLE XLVII

OPTIMIZED LARSON-MILLER PARAMETER ANALYSIS FOR SUPPLEMENTARY GRAIN SIZE STUDY SHEET

Regression Equation: $Y = \log t = C_1 + \frac{C_2}{T} + \frac{C_3}{T} \log S + \frac{C_4}{T} (\log S)^2$

A. Where T = Absolute temperature, Kelvin

t = Time to given creep strain, hours

S = Stress, MPa

Creep Strain	Equation Parameters				Fit of Test Data			
	C_1	C_2	C_3	C_4	Std. Error of Estimate	Correlation Coefficient	Number of Tests	RMS
0.5%	22.5517	31156.6	1534.94	-2028.90	.224	.955	9	.167
1.0%	20.9238	29122.2	2206.53	-2147.97	.180	.970	9	.135

B. Where T = Absolute temperature, degrees Rankine

t = Time to given creep strain, hours

S = Stress, ksi

0.5%	22.5517	55830.8	-3361.68	-3652.02	.224	.955	9	.167
1.0%	20.9238	53031.8	-2512.27	-3866.35	.180	.970	9	.135

131

TABLE OF CONTENTS

		Page	
SUMMARY		1	1/A7
1.0	INTRODUCTION	3	1/A9
2.0	CABOT BASELINE DATA	5	1/A11
	2.1 Materials	5	1/A11
	2.2 Texture	5	1/A11
	2.3 Tensile Properties	14	1/B7
	2.4 Stress Rupture Properties	17	1/B12
	2.5 Creep Properties	17	1/B12
	2.5.1 Creep life evaluation	17	1/B12
	2.5.2 Minimum creep rate evaluation	25	1/C9
	2.6 Static Oxidation Resistance	31	1/D5
	2.7 Dynamic Oxidation Resistance	31	1/D5
3.0	TEXTURE STUDY	39	1/E4
	3.1 Introduction	39	1/E4
	3.2 Initial Investigaton	40	1/E5
	3.2.1 Production of experimental sheet lots	40	1/E5
	3.2.2 Examination of crystallographic texture	40	1/E5
	3.2.3 Creep strength evaluation	61	1/G1
	3.3 Evaluation of Optimum Texture Sheets	65	1/G6
	3.3.1 Production of experimental sheet lots	65	1/G6
	3.3.2 Examination of grain size and crystallographic texture	65	1/G6

TABLE OF CONTENTS (Cont.)

		Page	
3.3.3	Bend ductility	65	1/G6
3.3.4	Tensile properties	65	1/G6
3.3.5	Stress rupture properties	67	1/G8
3.3.6	Creep life evaluation	67	1/G8
3.3.7	Minimum creep rate evaluation	79	2/B3
3.3.8	Examination of microstructure after creep testing	79	2/B3
3.3.9	Residual room temperature tensile properties after creep testing	88	2/C2
4.0	GRAIN SIZE STUDY	92	2/C8
4.1	Investigation of the Dependence of Creep Strength on Grain Size	92	2/C8
4.1.1	Production of experimental sheet lots	92	2/C8
4.1.2	Examination of crystallographic texture	92	2/C8
4.1.3	Creep strength evaluation	97	2/D3
4.1.4	Apparent activation energies for creep	101	2/D9
4.2	Evaluation of ASTM 5-6 Grain Size Sheets	103	2/D12
4.2.1	Production of experimental sheet lots	103	2/D12
4.2.2	Tensile properties	107	2/E2
4.2.3	Stress rupture properties	107	2/E2
4.2.4	Creep life evaluation	107	2/E2
4.2.5	Minimum creep rate evaluation	120	2/F11
4.3	Supplementary Grain Size Study: Investigation of the Dependence of Creep Strength on Sheet Thickness	120	2/F11
4.3.1	Production of experimental sheet	124	2/G3
4.3.2	Examination of crystallographic texture	124	2/G3

TABLE OF CONTENTS (Cont.)

	Page	
4.3.3 Tensile properties	124	2/G3
4.3.4 Stress rupture properties	128	2/G8
4.3.5 Creep life evaluation	128	2/G8
4.3.6 Minimum creep rates	140	3/B7
5.0 PRESTRAIN STUDY	144	3/B12
5.1 Materials and Experimental Procedure	144	3/B12
5.2 Creep Test Results	144	3/B12
5.3 Examination of Microstructures after Creep Testing	147	3/C3
6.0 DYNAMIC OXIDATION RESISTANCE OF EXPERIMENTAL SHEETS	154	3/C10
6.1 Materials and Experimental Procedure	154	3/C10
6.2 Dynamic Oxidation Test Results	154	3/C10
7.0 DISCUSSION AND CONCLUDING REMARKS	158	3/D2
APPENDIX A - Conversion of U.S. Customary Units to SI Units	160	3/D4
APPENDIX B - Creep Test Procedure	164	3/D8
APPENDIX C - Baseline Creep Test Data	168	3/D13
APPENDIX D - Texture Study Creep Test Data	173	3/E9
APPENDIX E - Grain Size Study Creep Test Data	179	3/F7
REFERENCES	186	3/G7

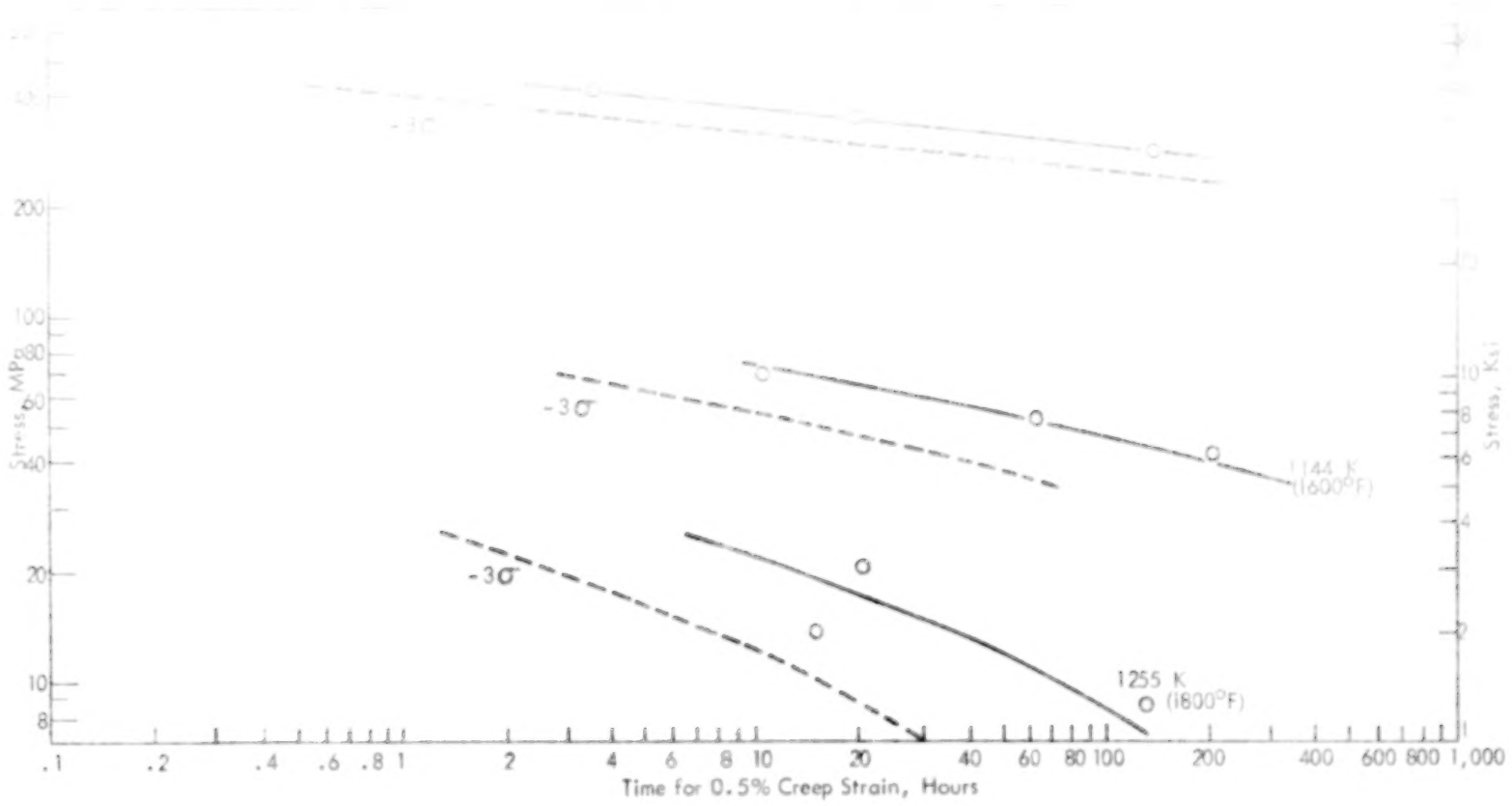

Figure 54: Stress vs. 0.5% Creep Life of Supplementary Grain Size Study Sheet (Actual Data and Parametric Evaluation)

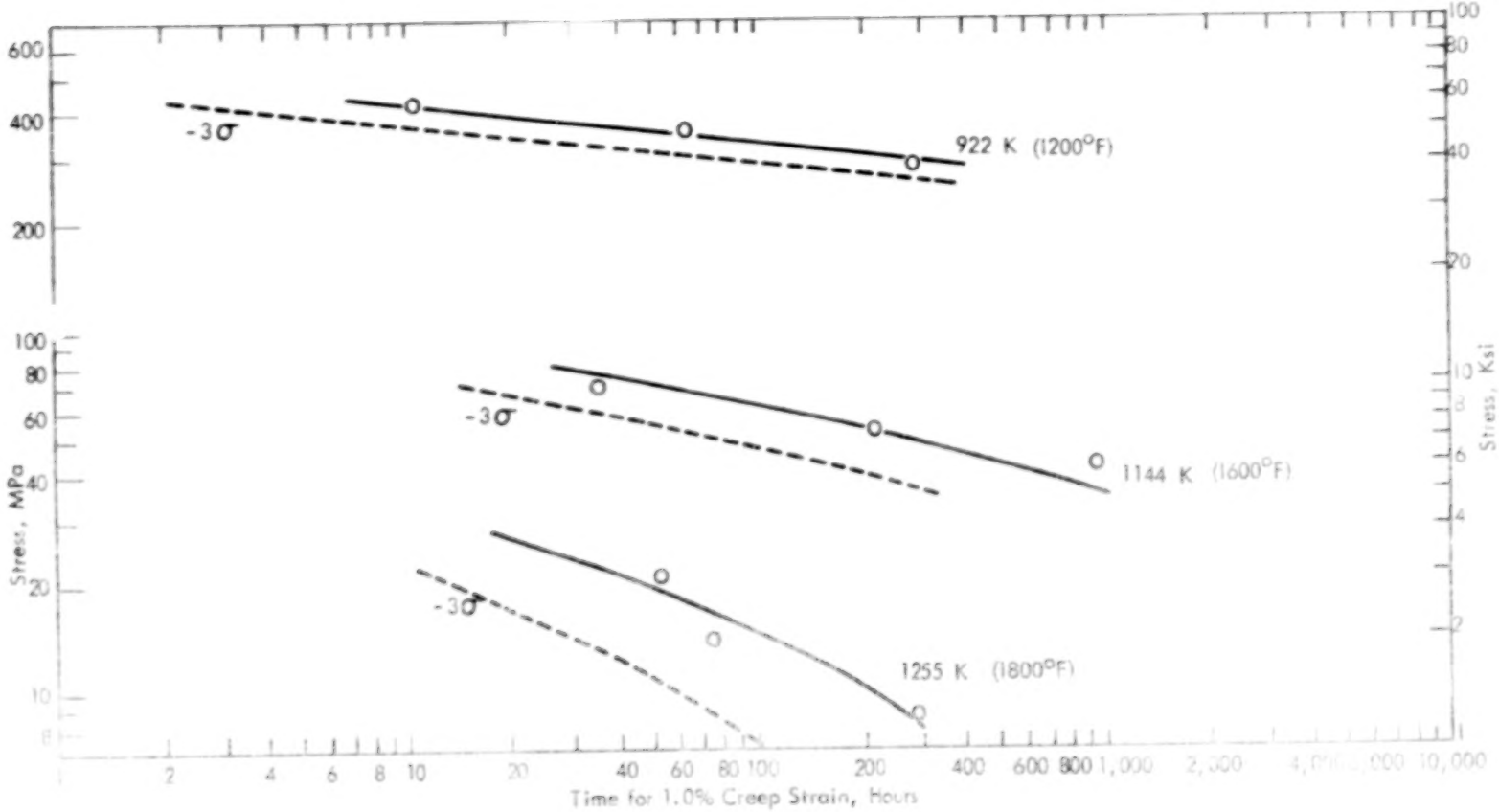

igure 55: Stress vs. 1.0% Creep Life of Supplementary Grain Size Study Sheet (Actual Data and Parametric Evaluation)

TABLE XLVIII

FORCE-FIT ANALYSIS OF SUPPLEMENTARY GRAIN SIZE STUDY SHEET TO LARSON-MILLER PARAMETER EQUATION WITH A LARSON-MILLER CONSTANT OF 17

Regression Equation: $P = T (\log t + 17) = C_2 + C_3 \log S + C_4 (\log S)^2$

A. Where T = Absolute temperature, Kelvin

t = Time to given creep strain, hours

S = Strain, MPa

Creep Strain	Equation Parameters C_2	C_3	C_4	Std. Error of Estimate, LM Parameter Units	Correlation Coefficient	Number of Tests	RMS
0.5%	23932.5	1318.98	-1618.25	295.84	.996	9	.203
1.0%	23960.8	2120.11	-1875.50	222.89	.998	9	.157

B. Where T = Absolute temperature, degrees Rankine

t = Time to given creep strain, hours

S = Stress, ksi

0.5%	43021.3	-2510.79	-2912.85	532.51	.996	9	.203
1.0%	43955.7	-1845.31	-3375.90	401.21	.998	9	.157

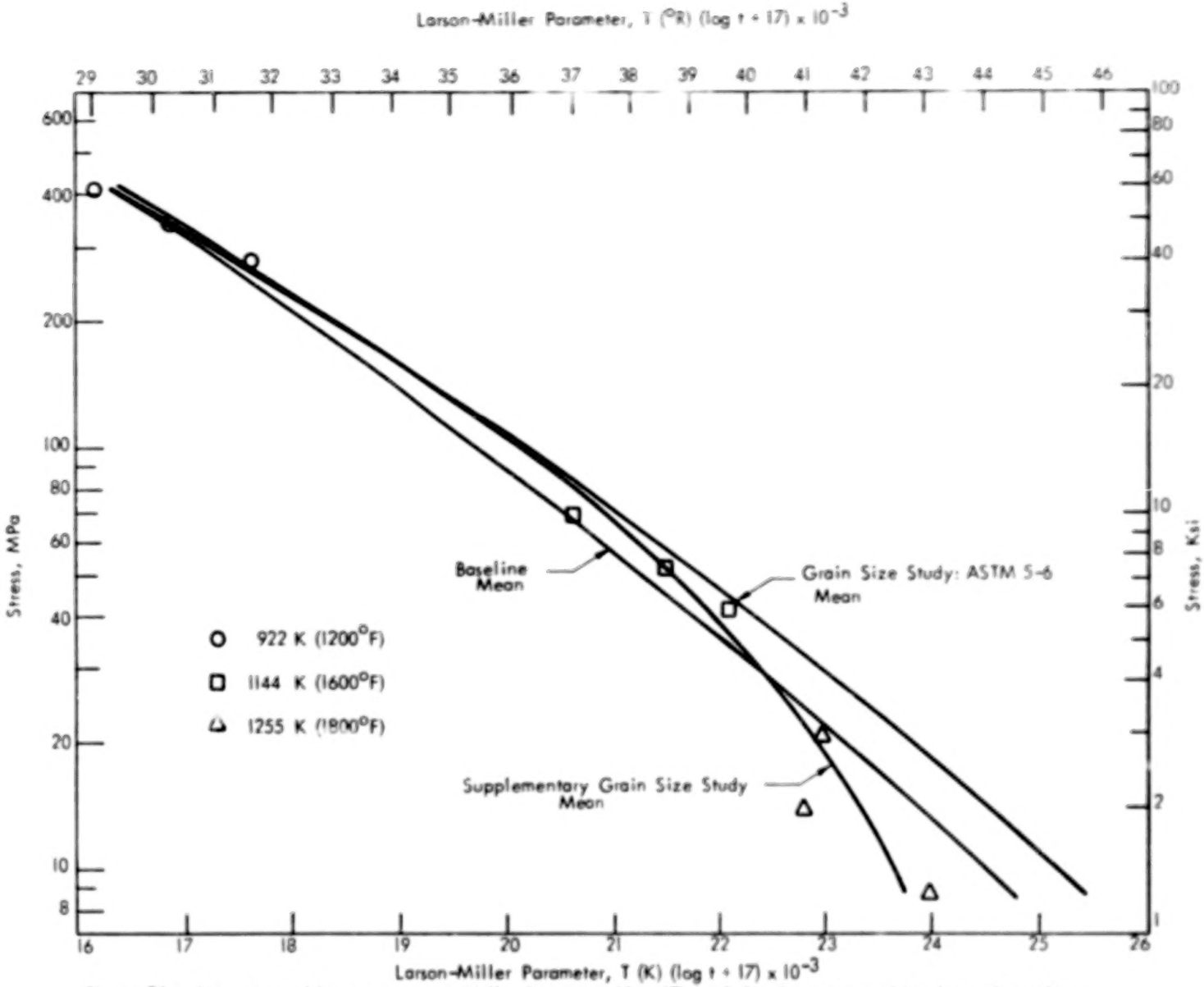
Larson-Miller Parameter, T (°R) (log t + 17) x 10⁻³
29 30 31 32 33 34 35 36 37 38 39 40 41 42 43 44 45 46
600 400 200 100 80 60 40 20 10 8
Stress, MPa
100 80 60 40 20 10 8 6 4 2 1
Stress, Ksi
Baseline Mean
Grain Size Study: ASTM 5-6 Mean
922 K (1200°F)
1144 K (1600°F)
1255 K (1800°F)
Supplementary Grain Size Study Mean
16 17 18 19 20 21 22 23 24 25 26
Larson-Miller Parameter, T (K) (log t + 17) x 10⁻³

Figure 56: Comparison of Stress vs. Larson-Miller Parameter (C_1 = 17) for 0.5% Creep Lives of Baseline, Grain Size Study and Supplementary Grain Size Study Sheets.

135

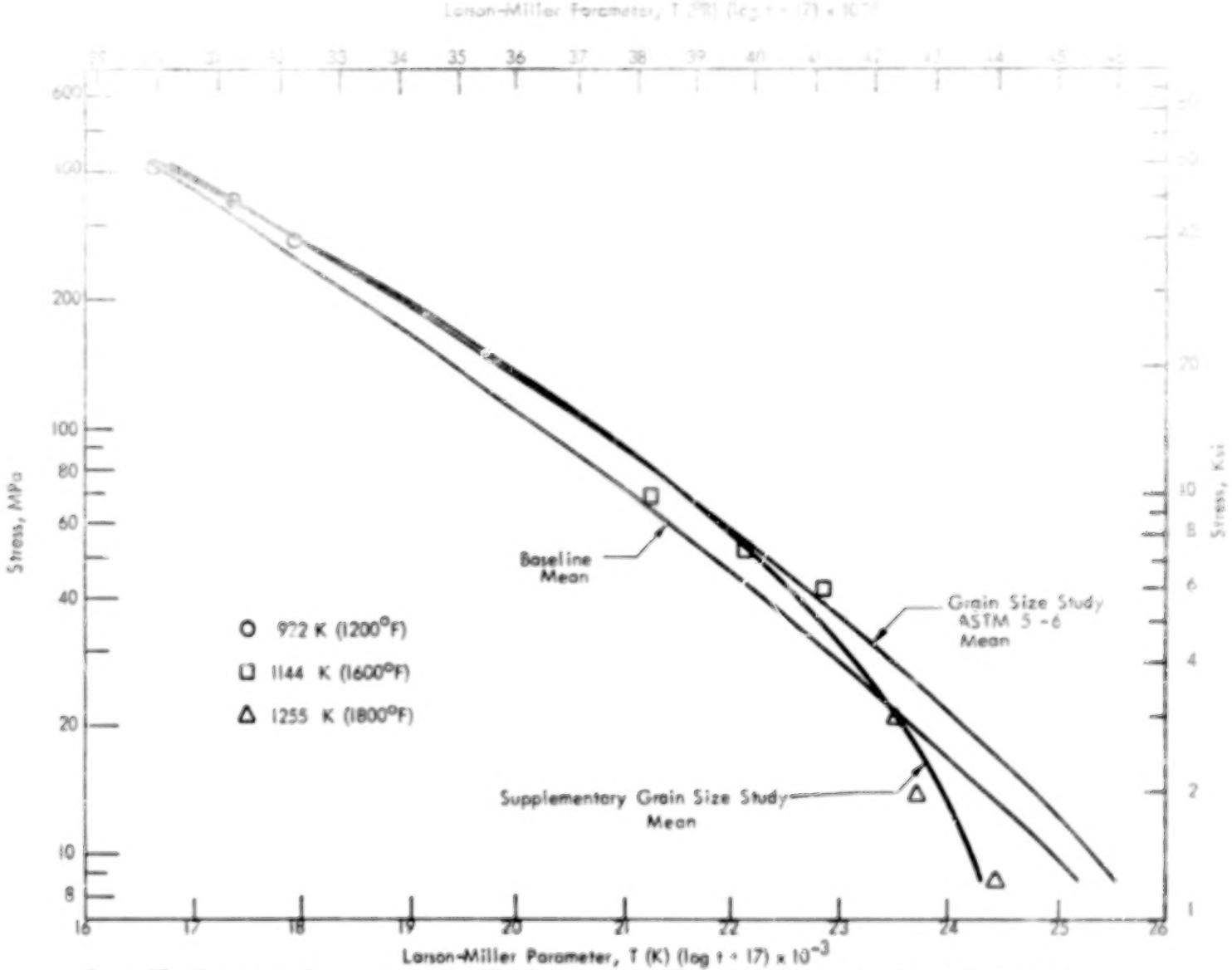

Figure 57: Comparison of Stress vs. Larson-Miller Parameter (C_1 = 17) for 1.0% Creep Lives of Baseline, Grain Size Study and Supplementary Grain Size Study Sheets.

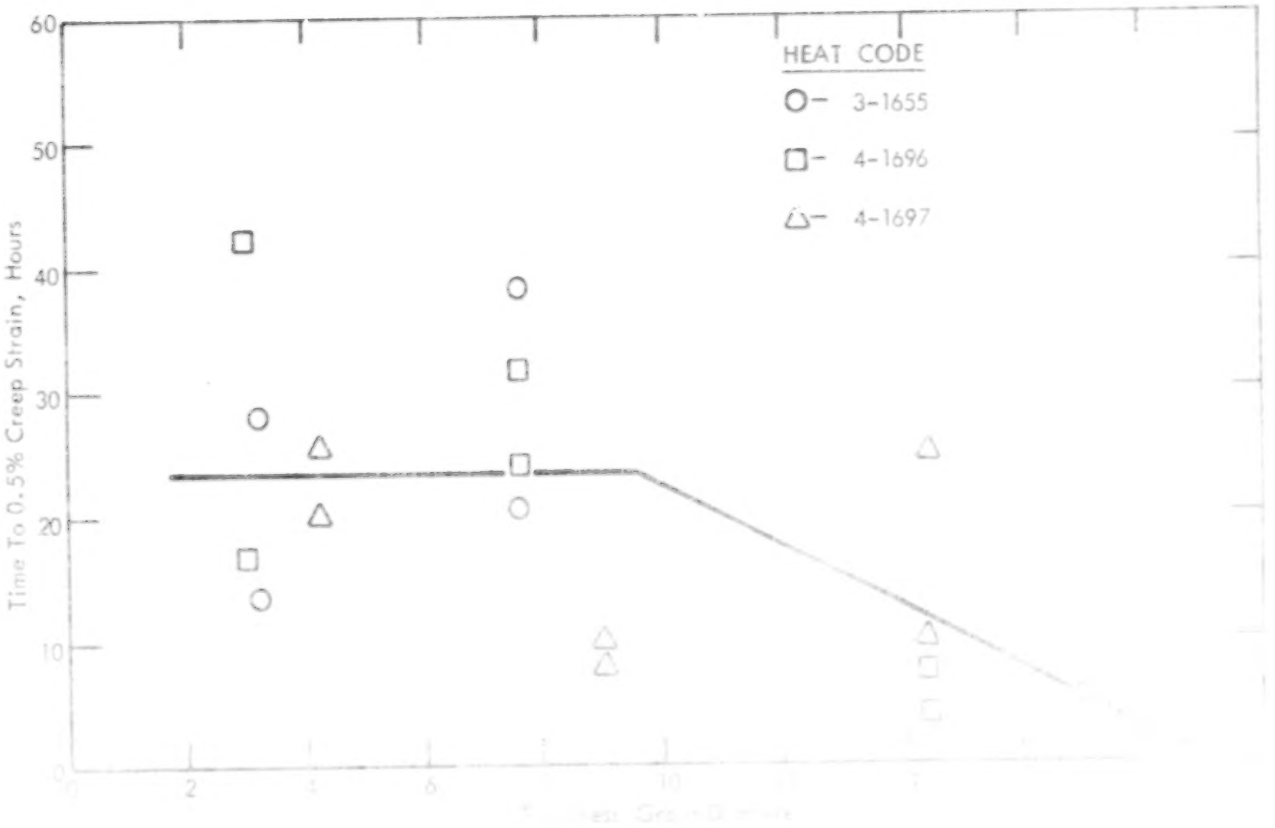

BEST DOCUMENT AVAILABLE

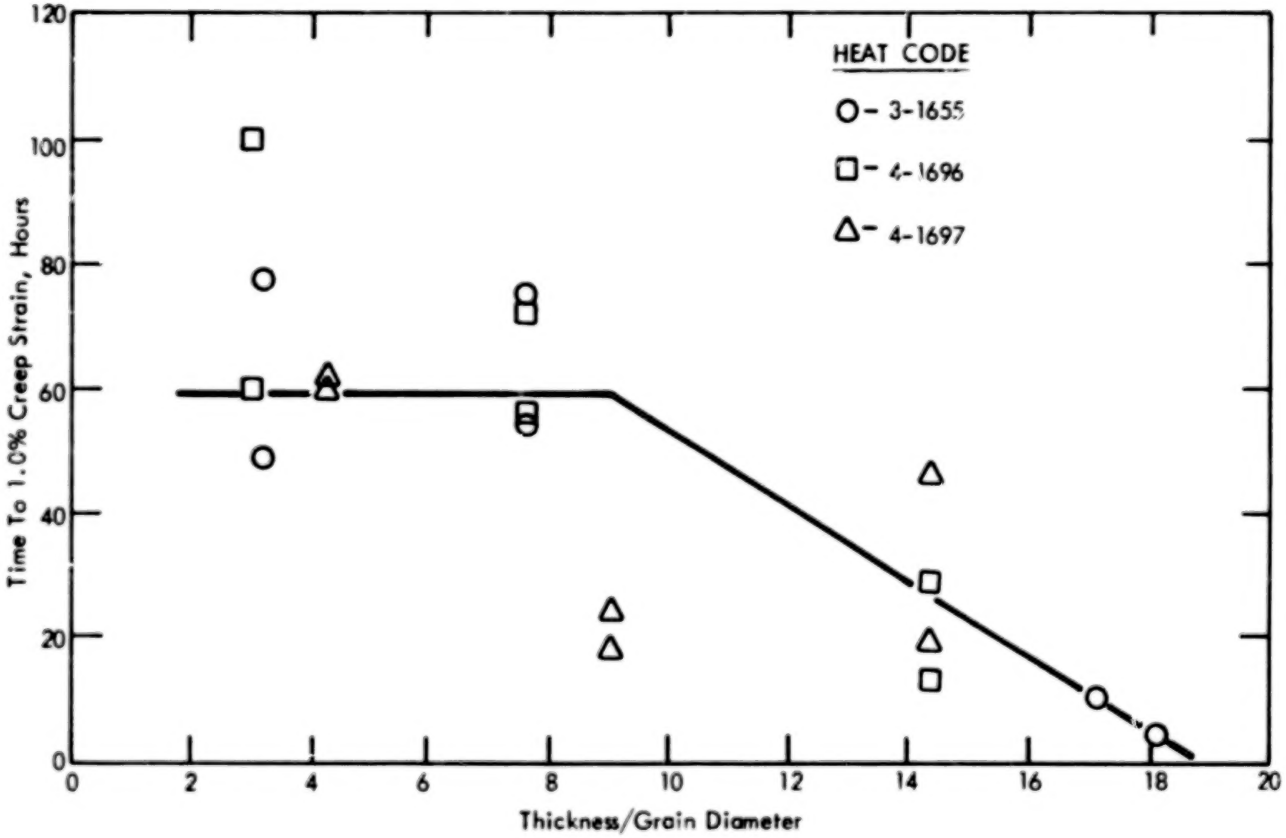

Figure 59: Time to 1.0% Creep Strain vs. Thickness - to - Grain Diameter Ratio for 1200 K/41.4 MPa (1700°F/6 k.s.i.) Tests of Grain Size Study Thin Gauge Strips.

TABLE XLIX

SUMMARY OF 1200 K/41.4 MPa (1700°F/6 ksi) CREEP DATA
FOR SUPPLEMENTARY GRAIN SIZE STUDY SHEET

Number of Tests, N	0.5% CREEP STRAIN			1.0% CREEP STRAIN		
	Avg. Log Time*	Antilog, Hrs	Std. Dev.**	Avg. Log Time*	Antilog, Hrs	Std. Dev.**
4	1.523	33.4	.346	1.828	67.3	.331

* $\log \bar{t} = \frac{\Sigma \log t_i}{n}$ where t_i = observed time to given creep strain

n = No. of observations

** log units

those obtained for the ASTM 2-4 and ASTM 5-6 thin gauge strips. These facts lead to the conclusion that low strain creep strength is dependent on grain size alone and not on thickness-to-grain diameter ratio within the range of grain sizes and thicknesses investigated.

4.3.6 Minimum creep rates. - The minimum creep rates determined for the supplementary grain size study sheet were examined by multiple regression analyses assuming both a power and an exponential dependence on stress as described in Section 2.5.2. Results of these analyses are presented in Tables L and LI. As was seen in the analyses for all previous materials, the fit of the data to either stress relationship was approximately equivalent. The explanation based on the hyperbolic sine law which was described in Section 2.5.2 is again thought to apply. Plots of the data corresponding to the power function of stress are illustrated in Figure 60. The minimum creep rates obtained at test temperatures of 922K (1200°F) and 1144K (1600°F) were equivalent to those of the ASTM 5-6 thin gauge grain size study sheets (Figure 52) and the baseline sheets (Figure 11). At 1255K (1800 F), however, the minimum creep rates of the supplementary grain size study sheet were higher than those of the grain size study sheets, but within the scatter band of the baseline sheets. These trends are consistent with the findings of the 0.5 percent and 1.0 percent creep life evaluations of the previous section.

The power function parameters listed in Table L indicate that the stress sensitivity and the "structure factor" at 922K (1200°F) were comparable to those obtained for the grain size study sheets (Table XLI). At 1144K (1600°F), the stress sensitivity of the supplementary grain size study sheet was higher, but its effect on the resulting minimum creep rates was offset by a low "structure factor" value. At 1255K (1800°F), the minimum creep rate response was very much different. The stress sensitivity was much lower, and the "structure factor" term was much higher.

TABLE L

ANALYSIS OF MINIMUM CREEP RATES OF SUPPLEMENTARY GRAIN SIZE STUDY SHEET AS A POWER FUNCTION OF STRESS*

Temp.	log A		n	Std. Error of Estimate, Log Units	Correlation Coefficient
	Stress as MPa	Stress as KSI			
922 K (1200°F)	-19.156	(-13.451)	6.80	.117	.991
1144 K (1600°F)	-14.822	(-8.848)	7.12	.007	1.000
1255 K (1800°F)	-4.626	(-2.837)	2.13	.072	.992

* $\log \dot{\epsilon}_{min} = \log A + n \log S$

$\dot{\epsilon}_{min}$ = minimum creep rate, %/hr

S = Stress (MPa or KSI)

A, n = constants estimated by method of least squares

TABLE LI

ANALYSIS OF MINIMUM CREEP RATES OF SUPPLEMENTARY GRAIN SIZE STUDY SHEET AS AN EXPONENTIAL FUNCTION OF STRESS*

Temp.	log A'	β		Std. Error of Estimate, Log Units	Correlation Coefficient
		Stress as MPa	Stress as KSI		
922 K (1200°F)	-4.951	.0088	(.0604)	.067	.997
1144 K (1600°F)	-5.613	.0568	(.3913)	.072	.998
1255 K (1800°F)	-3.156	.0655	(.4516)	.143	.969

* $\log \dot{\epsilon}_{min} = \log A' + \beta S$

$\dot{\epsilon}_{min}$ = minimum creep rate, %/hr

S = Stress (MPa or KSI)

A', β = constants estimated by method of least squares

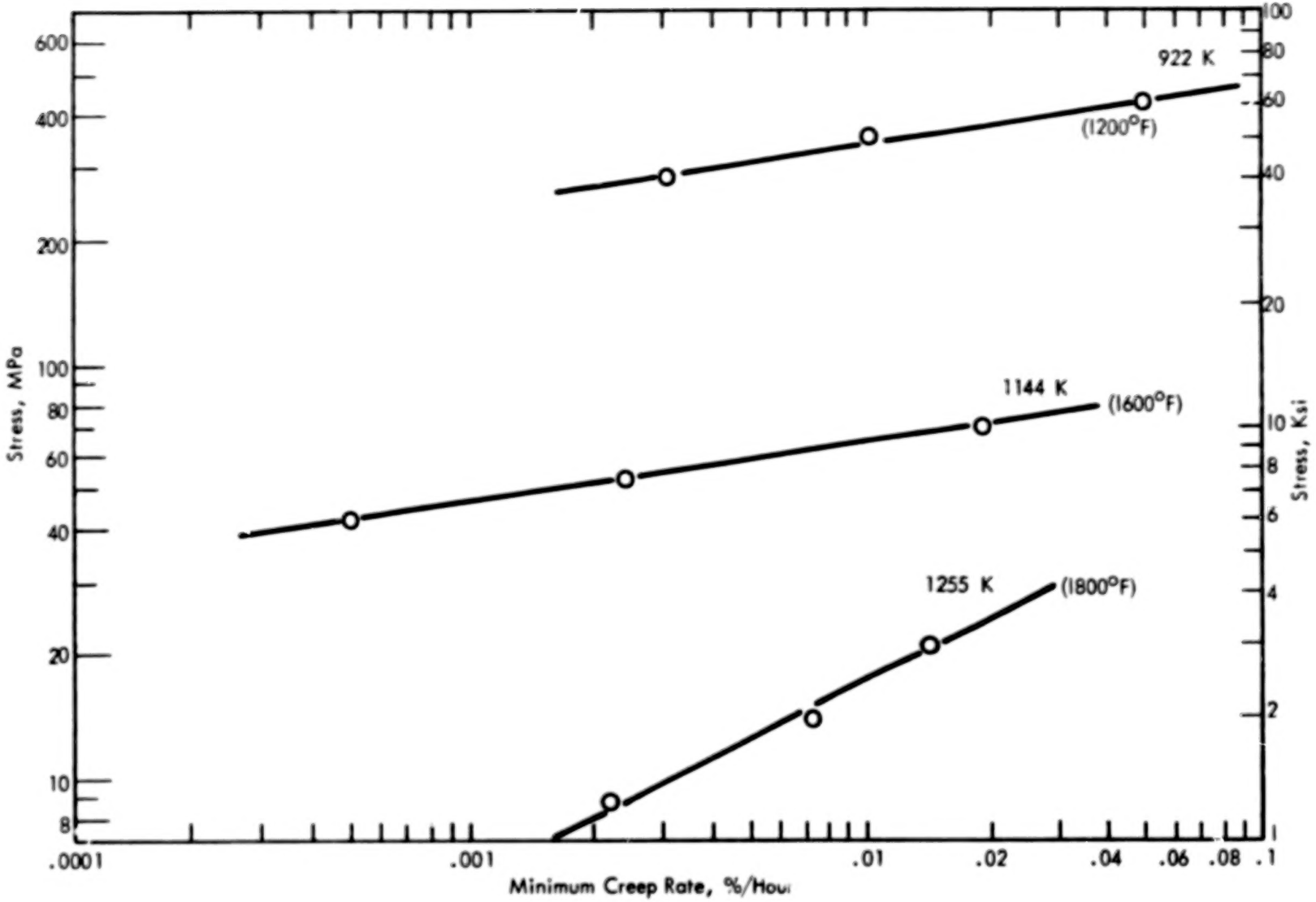

Figure 60: Stress vs. Minimum Creep Rate for Supplementary Grain Size Study Sheet.

5.0 PRESTRAIN STUDY

5.1 Materials and Experimental Procedure

A brief investigation was performed to determine the effects of prestrain on the creep strength of standard production HAYNES alloy No. 188 thin gauge sheet. The material used for this purpose was arbitrarily selected from baseline Heat 2-1604. Longitudinal samples of the same configuration as that illustrated in Appendix B were prepared from the sheet. Duplicate samples were then strained in a tensile testing machine to prestrain values of 1, 2, 4, 6, 10, 15, and 20 percent using the engineering definition of strain. After prestraining, the samples were creep tested at a condition of 1200K/41.4 MPa (1700°F/6 ksi) in accordance with the procedure given in Appendix B.

5.2 Creep Test Results

Results of the creep tests are listed in Table LII along with the original baseline tests for this heat for 0 percent prestrain reference. The data indicate a number of prestrain effects which can be summarized as follows:

(1) Creep Strength

Based on the amount of time to a given creep strain, the creep strength increased with prestrain up to a level of 4 percent. Prestrain amounts of 1 percent and 2 percent had essentially the same effect, and a slight but definite improvement over the baseline was observed. A two-fold improvement was obtained with 4 percent prestrain. From 4 percent through 10 percent prestrain, the increased creep strength was maintained but not improved. Above 10 percent prestrain, the creep strength began to decrease, falling to below that of the baseline at the 20 percent prestrain level.

(2) Minimum Creep Rate

The minimum creep rate was found to decrease with increasing prestrain up to a level of 4 percent. Prestrain amounts of 1 percent and 2 percent both provided approximately a 30 percent decrease in minimum creep rate from the baseline values. At 4 percent prestrain, the minimum creep rate was about half that of the baseline. From 4 percent to 10 percent prestrain, the reduced minimum creep rate was maintained. At 15 percent prestrain, the minimum creep rate rose to near that of the baseline, and at 20 percent prestrain it was roughly twice the baseline rate.

(3) Primary Creep

The amount of primary creep, viewed both in terms of creep strain and duration, was found to increase slightly above the baseline with 1 percent

TABLE LII

1200 K/41.4 MPa (1700°F/6,000 psi) CREEP DATA FOR THE PRESTRAIN STUDY: HEAT 2-1604

Time for Indicated Creep Strain, Hrs							Min. Creep Rate	Min. Creep Rate Intercept	Primary Creep Strain	Time of Primary Creep
0.1%	0.2%	0.3%	0.4%	0.5%	0.75%	1.0%	%/Hr	%	%	Hrs
Baseline 0% Prestrain										
1.5	3.5	6.0	9.0	13.0	23.0	33.0	.0245	.186	.43	10.0
1.0	3.0	6.0	10.0	14.0	25.0	35.6	.0231	.173	.40	10.0
1% Prestrain										
1.0	4.0	8.0	13.2	19.1	35.5	51.8	.0154	.198	.51	20.0
1.2	4.4	8.3	13.0	18.4	33.0	47.5	.0171	.182	.53	20.0
2% Prestrain										
1.5	4.8	9.2	14.2	19.7	33.5	47.2	.0181	.148	.51	20.0
.5	3.0	7.7	13.7	19.7	34.5	49.4	.0167	.171	.34	10.0
4% Prestrain										
2.0	7.5	14.5	22.0	29.2	47.3	62.8	.0135	.099	.24	10.0
2.0	7.0	14.5	23.0	30.7	52.5	70.0	.0121	.112	.25	10.0
6% Prestrain										
1.6	7.3	15.3	23.8	32.2	53.5	74.3	.0115	.121	.24	10.0
2.1	8.7	15.5	22.3	29.2	46.3	63.3	.0145	.073	.15	5.0
10% Prestrain										
2.5	8.0	14.3	20.8	27.5	43.0	56.5	.0152	.076	.19	7.5
2.4	8.3	15.5	22.7	30.0	47.0	61.3	.0138	.080	.17	6.0

145

TABLE LII (Cont.)

Time for Indicated Creep Strain, Hrs							Min. Creep Rate	Min. Creep Rate Intercept	Primary Creep Strain	Time of Primary Creep
0.1%	0.2%	0.3%	0.4%	0.5%	0.75%	1.0%	%/Hr	%	%	Hrs
			15% Prestrain							
3.5	7.9	12.3	16.7	21.2	31.2	39.2	.0227	.015	.08	2.5
1.5	6.2	10.9	16.7	20.7	31.2	40.7	.0205	.069	.12	2.5
			20% Prestrain							
.9	2.7	4.5	6.2	7.6	10.6	12.0	.0512	.058	.11	1.0
1.1	3.2	5.3	6.9	8.1	10.6	12.8	.0454	.043	.09	1.0

prestrain. It then decreased in a rather continuous fashion as the amount of prestrain increased through 20 percent.

These observations are in agreement with the findings of other investigators (ref. 5, p. 41). The beneficial effects of prestrain result from a reduction in primary creep and minimum creep rate. Adverse effects at high levels of prestrain can be associated with structural instability and the promotion of recrystallization. Although significant improvements over baseline 1200K/41.4 MPa (1700°F/6 ksi) creep strength were obtained by prestraining, the strength levels achieved were not as great as those observed in the textured sheets.

5.3 Examination of Microstructures After Creep Testing

Samples used in the prestrain study were examined metallographically to determine whether any microstructural changes had occurred during creep testing. Representative micrographs of these samples are presented in Figure 61. In comparison to the baseline, the prestrain samples appeared to have precipitated more carbides randomly within the grains and at twin boundaries. Changes in grain size were also observed. The grain size readings obtained from the samples are listed in Table LIII. Essentially no change in grain size was found in the samples prestrained 1 percent and 2 percent. Those samples prestrained 4 percent through 10 percent exhibited slight grain coarsening. At prestrain levels of 15 percent and 20 percent, recrystallization occurred, yielding a finer grain size than the baseline samples. The recrystallized samples contained remnant grain boundary carbide networks which are prominent in the micrographs. The new grain boundaries were essentially carbide free and are not easily discernible in the photographs.

To complement the metallographic evaluation, the prestrained samples were also examined by transmission electron microscopy. Electron micrographs illustrating typical structures observed in the samples are presented in Figure 62. Comparisons to the baseline (0 percent prestrain) can be made with reference to Figure 38a. The photographs clearly show the expected increase in dislocation density with increasing amounts of prestrain. At prestrains of 1-4 percent, the dislocation configurations consisted principally of tangles and pile-ups at grain boundaries and carbide particles. Cellular wall configurations were prominent at prestrains of 6 percent and above. The recrystallization process is evident at prestrain levels of 15 percent and 20 percent. Figure 62g clearly reveals a recrystallization front moving into a heavily deformed region in a sample prestrained 20 percent.

The observed structures indicate that improved creep resistance can be associated with configurations which provide effective dislocation locking. Above 10 percent prestrain, the recrystallization process begins to eliminate the locked in dislocation networks, and creep resistance is reduced. Creep strengths below the baseline values result when fine recrystallized grains with essentially carbide-free boundaries are produced. This strongly suggests

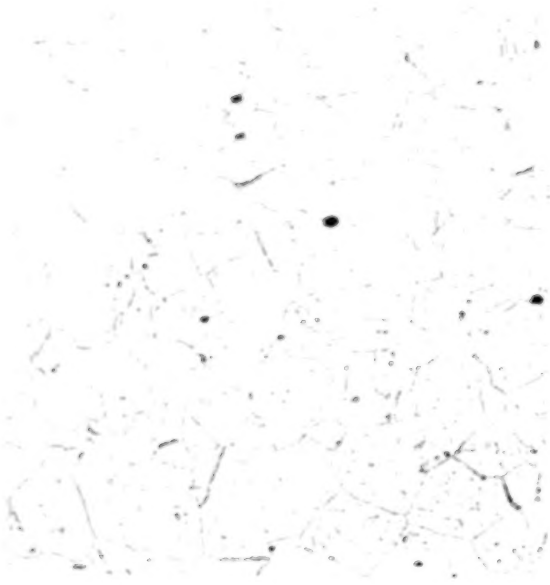

(a) Baseline - 0% Prestrain

(b) 1% Prestrain

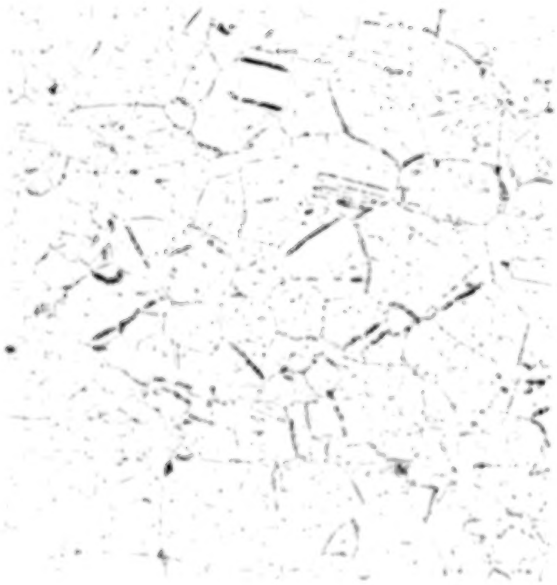

(c) 2% Prestrain

(d) 4% Prestrain

Figure 61: Samples from Prestrain Study after Creep Testing at 1200K/ 41.4 MPa (1700°F/6,000 psi) - Heat 2-1604. X300.

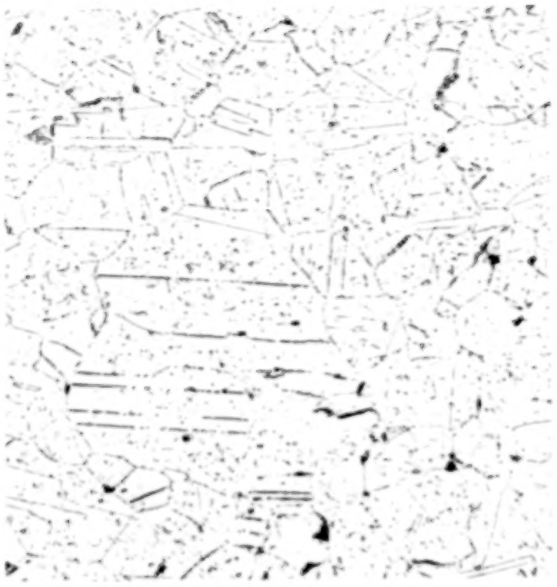

(e) 6% Prestrain

(f) 10% Prestrain

(g) 15% Prestrain

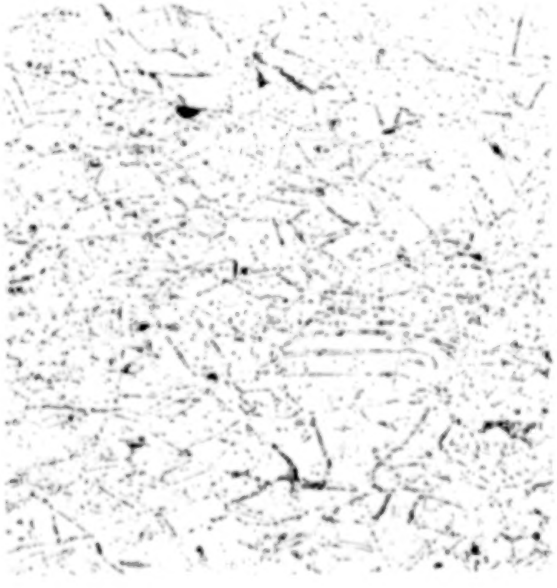

(h) 20% Prestrain

Figure 61 (continued): Samples from Prestrain Study after Creep Testing at 1200K/41.4 MPa (1700°F/6,000 psi) - Heat 2-1604. X300.

TABLE LIII

GRAIN SIZE ANALYSIS OF PRESTRAIN STUDY SAMPLES
AFTER CREEP TESTING AT 1200 K/41.4 MPa (1700°F/6,000 PSI)
HEAT 2-1604

Prestrain Amount	ASTM Grain Size
0%	6-1/2
1%	6-1/2
2%	6-1/2 to 7
4%	6 to 6-1/2, predominantly 6
6%	5-1/2 to 6-1/2
10%	5-1/2 to 6-1/2, predominantly 6
15%	6 to 8, predominantly 6 to 6-1/2
20%	7 to 8-1/2

(a) 1% Prestrain. X15,100.

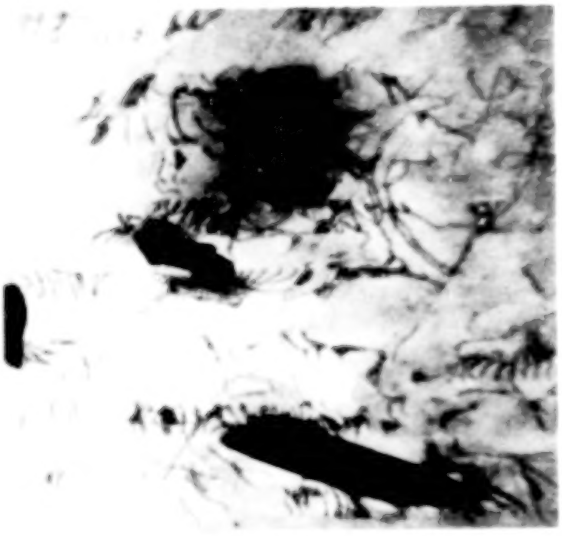

(b) 2% Prestrain. X23,900.

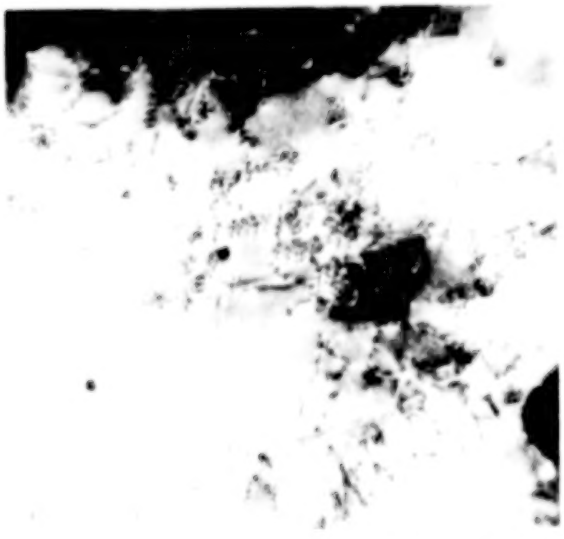

(c) 4% Prestrain. X15,100.

(d) 6% Prestrain. X15,100.

Figure 62: Substructures Observed in Prestrained Samples after Creep Testing at 1200K/41.4 MPa (1700°F/6 ksi). Heat 2-1604.

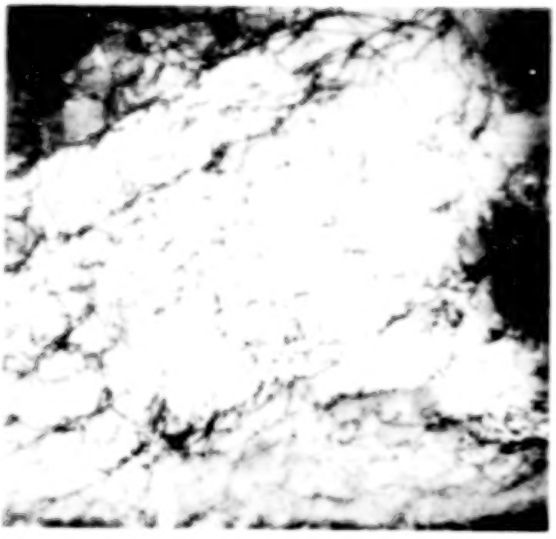

(e) 10% Prestrain. X23,900.

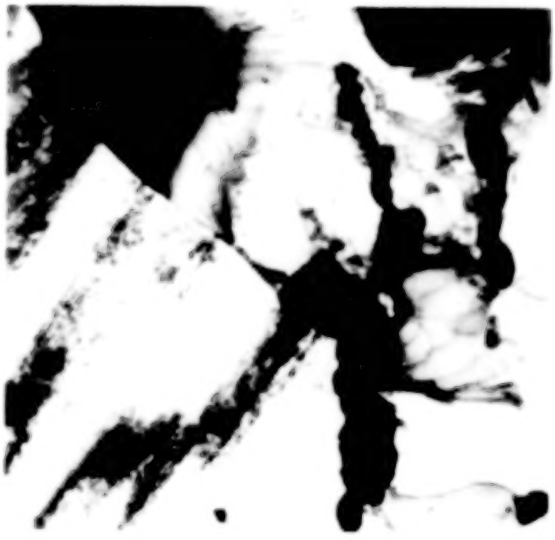

(f) 15% Prestrain. X9,500.

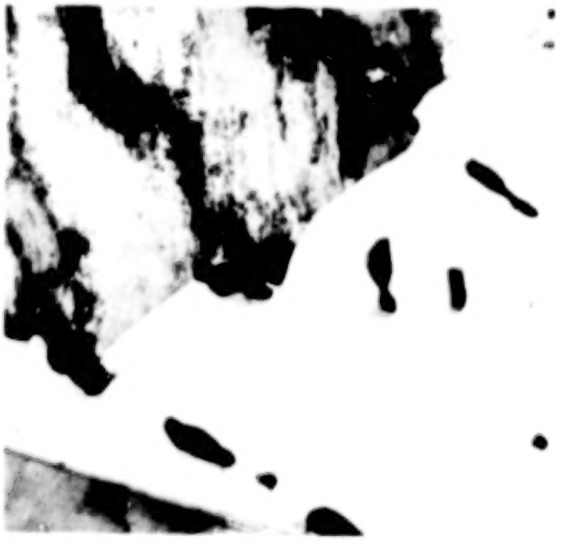

(g) 20% Prestrain. X9,500.

Figure 62 (continued): Substructures Observed in Prestrained Samples after Creep Testing at 1200K/41.4 MPa (1700°F/6 ksi). Heat 2-1604.

that grain boundary sliding becomes a significant factor in the deformation process.

6.0 DYNAMIC OXIDATION RESISTANCE OF EXPERIMENTAL SHEETS

6.1 Materials and Experimental Procedure

Duplicate samples from the baseline sheets and from each of the sheets produced for the texture, grain and supplementary grain size experimental studies were dynamic oxidation tested in order to determine any effects of TMP on dynamic oxidation resistance. The test was performed at a temperature of 1366K (2000°F) for 100 hours in a flame tunnel type rig which provided a gas velocity of Mach 0.3. The equipment, sample preparation and test procedures were the same as those described in Section 2.7.

6.2 Dynamic Oxidation Test Results

A summary of the weight change and metallographic results of the test are presented in Table LIV. A graphical presentation of the average weight change data is also given in Figure 63. Except for the 20-hour results, the weight change data for all of the expeirmental sheets were well within the scatter band of the baseline. The metallographic results, which provide a more reliable and unambiguous assessment of oxidation resistance, also indicate that all of the experimental sheets were within the baseline scatter band. It is concluded, therefore, that the TMP used in the experimental studies had no detrimental effects on the dynamic oxidation resistance of HAYNES alloy No. 188 sheet.

TABLE LIV

RESULTS OF DYNAMIC OXIDATION TESTING AT 1366 K (2000°F) FOR 100 HOURS
FOR BASELINE AND EXPERIMENTAL SHEETS

Heat No.	Weight Change, mg/cm^2				Metal Loss		Continuous Penetration		Maximum Penetration		Total Metal Affected	
	20 Hrs	40 Hrs	62 Hrs	100 Hrs	mm/Side	(Mils/Side)	mm/Side	(Mils/Side)	mm/Side	(Mils/Side)	mm/Side	(Mils/Side)
Baseline												
2-1604	.085	-.220	-.896	-3.3	.0038	(.15)	.0239	(.94)	.0465	(1.83)	.0503	(1.98)
	.120	-.169	-.692	-3.4	.0038	(.15)	.0231	(.91)	.0429	(1.69)	.0465	(1.83)
3-1622	-	-.587	-1.06	-1.71	.0165	(.65)	.0180	(.71)	.0450	(1.77)	.0615	(2.42)
	-.094	-.667	-1.21	-1.92	.0076	(.30)	.0216	(.85)	.0404	(1.59)	.0480	(1.89)
4-1671	.141	-.049	-.403	-.918	.0038	(.15)	.0188	(.74)	.0404	(1.59)	.0439	(1.73)
	.198	-.028	-.529	-1.11	.0038	(.15)	.0221	(.87)	.0467	(1.84)	.0506	(1.99)
Average	.090	-.287	-.798	-2.06	.0066	(.26)	.0213	(.84)	.0437	(1.72)	.0501	(1.97)
Std. Dev.	.111	.274	.312	1.07	.0051	(.20)	.0024	(.09)	.0029	(.11)	.0061	(.24)
Grain Size Study: ASTM 5-6												
3-1655	-.198	-.481	-.948	-1.69	.0152	(.60)	.0173	(.68)	.0361	(1.42)	.0513	(2.02)
	-.168	-.427	-.932	-1.96	.0064	(.25)	.0229	(.90)	.0396	(1.56)	.0460	(1.81)
4-1696	.085	-.106	-.524	-1.17	.0102	(.40)	.0147	(.58)	.0391	(1.54)	.0493	(1.94)
	.064	-.127	-.567	-1.15	.0114	(.45)	.0157	(.62)	.0361	(1.42)	.0475	(1.87)
4-1697	-.276	-.608	-1.06	-1.67	.0102	(.40)	.0188	(.74)	.0356	(1.40)	.0457	(1.80)
	-.315	-.679	-1.17	-1.86	.0102	(.40)	.0191	(.75)	.0366	(1.44)	.0467	(1.84)
Average	-.135	-.405	-.867	-1.58	.0106	(.42)	.0181	(.71)	.0372	(1.46)	.0478	(1.88)
Std. Dev.	.171	.241	.264	.36	.0028	(.11)	.0029	(.11)	.0017	(.07)	.0022	(.09)
Supplementary Grain Size Study: ASTM 5-6												
4-1697	-.101	-.527	-1.08	-1.96	.0203	(.80)	.0163	(.64)	.0330	(1.30)	.0533	(2.10)
	-.143	-.565	-1.10	-1.96	.0114	(.45)	.0165	(.65)	.0320	(1.26)	.0434	(1.71)
Average	-.122	-.546	-1.09	-1.96	.0159	(.63)	.0164	(.65)	.0325	(1.28)	.0484	(1.91)
	.030	.027	.01	.00	.0063	(.25)	.0001	(.01)	.0007	(.03)	.0070	(.28)

155

TABLE LIV (Cont.)

Test No.	Weight Change, mg/cm^2 20 Hrs	40 Hrs	62 Hrs	100 Hrs	Metal Loss mm/Side	(Mils/Side)	Continuous Penetration mm/Side	(Mils/Side)	Maximum Penetration mm/Side	(Mils/Side)	Total Metal Affected mm/Side	(Mils/Side)
						Texture Study						
3-1695	-.107	-.398	-.847	-1.92	.0076	(.30)	.0180	(.71)	.0396	(1.56)	.0472	(1.86)
	-.050	-.351	-.896	-2.66	.0038	(.15)	.0193	(.76)	.0417	(1.64)	.0455	(1.79)
4-1696	.014	-.176	-.647	-1.26	.0127	(.50)	.0202	(.80)	.0422	(1.66)	.0549	(2.16)
	.092	-.191	-.713	-1.39	.0102	(.40)	.0193	(.76)	.0399	(1.57)	.0500	(1.97)
4-1697	-.262	-.672	-1.18	-1.93	.0114	(.45)	.0165	(.65)	.0422	(1.66)	.0536	(2.11)
	-.254	-.684	-1.19	-1.89	.0140	(.55)	.0188	(.74)	.0447	(1.76)	.0587	(2.31)
Average	-.095	-.409	-.912	-1.84	.0100	(.39)	.0187	(.74)	.0417	(1.64)	.0517	(2.03)
Std. Dev.	.143	.219	.230	.50	.0037	(.15)	.0013	(.05)	.0019	(.07)	.0050	(.20)

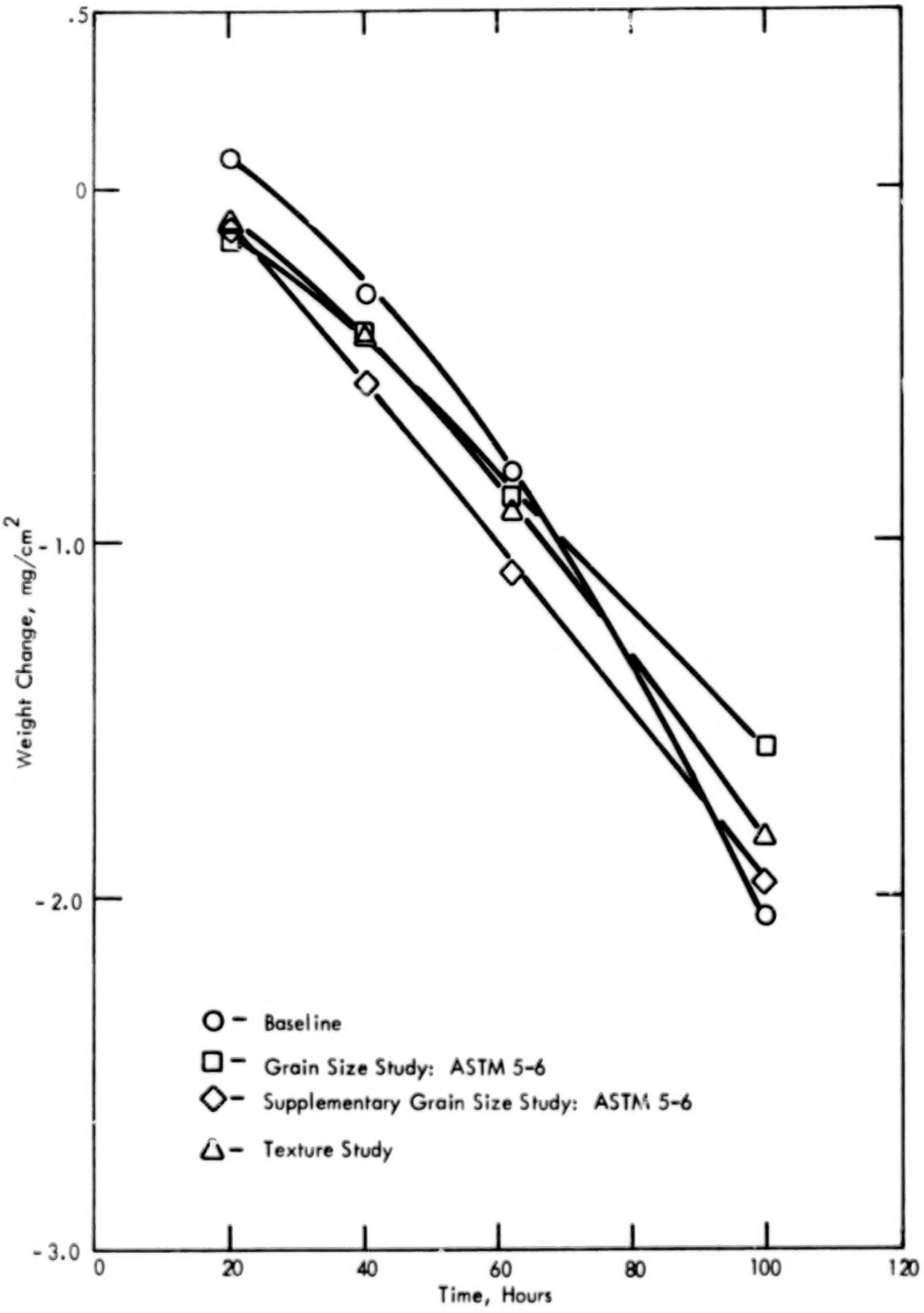

Figure 63: Weight Change vs. Time for Baseline and Experimental Sheets. Dynamic Oxidation Tested at 1366 K (2000°F) for 100 Hours With a Mach 0.3 Combustion Gas Velocity.

7.0 DISCUSSION AND CONCLUDING REMARKS

The primary objective of the program was to obtain improvements in the low strain ($\leq$ 1 percent) creep strength of HAYNES alloy No. 188 thin gauge sheet by means of TMP. To achieve this goal, two major approaches were taken. One focused attention on TMP designed to promote a preferred crystallographic texture after recrystallization. The other concentrated on grain size control. In addition, brief studies were conducted to examine the effects of thickness-to-grain diameter ratio and prestrain on low strain creep strength.

Of the two major approaches, the most significant improvements in creep strength were obtained in sheet having a strong recrystallized texture. Based on a stress versus Larson-Miller parameter correlation, the minus 3-sigma limits for 0.5 percent and 1.0 percent creep lives obtained for the textured sheets were found to be above the baseline average values over a range of test conditions corresponding to approximately 206.8 MPa/18 x 10^3 LMP-K (30 ksi/32.5 x 10^3 LMP-°R) to 17.2 MPa/23.5 x 10^3 LMP-K (2.5 ksi/42.3 x 10^3 LMP-°R). At the two extremes of this range, the average creep lives of the textured sheets approached those of the baseline sheets. However, when consideration is given to creep life minimums predicted by the minus 3-sigma limits and the amount of scatter as represented by the 1-sigma values obtained, definite improvements are indicated for the textured sheets at these two extremes of test conditions.

With regard to other properties, results of room temperature bend tests indicated that the presence of a preferred crystallographic texture did not adversely affect fabricability. The tensile and stress rupture properties of the textured sheets were equivalent or superior to those of the baseline sheets except for ductility values under certain test conditions. Specifically, the elongations obtained in tensile tests at temperatures of 1144K (1600°F) and above, in stress rupture tests performed at 1089K/165.4 MPa (1500°F/24 ksi), and in tensile tests conducted on samples which had been creep tested at 922K (1200°F) and at 1255K (1800°F) were less than those obtained in the baseline sheets. In all cases, however, the ductility values obtained for the textured sheets were at levels which would be considered acceptable.

The investigation to improve creep strength by optimizing grain size also yielded some promising end results, although the improvements found were not as great as those obtained in the textured sheets. Initially, the study to determine the dependence of creep strength on grain size at the 1200K/41.4 MPa (1700°F/6 ksi) quality control test condition did not reveal any significant improvements over the baseline sheets. However, the deterioration in creep strength at a grain size of ASTM 7-8, and the increase in the amount of primary creep strain at a grain size of ASTM 2-4 were important findings. Due to an apparent strain-aging effect, the determination of the apparent activation energies for creep did not lead to an understanding of the role of grain size on creep strength. In the final phase of the study, the evaluation of creep properties of thin gauge sheet with an ASTM 5-6 grain size indicated that

improvements over the baseline sheets were obtained. These improvements were evidenced by increases in the creep life average values and the minimums predicted by the minus 3-sigma limits for both 0.5 percent and 1.0 percent creep strain levels. In addition, the 1-sigma values determined for the ASTM 5-6 grain size sheets were approximately two-thirds of the values obtained for the baseline sheets.

The evaluation of tensile and stress rupture properties of the ASTM 5-6 thin gauge sheets revealed trends similar to those observed in the textured sheets. Tensile and stress rupture strengths were equivalent or superior to those of the baseline sheets, but elongation values obtained in tensile tests at 1144K (1600°F) and above and in stress rupture tests performed at 1089K/165.4 MPa (1500°F/24 ksi) were less than the baseline values. However, the ductilities observed were judged to be at acceptable levels.

The effect of thickness-to-grain diameter ratio on creep strength was also investigated. A sheet 0.76 mm (0.030 inch) thick having a grain size of ASTM 5-6 was produced and evaluated, and comparisons were made to the ASTM 5-6 thin gauge sheets. In addition, creep data generated on the initial grain size study sheets were re-analyzed in terms of thickness-to-grain diameter ratio. Results of this investigation revealed no meaningful correlation between creep properties and thickness-to-grain diameter ratio. Instead, the observed creep lives appeared to be related to grain size alone.

In a final study, the effect of prestrain on creep strength at the 1200K/41.4 MPa (1700°F/6 ksi) quality control test condition was examined using one of the baseline heats of production thin gauge sheet. Significant improvements were found with prestrains of 4-10 percent. Above 10 percent prestrain, recrystallization occurred, and creep properties were degraded. The improvements obtained with prestrain were not as great as those obtained in the textured sheets. Furthermore, it is doubtful whether the structures produced by 4-10 percent prestrain would be stable with respect to both recovery and recrystallization processes at other conditions of temperature and stress.

In summary, the low strain ($\leq$ 1 percent) creep strength of HAYNES alloy No. 188 thin gauge sheet was significantly improved through TMP which provided a sheet having a strong crystallographic texture after recrystallization. It must be emphasized that all of the development work was performed with laboratory produced sheet. Additional work will, therefore, be required to determine whether the method can be applied in the production of full-size sheets.

A final comment must be made regarding properties. In the evaluation of the textured sheets, no serious property limitation was discovered. However, the evaluation did not include many properties relevant to high temperature applications such as weldability and weld strength efficiency, formability, property response to forming and annealing operations, isothermal low cycle fatigue, and thermal stability to mention a few. These areas will have to be investigated if such a material is to receive serious design consideration.

APPENDIX A

CONVERSION OF U.S. CUSTOMARY UNITS TO SI UNITS

APPENDIX A

CONVERSION OF U.S. CUSTOMARY UNITS TO SI UNITS

The international System of Units (designated SI) was adopted by the Eleventh General Conference on Weights and Measures in 1960. The units and conversion factors used in this report are taken from or based on NASA SP-7012, "The International System of Units, Physical Constants and Conversion Factors - Revised, 1973."

The following table expresses the definitions of miscellaneous units of measure an exact numerical multiples of coherent SI units, and provides multiplying factors for converting numbers and miscellaneous units to corresponding new numbers of SI units.

The first two digits of each numerical entry represent a power of 10. An asterisk follows each number that expresses an exact definition. For example, the entry "-02 2.54*" expresses the fact that 1 inch = 2.54×10^{-2} meter, exactly, by definition. Most of the definitions are extracted from National Bureau of Standards documents. Numbers not followed by an asterisk are only approximate representations of definitions, or are the results of physical measurements.

ALPHABETICAL LISTING

To convert from	to	multiply by
Calorie (cal, thermochemical)	joule (J)	+ 00 4.184*
Fahrenheit (°F)	kelvin (K)	$t_K = (5/9)\ (t_F + 459.67)$
foot (ft)	meter (m)	-01 3.048*
inch (in)	meter (m)	-02 2.54*
mil	meter (m)	-05 2.54*
pound force (lbf)	newton (N)	+00 4.448*
Rankine (°R)	kelvin (K)	$t_K = (5/9)\ t_R$

PHYSICAL QUANTITY LISTING

Area

To convert from	to	multiply by
$foot^2$ (ft^2)	$meter^2$ (m^2)	-02 9.290*
$inch^2$ (in^2)	$meter^2$ (m^2)	-04 6.452*
$inch^2$ (in^2)	$centimeter^2$ (cm^2)	+00 6.452

Energy

To convert from	to	multiply by
Calories (cal, thermochemical)	joule (J)	+00 4.184

Force

pound force (lbf)	newton (N)	+00 4.448*

Length

foot (ft)	meter (m)	-01 3.048*
inch (in)	meter (m)	-02 2.54*
mil	meter (m)	-05 2.54*

Pressure

pound/inch^2 (psi, lbf/in^2)	pascal (Pa)	+03 6.895

Temperature

Fahrenheit (°F)	kelvin (K)	$t_K = (5/9)\ (t_F + 459.67)$
Rankine (°F)	kelvin (K)	$t_K = (5/9)\ t_R$

PREFIXES

The names of multiples and submultiples of SI units may be formed by application of the prefixes:

Multiple	Prefix
10^{-6}	micro (μ)
10^{-3}	milli (m)
10^{-2}	centi (c)
10^{-1}	deci (d)
10^{3}	kilo (k)
10^{6}	mega (M)
10^{9}	giga (G)

APPENDIX B

CREEP TESTING PROCEDURE

APPENDIX B

CREEP TESTING PROCEDURE

All creep tests were carried out in air. The specimen configuration employed is shown in Figure B-1. To prevent distortion around the pinning holes, tabs were spot welded to the grip ends of each sample. A rigid frame extensometer was fastened to the double radius shoulder of the specimen outside of the reduced test section as illustrated in Figure B-2. The knife edges of the extensometer were spaced 50.8 mm (2 inches) apart. All of the measured creep elongation was assumed to have occurred in the gage section of the specimen.

Two thermocouples were wired to the sample test section. One was used to control the furnace temperature, while the other was used to obtain an independent check of specimen temperature. Throughout each test, the temperature was maintained to within ± 1.7K (± 3°F) of the required temperature. Before the test load was applied, the assembly was allowed to soak at temperature for at least 1/2 hour.

Creep deformation, exclusive of the instantaneous loading strain, was measured using a single linear variable differential transformer (LVDT). The resolution of the LVDT measuring system was 2.54×10^{-4} mm (1×10^{-5} in.). For some of the initial tests, the measured creep strain was recorded as a function of elapsed time on a strip chart. When a fully automated system became operational at Stellite, the test data were electronically stored and read out after test by a computer. Tests were discontinued after a creep strain greater than 1% had been reached. Minimum creep rate parameters were determined using a straight line least squares fit of the data points judged to lie within the minimum creep rate portion of the creep curve.

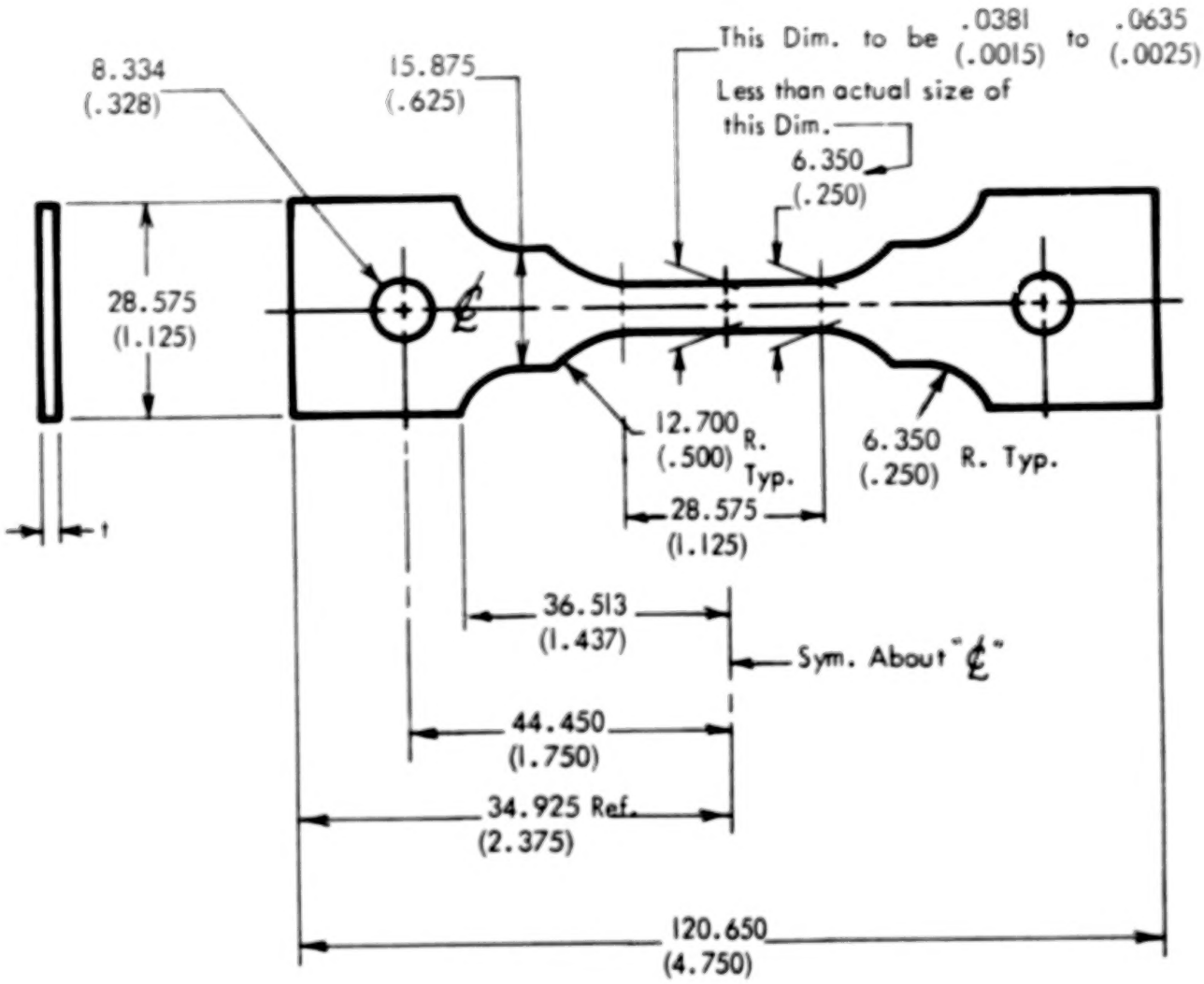

Figure B-1: Sheet Specimen Configuration. Dimensions are given in millimeters (inches)

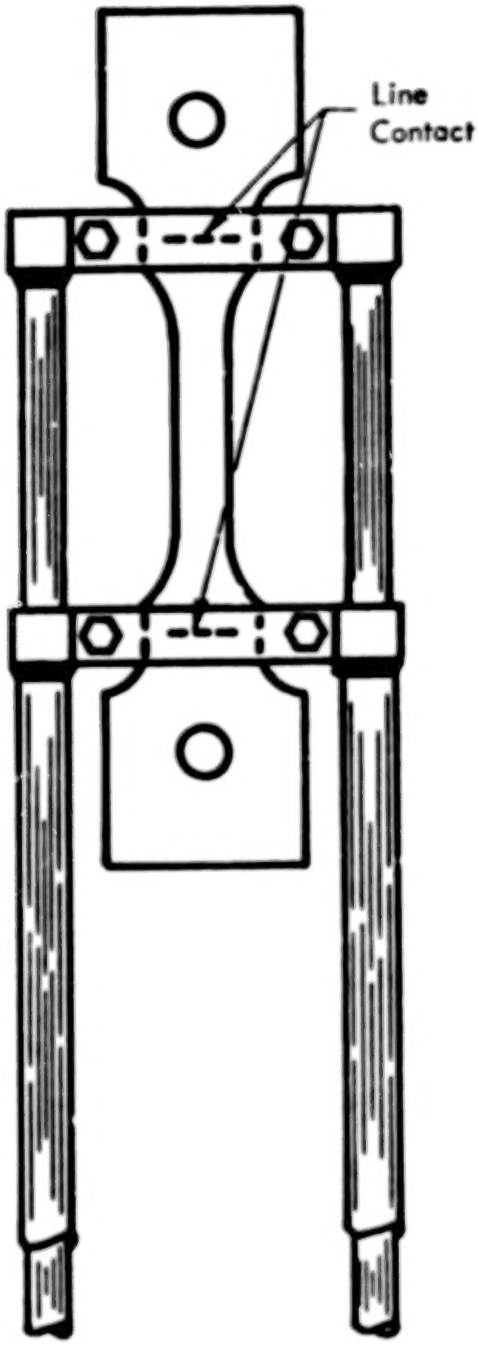

Figure B-2: Creep Extensometer System

APPENDIX C

BASELINE CREEP TEST DATA

TABLE C-I

BASELINE CREEP TEST DATA

Sample Orientation	Stress MPa	Stress (ksi)	Time for Indicated Creep Strain, Hrs. 0.1%	0.2%	0.3%	0.4%	0.5%	0.75%	1.0%	Min. Creep Rate, %/Hr	Primary Creep Strain, %	Time of Primary Creep, Hr.
Heat 2-1604												
922 K (1200°F)												
T	413.7	(60.0)	0.4	0.[illegible]	1.0	1.6	2.3	4.2	6.3	0.1014	1.40	10.0
L	344.7	(50.0)	0.9	3.0	5.5	8.9	12.5	22.0	33.5	0.0229	0.68	19.0
L	275.8	(40.0)	25.0	40.0	98.0	133.0	169.0	240.0	317.0	0.00185	0.20	40.0
L	206.8	(30.0)	10.0	54.0	100.0	230.0	360.0	630.0	865.0	0.00082	0.34	150.0
T	172.4	(25.0)	60.0	235.0	420.0	600.0	765.0	1070.0	1350.0	0.00056	0.12	100.0
1033 K (1400°F)												
T	172.4	(25.0)	1.5	2.5	4.0	5.0	5.8	7.5	10.3	0.0683	3.35	35.0
T	137.9	(20.0)	1.5	3.8	6.7	9.5	12.5	19.5	27.3	0.0312	0.73	19.0
L	103.4	(15.0)	1.1	3.2	8.7	15.0	23.0	48.0	78.0	-	-	-
L	96.5	(14.0)	6.8	17.0	30.0	49.5	67.0	125.0	220.0	-	-	-
T	86.1	(12.5)	10.0	27.5	46.0	64.0	90.0	160.0	327.0	0.0015	0.90	250.0
L	68.9	(10.0)	9.0	25.0	63.0	113.0	161.5	475.0	770.0	0.00077	0.75	475.0
1144 K (1600°F)												
T	68.9	(10.0)	0.9	2.0	3.4	4.8	6.6	11.8	17.6	0.0435	0.71	11.0
L	51.7	(7.5)	0.1	0.9	2.9	6.5	13.0	34.0	63.0	-	-	-
L	41.4	(6.0)	1.2	5.0	13.0	25.0	43.0	100.0	194.0	-	-	-
L	34.5	(5.0)	5.0	15.0	33.0	58.0	87.5	193.0	450.0	0.00080	0.90	325.0
T	27.6	(4.0)	9.0	38.0	85.0	160.0	275.0	920.0	1940.0	0.00022	0.73	800.0
1200 K (1700°F)												
T	41.4	(6.0)	1.5	3.5	6.0	9.0	13.0	23.0	33.0	0.0245	0.43	10.0
T	41.4	(6.0)	1.0	3.0	6.0	10.0	14.0	25.0	35.6	0.0231	0.40	10.0

169

TABLE C-I (Continued)

Sample Orientation	Stress MPa	(ksi)	Time for Indicated Creep Strain, Hrs. 0.1%	0.2%	0.3%	0.4%	0.5%	0.75%	1.1%	Min. Creep Rate, %/Hr	Primary Creep Strain, %	Time of Primary Creep, Hr.
1255 K (1800°F)												
T	34.5	(5.0)	0.9	2.7	4.7	6.8	8.8	11.7	18.0	0.0994	0.17	2.0
L	31.0	(4.5)	0.1	0.2	0.4	0.5	0.9	2.4	4.8	0.0838	1.00	4.8
L	27.6	(4.0)	0.7	2.0	4.0	6.5	9.0	15.3	20.9	0.0398	0.30	4.0
L	20.7	(3.0)	3.5	11.0	24.0	38.0	52.0	81.3	100.0	0.0070	0.28	20.0
T	13.8	(2.0)	9.0	47.0	103.0	167.0	218.0	318.0	390.0	0.0016	0.23	75.0
T	10.3	(1.5)	12.5	35.0	60.0	95.0	150.0	300.0	460.0	0.0013	0.66	250.0
T	8.6	(1.25)	40.0	300.0	875.0	1500.0	2100.0	3660.0	5225.0	0.00017	0.24	500.0
						Heat 3-1622						
922 K (1200°F)												
T	413.7	(60.0)	1.5	5.3	10.5	16.0	21.4	35.0	48.5	0.0185	0.29	10.0
L	344.7	(50.0)	2.7	9.5	16.8	23.2	30.0	46.0	63.5	0.0151	0.10	2.7
L	275.8	(40.0)	17.0	45.0	77.0	115.0	155.0	254.0	335 5	0.0023	0.37	100.0
L	206.8	(30.0)	37.0	100.0	190.0	295.0	400.0	660.0	900.0	0.00097	0.31	200.0
T	172.4	(25.0)	110.0	400.0	750.0	1100.0	1450.0	2540.0	3925.0	0.00017	-	-
1033 K (1400°F)												
T	172.4	(25.0)	2.0	4.3	7.0	9.5	12.2	2-.5	29.0	0.0162	1.50	51.0
T	137.9	(20.0)	2.0	6.0	10.0	15.0	22.0	43.0	75.0	-	-	-
L	103.4	(15.0)	4.5	11.0	25.0	50.0	95.0	264.0	540.0	0.00092	0.87	400.0
L	96.5	(14.0)	30.0	82.0	180.0	300.0	500.0	900.0	1540.0	0.00031	0.85	1050.0
T	86.1	(12.5)	20.0	70.0	210.0	450.0	810.0	1950.0	3090.0	0.00023	0.50	810.0
L	68.9	(10.0)	550.0	1050.0	Discontinued at 0.25%, 1656.5 Hrs.							

TABLE C-I (Continued)

Sample Orientation	Stress MPa	Stress (ksi)	Time for Indicated Creep Strain, Hrs. 0.1%	0.2%	0.3%	0.4%	0.5%	0.75%	1.0%	Min. Creep Rate, %/Hr	Primary Creep Strain, %	Time of Primary Creep, Hr.
1144 K (1600°F)												
T	68.9	(10.0)	1.0	2.7	6.3	11.0	16.5	33.3	50.2	0.0147	0.55	20.0
L	51.7	(7.5)	3.0	16.0	50.0	85.0	120.0	205.0	345.0	-	-	-
L	41.4	(6.0)	26.0	94.0	180.0	288.0	430.0	770.0	1105.0	0.00073	0.45	350.0
L	34.5	(5.0)	5.0	25.0	85.0	167.0	265.0	610.0	1120.0	0.00047	0.80	700.0
T	27.6	(4.0)	15.0	110.0	330.0	750.0	1910.0	5700.0	7850.0	0.000069	0.48	1500.0
1200 K (1700°F)												
T	41.4	(6.0)	2.5	8.0	18.0	25.0	33.5	55.0	76.5	0.0117	0.18	5.0
T	41.4	(6.0)	5.0	17.0	32.0	50.0	71.0	115.0	156.0	0.0051	0.24	20.0
1255 K (1800°F)												
T	34.5	(5.0)	1.2	3.1	5.5	7.9	10.1	14.4	18.3	0.0398	0.24	4.0
L	31.0	(4.5)	2.2	5.2	9.0	12.6	16.5	26.0	33.2	0.0264	0.20	5.0
L	27.6	(4.0)	1.7	5.5	10.0	16.0	20.8	30.7	42.0	0.0184	0.30	10.0
L	20.7	(3.0)	2.0	9.0	19.0	30.0	43.0	74.0	95.0	0.0071	0.42	35.0
T	13.8	(2.0)	7.0	25.0	55.0	90.0	122.0	204.0	259.0	0.0030	0.36	75.0
T	10.3	(1.5)	12.0	55.0	150.0	300.0	475.0	800.0	980.0	0.00060	0.30	155.0
T	8.6	(1.25)	10.0	38.0	105.0	225.0	405.0	815.0	1040.0	0.00051	0.44	300.0
Heat 4-1671												
922 K (1200°F)												
T	413.7	(60.0)	0.8	1.8	2.8	4.2	5.7	9.2	13.4	0.0606	0.92	12.0
L	344.7	(50.0)	1.1	3.8	7.5	11.0	15.2	27.5	40.2	0.0198	0.50	15.2
L	275.8	(40.0)	5.5	19.5	34.5	50.3	69.0	96.5	137.2	0.0070	0.14	10.0
L	206.8	(30.0)	44.0	130.0	200.0	265.0	320.0	440.0	530.0	0.0011	0.10	44.0
T	172.4	(25.0)	110.0	240.0	357.0	467.0	575.0	840.0	1150.0	0.00081	-	-

TABLE C-I (Concluded)

Sample Orientation	Stress MPa	Stress (ksi)	Time for Indicated Creep Strain, Hrs. 0.1%	0.2%	0.3%	0.4%	0.5%	0.75%	1.0%	Min. Creep Rate, %/Hr	Primary Creep Strain, %	Time of Primary Creep, Hr.
1033 K (1400°F)												
T	172.4	(25.0)	2.5	3.2	4.5	5.3	6.3	8.2	10.8	0.0647	3.15	35.0
T	137.9	(20.0)	1.5	3.2	5.2	7.1	9.0	13.4	18.3	-	-	-
L	103.4	(15.0)	3.8	9.5	15.5	23.0	34.0	66.0	109.0	-	-	-
L	96.5	(14.0)	5.0	13.0	22.5	35.0	50.0	106.0	185.0	-	-	-
T	86.1	(12.5)	32.0	67.0	110.0	166.0	245.0	480.0	775.0	-	-	-
L	68.9	(10.0)	8.7	25.0	71.0	143.0	257.0	680.0	1195.0	0.00042	0.70	600.0
1144 K (1600°F)												
T	68.9	(10.0)	0.8	1.9	3.2	4.5	6.0	9.8	13.7	0.0655	0.43	5.0
L	51.7	(7.5)	0.2	0.7	4.0	10.0	17.8	44.0	82.0	-	-	-
L	41.4	(6.0)	6.5	16.0	32.0	48.0	68.0	130.0	208.0	-	-	-
L	34.5	(5.0)	7.0	17.0	40.0	70.0	110.0	245.0	475.0	-	-	-
T	27.6	(4.0)	30.0	105.0	200.0	375.0	980.0	2380.0	3295.0	0.00013	0.45	600.0
1200 K (1700°F)												
T	41.4	(6.0)	1.0	2.5	4.8	6.9	8.9	14.1	17.9	0.0479	0.17	2.0
T	41.4	(6.0)	2.0	4.0	7.0	10.0	12.5	18.5	24.5	0.0359	0.10	2.0
1255 K (1800°F)												
T	34.5	(5.0)	0.4	0.8	1.2	1.6	2.0	2.9	6.8	0.2956	0.15	0.6
L	31.0	(4.5)	0.5	1.1	1.8	2.5	3.0	4.6	5.9	0.1583	0.10	0.5
L	27.6	(4.0)	0.8	2.1	3.5	4.9	6.0	8.7	11.0	0.0730	0.10	0.8
L	20.7	(3.0)	0.9	3.5	6.5	10.5	14.5	23.3	30.1	0.0257	0.23	5.0
T	13.8	(2.0)	1.7	4.5	8.8	17.0	30.0	59.0	77.5	0.0081	0.41	20.0
T	10.3	(1.5)	4.5	15.5	44.0	84.0	124.0	188.0	236.0	0.0020	0.31	50.0
T	8.6	(1.25)	15.0	41.0	70.0	100.0	130.0	190.0	238.0	0.0035	0.16	30.0

APPENDIX D

TEXTURE STUDY CREEP TEST DATA

TABLE D-I

LONGITUDINAL CREEP TEST DATA AT 1200 K/41.4 MPa (1700°F/6 ksi)
FOR INITIAL TEXTURE STUDY EXPERIMENTAL STRIPS

Time for Indicated Creep Strain, Hrs.							Min. Creep Rate %/Hr	Primary Creep Strain %	Time of Primary Creep Hrs
0.1%	0.2%	0.3%	0.4%	0.5%	0.75%	1.0%			
					7A*				
0.1	0.3	0.4	0.6	0.8	1.1	1.6	0.619	0.67	1.0
0.1	0.2	0.4	0.5	0.7	1.1	1.4	0.653	0.31	0.4
					7B*				
1.0	3.2	7.1	10.5	14.0	22.3	30.5	0.028	0.25	5.0
1.1	4.9	10.5	16.0	21.3	34.2	46.7	0.018	0.20	5.0
					7C*				
2.5	7.0	13.5	26.0	36.0	57.0	79.0	0.0095	0.38	24.0
2.0	10.0	21.0	36.0	45.0	71.0	92.0	0.0078	0.34	25.0
3.5	12.0	26.0	39.5	53.0	84.0	109.0	0.0071	0.22	15.0
10.0	13.0	36.0	49.0	61.5	87.0	109.0	0.0075	0.15	15.0
1.8	7.5	16.5	27.3	37.8	64.0	86.0	0.0093	0.30	17.0
					8A*				
0.08	0.17	0.27	0.38	0.51	0.76	1.10	0.825	0.40	0.4
0.13	0.29	0.47	0.65	0.82	1.18	1.51	0.550	0.15	0.2
					8B*				
0.7	2.8	5.5	8.0	10.6	20.4	21.3	0.039	0.21	3.0
0.8	2.3	4.8	7.3	9.7	15.0	20.0	0.043	0.31	5.0
					8C*				
5.0	21.0	42.0	60.0	78.0	114.0	144.0	0.0054	0.19	20.0
4.0	20.5	44.0	67.0	90.0	140.0	183.0	0.0044	0.18	14.0

TABLE D-I (Concluded)

Time for Indicated Creep Strain, Hrs.							Min. Creep Rate %/Hr	Primary Creep Strain %	Time of Primary Creep Hrs
0.1%	0.2%	0.3%	0.4%	0.5%	0.75%	1.0%			
12.0	32.0	54.0	72.0	90.0	129.0	160.0	0.0047	0.10	10.0
3.0	13.0	26.5	40.0	53.0	86.0	118.0	0.0078	0.21	15.0
4.5	14.5	30.0	47.0	64.0	106.0	141.0	0.0061	0.26	24.0
					9A*				
0.10	0.20	0.33	0.46	0.60	0.97	1.35	0.672	0.51	200.0
0.12	0.27	0.45	0.65	0.87	1.48	2.06	0.450	1.40	3.0
					9B*				
0.5	1.1	1.9	2.8	3.7	5.9	7.9	0.115	0.31	2.0
0.8	3.6	7.5	11.2	15.0	25.0	32.3	0.026	0.24	5.0
					9C*				
8.5	28.0	46.0	63.5	82.0	120.0	151.0	0.0053	0.17	20.0
0.5	6.5	15.0	25.0	33.0	59.0	63.5	0.0110	0.20	6.0
9.0	33.0	56.0	80.0	107.0	166.0	216.0	0.0040	0.16	20.0
4.0	21.0	45.0	74.0	102.0	176.0	242.0	0.0035	0.35	60 0
12.0	33.0	58.0	84.0	106.0	156.0	200.0	0.0039	0.20	34.0

* 7, 8 and 9 indicate Final Cold Reductions of 70%, 80% and 90%, respectively; A, B and C indicate Final Annealing Temperatures of 1394 K (2050°F), 1450 K (2150°F) and 1505 K (2150°F), respectively.

175

TABLE D-II

CREEP TEST DATA FOR TYPE 8C* TEXTURE STUDY SHEETS

Sample Orientation	Stress MPa	Stress (ksi)	Time for Indicated Creep Strain, Hrs. 0.1%	0.2%	0.3%	0.4%	0.5%	0.75%	1.0%	Min. Creep Rate, %/Hr	Primary Creep Strain, %	Time of Primary Creep, Hrs
Heat 3-1655												
922 K (1200°F)												
L	413.7	(60.0)	0.6	2.0	3.7	5.7	8.0	16.3	26.5	0.0244	0.69	14.0
L	344.7	(50.0)	3.0	9.5	19.0	32.0	49.0	93.0	131.0	0.0057	0.46	42.0
L	275.8	(40.0)	10.0	36.0	85.0	138.0	190.0	323.0	455.0	0.0019	0.24	55.0
1144 K (1600°F)												
L	68.9	(10.0)	1.5	7.0	20.0	40.0	66.0	130.0	189.5	0.0039	0.40	40.0
L	51.7	(7.5)	10.0	58.0	140.0	250.0	375.0	750.0	1210.0	0.00054	0.78	800.0
L	41.4	(6.0)	11.0	50.0	120.0	220.0	325.0	615.0	1130.0	0.00044	-	-
1200 K (1700°F)												
L	41.4	(6.0)	7.0	24.0	45.0	68.0	91.0	149.0	207.0	0.0045	0.37	60.0
L	41.4	(6.0)	2.5	12.0	31.5	54.0	76.0	132.0	177.0	0.0044	0.29	30.0
T	41.4	(6.0)	2.5	9.5	21.0	37.0	55.5	103.0	150.5	0.0053	0.36	30.0
T	41.4	(6.0)	2.5	15.0	35.0	58.0	83.0	151.0	218.0	0.0035	0.53	90.0
1255 K (1800°F)												
L	34.5	(5.0)	1.8	5.5	10.3	15.0	19.0	30.5	39.5	0.0207	0.19	5.0
L	20.7	(3.0)	8.0	25.0	52.5	91.0	142.0	272.0	398.0	0.0019	0.42	100.0
L	13.8	(2.0)	8.0	23.0	53.0	109.0	188.0	542.0	975.0	0.00055	0.70	450.0
Heat 4-1696												
922 K (1200°F)												
L	413.7	(60.0)	0.8	1.8	2.8	4.0	5.5	9.1	13.9	0.0503	0.86	13.0
L	344.7	(50.0)	4.5	12.0	22.3	36.0	53.0	93.7	124.5	0.0057	0.43	40.0
L	275.8	(40.0)	13.0	42.0	87.5	133.0	180.0	320.0	472.0	0.0016	-	-

APPENDIX D-CONTINUED

TABLE D-11 (Continued)

Sample Orientation	Stress MPa	Stress (ksi)	Time for Indicated Creep Strain, Hrs. 0.1%	0.2%	0.3%	0.4%	0.5%	0.75%	1.0%	Min. Creep Rate, %/Hr	Primary Creep Strain, %	Time of Primary Creep, Hrs
1144 K (1600°F)												
L	68.9	(10.0)	2.0	8.5	20.0	34.5	51.0	94.0	137.0	0.0058	0.49	49.0
L	51.7	(7.5)	28.0	71.0	125.0	182.0	238.0	378.0	520.0	0.0019	0.35	150.0
L	41.4	(6.0)	10.0	85.0	225.0	360.0	515.0	1360.0	4557.0	0.000057	0.87	2500.0
1200 K (1700°F)												
L	41.4	(6.0)	0.2	2.8	12.0	24.0	38.0	72.5	101.0	0.0073	0.36	19.0
L	41.4	(6.0)	11.0	32.5	54.5	76.5	100.0	162.0	228.5	0.0039	-	-
T	41.4	(6.0)	1.7	8.5	19.5	30.5	42.0	60.7	93.0	0.0090	0.24	13.0
T	41.4	(6.0)	1.5	5.0	11.8	20.0	28.0	49.0	69.0	0.0119	0.34	15.0
1255 K (1800°F)												
L	34.5	(5.0)	1.8	7.2	12.5	17.7	23.0	34.3	43.0	0.0187	0.12	2.5
L	20.7	(3.0)	5.5	19.5	39.0	69.0	117.7	255.0	386.0	0.0917	0.47	100.0
L	13.8	(2.0)	12.0	31.0	62.0	100.0	154.0	368.0	591.0	0.0011	0.49	150.0
						Heat 4-1697						
922 K (1200°F)												
L	413.7	(60.0)	0.5	1.3	2.2	3.4	4.8	8.9	14.2	0.0447	0.85	10.8
L	344.7	(50.0)	2.2	6.0	11.0	17.8	26.0	56.0	86.0	0.0078	0.63	40.0
L	275.8	(40.0)	22.0	85.0	163.0	240.0	315.0	535.0	750.0	0.0011	-	-
1144 K (1600°F)												
L	68.9	(10.0)	4.5	13.5	27.0	41.5	56.0	92.0	127.3	0.0070	0.25	20.0
L	51.7	(7.5)	25.0	105.0	210.0	345.0	500.0	980.0	1530.0	0.00039	0.77	1030.0
L	41.4	(6.0)	90.0	300.0	402.0	595.0	812.0	2000.0	3680.0	0.00016	0.66	1400.0

APPENDIX D-CONTINUED

177

TABLE D-II (Concluded)

Sample Orientation	Stress MPa	Stress (ksi)	Time for Indicated Creep Strain, Hrs. 0.1%	0.2%	0.3%	0.4%	0.5%	0.75%	1.0%	Min. Creep Rate, %/Hr	Primary Creep Strain, %	Time of Primary Creep, Hrs
1200 K (1700°F)												
L	41.4	(6.0)	2.5	18.0	39.0	60.0	82.0	128.0	162.0	0.0046	0.19	15.0
L	41.4	(6.0)	3.2	13.2	25.0	36.7	48.5	82.8	93.0	0.0083	0.17	10.0
T	41.4	(6.0)	5.0	18.0	52.0	106.0	165.0	316.0	468.0	0.0016	0.43	125.0
T	41.4	(6.0)	5.5	16.0	31.0	49.5	69.0	116.0	153.0	0.0050	0.35	40.0
1255 K (1800°F)												
L	34.5	(5.0)	5.9	13.5	20.3	27.7	35.5	51.0	63.7	0.0130	0.09	5.0
L	20.7	(3.0)	8.0	26.0	58.0	107.0	160.0	281.0	370.0	0.0019	0.33	70.0
L	13.8	(2.0)	17.0	62.0	142.0	265.0	398.0	672.0	875.0	0.00076	0.35	209.00

* 80% Final Cold Work + Final Anneal at 1505 K (2250°F)/10 min.

APPENDIX E

GRAIN SIZE STUDY CREEP TEST DATA

TABLE E-I

LONGITUDINAL CREEP TEST DATA AT 41.4 MPa (6 ksi) FOR INITIAL GRAIN SIZE STUDY EXPERIMENTAL STRIPS

Sample Orientation	Temperature K	Temperature (°F)	Time for Indicated Creep Strain, Hrs. 0.1%	0.2%	0.3%	0.4%	0.5%	0.75%	1.0%	Min. Creep Rate, %/Hr	Primary Creep Strain, %	Time of Primary Creep, Hrs
						ASTM 2-4						
	Heat 3-1655											
	1172	(1655)	2.0	6.5	14.5	26.5	41.5	90.0	160.0	0.0023	1.03	170.0
	1200	(1700)	0.7	2.0	4.9	8.6	13.7	29.4	49.0	0.0113	0.94	44.0
	1200	(1700)	2.2	6.8	12.8	20.2	28.1	51.5	77.5	0.0085	1.08	85.0
	1227	(1750)	0.8	3.0	6.4	10.5	15.1	27.0	38.8	0.0209	0.45	12.5
	1255	(1800)	0.5	1.1	1.8	2.6	3.5	5.5	7.6	0.1230	1.10	4.0
	Heat 4-1696											
	1172	(1650)	13.5	32.5	53.0	73.0	98.0	218.0	307.0	0.0016	0.91	250.0
	1200	(1700)	0.6	2.4	6.0	10.8	17.0	36.0	60.0	0.0095	0.90	50.0
	1200	(1700)	3.2	10.5	20.0	30.8	42.2	71.2	100.2	0.0083	0.59	52.0
	1227	(1750)	3.5	9.2	15.6	22.2	28.6	44.0	57.3	0.0309	0.42	10.0
	1255	(1800)	0.5	1.4	2.5	4.8	5.1	8.3	11.6	0.0776	0.42	4.0
	Heat 4-1697											
	1172	(1650)	3.5	16.0	34.0	57.0	82.5	165.0	300.0	0.0016	0.89	230.0
	1200	(1700)	1.5	4.3	8.5	13.6	20.0	39.5	59.5	0.0124	0.64	30.0
	1200	(1700)	2.5	7.2	13.0	19.3	25.7	43.0	62.2	0.0127	0.78	45.0
	1227	(1750)	2.0	3.8	5.5	7.4	9.6	15.1	20.6	0.0449	0.52	10.0
	1255	(1800)	0.4	0.8	1.4	2.1	2.8	4.6	6.4	0.1394	0.80	2.0
						ASTM 5-6						
	Heat 3-1655											
	1172	(1650)	4.7	16.0	31.0	46.0	61.0	96.0	133.5	0.0065	0.23	20.0
	1200	(1700)	1.5	9.5	19.0	28.6	38.2	58.2	75.5	0.0105	0.20	10.0
	1200	(1700)	0.9	2.8	7.3	13.8	20.8	38.2	54.9	0.0142	0.42	15.0
	1227	(1750)	0.7	2.5	5.8	9.7	13.3	21.5	28.9	0.0261	0.24	3.5
	1255	(1800)	0.2	0.5	1.0	1.5	2.0	3.2	4.5	0.2040	0.6	1.0

TABLE E-1 (Continued)

Sample Orientation	Temperature K	Temperature (°F)	Time for Indicated Creep Strain, Hrs. 0.1%	0.2%	0.3%	0.4%	0.5%	0.75%	1.0%	Min. Creep Rate, %/Hr	Primary Creep Strain, %	Time of Primary Creep, Hrs
		Heat 4-1696										
	1172	(1650)	11.5	23.5	42.5	62.0	84.0	147.0	216.0	0.0037	0.64	118.0
	1200	(1700)	1.2	6.5	15.0	23.3	31.9	52.9	72.7	0.0118	0.24	9.5
	1200	(1700)	0.8	4.3	11.2	17.2	24.3	41.9	56.5	0.0141	0.30	10.0
	1227	(1750)	2.2	5.5	9.0	12.6	16.3	24.2	30.5	0.0269	0.12	3.0
	1255	(1800)	0.7	2.5	4.3	5.8	7.2	10.3	12.5	0.0556	0.12	1.0
		Heat 4-1697										
	1172	(1650)	1.8	6.5	14.5	26.3	30.0	71.0	103.2	0.0080	0.39	25.0
	1200	(1700)	0.8	2.2	4.1	6.6	9.8	17.0	24.4	0.0340	0.21	7.2
	1200	(1700)	0.5	1.7	3.4	4.5	7.8	12.2	18.1	0.0469	0.33	4.0
	1227	(1750)	0.6	1.3	2.1	3.0	3.8	5.8	7.5	0.1237	0.22	1.5
	1255	(1800)	0.2	0.5	0.9	1.3	1.8	2.8	3.8	0.2355	0.23	0.6
						ASTM 7-8						
		Heat 3-1655										
	1172	(1650)	2.0	8.0	17.5	27.5	37.3	62.0	84.5	0.0096	0.23	10.0
	1200	(1700)	0.3	0.7	1.2	1.7	2.1	3.2	4.5	0.2197	0.26	1.0
	1200	(1700)	0.5	1.6	2.8	4.0	5.2	8.5	10.4	0.0853	0.15	1.0
	1227	(1750)	0.5	1.3	2.3	3.3	4.3	6.7	9.2	0.1004	0.21	1.4
	1255	(1800)	0.2	0.4	0.6	0.8	1.0	1.6	2.1	0.4838	0.10	0.2
		Heat 4-1696										
	1172	(1650)	2.5	8.5	15.5	22.5	29.5	46.5	70.0	0.0084	-	-
	1200	(1700)	1.0	2.6	4.2	6.0	7.4	10.6	13.4	0.0629	0.15	2.0
	1200	(1700)	1.1	4.0	7.3	10.7	14.0	22.2	29.0	0.0301	0.18	3.0
	1227	(1750)	1.5	3.0	4.5	5.9	7.1	9.6	11.8	0.0634	0.00	0.0
	1255	(1800)	0.7	1.3	1.8	2.3	2.8	3.7	4.5	0.1780	0.07	0.5

181

TABLE B-I (Concluded)

Sample Orientation	Temperature K	Temperature (°F)	Time for Indicated Creep Strain, Hrs. 0.1%	0.2%	0.3%	0.4%	0.5%	0.75%	1.0%	Min. Creep Rate, %/Hr	Primary Creep Strain, %	Time of Primary Creep, Hrs
		Heat 4-1697										
	1172	(1650)	12.0	42.0	70.0	96.5	120.0	175.0	226.0	0.0035	0.13	20.0
	1200	(1700)	0.8	2.5	4.8	7.3	9.8	15.4	19.6	0.1043	0.27	4.0
	1200	(1700)	2.0	8.0	14.0	20.0	25.0	36.5	46.4	0.0670	0.32	3.0
	1227	(1750)	1.6	3.9	6.0	8.0	9.6	12.8	15.5	0.0716	0.12	2.5
	1255	(1800)	0.5	1.4	2.2	3.2	4.1	4.4	6.8	0.1118	0.15	0.6

APPENDIX B-CONTINUED

TABLE E-II

CREEP TEST DATA FOR ASTM 5-6 GRAIN SIZE STUDY SHEETS

Sample Orientation	Stress MPa	Stress (ksi)	Time for Indicated Creep Strain, Hrs. 0.1%	0.2%	0.3%	0.4%	0.5%	0.75%	1.0%	Min. Creep Rate, %/Hr	Primary Creep Strain, %	Time of Primary Creep, Hrs
Heat 3-1655												
922 K (1200°F)												
L	413.7	(60.0)	0.8	1.6	2.6	3.6	4.7	8.2	12.5	0.056	0.74	8.0
L	344.7	(50.0)	3.3	8.0	14.0	22.0	32.5	61.5	90.0	0.0086	0.48	30.0
L	275.8	(40.0)	11.5	29.5	59.0	93.0	128.0	213.0	300.0	0.0029	0.30	60.0
1144 K (1600°F)												
L	68.9	(10.0)	0.4	1.4	3.1	5.6	8.8	19.2	31.8	0.0202	0.76	20.0
L	51.7	(7.5)	7.5	25.5	56.0	90.9	124.0	204.0	275.0	0.0029	0.25	40.0
L	41.4	(6.0)	8.0	37.0	80.0	130.0	187.0	345.0	520.0	0.0015	0.76	350.0
1255 K (1800°F)												
L	34.5	(5.0)	2.5	5.0	7.6	10.1	12.2	16.5	20.2	0.0400	0.08	2.5
L	20.7	(3.0)	27.5	63.0	83.0	99.0	112.5	142.5	170.0	0.0019	0.05	5.0
L	13.8	(2.0)	10.0	25.0	60.0	140.0	730.0	Discontinued at 0.68%, 3220.0 Hrs.		0.000074	0.49	700.0
Heat 4-1696												
922 K (1200°F)												
L	413.7	(60.0)	0.7	1.5	2.5	3.6	4.8	8.6	13.6	0.0446	1.02	14.0
L	344.7	(50.0)	3.8	9.0	15.0	24.0	34.0	59.0	84.5	0.0097	0.46	30.0
L	275.8	(40.0)	12.0	35.0	72.5	112.0	150.0	247.5	340.0	0.0027	0.24	50.0
1144 K (1600°F)												
L	68.9	(10.0)	1.5	6.5	14.5	25.0	36.0	63.5	91.0	0.0091	0.36	20.0
L	51.7	(7.5)	4.0	18.0	37.0	62.0	90.0	171.0	275.0	0.0023	0.88	225.0
L	41.4	(6.0)	55.0	120.0	200.0	293.0	395.0	755.0	1390.0	0.00038	0.72	700.0

183

TABLE E-II (Concluded)

Sample Orientation	Stress MPa	Stress (ksi)	Time for Indicated Creep Strain, Hrs. 0.1%	0.2%	0.3%	0.4%	0.5%	0.75%	1.0%	Min. Creep Rate, %/Hr	Primary Creep Strain, %	Time of Primary Creep, Hrs
1255 K (1800°F)												
L	34.5	(5.0)	0.7	2.1	3.6	5.2	6.7	10.2	13.2	0.0655	0.13	1.0
L	20.7	(3.0)	3.5	7.7	12.0	16.3	20.5	30.6	38.7	0.0234	0.08	2.5
L	13.8	(2.0)	5.0	30.0	100.0	250.0	770.0	3040.0	Discontinued at 0.77%, 3191.4 Hrs	0.00010	0.51	800.0
						Heat 4-1697						
922 K (1200°F)												
L	413.7	(60.0)	0.5	1.2	2.0	2.8	3.8	6.4	9.6	0.0601	1.10	11.0
L	344.7	(50.0)	1.8	4.5	8.3	13.0	19.5	39.0	64.5	0.0096	0.86	50.0
L	275.8	(40.0)	7.0	25.5	56.0	93.0	129.0	220.0	311.0	0.0028	0.31	60.0
1144 K (1600°F)												
L	68.9	(10.0)	3.0	10.5	25.0	39.5	54.0	88.0	116.5	0.0067	0.23	15.0
L	51.7	(7.5)	1.9	7.0	18.0	31.0	47.5	102.0	183.0	0.0024	1.01	186.0
L	41.4	(6.0)	10.0	40.0	95.0	170.0	260.0	605.0	1125.0	0.00046	0.75	600.0
1255 K (1800°F)												
L	34.5	(5.0)	3.0	7.0	10.7	14.5	18.0	24.3	29.8	0.0260	0.09	2.5
L	20.7	(3.0)	6.0	16.7	28.5	45.5	63.0	105.0	139.0	0.0057	0.37	40.0
L	13.8	(2.0)	12.0	30.0	55.0	90.0	150.0	515.0	1155.0	0.00042	0.61	320.0

TABLE E-III

CREEP TEST DATA FOR SUPPLEMENTARY GRAIN SIZE STUDY SHEET
[HEAT 4-1697, 0.76 mm (0.030-inch) THICK, ASTM 5-6]

Sample Orientation	Stress MPa	Stress (ksi)	Time for Indicated Creep Strain, Hrs. 0.1%	0.2%	0.3%	0.4%	0.5%	0.75%	1.0%	Min. Creep Rate, %/Hr	Primary Creep Strain, %	Time of Primary Creep, Hrs
922 K (1200°F												
L	413.7	(60.0)	0.3	0.9	1.6	2.5	3.6	6.8	10.7	0.0500	1.18	14.0
L	344.7	(50.0)	1.5	5.0	9.0	14.0	20.0	42.5	64.5	0.0103	0.74	40.0
L	275.8	(40.0)	18.0	44.0	74.0	107.0	139.0	220.0	288.0	0.0031	0.32	80.0
1144 K (1600°F)												
L	68.9	(10.0)	0.4	1.7	4.2	7.2	10.5	22.5	35.4	0.0190	0.65	17.0
L	51.7	(7.5)	10.0	20.0	32.0	46.5	63.5	121.0	214.0	0.0024	0.87	160.0
L	41.4	(6.0)	4.0	25.0	75.0	136.0	205.0	450.0	920.0	0.00050	0.90	700.0
1200 K (1700°F)												
L	41.4	(6.0)	1.8	4.5	7.2	10.0	12.6	18.0	22.7	0.0368	0.15	3.0
L	41.4	(6.0)	12.0	25.0	38.0	51.5	65.0	92.5	113.0	0.0075	0.15	7.5
T	41.4	(6.0)	0.4	1.7	6.2	14.5	24.0	47.0	69.0	0.0106	0.39	13.0
T	41.4	(6.0)	7.5	20.0	34.0	48.7	63.0	93.5	115.8	0.0065	0.21	21.0
1255 K (1800°F)												
L	20.7	(3.0)	1.2	3.6	7.9	13.8	20.7	38.5	52.1	0.0141	0.42	15.0
L	13.8	(2.0)	0.2	1.2	3.0	7.0	15.0	47.5	74.5	0.0073	0.50	15.0
L	8.6	(1.25)	1.8	14.0	46.5	90.0	132.0	232.0	279.0	0.0022	0.29	42.0

185

REFERENCES

1. Davis, J. W.; and Cramer, B. A.: Prediction and Verification of Creep Behavior in Metallic Materials and Components for the Space Shuttle Thermal Protection System - Phase I - Cyclic Materials Creep Predictions. NASA CR-132605-1, 1974.

2. Herchenroeder, R. B.; Matthews, S. J.; Tackett, J. W.; and Wlodek, S. T.: HAYNES alloy No. 188, Cobalt, No. 54, March 1972, pp 3-13.

3. Klappholy, J. J.; Waxman, S.; and Feng, C.: A Computerized Technique of Plotting a Complete Polefigure by an X-ray Reflection Method. Advances in X-ray Analysis, Vol. 15, Plenum Press, 1972, pp 365-372.

4. Conway, J. B.: Stress Rupture Parameters: Origin, Calculation and Use. Gordon and Breach, Science Publishers, Inc., 1969, pp 21-84.

5. Garofalo, F.: Fundamentals of Creep and Creep-Rupture in Metals. The MacMillan Company, 1965, pp 48-53.

6. Herchenroeder, R. B.: HAYNES alloy No. 188 Aging Characteristics. Proceedings of the International Symposium on Structural Stability in Superalloys. Seven Springs, Pa., Sept. 4-8, 1968, Vol. II, pp 460-500.

7. Barrett, C. R.; Lytton, J. L.; and Sherby, O. D.: Effect of Grain Size and Annealing Treatment on Steady-State Creep of Copper, Trans. AIME, Vol. 239, February, 1967, pp 170-180.

8. Cullity, B. D.: Elements of X-ray Diffraction. Addison-Wesley Publishing Company, Inc., 1956, pp 280-285.

9. Dieter, G. E., Jr.: Mechanical Metallurgy, McGraw-Hill Book Company, Inc., 1961, pp 432-434.

10. Rhines, F. N.; and Wray, P. J.: Investigation of the Intermediate Temperature Ductility Minimum in Metals. ASM Trans., Vol. 54, 1961, pp 117-128.

11. Garofalo, F.; Domis, W. F.; and von Gemmingen, F.: Effect of Grain Size on the Creep Behavior of an Austenitic Iron-Base Alloy. Trans. AIME, Vol. 230, October, 1964, pp 1460-1467.

12. Wohlbier, F. H., Editor: Diffusion and Defect Data. H. Merkal & Company, Switzerland, Vol. 8, No. 1-4, 1974.

13. Conrad, H.; Bernett, E.; and White, J.: Correlation and Interpretation of High Temperature Mechanical Properties of Certain Superalloys. Joint Intl. Conf. on Creep, Inst. of Mech. Engr., London, 1963, pp 1-9-15.

14. Dorn, J. E., Editor: Mechanical Behavior of Materials, McGraw-Hill, New York, 1961, pp 192-194.

15. Richards, E. G.: Influence of Specimen Size and Grain Size on the Creep-Rupture Strength of Some Nickel-Base High-Temperature Alloys, J. Inst. of Metals, Vol. 96, 1968, pp 365-370.

16. Stickley, G. W.; and Brownhill, D. J.: Elongation and Yield Strength of Aluminum Alloys Related to Gage Length and Offset, Proc. ASTM, Vol. 65, 1965, pp 597-616.

1 Report No	2 Government Accession No	3 Recipient's Catalog No
NASA CR-3013		

4 Title and Subtitle	5 Report Date
Thermomechanical Processing of HAYNES® Alloy No. 188 Sheet to Improve Creep Strength	August 1978
	6 Performing Organization Code

7 Author(s)	8 Performing Organization Report No
D. L. Klarstrom	
	10 Work Unit No

9 Performing Organization Name and Address	11 Contract or Grant No
Stellite R & D. Department Cabot Corporation 1020 W. Park Avenue Kokomo, Indiana 46901	NAS1-13837
	13 Type of Report and Period Covered
12 Sponsoring Agency Name and Address	Contractor Report/Final
National Aeronautics and Space Administration Washington, D.C. 20546	14 Sponsoring Agency Code

15 Supplementary Notes

Technical Representative of The Contracting Officer:
Donald R. Rummler, Materials Division, Materials Research Branch,
NASA-Langley Research Center, Hampton, Va. 23665

16 Abstract

An investigation was performed to seek improvements in the low strain (≤ 1 percent) creep strength of HAYNES alloy No. 188 thin gauge sheet by means of thermomechanical processing (TMP). Processing methods designed to develop a sheet with strong crystallographic texture after recrystallization and to optimize grain size were principally studied. The effects of thickness-to-grain diameter ratio and prestrain on low strain creep strength were also briefly examined. Results of the program indicate that the most significant improvements were obtained in the sheets having a strong crystallographic texture. The low strain creep strength of the textured sheets was observed to be superior to that of standard production sheets in the 922 K (1200°F) to 1255 K (1800°F) temperature range. Tensile, stress rupture, fabricability and surface stability properties of the experimental sheets were also measured and compared to property values reported for the baseline production sheets.

17 Key Words (Suggested by Author(s))	18 Distribution Statement
Thermomechanical Processing, High Temperature Creep Strength, Cobalt-Base Alloy (HAYNES alloy No. 188), High Temperature Alloy Sheet, Mechanical Properties	Unclassified - Unlimited Subject Category 26

19 Security Classif (of this report)	20 Security Classif (of this page)	21 No of Pages	22 Price*
Unclassified	Unclassified	191	$9.00

* For sale by the National Technical Information Service, Springfield, Virginia 22161

NASA-Langley, 1978

END

DEC 21 1978